UNIVERSITÄT ZU LÜBECK

From the Institute of Biochemistry

of the University of Lübeck

Director: Prof. Dr. Rolf Hilgenfeld

Implications of T-lymphocyte homing in Lassa fever pathogenesis and transmission

Dissertation

for Fulfillment of

Requirements

for the Doctoral Degree

of the University of Lübeck

from the Department of Natural Sciences

submitted by

Julia Rebecca Port

from Gelnhausen

Lübeck, 2019

First referee: Prof. Dr. rer. nat. Lars Redecke

Second referee: Prof. Dr. rer. nat. Tamás Laskay

Date of oral examination: 19.12.2019

Approved for printing. Lübeck, 03.01.2020

I. TABLE OF CONTENTS

II. ABBREVIATIONS

ALT	alanine transaminase
ANN	artificial neural network
ANOVA	analysis of variance
APC	antigen presenting cell
APC	-allophycocyanin
AST	aspartate aminotransferase
B cell	B lymphocyte
Ba366	Bantou 366 (strain)
BNITM	Bernhard Nocht Institute for Tropical Medicine
BSA	bovine serum albumin
BSL-4	biosafety level 4
BUV	brilliant ultraviolet
BV	brilliant violet
ca	circa
CCL	CC-chemokine ligand
CCR	CC chemokine receptor
CD	cluster of differentiation
CD40L	CD40 ligand
CD62L	L-selectin
CDC	Centers for Disease Control
CEPI	Coalition for Epidemic Preparedness and Innovations
CFR	case fatality rate
CHAPV	Chapare virus
CI	confidence intervals
CLA	cutaneous lymphocyte antigen
CM	central memory
CTLA	cytotoxic T-lymphocyte-associated protein
Cy	cyanine
d	distilled
DC	dendritic cell
DC-SIGN	(DC)-specific intracellular adhesion molecule 3 -grabbing nonintegrin
DMEM	Dulbecco's Modified Eagle's Media
DMSO	dimethyl sulfoxide
DNA	Deoxyribonucleic acid
DPI	days post infection
DPO	days post-onset
ds	double-stranded
DTT	dithiothreitol
EBOV	Ebola virus
EBV	Epstein-Barr virus
EDTA	ethylendiamintetraacetate

eff	effector
ELISPOT	Enzyme-linked Immunospot
EM	effector memory
EVD	Ebola virus disease
FCS	fetal calve serum
FFU	focus forming units
FITC	Fluoresein isothiocyanate
GP	glycoprotein precursor
GPC	glycoprotein
GTOV	Gunarito virus
HBSS	Hank's Balanced Salt Solution
HEV	high endothelial venules
HIV	human immunodeficiency virus
HLA	human leukocyte antigen
HRP	horseradish peroxidase
HS	human serum
HSV	herpes simplex virus
i.d.	intradermal
i.n.	intranasal
i.v.	intravenous
IC_{50}	half maximal inhibitory concentration
ICAM	intracellular adhesion molecule
ICS	intracellular cytokine staining
IEDB	immune epitope data base
IFA	immunofocus assay
IFN	interferon
IFNAR chimeras	bone marrow-chimeric IFNAR knock-out mice with C57BL/6 bone marrow
$IFNAR^{KO}$	type I interferon receptor knockout mice
IgG	immunoglobulin class G
IgM	immunoglobulin class M
IGR	intergenic region
IKKε	IκB kinase ε
IL	interleukin
IP	IFN inducible protein
IRF	interferon regulatory factor
ISGs	IFN-stimulated genes
ISTH	Irrua Specialist Teaching Hospital
ITGA1	alpha 1 integrin/CD49a
ITGA4	alpha 4 integrin/CD49d
ITGAE	alpha E integrin/CD103
ITGB1	beta 1 integrin/CD29
ITGB7	beta 7 integrin
IU	international units

IVC	individually ventilated cages
kb	kilo base
kDA	kilo Dalton
L	liter
L-segment	large segment
LAMP	lysosomal membrane protein
LASV	Lassa virus
LCMV	lymphocytic choriomeningitis mammarenavirus
LF	Lassa fever
LFA	leucocyte function associated molecule
LGA	local government area
LSCtin	lymph node sinusoidal endothelial cell C-type lectin
LUJV	Lujo virus
Ly5.1	natural allelic isoform of CD45 known as CD45.1
M. natalensis	*Mastomys natalensis*
MACV	Machupo virus
MadCAM-1	mucosal addressin cell adhesion molecule 1
MAVS	mitochondrial antiviral-signaling protein
MDA5	Melanoma differentiation- associated protein 5
mDC	monocyte derived DC
MHC	major histocompatibility complex
mL	milliliter
mo	monocyte derived
MOI	multiplicity of infection
MORV	Morogoro virus
mRNA	messenger RNA
NF-κB	nuclear factor kappa-light-chain-enhancer of activated B cells
NHP	non-human primate
NK cell	natural killer cell
NLR	NOD-like receptor
nm	nanometer
NP	nucleoprotein
OT-I	ovalbumin-specific TCR
OVA	ovalbumin
p.o.	per os
PAMP	pathogen associated molecular patterns
PBMC	peripheral blood mononuclear cell
PBS	phosphate buffered saline
PCR	polymerase chain reaction
PE	-phycoerythrin
PerCp	Peridinin-chlorophyll-protein
PHA	Polyhydroxyalkanoate
PMA	Phorbol myristate acetate

PNAd	peripheral lymph node addressin
PRR	pattern recognition receptor
RA	retinoic acid
RBC	red blood cell
RIG	retinoic-acid inducible gene
RLRS	(RIG)-I-like receptors
RM	resident memory
RNA	Ribonucleic acid
RPMI	Roswell Park Memorial Institute
RT	room temperature
RT-PCR	real-time PCR
S-segment	small segment
SABV	Sabia virus
SCM	stem cell memory
SD	standard deviation
SEM	standard error of the mean
SFC	Single Focus Forming Cells
SIV	simian immunodeficiency virus
SSP	stable signal peptide
T cell	T lymphocyte
TAE	TRIS-Acetat-EDTA-buffer
$TCID_{50}$	median 50 % tissue culture infective dose
TCR	T cell receptor
TGF	transforming growth factor
TLR	Toll-like receptor
TMB	Tetramethylbenzidine
TNF	tumor necrosis factor
U	enzyme unit
UTRs	untranslated regions
UV	ultraviolet
VCAM-1	vascular cell adhesion molecule
VSV	vesicular stomatitis virus
WHO	World Health Organization
WT	wildtype
Z	RING finger zinc-binding protein
α-	anti-
µL	microliter

1 ABSTRACT/ZUSAMMENFASSUNG

Lassa virus is endemic in several West African countries and causes around 300,000 cases of Lassa fever (LF) annually. Previous work has highlighted the role of T-cell-mediated immunity in LF survival. However, the relationship between T cells and pathophysiology is poorly understood and data from human LF is scarce. The goal of the present study was to increase the current understanding of T-cell-mediated immunity and pathogenesis in LF. In particular the role of T-cell homing, which allows trafficking of T cells to infected tissues, was investigated in relation to disease pathogenesis and outcome. It was also investigated whether T-cell homing signatures were related to viral transmission routes.

Clinical immunological research was performed on LF patient samples in the context of studies conducted at the Irrua Specialist Teaching Hospital, in Edo state, Nigeria. To explore the biological implications of the data collected in patients, natural routes of exposure were mimicked in a mouse model of infection with functional hematopoietic immunity and the impact on disease and T-cell response characterized.

The findings presented here indicate distinct T-cell phenotypes and signatures in humans that define LF survival and severity. Within survivors, mild cases mounted a controlled and antigen-specific T-cell response characterized by moderate levels of activation and response to re-stimulation with LASV antigens *ex vivo*. Conversely, severe cases showed high levels of T-cell activation, including T cells that did not respond to LASV re-stimulation. Severe cases showed an increased T-cell homing pattern that suggested recruitment to the intestinal mucosa, a pattern that was recapitulated by oral administration of LASV in a mouse model, while fatal cases showed increased non-specific homing signatures targeting especially $CD4^+$ T cells towards inflammation.

The data presented here suggests that a controlled and effective T-cell immune response is important for recovery of LF. I speculate that inflammation and inflammation-driven activation of T cells and their subsequent recruitment to sites of infection, such as the gastrointestinal tract, are important drivers of LF pathogenesis. Finally, T-cell homing signatures may function as a biomarker of disease severity and can provide insight into putative routes of LASV transmission.

Das Lassa-Virus (LASV) ist endemisch in mehreren westafrikanischen Ländern und löst jährlich 300,000 Fälle des Lassafiebers (LF) aus. Vorangegangene Arbeiten haben die Rolle von T-Zell-vermittelter Immunität in LF untersucht. Bis heute ist der Einfluss von T-Zellen auf die Pathophysiologie von LF nicht aufgeklärt. Ein Grund dafür ist, dass humane Daten über LF rar sind. Das Ziel dieser Studie war es, das Verständnis des Zusammenhangs von T-Zell-vermittelter Immunität und Pathogenese in LF zu verbessern. Im Speziellen sollte die Rolle des T-Zell-Homings, welches die Rekrutierung von T-Zellen in infizierte Gewebe ermöglicht, im Hinblick auf die Beziehung zu Krankheitsverlauf und Pathogenese untersucht werden. Weiterhin sollte gezeigt werden, ob Signaturen des T-Zell-Homings in Beziehung zu der Transmissionsroute stehen.

Die klinisch-immunologische Forschung dieser Arbeit wurde an LF Patientenproben im Kontext von Studien am Irrua Specialist Teaching Hospital im Bundesstaat Edo in Nigeria durchgeführt. Um die biologischen Implikationen der im Menschen gesammelten Daten weiter zu untersuchen, wurden natürliche Transmissionsrouten in einem Infektions-Mausmodell mit funktionaler Immunität nachgestellt und die Auswirkung auf Krankheit und T-Zell Antwort charakterisiert.

Die hier präsentierten Ergebnisse indizierten distinkt verschiedene T-Zell-Phänotypen und Signaturen im Menschen, die Überleben und Schweregrad von LF definieren. Innerhalb der Gruppe der Überlebenden bildeten Patienten mit milden Krankheitsverläufen eine kontrollierte und antigen-spezifische T-Zell-Antwort aus, die durch moderate Aktivierung und Reaktion auf Restimulation mit LASV-Antigenen *ex vivo* charakterisiert war. Im Gegensatz zeigten Patienten mit schweren Verläufen hohe T-Zell-Aktivierung und eine Antwort, die auch T-Zellen, die nicht auf LASV Restimulation reagierten, beinhaltete. Hier konnte vermehrt eine T-Zell-Homingsignatur gezeigt werden, die die Rekrutierung in die intestinale Mukosa suggeriert. Diese Signatur konnte durch orale Administration von LASV im Mausmodell rekapituliert werden. Im Gegensatz dazu konnte in Patienten mit fatalem Verlauf vermehrt unspezifische Homingsignaturen nachgewiesen werden, die speziell auf die Infiltration von $CD4^+$-T-Zellen in entzündete Gewebe hinzielt.

Die hier gezeigten Daten suggerieren, dass eine kontrollierte und effektive T-Zell-Immunantwort für das Überleben von LF wichtig ist. Weiter kann spekuliert werden, dass Entzündung und entzündungsbedingte Aktivierung von T-Zellen, sowie die darauffolgende Rekrutierung dieser zu Infektionsherden wie dem gastrointestinalen Trakt, wichtige Treiber der LF Pathogenese sind. Schließlich implizieren die Daten, dass T-Zell-Homingsignaturen

als Biomarker zur Einschätzung des Krankheitsverlaufs fungieren könnten und einen Einblick auf mutmaßliche Transmissionsrouten erlauben.

2 INTRODUCTION

2.1 PART I: LASSA FEVER: A RE-EMERGING HEMORRHAGIC FEVER

2.1.1 THE ETIOLOGICAL AGENT

PHYLOGENETIC CONTEXT

Lassa virus (LASV) is the etiological agent of Lassa fever (LF), a viral zoonosis endemic in West Africa. The natural host and reservoir of LASV is the multimammate rat *Mastomys natalensis.* LASV is a member of the virus family *Arenaviridae* and, due to its mammalian host, the genera *Mammarenavirus*. At least seven viruses of this family have been found to be highly pathogenic for humans and cause hemorrhagic fever. In addition to LASV, other arenaviruses such as Lujo (LUJV), Machupo (MACV), Guanarito (GTOV), Sabia (SABV) and Chapare (CHAPV) viruses fall into this category (Yun and Walker, 2012). While CHAPV has not been classified yet, as of 2018, the Bundesamt für Arbeitsschutz und Arbeitsmedizin has classified all others as risk group 4 pathogens (Technische Regeln für Biologische Arbeitsstoffe 462). Accordingly, any work with these viruses may only be performed under biosafety level 4 (BSL-4) laboratory conditions.

Broadly, mammalian arenaviruses are subdivided into two complexes based on geographic distribution, as well as antibody cross-reactivity (Wulff, Lange, and Webb, 1978) and sequence phylogeny (Bowen, Peters, and Nichol, 1997), **(Figure 2.1).** New World arenaviruses are found in North and South America, while members belonging to the Old World arenaviruses are distributed over Africa, Europe and Asia. Besides LASV, only the human pathogenic arenavirus LUJV has been found in the African continent recently (Briese et al., 2009). Only one arenavirus (Tacaribe virus) has been isolated from frugivorous bats (Downs, Anderson, Spence, Aitken, and Greenhall, 1963), while all other known arenaviruses have been shown to share host reservoirs within the family *Muridae*. It is assumed that these viruses share a long history of co-evolution with their hosts, which has contributed to their high genetic diversity (Bowen, Peters, and Nichol, 1997).

Consequently, as different *Muridae* species are subject to limitations in their geographic range and habitation, the distribution of arenaviruses is equally restricted. LASV has a limited geographic spread across several West African countries. Interestingly, the main natural host has a far wider geographic distribution. *Mastomys natalensis* is the host species for multiple arenaviruses, can be found across all Sub-Saharan Africa, and is in fact considered Africa's most predominant rodent species (Colangelo et al., 2013). It remains unknown why LASV

has only been found in two phylogroups found in West Africa, but has not spread further, even though other *Mastomys natalensis* phylogroups are also susceptible to infection (Gryseels et al., 2017).

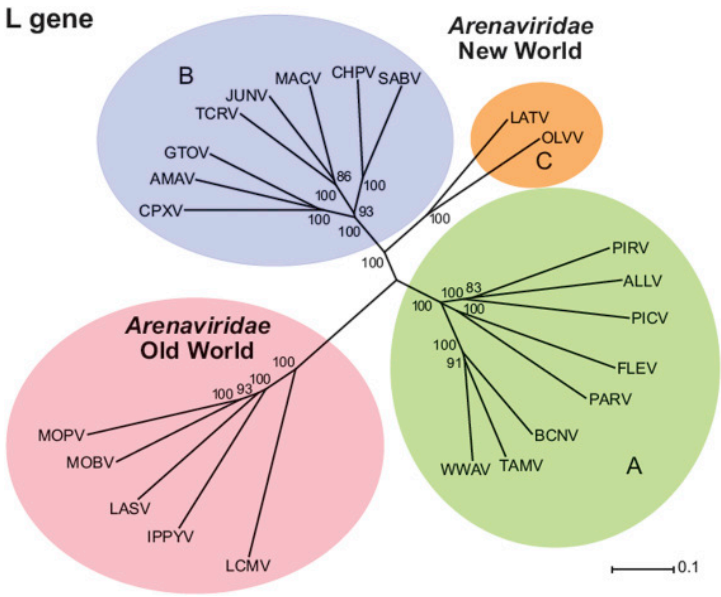

Figure 2.1: Arenavirus phylogeny. Arenaviruses are divided into three New World and one Old World clusters. Based on the viral L-gene sequence homology, LASV is found in the clade of Old World viruses. (Adapted from International Committee on Taxonomy of Viruses, 2012).

VIRAL STRUCTURE

LASV, like all members of the *Arenaviridae* family, is an enveloped, ambisense single-stranded RNA virus that has a segmented genome (Buchmeier, Peters, and De la Torre, 2007). Virions carry a lipid envelope around the inner nucleocapsid and range between 40 to 200 nm in diameter **(Figure 2.2)**. The RNA genome is comprised of two segments, which are ambisense in orientation. The largest genomic segment (ca. 7 kb) encodes for the RNA-dependent RNA polymerase (L) and the small RING finger zinc-binding protein (Z), while the nucleoprotein (NP), which forms the nucleocapsid, and the glycoprotein precursor protein (GP) are encoded on the smaller S segment (~3.4 kb). Post-translational cleavage of GP results in the formation of GP1 and GP2, which form the envelope, and a stable signal peptide (SSP). GP1 binds to glycoprotein target cell receptors, while GP2 has structural consistency to transmembrane fusion proteins (Cao et al., 1998; Illick et al., 2008; Van Breedam et al., 2014; Gallaher, DiSimone, and Buchmeier, 2001). The replication of LASV is classified as non-lytic and replication is cytosolic. Uptake into target cells occurs through receptor mediated endocytosis and macropinocytosis (Torriani, Galan-Navarro, and Kunz, 2017). The first important cellular receptor that has been described is dystroglycan, which is ubiquitously expressed but requires post-translational tissue-specific modification to function as an entry receptor for LASV (Cao et al., 1998; Goddeeris et al., 2013). More recently, lymph node sinusoidal endothelial cell C-type lectin (LSCtin) and dendritic cell (DC)-specific

intracellular adhesion molecule 3 (ICAM-3)-grabbing nonintegrin (DC-SIGN) have been investigated as entry receptors. Both have a restricted expression pattern and only facilitate entry to selective cell populations, including DCs, an important immune cell population relevant to developing an adaptive anti-viral immune response. DCs have been shown to be important early target cells for initial viral replication at the first entry site (Shimojima, Stroher, Ebihara, Feldmann, and Kawaoka, 2012; Van Breedam et al., 2014). Infection of DCs, monocytes or macrophages, as well endothelial cells, does not lead to cell death and tissue damage by itself *in vitro* (Lukashevich et al., 1999).

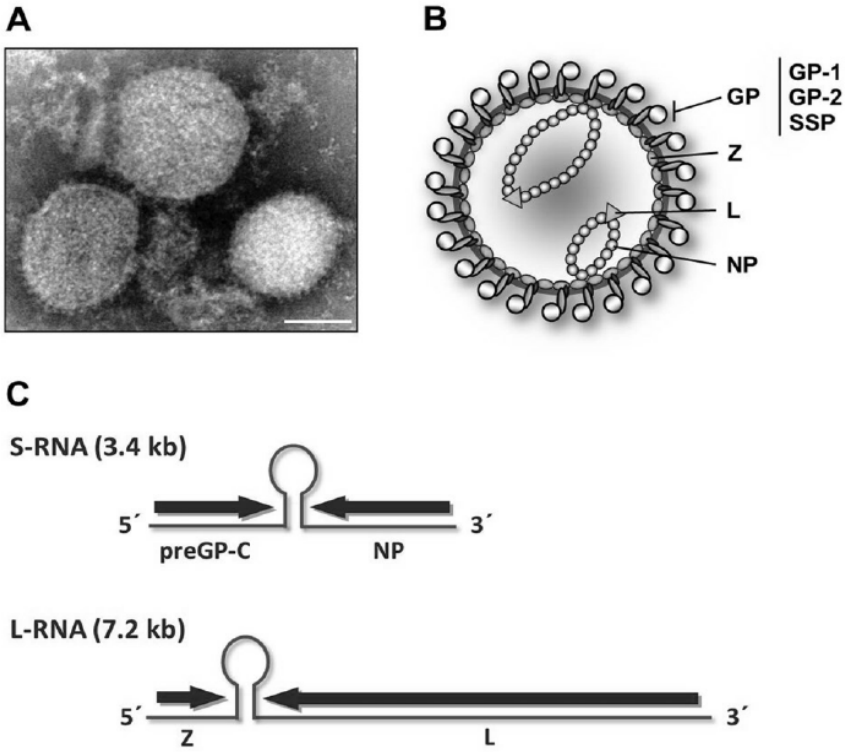

Figure 2.2. Lassa virus structure and genomic orientation: Electron microscopy of Lassa virus (A) and overview of virus proteins and RNA, which comprises the virion structure (B). The LASV genome is divided into two segments and has ambisense orientation (C). The glycoprotein (GPC) is encoded on the smaller (S) segment in positive-sense orientation, the nucleoprotein (NP) in negative-sense orientation, separated by an intergenic region (IGR). On the larger (L) segment the Z matrix protein is encoded in positive, the L polymerase in negative-sense orientation, also separated by an IGR. Adapted from (Fehling, Lennartz, and Strecker, 2012).

2.1.2 THE DISEASE

EPIDEMIOLOGY AND ECOLOGY

Lassa fever is a hemorrhagic disease endemic in multiple West African countries that occurs after infection with LASV. LF was first described in 1969, in the small town of Lassa in the Northeast of Nigeria. The first known case was a missionary nurse that contracted a febrile

disease and died about one week after the onset of symptoms. It is assumed that infection occurred from contact with an obstetrical patient. Two additional nurses acquired the disease. Isolation and description of LASV was possible from all three cases and the disease came to be known as “Lassa” fever (Buckley and Casals, 1970).

LASV seroprevalence is widespread across multiple West African countries, but shows great variability depending on the geographic location (McCormick, Webb, et al., 1987). Sierra Leone (McCormick, Webb, et al., 1987), Guinea (Bausch et al., 2001; Lukashevich, Clegg, and Sidibe, 1993), Liberia and Nigeria (Asogun et al., 2012; Tomori, Fabiyi, Sorungbe, Smith, and McCormick, 1988) are considered LASV-endemic countries, while evidence suggests that LASV can also be found in Ivory Coast, Mali, Central African Republic, Togo and Benin (Safronetz et al., 2010).

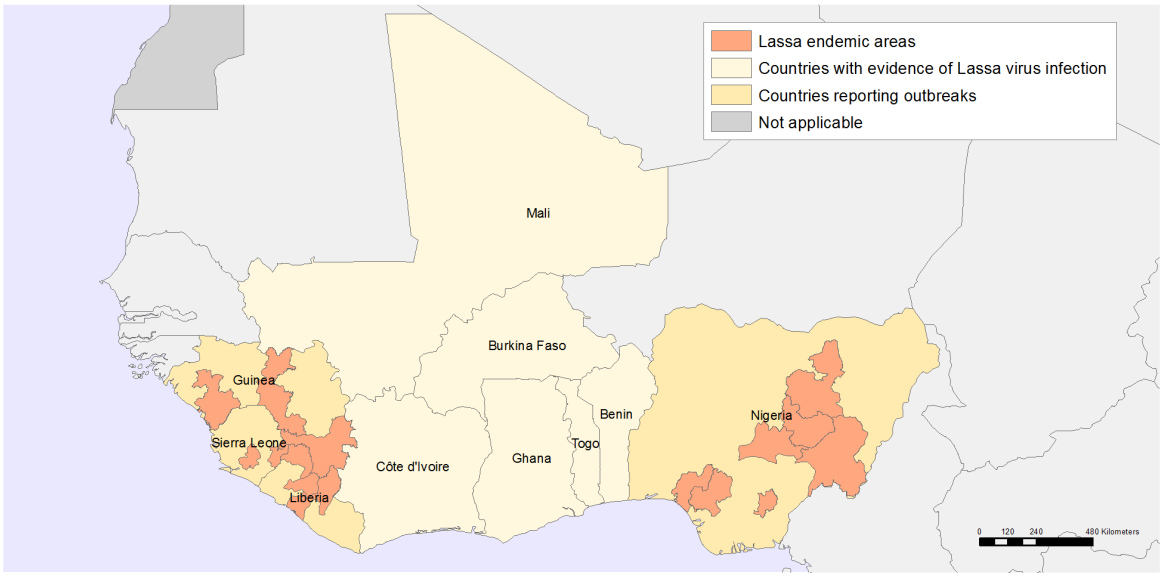

Figure 2.3: Lassa affected countries. Countries considered to be LASV-endemic include Nigeria, Sierra Leone, Liberia and Guinea. Adapted from (World Health Organization, 2018).

While few LF cases have been reported in Burkina Faso, Ghana, Senegal, Ivory Coast, Gambia and Mali, sizeable outbreaks have only been reported in Nigeria and Sierra Leone, with less severe outbreaks also occurring in Liberia, Benin, Guinea and the Central African Republic (Richmond and Baglole, 2003; Shaffer et al., 2014) **(Figure 2.3)**. Overall, eastern Nigeria and the Mona River region (Liberia, Sierra Leone, Guinea) are most affected, which, interestingly, leaves two distinct and separate regions where LF can be considered as truly endemic (Fichet-Calvet and Rogers, 2009). It is estimated that 100,000 - 300,000 infections occur each year with approximately 5,000 deaths (McCormick, 1986). However, the seroprevalence ranges from 1.8 % to 55 % in endemic regions and the annual incidence of

seroconversion has been reported to range from 5 – 20 %, indicating that most infections progress to mild disease or are asymptomatic (Yun and Walker, 2012).

Prevalence in the host reservoir fluctuates both seasonally and geographically (Fichet-Calvet et al., 2007; Monath, Newhouse, Kemp, Setzer, and Cacciapuoti, 1974). Zoonotic LF transmission is dependent on seasonal factors such as food abundance for rodents and their corresponding behavior. The rodent reservoir lives in close contact with the human population. It has been observed that during the dry season (December to March) a higher number of rats are found around and inside houses. However, they are more commonly encountered in agricultural fields surrounding settlements in the wet season (April to November). The viral prevalence in rats has been found to be two to three times higher during the wet season (Fichet-Calvet et al., 2007). Recently, additional rodent species have been reported to act as natural hosts, although their overall contribution to transmission into humans is thought to be less significant compared to *Mastomys* (Olayemi et al., 2016). In endemic regions studies have found that 30 % of *Mastomys* carry the virus.

Animal-to-human transmission is thought to occur either through direct or indirect contact with the host species. LASV is shed in the urine and feces of rats and is assumed to remain infectious in the environment. Human exposure and infection may occur through inhalation of aerosolized virus particles (Stephenson, Larson, and Dominik, 1984) or through direct contact with rodent saliva, blood, urine or feces. Furthermore, infection can occur via contact with fomites. Oral infection through rodent consumption as bush meat is also possible (Malhotra et al., 2013). Human-to-human transmission is rare, and outbreaks are characterized by multiple spillover events. It is estimated that only 10 % of disease transmission occurs through direct or indirect contact among infected humans. Human-to-human transmission may occur in nosocomial settings. Consequently, primarily healthcare workers are at higher risk of becoming infected in this manner. Also, close contact while sharing a household with an infected person or exposure to infected human body fluids poses a risk. Patient care of family members outside and inside of quarantine stations is not uncommon, especially before positive diagnosis is confirmed.

CLINICAL MANIFESTATION

Even though LF is considered a viral hemorrhagic disease, symptoms of hemorrhage are rarely observed in patients. The symptoms of LF are non-specific and do not allow for an easy differential diagnosis when compared to other febrile illnesses frequently found in the affected region (Yun and Walker, 2012). After an incubation period of 7 to 21 days, flu-like

symptoms such as fever, general weakness, headaches, sore throat, coughing, joint pain and malaise are observed. The first few days of disease are typically only characterized by fever, general weakness and fatigue.

While the majority of symptomatic patients only present with mild disease, approximately 20 % of patients suffer from severe LF. For mild LF, the recovery period already begins as early as 8 days after the onset of symptoms, while in severe LF the rapid deterioration of patients begins between 6 to 10 days after disease onset. In cases of severe disease progression and fatal outcome, facial and pulmonary edema, pleural and pericardial effusions, acute respiratory distress and signs of terminal hypovolemic shock can be observed. Additionally, the gastrointestinal and neurological systems can be affected, producing symptoms such as vomiting, nausea and diarrhea as well as clinical signs of encephalopathy and even coma or seizures (McCormick, King, et al., 1987; Bausch et al., 2001; Khan et al., 2008). In this severe disease state moderate bleeding from mucosal surfaces can occur. In hemorrhagic cases, inhibition of platelet aggregation and thrombocytopenia are common (Cummins et al., 1989; Fisher-Hoch et al., 1988). Despite the disease progression being well characterized, LF pathogenesis, particularly for fatal outcome and severe disease, is not well understood. It is likely however, that changes in the vascular endothelium, liver, adrenal gland and other organs contribute to the final terminal shock syndrome. Blood loss alone and lesions observed in organ tissues cannot explain the resulting death in fatal cases (Walker et al., 1982). Interestingly, while cytokine storm due to activation of target cells such as monocytes has been shown to be the cause of vascular breakage in other hemorrhagic infections, it is not observed in LF (Mahanty et al., 2001; Yun and Walker, 2012).

Early viral replication in humans occurs first at the site of entry and then disseminates through the blood stream to spleen, lymph nodes, and liver. The highest levels of viremia are observed usually between days 4 and 9 after onset of symptoms. Early viral load has been shown to be a good predictor of disease outcome. Patients with a systemic viral load < 10^3 median 50 % tissue culture infective dose ($TCID_{50}$)/mL were less likely to succumb to disease compared to patients with higher viral loads (Yun and Walker, 2012). Statistically, fatal outcome is more likely if patients present with serum level of aspartate aminotransferase (AST) ≥ 150 international units (IU)/L, which is a strong indicator of liver damage. Indeed, post-mortem investigation of tissue damage has revealed that LF leads to lesions in the liver (Winn et al., 1975; McCormick et al., 1986). Overall, severe LF is associated with raised AST levels, as well as raised alanine transaminase (ALT), another liver enzyme, and a raised hematocrit. In late stages and convalescence deafness may

occur. This deafness has been reported in up to 20 % of infections and can occur transiently, but may also be permanent. (Cummins et al., 1990)

As not all cases of LF are reliably diagnosed, it has been difficult to establish the actual case fatality ratio (CFR), but it is believed to be between 1 % and 2 % of all infections (McCormick and Fisher-Hoch, 2002). For hospitalized LF the case CFR is estimated to be between 15 % - 20 %, though this rate may increase during nosocomial outbreaks (Fisher-Hoch et al., 1995; McCormick et al., 1987). Two population groups especially at risk of severe LF are pregnant woman and young children. Even though mortality overall is not high, it is significantly increased in woman in their third trimester of pregnancy (30 %). In infants less than two years old “swollen baby syndrome” or anasarca can occur and is also linked to high mortality (World Health Organization, 2018).

ANIMAL MODELS FOR LASSA FEVER

Multiple animal models have been established for LF and LASV infection. Interestingly, experimental LASV infection in wildtype mice, *Mus musculus* (such as the laboratory strain C57BL/6), is characterized by fast viral clearance without clinical manifestations. It has been shown, that mice will become susceptible to infection and show severe disease progression if they are expressing human leukocyte antigen (HLA)-I (Flatz et al., 2010).

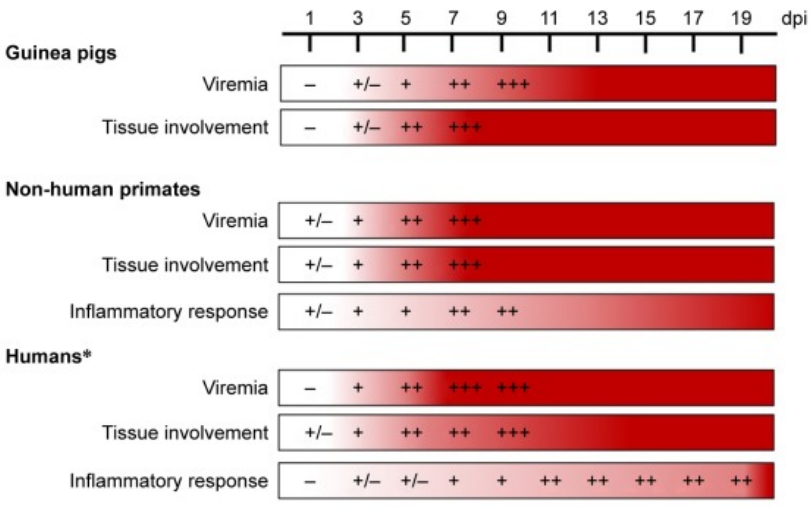

Figure 2.4. LF disease in humans and model animal species: Relevant features of disease are depicted in a time dependent manner. Guinea pigs and non-human primates replicate to a certain degree viremia, tissue involvement and inflammatory response. *in humans days post infection (dpi) refers to days post clinical manifestation and onset of symptoms. Adapted from (Warner, Safronetz, and Stein, 2018).

Therefore, guinea pigs and non-human primates (NHPs) have been used as model organisms for LF/LASV infection and can adequately replicate selected aspects of human disease **(Figure 2.4)** (Yun and Walker, 2012). Infection in guinea pigs is not always successful for all LASV isolates and pathogenesis develops differently than in humans

(Jahrling, Frame, Smith, and Monson, 1985; Walker, Wulff, Lange, and Murphy, 1975). NHPs are preferred over guinea pigs to mimic human infection. While it can be argued that NHPs are the gold standard animal model for LF disease (Warner et al., 2018), ethical and practical considerations make this model approach difficult.

Recently, an immune competent mouse model susceptible to infection and disease has been developed, and this model reproduces many key features of human LF (Oestereich, Lüdtke et al., 2016). Interferon (IFN)-I knock-out mice ($IFNAR^{KO}$) present with an IFN-I signaling deficiency. This strain has previously been shown to be susceptible to LASV infection. However, this strain lacks a competent immune response. Oestereich et al. demonstrated, that by irradiating this strain and transplanting wild type bone marrow progenitor cells, a model is generated in which the IFN-I signaling deficiency is limited to radioresistant cells (mostly stromal) and functional reconstitution of the hematopoietic system is observed ($IFNAR^{B6}$, referred to as “IFNAR chimeras”). These mice were also susceptible to infection with LASV; infection was characterized by lethal outcome, viremia, liver damage and edema (Oestereich, Lüdtke et al., 2016). In this chimeric model studies of the cellular immune response in an IFN-competent environment are possible (Lüdtke et al., 2017).

2.1.3 CURRENT AND FUTURE RELEVANCE

A RE-EMERGING INFECTION

While export of very few LF cases has occurred in the past, the highest risk for infection is limited geographically and the population at risk is mostly limited to rural areas in West Africa **(Figure 2.5)**, where close contact with the reservoir rodent species is common. It can be assumed that case numbers are underestimated due to both previous and current political conflicts that prevent disease surveillance and the lack of an established clinical management or diagnostic infrastructure in affected countries (Ii and Wohl, 2017). Laboratory research of LF is complicated and limited because the highest biosafety level is required to handle LASV. In recent years, an increase in incidence and severity of cases has been observed and reported by the World Health Organization (WHO) (World Health Organization, 2016). The largest outbreak hitherto, which far surpassed any recorded previous outbreaks, recorded 1,495 suspected cases and 376 confirmed cases and affecting more than 18 Nigerian states by 18 March in 2018 (Roberts, 2018; “WHO | Lassa Fever – Nigeria,” 2018). Consequently, when the WHO published its “Research and Development Blueprint” in 2016 to highlight emerging infections of importance, LASV was listed (Mehand, Al-Shorbaji, Millett, and Murgue, 2018; WHO, 2016). As such, affected countries have increased LF awareness

programs in recent years, heightening public preparedness and knowledge especially as a result of the 2018 outbreak.

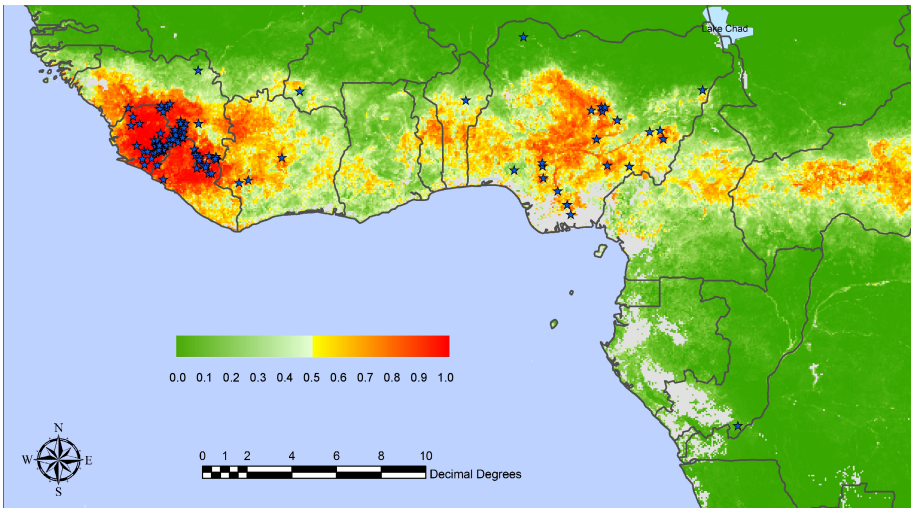

Figure 2.5. Risk map of West Africa. Risk of Lassa infection is indicated across West Africa (no risk = 0.0, high risk = 1.0) based on geography and weather patterns. Stars mark confirmed locations. Adapted from (Fichet-Calvet and Rogers, 2009).

TREATMENT AND VACCINE DEVELOPMENT

No LASV-specific treatment has been licensed for LF yet. Current treatment strategies rely mostly on supportive care and use of the drug ribavirin, which is a broad-spectrum antiviral. Ribavirin has been proposed to reduce mortality if administered in the early phase of disease (McCormick et al., 1986b), however its effectiveness at later stages is low. In addition, the side effects of ribavirin, in particular its liver toxicity, remain problematic (Günther and Lenz, 2004). Currently, there are no licensed vaccines available. However, the Coalition for Epidemic Preparedness and Innovations (CEPI) has declared LF as one of three diseases in which funding should be invested to move vaccine candidates into Phase III trials. Multiple strategies are being pursued to develop a successful vaccine candidate. Currently, the Vesicular Stomatitis virus (VSV)-LASV-GPC vaccine candidate appears to be the most promising (Yun and Walker, 2012; Fisher-Hoch et al., 2000). Also, under development and with documented protective efficiency in animal models are a recombinant Vaccinia virus vaccine expressing LASV NP and the re-assorted ML29 platform that uses the L-Segment RNA from the non-pathogenic arenavirus Morogoro (MORV) in combination with the S-Segment from LASV **(Figure 2.6)**.

Little work has been done on actual human patient material to investigate the human immune response to LASV further. Classically, for viral infections it is most often the cellular adaptive response of the immune system that is key, with viral clearance mediated through killing of

infected cells by cytotoxic T cells and NK cells (Koszinowski, Reddehase, and Jonjic, 1991; Paust, Blish, and Reeves, 2017). Unfortunately, the LASV-specific adaptive immune response in humans is currently still poorly understood. Few predictors of survival have been described. In order to further develop vaccine and antivirals it is therefore essential to understand the human immune responses to LASV, and their role in disease pathogenesis and survival.

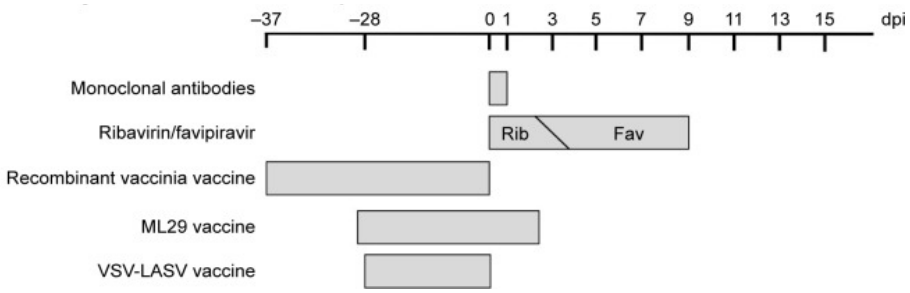

Figure 2.6. LF therapeutics and vaccines under development. Successful treatments and pre-clinical vaccine candidates are depicted with the time frame of their efficacy. Ribavirin and Favipiravir are useful in treatment after infection. A recombinant vaccinia vaccine, the ML29 vaccine and the VSV-LASV vaccine have shown protective capacity in animal models if administered at the indicated time points prior to infection. Adapted from (Warner et al., 2018).

2.2 PART II: IMMUNE RESPONSES TO LASSA VIRUS INFECTION

Every viral infection is a race between viral replication and the immune response of the host. Viral clearance and host survival depend strongly on the body's ability to mount not only an effective, but also a controlled immune response. Depending on the type of infection, multiple factors can be of relevance in determining outcome. The human immune system can be broadly divided into the innate and the adaptive arms. Innate immune responses serve to generate a first line of defense against pathogens, which is fast, robust and reliable. On the other side, the adaptive immune response comes into play later and generates a host-specific response that is highly accurate to match the specific characteristics of the invading pathogen and to develop lasting memory against it (Koszinowski et al., 1991; Koyama, Ishii, Coban, and Akira, 2008). Among the key cellular players of the innate response are macrophages and DCs.

DCs function as the bridge between the innate and the adaptive system and are referred to as antigen presenting cells (APCs). They process and present antigens of the detected pathogen to T cells, leading to activation of pathogen-specific immunity. The adaptive

response generally starts later after initiation of the innate response. Its aim is to generate pathogen-specific responses and lasting memory. It can be divided into two branches. The humoral anti-viral response relies on antibody production by B cells. These antibodies bind to free viral particles and can neutralize them or mediate their destruction by phagocytes, agglutination or the complement system. However, the cellular response, driven by $CD8^+$ cytotoxic T cells, can directly target infected cells. Effector $CD4^+$ T cells serve multiple purposes. T_H1 cells secrete IFN-γ, tumor necrosis factor (TNF)-β and various pro-inflammatory cytokines. This subset serves to initiate cell-mediated functions and activates cytotoxic T cell. The second subset, T_H2 secretes interleukin (IL)-4, IL-5, IL-6 and IL-10, which assists in the humoral response. Specifically, T_H2 cells function in B cell activation and class switching of the antibody response. A third important subset of T cells is comprised of regulatory $CD4^+$ T cells that can modulate and down regulate the inflammatory response through IL-10 and transforming growth factor (TGF)-β secretion. Cytotoxic $CD8^+$ T cells can be subdivided into either IFN-γ and TNF-α producing or IL-4 and IL-10 producing subsets. A subset of antigen-experienced T cells, either $CD4^+$ or $CD8^+$, will adopt a memory phenotype and remain in the body long term. These cells form the basis of the cellular immune memory, which allows fast response in case of secondary infection; memory T cells can revert to an activated effector state in the case of renewed antigen encounter. In the context of infection with LASV, both the innate and the adaptive responses are modulated by viral proteins.

2.2.1 THE INNATE IMMUNE RESPONSE IN LASSA FEVER

The aim of the innate anti-viral response is the prevention of viral replication and spread before the adaptive response can be initiated. The innate immune response relies on early and fast identification of foreign molecules in the system. To achieve reliable identification of such molecules, the body relies on recognizing evolutionary conserved “danger patterns” common across multiple pathogens, collectively referred to as pathogen associated molecular patterns (PAMPs). To recognize these PAMPs, cells of the local tissue environment and innate immune cells possess three main protein families called pattern recognition receptors (PRRs), that can recognize specific PAMPs (Koyama et al., 2008). These include the Toll-like receptor (TLRs), NOD-like receptors (NLRs) and retinoic-acid inducible gene (RIG)-I-like receptors (RLRs). In the case of viruses, common PAMPs to be recognized by these PRRs are double-stranded (ds)RNA or 5’-triphosphorylated RNA generated during viral replication; both structures do naturally not occur in the host cell (Marcus, Svitlik, and Sekellick, 1983; Marcus and Sekellick, 1977; Kim, Shin, and Nahm, 2016; Thompson and Iwasaki, 2008; Yoneyama et al., 2015; Loo and Gale, 2011).

After PAMPs are recognized, the signal is transduced through cellular adapter proteins, such as mitochondrial antiviral-signaling protein (MAVS) and IKKε, and induces the activation of multiple transcription factors, including interferon regulatory factor 3 (IRF3), IRF7 and nuclear factor kappa-light-chain-enhancer of activated B cells (NF-κB) (Ikushima, Negishi, Taniguchi, 2013; Oeckinghaus and Ghosh, 2009). These transcription factors then induce or increase transcription of type I IFN genes, inducing the type I IFN production. This pathway leads to engagement of the IFN receptor in infected and bystander cells which leads to the expression of IFN-stimulated genes (ISGs). This combats viral replication either through direct effects on viral replication or through changes in the infected cell or cells in the vicinity that counteract viral replication indirectly. These effects are strengthened by positive feedback loops in the signaling cascade (Haller, Kochs, and Weber, 2006). Additionally, upon PRR recognition, infected cells will release cytokines that can modulate and increase the adaptive immune response. Importantly, this will activate APCs. These cells take up pathogens or fragments thereof, process them and present antigens to effector cells, such as T cells, of the adaptive response. These cytokines can also influence adaptive effector cells directly and lead to activation and maturation of these cells.

To clear infection successfully, the above-described activation of the type I IFN response by LASV infected cells to activate the adaptive response is necessary. Mice lacking type I IFN receptors fail to control LASV infection and die (Yun et al., 2012; Oestereich, Lüdtke et al. 2016). In addition, in NHPs survival is characterized by an early type I IFN response, while IFN-α, an important type I IFN, appeared only shortly before death in fatally-infected animals (Baize et al., 2009). In a longitudinal study of one human patient, an early peak of IFN-α was observed and the kinetics of this cytokine expression correlated with viremia (McElroy et al., 2017).

However, a key feature of arenaviruses and LASV infection is the virus-mediated disruption of the innate immune system. In fact, type I IFN signaling is hindered by arenavirus infection (Meyer and Ly, 2016). Multiple mechanisms have been described through which the IFN response is affected by LASV. During LASV infection dsRNA is produced, which is involved in replication, transcription and translation. As it is not found in the host cell physiologically, dsRNA is a strong indicator of viral presences and induces innate immune signaling. Viral dsRNA would normally be recognized, as described above, as foreign through either the RIG-I-MAVS or the melanoma differentiation-associated protein 5 (MDA5)-MAVS pathway, activating IRF3 and IRF7, leading to the production of type I IFN and upregulation of ISGs (Koyama et al., 2008; Meyer and Ly, 2016). However, *in vitro* analyses have shown multiple functions of LASV Z protein and NP which inhibit sensing of dsRNA either directly or have

adverse impact on the signaling cascade downstream (Prescott et al., 2017) **(Figure 2.7)**. LASV Z protein has been demonstrated to inhibit RIG-1 and MDA5, which sense viral dsRNA, through binding to both proteins and preventing binding to the downstream adaptor MAVS. The LASV NP was shown to exhibit two functions in inhibiting sensing of viral dsRNA. First, an exonuclease activity is encoded into NP, which can degrade viral dsRNA that is not currently involved in viral functions, minimizing the pool of dsRNA which could be recognized by cellular receptors (Hastie, King, Zandonatti, and Saphire, 2012). In addition, NP was shown to prevent transcription factor IRF3 and NF-κB activation by binding IKKε (Pythoud et al., 2012). It has also been shown that LASV may use TAM receptors, AXL and TYRO3, for cell entry, which leads to upregulation of suppressor cytokine signaling proteins. This can also facilitate inhibition of the type I IFN response signaling (Hastie et al., 2017; Jiang et al., 2013). Consequently, if the innate response is adversely affected, this will also affect the adaptive response. However it remains unclear to which degree this effects disease outcome in humans, as these findings need to be further validated *in vivo* (Prescott et al., 2017).

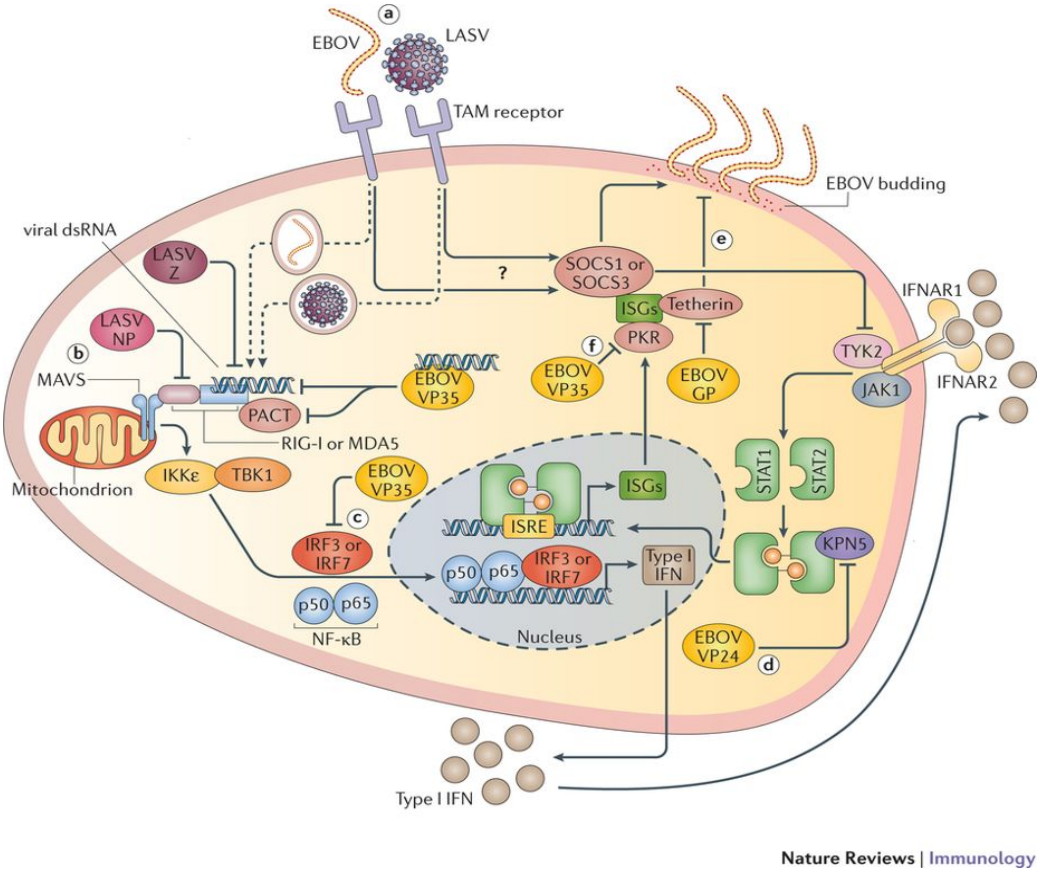

Figure 2.7. LASV interferes with type I IFN pathway. LASV proteins NP and Z interfere with the intrinsic cellular anti-viral upregulation of type I IFN production and ISGs. NP and Z negatively affect dsRNA sensing directly, through NP endonuclease activity, or indirectly through interaction with IKKε or RIG-1 and MDA5, respectively. Adapted from (Prescott et al., 2017).

2.2.2 THE HUMORAL IMMUNE RESPONSE IN LASSA FEVER

Evidence points towards the direction that the humoral immunity plays a minimal role during acute LF (Yun and Walker, 2012). While immunoglobulin M (IgM) and IgG antibodies against LASV exist in LF patients, their presence is not correlated with viral clearance or survival (Johnson et al., 1987). Neutralizing antibodies only appear late in disease and throughout convalescence (Jahrling, Frame, Rhoderick, and Monson, 1985). While some antibodies recognize LASV-specific epitopes, others have cross-reactivity against other arenaviruses (Ruo et al., 1991). Antibodies are generally targeted towards GPC, NP or the Z protein. An increase in antibody serum levels has been observed after viral clearance, even up to several months after convalescence (Günther et al., 2001; Lloyd et al., 1989; Ter Meulen et al., 1998). This may imply that residual viral replication still occurs, which facilitates low-level B-cell activation. Taken together, these data suggest that the role of the humoral response is less relevant throughout acute disease. As such, successful viral clearance must be achieved through cellular immunity and is therefore T-cell mediated.

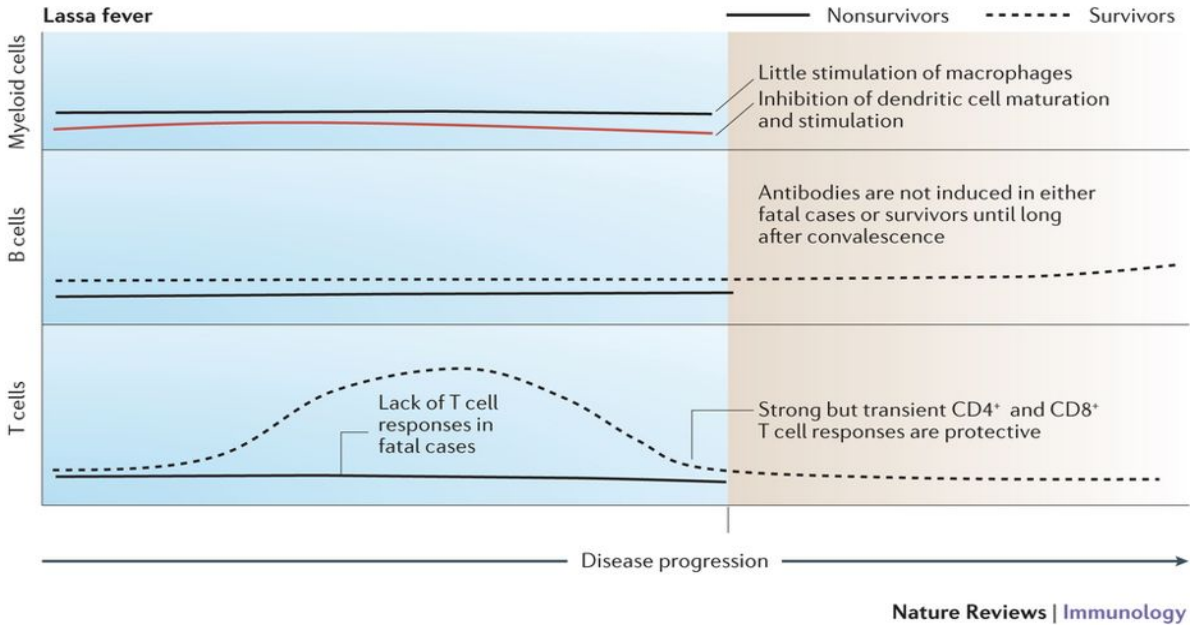

Figure 2.8. Development of Immune cell population throughout LF. Myeloid cells are adversely affected by infection with LASV and the activation capacity of T cells is deregulated. B cells fail to produce protective antibody responses throughout acute disease, but neutralizing antibodies appear after convalescence. This implies that T cells are vital to viral clearance and the lack of a T-cell response is often fatal. Adapted from (Prescott et al., 2017)

2.2.3 PRIMING OF THE CELLULAR IMMUNE RESPONSE IN LASSA FEVER

To understand the antiviral function of T cells and their role in specific infections it is important to understand the extensive selection process and maturation T cells go through to

ensure disease-specific responses that do not harm the host body. T cells first pass through stringent negative and positive selection in the thymus before they circulate freely between the bloodstream and lymphoid system. This selection is based on the expression of surface molecules needed to communicate with APCs and to recognize antigens presented on these cells as well as infected target cells. Key to this interaction is the variable T-cell receptor (TCR), which will recognize antigens that are presented in the context of MHC molecules **(Figure 2.9)**. In humans the MHC molecules are often referred to as human leucocyte antigens (HLA). Part of the TCR is the CD3 molecule, which allows identification of T cells by this marker. Furthermore, CD4 or CD8 molecules are present to facilitate MHC-TCR interaction. T cells undergo selection in the thymus to ensure they are functional and not autoreactive. The TCR consists of an alpha and a beta subunit, which are independently encoded in the genome. Both chains undergo genomic rearrangement, referred to as somatic diversification, during T-cell selection in the thymus. Diversity results from recombination of V, J and D segments at the genomic level. This generates a near endless supply of unique TCR clonotypes and only 1 in 10^5 naïve T cells will recognize any given antigen (Laydon, Bangham, and Asquith, 2015; Six et al., 2013). Only T cells that recognize self-MHC molecules on other cells (positive-selection), do react adequately and do not recognize self-peptides (negative-selection) will survive and exit the thymus. At this stage T cells are considered immature and naïve.

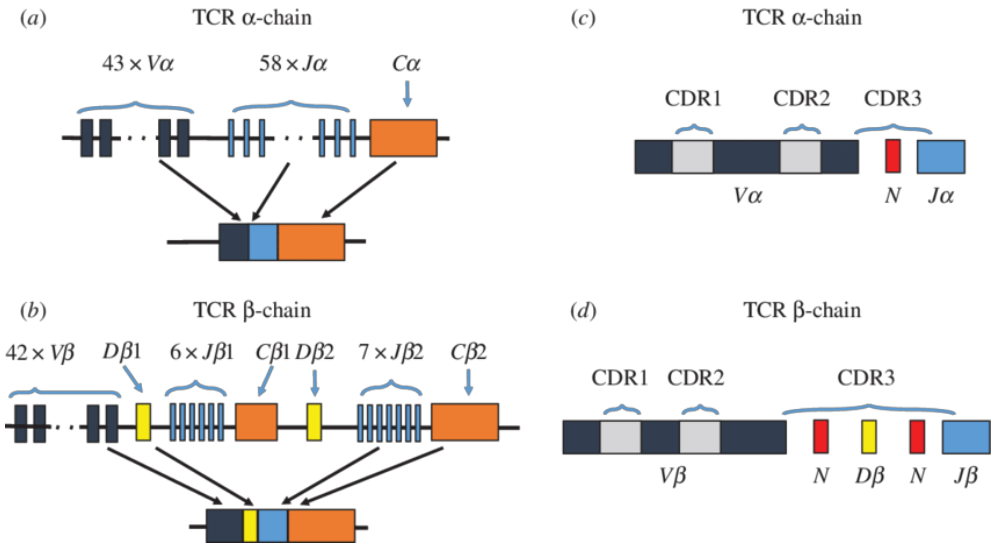

Figure 2.9: T-cell receptor. (*a/b*) Variable (*V*), joining (*J*) and constant regions (*C*) constitute both TCR chains, with an additional diversity (*D*) region only in the β-chain. Recombination of segments with additional nucleotide additions generates a rearranged TCR for each T cell. Hypervariable complementarity-determining regions (CDR1-CDR3) of the α-chain (*c*) and β-chain (*d*) are depicted, indicating that most variable CDR3 region straddles the *V*(*D*)*J* junction. Adapted from (Laydon et al., 2015).

In order to present antigens to naïve T cells and initiate an adaptive response APCs, such as DCs, take up extracellular pathogens through phagocytosis. This mechanism also allows the uptake of viral particles or cell debris containing viral proteins. Intracellular pathogens, such as LASV, may also infect those cells directly. Pathogens are transported through the cell in vesicles and fusion with a lysosome allows the particles to be digested. Processing of antigens by APCs follows either the endogenous (antigen found inside the cell) or the exogenous pathway (antigen taken up by the cell). Antigens then bind to MHC I or II molecules, respectively. These complexes are transported to the cell surfaces. In the specific case of viruses, it is possible that viral proteins synthesized by the infected cell can be degraded and loaded onto MHC I molecules. APCs migrate from the tissue where they encountered the pathogen to the corresponding draining lymph node, where activation and maturation of T cells is initiated. Naïve T cells circulate through the blood and lymphoid system. Only when they enter and temporarily reside in lymphoid organs such as lymph nodes and the spleen, encounter with antigens presented by APCs is possible. Cells will mature and differentiate only if they encounter antigen.

Cells of the myeloid lineage, such as monocytes, macrophages and DCs, are among the first cells infected with LASV and are thought to play a role in viral spread by carrying virus into the lymphoid organs (Prescott et al., 2017). An important consequence of LASV infection of these myeloid cells is the resulting immune suppression **(Figure 2.10)**.

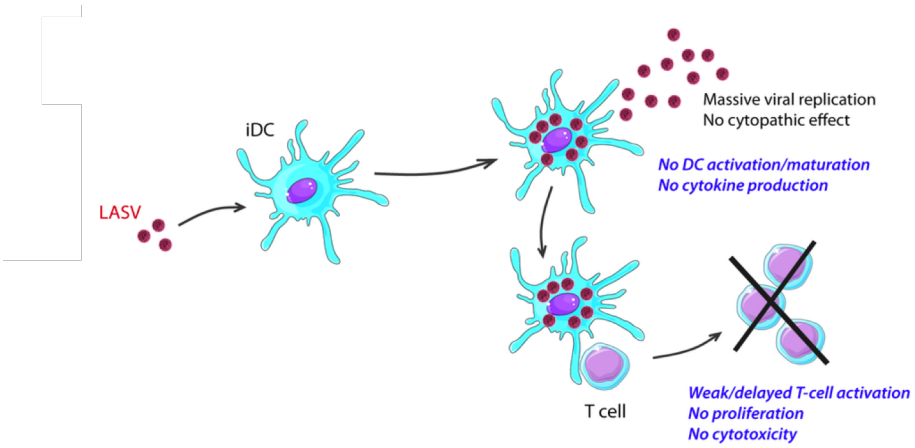

Figure 2.10: LASV infection of DCs. Infection of DCs by LASV leads to viral replication and no cytopathic effect. However, DC maturation and activation is adversely affected, and no cytokine production is observed. This leads to a lack of T-cell activation with decreased T-cell proliferation and cytotoxicity *in vitro*. Adapted from (Russier, Pannetier, and Baize, 2012)

Infection of human monocyte derived DCs (moDCs) and macrophages, both important APCs that are vital for the induction of a T cell-mediated response, functionally impairs these cell types (Schaeffer et al., 2018). Contrary to expectation, no activation of these APCs was observed, and no pro-inflammatory cytokines were released. Additionally, CD40, CD80 and CD86, co-stimulatory molecules required for proper APC-T-cell interaction were not upregulated on the cell surface of the APCs (Baize et al., 2004). This suggests, that also the T-cell response might be adversely affected.

2.2.4 THE CELLULAR IMMUNE RESPONSE IN LASSA FEVER

ACUTE RESPONSES

T-cell activation and maturation is initiated after interaction between the TCR and the MHC complex loaded with a peptide antigen. As described above, T cells are broadly divided into $CD4^+$ helper cells and $CD8^+$ cytotoxic cells. $CD4^+$ T cells require interaction with peptides presented in the context of MHC II, while $CD8^+$ T cells require presentation in the context of class I MHC complexes. This facilitates their proliferation and differentiation into effector and memory phenotypes. For activation, classically two signals are necessary. First, the antigenic peptide in the MHC complex must bind to the TCR-CD3 complex on the T cell. Second, unspecific co-stimulation through interaction of surface markers CD28 (T cell) and B7 proteins (APCs) must be present. B7 may also bind to cytotoxic T-lymphocyte-associated protein (CTLA)-4, which acts antagonistically to CD28. Anergy is induced if the second signal is missing. B7 and CD28 also induce IL-2 production and clonal expansion. Depending on the co-stimulatory background, the chemokines and cytokines present in the milieu during T-cell priming, both $CD4^+$ and $CD8^+$ naïve T cells can turn into multiple effector type subsets with variable memory capacity **(Figure 2.11)**. Naïve T cells can turn into short-lived effector T cells (T_{eff}) expressing CD45RA or into long-term effector memory T_{EM} cells. Generally, T_{eff} cells only have a limited lifespan of a few weeks (Farber, Yudanin, and Restifo, 2014).

Evidence suggests that survival of LF is linked to a successful cellular T-cell response. Experiments in NHPs, in particular in *Cynomolgus* monkeys, demonstrated that surviving animals had higher levels of activated T cells compared to those with fatal outcome (Baize et al., 2009). In NHPs, fatal outcome was associated with reduced expression of CD25 and CD69, markers for activation on effector T cells (Warner et al., 2018), T-cell proliferation and cytokine production. Only recently, a detailed study of the human response to LASV infection showed that the T-cell chemoattractants RANTES and CX3CL1 were upregulated during acute infection, and granzyme B, a T-cell effector cytokine, was found early on (McElroy et

al., 2017). The same authors also found that robust T-cell responses were characterized by a peak in activation of $CD4^+$ T-cell responses at day 14 post-onset. Furthermore, $CD8^+$ T cells presented a first response peak corresponding to viral clearance and a second at day 23 post-onset. This activation profile was accompanied by the upregulation of the proliferation marker Ki67 as well as degranulation. Furthermore, these $CD8^+$ T cells showed an overall effector-like phenotype with low BCL-2 and CD45RA expression but high PD-1 expression. The strongest LASV-specific $CD4^+$ T-cell response was observed at 20 - 30 days post-onset, while the $CD8^+$ T-cell response was strongest during convalescence (McElroy et al., 2017).

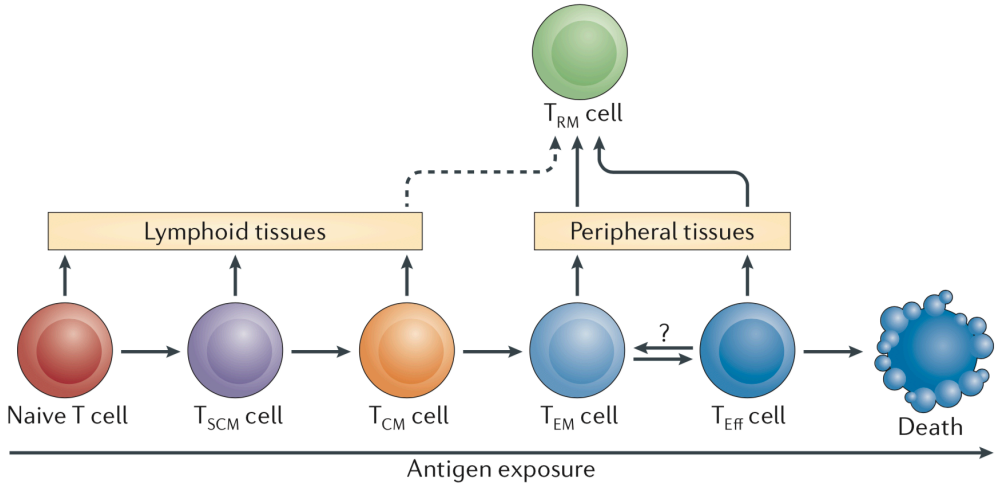

Figure 2.11: T-cell effector and memory subsets. Naïve T cells can change their phenotype after antigen encounter and turn into stem cell memory (SCM), central memory (CM), both of which circulate to the lymphoid tissue, or into short lived effector (Eff) or effector long-lived effector memory (EM) cells, which circulate to the periphery. Resident memory T cells (RM) can originate from effector, effector memory and central memory T cells. One naïve T-cell clone can give theoretically rise to all antigen-experienced subsets, which allows for an imminent effector response in addition to peripheral and central memory retention of the antigen. Adapted from (Farber et al., 2014).

Generally, activated effector-type $CD8^+$ T cells can induce apoptosis of the infected target cell through release of cytotoxic granules, in addition to the release of cytokines. The induction of apoptosis relies on perforins, which enables the uptake of these granules into the target cell, as well as granzymes and granulysin. TNF-α release also aids in the induction of apoptosis. IFN-γ induces an anti-viral state in surrounding cells. Importantly, it can also increase the efficacy of the $CD8^+$ response (Randall and Goodbourn, 2008; Rosendahl Huber, van Beek, de Jonge, Luytjes, and van Baarle, 2014). LASV-specific $CD8^+$ T cells appeared at day 10 post infection and also showed effector phenotype but were found at low frequency. Functionally, McElroy et al. demonstrated that LASV-specific T cells were able to

respond to LASV with production of TNF-α, IFN-γ and degranulation with granzyme B (McElroy et al., 2017).

CELLULAR IMMUNE MEMORY AFTER LASSA FEVER

A subset of T cells can further differentiate into a central memory T_{CM} phenotype that regains antigen experience but primarily circulates in the blood and secondary lymphoid organs. In the context of LF a strong $CD4^+$ T-cell memory response, mostly directed against epitopes of NP, was found in a seropositive human cohort (ter Meulen et al., 2000) Furthermore, LF survivors that presented no evidence of seroconversion still did not develop LF after reinfection, which implies that a memory cellular response is protective (Warner et al., 2018).

To establish effective immune surveillance, topographic memory formation must occur on local antigen experienced resident T cells that remain in the tissue long-term. Especially in barrier systems such as the skin, gut, respiratory tract and female genital mucosa (Gaide et al., 2015; Schenkel and Masopust, 2014; Thome et al., 2014; Watanabe et al., 2015), effective local immune surveillance and response memory are key. Colonization of these barrier tissues with resident T cells has been described for other viral infections and resident T cells are able to trigger both successful innate and adaptive responses in response to recurring infections (Ariotti et al., 2014; Schenkel et al., 2014).

IMMUNOPATHOGENESIS IN LASSA FEVER

Severe tissue damage is observed in fatal human LF cases after autopsy. It is assumed that host immune responses play a role in generating these pathological findings. As a consequence of LASV infection, a pro-inflammatory IFN−γ and TNF-α−mediated cytokine storm, similar to what is observed during septic shock, is hypothesized to contribute to fatal outcome (Gunther, 2000). However, this study relied on observation made on one fatal human case relocated to Germany for treatment and supporting evidence could not be verified in subsequent studies in all fatal patients, which implies that IFN-γ and TNF-α are either only upregulated in a subset of fatal cases or in a time-dependent manner (Yun and Walker. 2012; Mahanty et al.. 2001). Secondly, the above-described effects of LASV infection on DCs and macrophages may contribute not only to a malfunctioning T-cell activation but also to overall immunosuppression. While these studies only demonstrated downregulation of immune responses *in vitro* this observed suppression was supported by the observation that circulating levels of IL-8 and IFN inducible protein (IP)-10 were decreased in fatal patients during acute LF in humans *in vivo* (Mahanty et al., 2001).

Some studies have highlighted the potential role of T cells in pathogenesis. Results from NHP experiments and analysis of tissue-specific histopathology and immunity imply that that the adaptive response is negatively affected after LASV infection (Yun and Walker, 2012). Importantly, it has been shown in mice that a mouse strain which expresses the human MHC-I complex fails to survive LASV infection, while the depletion of T cells during LASV infection has been shown to prevent disease in mice (Flatz et al., 2010). These authors also demonstrated that LASV-specific T cells contributed to disease through macrophage activation. As a consequence, they observed cell-mediated inflammatory reactions and damage to secondary lymphoid organs (Flatz et al., 2010). This could suggest, that while T cells play an important part in viral clearance, if this fails a dysfunctional response or inadequate activation may be causative of damage instead.

If T-cell-mediated pathogenesis occurs in LF, then infiltration of T cells into tissues could play a key function. During the course of infection T cells can leave the blood flow through extravasation and infiltrate into inflamed tissues and organs. Site-specific extravasation is mediated by the expression of so-called homing markers on the surface of T cells matched to receptors primarily expressed on the endothelial cells of target tissues. This allows accurate infiltration of T cells and killing of infected tissue cells but may also be cause of tissue damage. While T cells are highly suspected to influence LF pathogenesis, T-cell homing and expression of tissue-specific signatures has not been investigated in the context of LF. Understanding these critical aspects of T-cell immunity in the context of LF could not only help increase our understanding of T cell-mediated pathology but such signatures could then also potentially server as biomarkers of pathology or inform future vaccine strategies by allowing better direction of the T-cell responses induces by said vaccines.

2.3 PART III: T-CELL HOMING

2.3.1 POSTCODES OF THE IMMUNE SYSTEM

While some viral infections, such as Human Immunodeficiency virus (HIV), infect circulating immune cells, many other viruses target cells found also in specific organs and tissues. Consequently, it is necessary for cells of the immune system to leave the blood stream or lymphatic system to facilitate an immune response at any given site in the body. The mammalian immune system is able to control infections and provide constant surveillance by allowing cells, including T cells, to re-circulate between blood or secondary lymphoid organs and other body tissues when required. This extravasation is a multi-step process of adhesion

steps that allows cells to leave the blood stream even under hemodynamic flow **(Figure 2.12)** (Sackstein, Schatton, and Barthel, 2017).

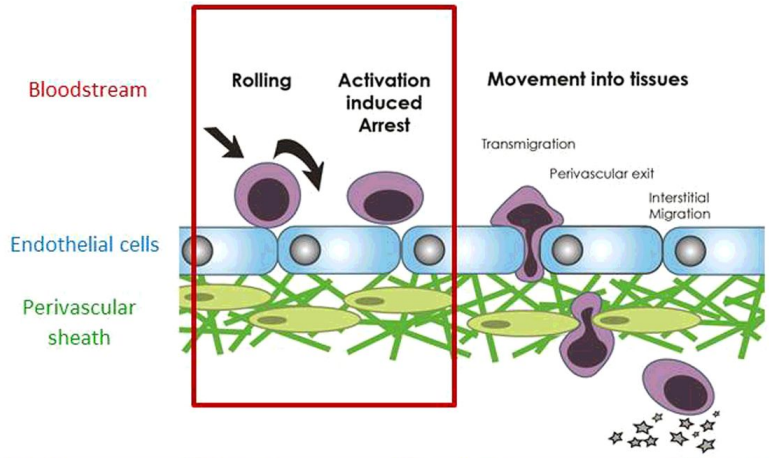

Figure 2.12: Lymphocyte extravasation. T cells are able to leave the blood stream and migrate into organ tissues. This process is multi-step. The receptors and ligands involved in rolling, activation and arrest of T cells may be referred to as a "homing address" or "homing signature" (red box). Adapted from (Ager, Watson, Wehenkel, and Mohammed, 2016)

The mechanistic steps necessary to securely adhere T cells to the endothelial layer against hemodynamic pressure and allow transmigration into organ tissues are well described. Key molecules in this process are tissue-specific selectins, integrins and chemokine receptors expressed on the T-cell surface. Transmigration of T cells can be divided into 4 steps: rolling, tethering, activation and arrest. First, lymphocytes will "roll" along the epithelial cell layer lining the blood vessels. Selectins expressed on the surface of lymphocytes promote adhesion of T cells to endothelial cells and enable their deceleration against the blood flow. Tethering is facilitated through the interaction of multiple surface molecules expressed on both lymphocytes and endothelial cells. Once cells are attached to the endothelial layer, chemokine receptors on T cells will allow chemokine-mediated signaling, which increases integrin activation and induces a conformational change in these migrating cells. This chemokine-mediated signaling is milieu-specific. Tissue or endothelial-derived chemokines are bound to the endothelial surface and encountered by the rolling T cell (Marelli-Berg, Cannella, Dazzi, and Mirenda, 2008; Rot and von Andrian, 2004). T cells tether to the endothelial cells and "arrest". After T cells stick to the endothelial layer, they then migrate laterally until a potential exit is located. Transmigration occurs as cells then move through the endothelial layer and exit the perivascular sheath. Once passed through this layer, interstitial migration within the organ tissue is possible (Bromley, Mempel, and Luster, 2008; Förster, Davalos-Misslitz, and Rot, 2008).

While some cell surface molecules are ubiquitously expressed throughout all organs systems, others are only present on epithelial cells belonging to specific tissue compartments. The complexity of the ligands and receptor molecules involved in this process collectively make up the “homing signature” of each T cell. When T cells undergo transformation from naïve to mature phenotype, they acquire multiple surface markers that allow for organotropic targeting of their effector function. T cells will express different “homing signatures” depending on multiple factors. Similar to a postal code, different and distinct homing addresses exist depending on activation status, inflammatory status and tissue-specificity of the T cell. Simplistically, these postal codes are a three-digit code comprised of a combination of one selectin, one chemokine receptor and one integrin molecule (Sackstein, Schatton, and Barthel, 2017).

2.3.2 HOMING IN INFECTION AND DISEASE

To date, homing markers and their impact on disease have been studied primarily in the context of cancer, but T cells with distinct homing signatures have also been described for viral infections (Rott et al., 1997; Jiang et al., 2008; Rivino, 2018; Mikhak, Strassner, and Luster, 2013). Interestingly, in the context of infectious diseases, viral infections in particular, looking at the T-cell homing profile during acute infection and at homing molecules expressed on memory T cells can provide information about the primary site of antigen encounter and organ tissues of immunological relevance or sites of persistent infection. Hypothetically, the route of transmission may even be extrapolated from the T-cell homing signature.

HOMING OF NAÏVE T CELLS TO SITES OF ANTIGEN PRESENTATION

In the search for their antigen naïve T cells circulate though the body via the intricate blood and lymphatic systems, through which they can reach secondary lymphoid organs such as the spleen and a multitude of lymph nodes spread throughout the body where antigen presentation by DCs can occur. They enter these secondary lymphoid organs in specialized postcapillary high endothelial venules (HEVs). The first steps of adhesion are mediated by glycan dependent receptor ligand binding. Specifically, for naïve T cells to enter secondary lymphoid tissues they require the expression of L-selectin (CD62L), which can bind to different ligands expressed on HEVs. These peripheral lymph node addressins are a family of sialylated mucins (Girard, Moussion, and Förster, 2012; Miyasaka and Tanaka, 2004; Rivera-Nieves et al., 2006). This binding allows naïve T cells to roll along the apical surface of the blood vessels. For lymphoid-tissue-specific homing, chemokine-mediated signaling

and integrin activation is mediated through the CC-chemokine receptor 7 (CCR7) expressed on the T cell. The activation of T-cell leucocyte function associated molecule (LFA)-1 ($\alpha L\beta 2$ integrin) is followed by binding of LFA-1 on T cells to intercellular adehesion-molecule-1 (ICAM-1) and ICAM-2 on endothelial cells (Fu, Ward, and Marelli-Berg, 2016; Marelli-Berg et al., 2008; Miyasaka and Tanaka, 2004). Strong arrest is facilitated by conformational changes of LFA-1. Once inside the lymph node, upregulation of chemokine receptors CCR4 and CCR5 allows naïve T cells to migrate towards DCs. (Griffith, Sokol, and Luster, 2014). As such, the three-digit code found on T cells required for lymphoid homing is comprised of CD62L, CCR7 and LFA-1.

Expression of tissue-specific homing markers is induced through the interaction of naïve T cells with DCs. This priming and imprinting process of T cells occurs in draining lymph nodes. Each organ system contains a lymph drainage system that is connected to select specific lymph nodes (Swartz, Hubbell, and Reddy, 2008). Specific mechanisms exist that allow for differential priming of T cells in order to retain their tissue-specific memory and preferred recirculation into the organs and tissues connected to the lymph node. DCs imprint on their cognate T cells a topographical memory of the original organ where the DC took up the antigen (Fu, Wang, Mauro, and Marelli-Berg, 2013). A tissue-specific imprinted homing signature will statistically enhance the likelihood that mature T cells will encounter their specific antigen again as they will preferentially return to the site of viral replication. However, not all aspects that determine this imprinting process are fully understood. Especially for viral infections of the intestine, the skin and the lung specific imprinting has been described.

TISSUE-TROPIC HOMING OF ANTIGEN-EXPERIENCED T CELLS

Antigen-experienced T cells preferentially migrate to inflamed tissues in order to clear the invading pathogen. To retain these cells within inflamed tissue, CD62L expression is lost through shedding and CCR7 expression is downregulated. T_{eff} cells will thus be prevented from recirculating and traveling back to uninflamed secondary lymphoid organs (Fu et al., 2013, 2016). However, as described, mature T cells are also imprinted during antigen presentation with a homing signature matched to the site of first antigen encounter. Gut homing signatures are comprised of α4β7 integrin and CCR9, which determine T-cell trafficking to the lamina propria **(Figure 2.13**).

α4β7 integrin binds to the mucosal addressin cell adhesion molecule 1 (MadCAM-1). This ligand is specifically expressed in HEVs located in intestinal tissue. CCR9 recognizes CC-chemokine ligand (CCL)25, a chemokine preferentially expressed by epithelial cells of the

intestine. It follows, that enteric viral infections that follow oral infection are characterized by expression of intestinal homing markers on antigen experienced T cells. It has been shown that rotavirus-specific $CD4^+$ T cells are characterized by a gut-homing phenotype (α4β7 $integrin^+$, $CCR9^+$) during acute infection (Parra et al., 2014; Rott et al., 1997). T-cell priming in the mesenteric lymph nodes is promoted through retinoic acid (RA), an vitamin A derivative (Gorfu, Rivera-Nieves, and Ley, 2009; Dzutsev et al., 2017; Mwanza-Lisulo et al., 2018; Zeng et al., 2013). In this context it was also shown that RA plays a role in induction of virus-specific T-cell migration to the intestine in swine after inoculation with gastroenteritis virus (Chen et al., 2016).

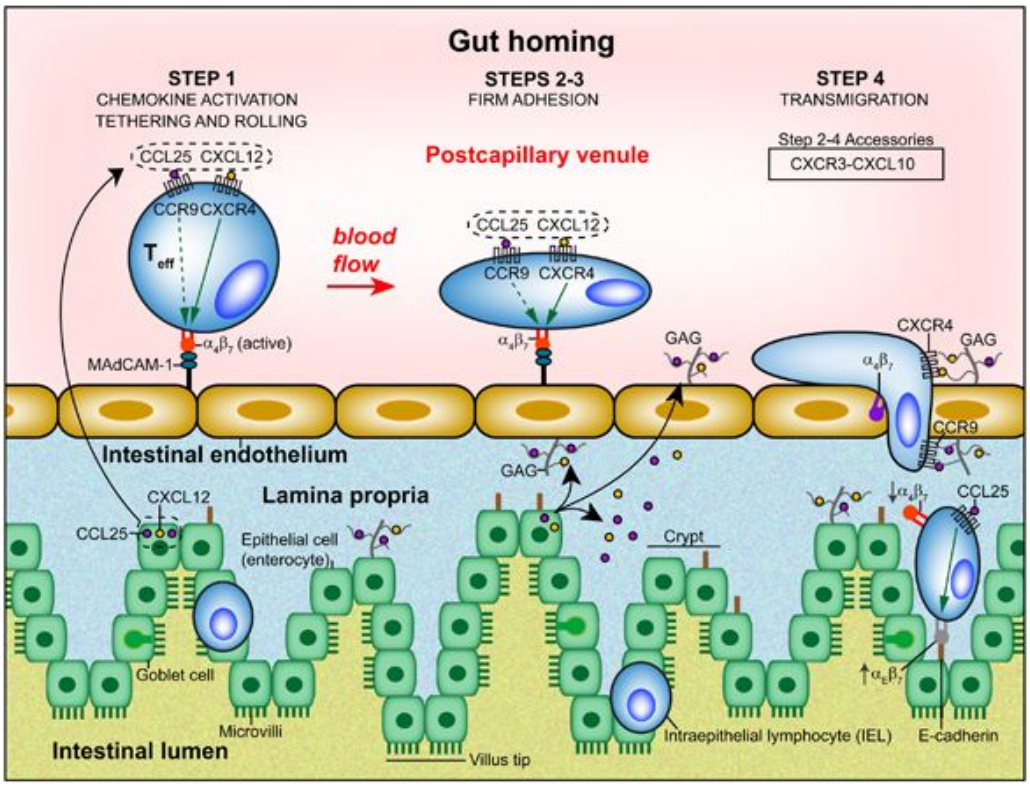

Figure 2.13: Gut homing. The first step of adhesion and tethering of gut-homing T cells to intestinal endothelium is mediated by binding of α4β7 integrin to MadCAM-1 of HEVs of the lamina propria. CCL25 and CXCL12 are produced by epithelial cells of the lamina propria and secreted into the blood stream, which allows binding to CCR9 and CXCR4 on the tethered T cell. This leads to activation of the integrin and firm adhesion of the T cell (step 2-3). Transmigration (step 4) is assisted by CXCR3 and CXCL10. Adapted from (Sackstein et al., 2017).

T-cell homing to the skin has also been well described. T cells with a skin-specific homing signature express cell-surface carbohydrate epitope cutaneous lymphocyte antigen (CLA) (Santamaria Babi et al., 1995) which interacts with E-selectin on dermal endothelium (Santamaria Babi et al., 1995). CCR4 and/or CCR10 are the chemokine receptors relevant to skin-homing both in steady-state conditions and during inflammation (Baekkevold et al., 2005; Kunkel et al., 2002; Reiss, Proudfoot, Power, Campbell, and Butcher, 2001). It has

been demonstrated that skin-tropic viruses induce T-cell homing to the skin. CCR10 expression has been shown on circulating human herpes simplex virus (HSV)-specific $CD8^+$ T cells, while CLA expression was shown on circulating $CD4^+$ T cells in humans (González et al., 2005; Hensel et al., 2017; Koelle, Huang, Hensel, and McClurkan, 2006). In Dengue virus infection, homing of dengue-specific T cells to the skin and expression of CLA was demonstrated during natural human infection (Rivino, 2018; Rivino et al., 2015).

Other organ tissues and their specific T-cell homing signatures are not understood as clearly as the skin and intestinal system **(Figure 2.14)**. CCR3 and CCR4 have been found to play a function in T-cell homing to the lung. Mucosal airways express the CCR3 ligand CCL28, as well as the CXCR4 ligand CXCL12 (Campbell, et al., 2001; Danilova et al., 2015; Mikhak et al., 2013). Additional markers used in the homing pathway to the bronchus-associated lymphoid tissue include L-selectin/peripheral lymph node addressin (PNAd), $\alpha4\beta1$-integrin/vascular cell adhesion molecule (VCAM)-1 and LFA-1 (Xu et al., 2003). For the respiratory infection with influenza virus it has been demonstrated that T cells imprinted by DCs in the lung and expressing CCR4 were most protective (Mikhak et al., 2013). Influenza A H7N9 specific-T cells were reported months after infection to express respiratory mucosa associated homing signatures (Zhao et al., 2018) and adoptive transfer experiments in mice have shown that lung homing properties rather than frequency is crucial for protection (Cerwenka, Morgan, and Dutton, 1999). Lung specific DCs have been shown to induce CCR4 expression on T cells in the context of influenza infection (Mikhak et al., 2013). In addition, also antigen presentation by lung DCs in lung-draining lymph nodes was shown for respiratory syncytial virus (Lukens, Kruijsen, Coenjaerts, Kimpen, and van Bleek, 2009).

Multiple studies have implicated CCR5 to be involved in liver specific homing (Grant, Lalor, Salmi, Jalkanen, and Adams, 2002; Kunkel et al., 2002). T-cell homing to the heart has been described to also include expression of CCR5 and CXCR3, as well as hepatic growth factor (Fu et al., 2016; Sackstein et al., 2017). Homing to the female genital tract has been shown to include CCR5, CXCR6, CCR2, and CD11c, though not exclusively (Qualai et al., 2016). $\alpha4\beta1$ integrin has also been shown to be highly relevant in genital tract infections (Davila, Olive, and Starnbach, 2014). Additionally, also homing to the brain, the bone marrow, the conjunctiva and testis have been investigated, though the defining signatures are poorly understood (Ntranos et al., 2019; Samaha et al., 2018; Goedhart et al., 2019; Davila, Olive, and Starnbach, 2014; Qualai et al., 2016; Fu et al., 2013).

While effector subsets lose expression of CCR7 and CD62L after antigen encounter, both markers are retained on the cells of the central memory compartment. This allows for the preferential recirculation of these cells to secondary lymphoid organs (Griffith et al., 2014). In addition, T_{CM} cells are able to traffic into specific tissues and may present a tissue-specific signature. However, in comparison to classical effector T cells, their tissue trafficking potential is limited and the expression of homing signatures less distinct (Fu et al., 2013; Griffith et al., 2014).

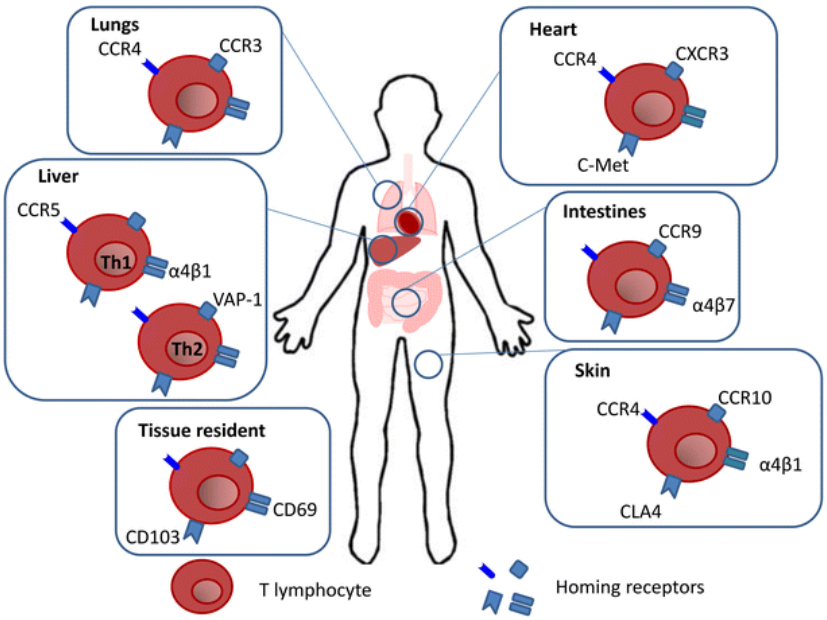

Figure 2.14: Homing receptors and organotropism. Previously described homing markers and their expression on T cells are shown for lung, heart, liver, intestine and skin. Additionally, residency markers are depicted. Adapted from (Fu et al., 2016)

T-CELL HOMING MARKERS IN DIAGNOSTICS AND THERAPY

While T-cell homing allows an effective T-cell response during acute infection as well as the formation of a successful defense against reinfection, this mechanism can also serve as a tool to investigate other aspects of disease, treatment options and vaccination strategies. Interestingly, some homing markers have been implicated as biomarkers of disease. CCR5 and CCR4 positive $CD4^+$ T cells in cutaneous psoriasis are associated with systemic inflammation (Sgambelluri et al., 2016). CLA has been suggested as a biomarker for atopic dermatitis (Czarnowicki, Santamaria-Babí, and Guttman-Yassky, 2017). CCR4 has also been investigated as a marker for latent and active tuberculosis management, though only in combination with CD27 (Gonzalo-Asensio et al., 2019). In the context of HIV infection $\alpha4\beta7$ integrin is thought to be a biomarker for intestinal microbial translocation and disease severity (Abad-Fernández et al., 2015). Also, in Ebola virus disease (EVD), $\beta7$ integrin expression has been linked to fatal outcome in humans (Speranza et al., 2018).

Antibody treatment to inhibit the expression of selected homing markers has also been employed for multiple different diseases. Especially integrins have been investigated as therapeutic targets (Cox, Brennan, and Moran, 2010). Use of the antibody Natalizumab is an effective strategy to combat multiple sclerosis. It acts by binding to β1 integrin on T cells, which modulates their brain homing capacity (Bauer et al., 2009). Also, chemokine receptors have been under investigation as treatment targets. The potential of CCR4-minibody gene transfer for treatment of skin cancers has been explored (Han et al., 2012). Hypothetical immunomodulatory targets for treatment also include active DNA methylation that is responsible for the increased or decreased expression of homing markers. Fumarates have been described to target the metabolic-epigenetic interplay in CCR6 brain-homing T cells in multiple sclerosis (Ntranos et al., 2019). RA was used to modify the response to generate effective T regulatory cells (Candia et al., 2017).

Modulating the homing capacity and signatures of T cells has also been considered as a means to increase the vaccination efficiency. T-cell homing signatures act as key factors required for a successful immune response during an acute infection and for tissue-specific memory formation. Generally, the generation of T_{RM} is also infection-route dependent, which can affect their protective capacities. Homing to preferred tissues facilitates formation of resident subsets that can protect against reinfection. This was shown in one study of Listeria infection in mice whereby oral infection with Listeria generated an enhanced resident T-cell population compared to other routes or infection (Sheridan et al., 2014). It has been shown that resident $CD8^+$ T cells in the lung are vital for protection against influenza virus (Wu et al., 2014). Vaccination-induced resident $CD8^+$ T cells have been shown to provide protection against melanoma in the skin (Gálvez-Cancino et al., 2018). Additional mucosal adjuvant treatment has been tried in order to elicit stronger lung-homing potential and localized responses induced by an live-attenuated influenza vaccination by increasing the potential of lung-priming DCs (Pérez-Girón et al., 2014). The benefits of additional RA treatment on oral vaccinations have also been investigated in order to increase gut homing potential (Mwanza-Lisulo et al., 2018) and for modulation of overall T-cell immunity (Bono et al., 2016).

While most treatment studies have focused on cancer or neurodegenerative diseases, potential to apply similar strategies also to treatment of viral infections exists. In the context of vaccine development, it has been shown, that detailed understanding of T-cell homing can increase vaccine success against viral infections. It can be hypothesized that, if homing signatures exist in LF, similar strategies may be employed to inform future treatment or vaccine development.

3 AIM OF THIS THESIS

The relationship between T-cell immunity and LF pathophysiology is poorly understood. Our current understanding of the role of T cells in LF relies on *in vitro* work and studies in animal models, but data from human Lassa fever is scarce.

The goal of this thesis is to characterize the role of T-cell immunity in recovery from LASV infection and its putative role in LF pathogenesis. In particular, three specific goals will be addressed:

1- Determine the putative role and response of LASV-specific and unspecific T cells in LF pathogenesis
2- Evaluate the relationship between T-cell homing and pathogenesis and transmission of LF
3- Explore the biological relevance of these findings in a dedicated animal model

To meet the first two goals, clinical immunological studies will be conducted on a hospital-based acute Lassa fever cohort in Nigeria during the 2017/2018 seasonal epidemics. These studies will combine immune assays done in the field with multiparametric analyses of samples performed in the BSL-4 laboratory at the Bernhard-Nocht-Institute for Tropical Medicine. To achieve the third goal, T-cell signatures will be also investigated *in vivo* in a susceptible immunocompetent mouse model. Finally, to put our putative findings in an epidemiological context with relevance for public health, a questionnaire-based epidemiological study of the risks associated with exposure of patients to LASV infection will be conducted.

The ultimate goal of this study is to provide a framework on the role of T-cell homing signatures in LF, their relevance as biomarkers, their putative use for vaccine design and therapeutics and their potential to inform about routes of LASV transmission.

4 RESULTS

4.1 CONTEXTUALIZATION OF A HUMAN LASSA FEVER PATIENT COHORT

While each year an estimated 300,000 cases of LF occur in endemic West African regions, it has proven challenging to conduct immunological research in humans. Affected countries suffer from political unrest and limited healthcare capabilities to support patient management and follow-up. Study sites equipped with the necessary biosafety and containment equipment are difficult to establish. This thesis was possible due to a collaborative project initiated in 2007 by Prof. Stephan Günther (BNITM) and the Irrua Specialist Teaching Hospital (ISTH) in Edo state, Nigeria. ISTH functions as a countrywide reference lab for LF diagnostics and is equipped with a Lassa treatment ward. For the work presented in this thesis we were able to set up a hospital-based acute patient pathogenesis study. Under the ethical framework of this study, immunological studies were performed and information on patient epidemiological data and disease progression was collected. In total, 242 confirmed LASV-positive patients were recruited and followed throughout the acute phase of disease for the purpose of this study between January 2017 and April 2018.

4.1.1 COHORT DESCRIPTION: DEMOGRAPHICS AND CLINICAL MANIFESTATIONS

To provide clinical and epidemiological context the patient cohort recruited was first characterized demographically. After informed consent was given, patients were asked to provide information including place of residence, gender, age and occupation. In total, 146 patients agreed to provide information. The majority of patients hospitalized at ISTH were from Edo state. **(Figure 4.1 A)**. The majority of patients enrolled in the study were male (62 %) **(Figure 4.1 B**). Age distribution ranged from <10 years to 75 years of age. The age distribution was unequal between age brackets with one third of patients (33 %) aged between 21 and 30 years of age **(Figure 4.1 C)**. The majority of patients reported to be students (44 %), which included training jobs and non-permanent employment. Few patients were from the agricultural sector (6 %), clergy (4 %) and healthcare (7 %), occupations we hypothesized to have increased chances of contact with rodents or risk of human-to-human transmission **(Figure 4.1 D)**.

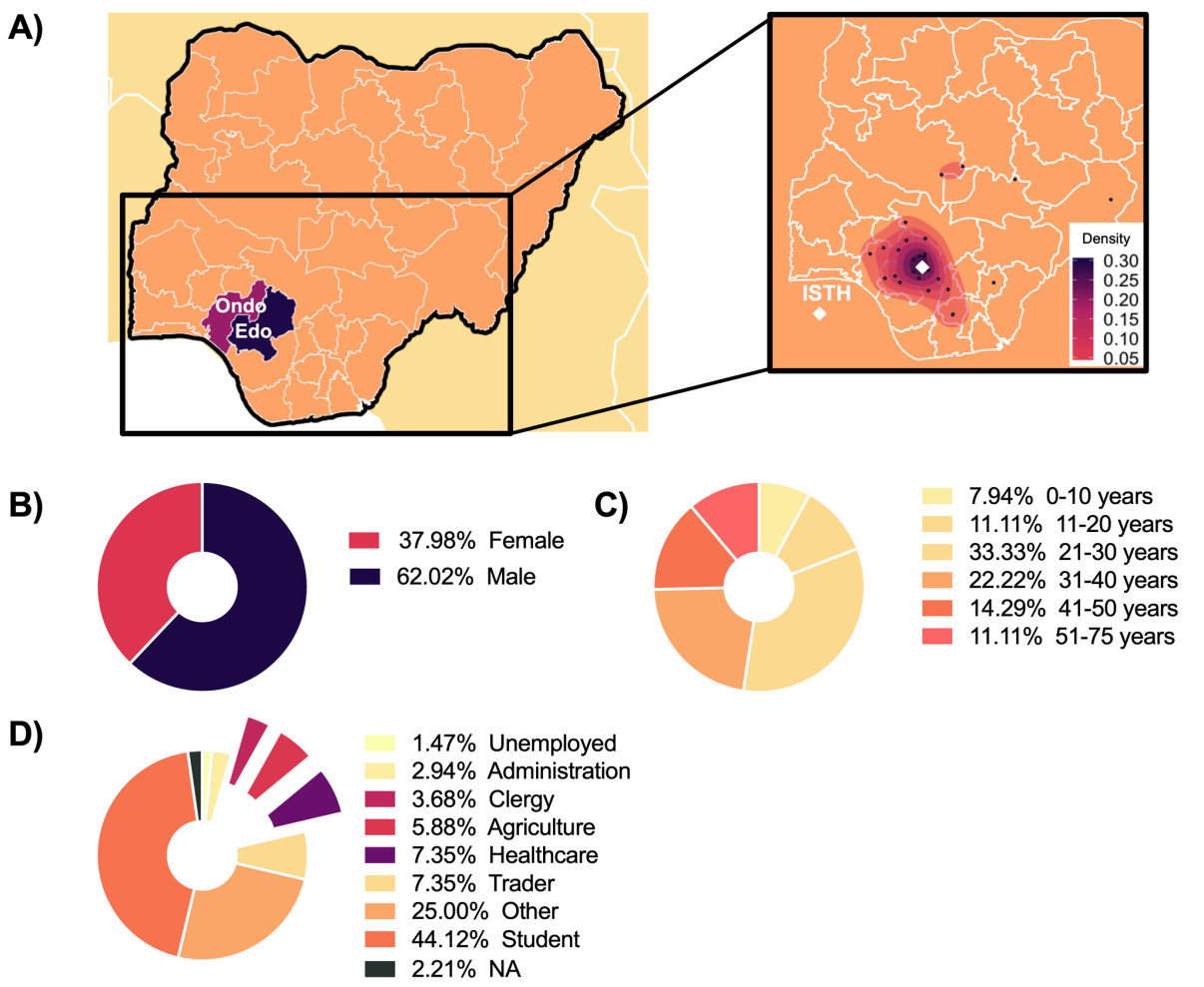

Figure 4.1: Patient demographics. Patients were asked to provide current place of residence (N = 112) (A), which was mapped using geographic coordinates on city level and depicted for each patients (dots) and indicating density (color bar). Gender (N = 129) (B), age (N = 76) (C) and occupation (N = 136) (D) are shown. Information on responders was summarized and percentage of patients (%) is shown. Pie chart colors refer to legends to the right. Abbreviations: ISTH, Irrua Specialist Teaching Hospital.

Clinically, LF presents with non-specific symptoms (Yun and Walker, 2012). Once stationed on the ward, patients were asked to report their symptoms since onset **(Figure 4.2 A)**. As expected, nearly all patients reported to have experienced fever (98.5 %), while more than 50 % reported general weakness, headache, abdominal pain and vomiting. Bleeding was observed in 6.8 % of patients and other symptoms such as pharyngitis (5.4 %), conjunctivitis (4.6 %), facial edema (1.5 %) and deafness (1.5 %) were rare. While overall mortality of LF is expected to be low, previous work has documented that the case-fatality rate of hospitalized patients may be of up to 22 % (Warner et al., 2018). In accordance with this previous report, the overall case-fatality rate of patients included in our study was 15.3 % **(Figure 4.2 B)**.

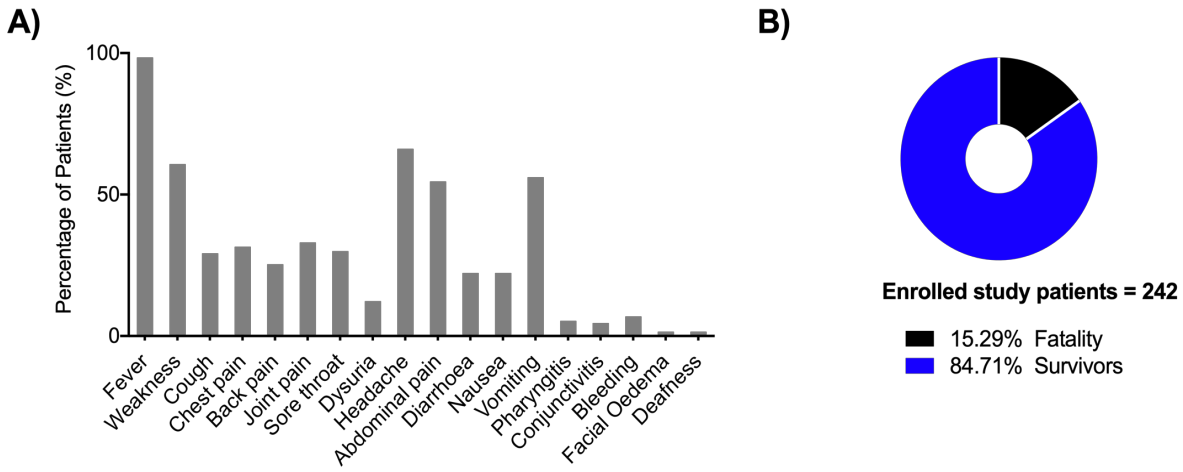

Figure 4.2. Symptoms and outcome of disease: Patients were asked to self-report the symptoms they experienced since onset (A). Percentage of patients (%) that provided information (N = 146) is shown. Outcome is shown for all patients enrolled in this study 2017 and 2018 (B).

4.1.2 Epidemiological risk factors of Lassa fever include direct and indirect exposure to rodents

Awareness of the risk factors to contract LF has increased in Edo state in recent years due to outreach campaigns led by ISTH. However, there is a lack of data regarding the most common risk behaviors of LF patients. To better understand the epidemiological context of the patient cohort recruited, a questionnaire was given to LF patients treated at ISTH. Patients reported information on their behaviors within the last month prior to disease onset **(Figure 4.3 A)**. Very few patients reported to have been living in the same house as a confirmed LF case or to have been personally taking care of one. Only 12.5 % of patients reported direct contact with live rodents through touch or bites. However, patients reported risk behaviors that were linked to putative respiratory, skin and oral exposure. For example, a possible route of infection is through the respiratory mucosa while sweeping floors similarly to what has been previously described for hantavirus infection (Armstrong et al., 1995; Childs et al., 1995), which over half of the patients confirmed to have performed (57 %). Skin contact with infected body fluids may also occur through scratches in the skin while in contact with rats (46 %) or while washing dishes containing contaminated food (53 %). Moreover, a majority of patients reported consumption of uncooked or uncovered food, which poses a potential risk of oral infection (71 %). Of those that reported to have consumed uncooked or uncovered food items, most confirmed that they consumed groundnuts (82.5 %), which is the local name for peanuts that are roasted on open roads. More than half consumed Garri (57.28 %), while less recalled rice, soup or other food items **(Figure 4.3 B)**. Taken together, the data gathered from the questionnaire indicated that patients were encountering risk scenarios of direct and indirect contact with the rodent host. Interestingly,

behaviors that could precede infection through mucosal surfaces were most common. These data also support the notion that human-to-human transmission is rare (Kafetzopoulou et al., 2019; Siddle et al., 2018).

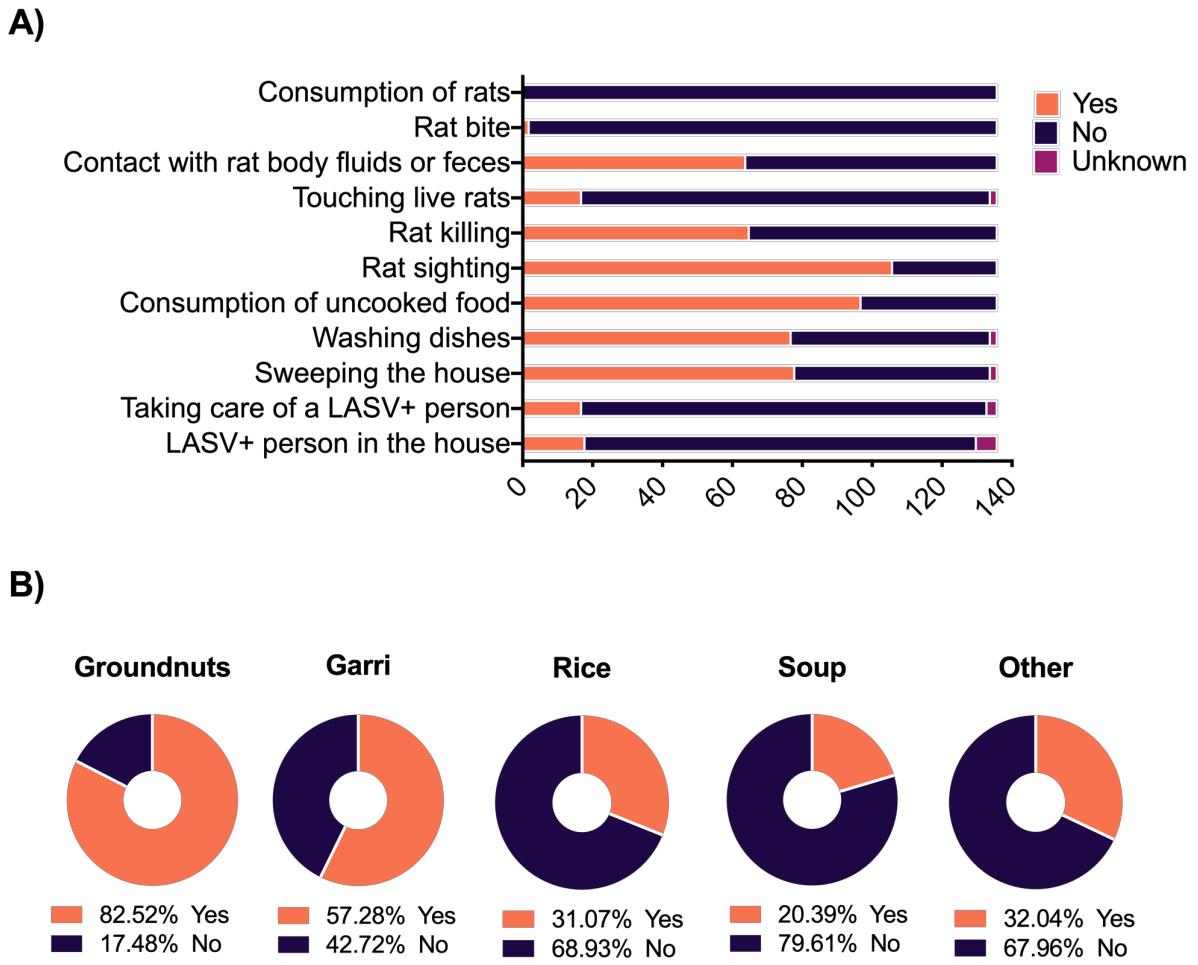

Figure 4.3: Exposure risks and interaction with rats. Patients were provided a questionnaire-based survey and information on behavior and interaction with rodents was collected (A). Number of patients out of the total of patients that complete completed the questionnaire (N = 136) that confirmed to have pertained in the behavior is shown in orange, patients that did not recall such behavior are shown in dark purple and, if unknown, in pink. For further clarification, patients provided information which food items were consumed uncooked or uncovered (B). Percentage of patients (%) is given.

4.2 Characterization of the T-cell response

Previous findings in our laboratory provided a link between T-cell responses and LF immunopathology (Oestereich, Lüdtke et al., 2016). Therefore, we next sought to determine the relationship between human T-cell responses to LASV and the severity of LF. To this end, up to 2 mL of EDTA blood were drawn from patients every second day after admission.

Patients were classified as “mild” and “severe” cases who survived infection, as well as patients who suffered fatal disease, henceforth referred to as “Fatals”. Disease severity in survivors was determined based on the levels of serum AST, which is a sign of liver damage and has been used as indicator for severity (McCormick, King, et al., 1987; McCormick et al., 1986a) **(Figure 4.4 A)**. Survivors with AST serum levels > 300 were classified as “Severe Cases”, survivors with AST serum levels consistently < 300 were classified as “Mild Cases”. Overall, 17.36 % of patients presented with severe disease. Patient groups will henceforth be referred to as “Fatals”, “Mild Cases” and “Severe Cases”. The majority of patients presented as Mild Cases **(Figure 4.4 B)**. Peripheral blood mononuclear cells (PBMCs) were isolated and T cells analyzed for activation, expansion and antigen-specificity.

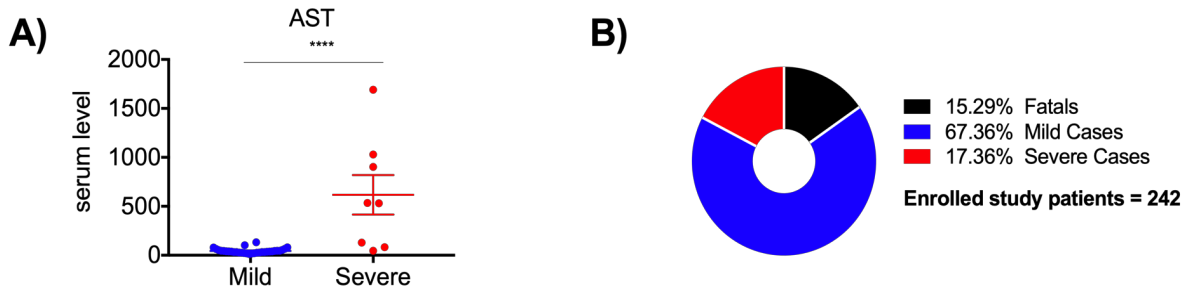

Figure 4.4: Patient classification. Patients, who survived, were classified as “mild” or “severe” based on serum level AST. Serum level AST (U/L) is depicted for survivors (A). Graphs are presented with mean and standard error of the mean (SEM). Mild Cases (N = 32) = blue and Severe Cases (N = 8) = red. An overview of outcome distribution is depicted in (B). Pie colors refer to legend on the right. Statistical significance was determines using unpaired Mann-Whitney test. Significance levels are presented as follows: ns = $p > 0.05$; * = $p \leq 0.05$; ** = $p \leq 0.01$; *** = $p \leq 0.001$; **** = $p \leq 0.0001$. Abbreviations: AST, aspartate transaminase.

4.2.1 T-CELL ACTIVATION IS INCREASED IN SEVERE LASSA FEVER

In the NHP model of LF, T-cell activation early after infection was correlated with survival (Baize et al., 2009). However, whether this observation reflects human LF is now known. Using flow-cytometric analysis, T-cell activation was characterized longitudinally across LF patients with different outcome. Co-expression of CD38 and HLA-DR was used to identify activated $CD4^+$ or $CD8^+$ T-cell populations (Lindgren et al., 2011; McElroy et al., 2015; Miller et al., 2008; Ruibal et al., 2016).

Levels of co-expression of activation markers were higher in $CD8^+$ T cells compared to $CD4^+$ T cells. Across patients, activation levels decreased in the $CD8^+$ T compartment over time but peaks of activation were observed at days 15/16 and 23/24 post-onset **(Figure 4.5 A)**. Activation peaked in the $CD4^+$ compartment from day 14 to day 18 post-onset and a second

activation peak was observed at day 24/25 post-onset. When comparing mild, severe and lethal LF, we observed that Mild Cases presented overall with the lowest levels of activated $CD4^+$ and $CD8^+$ T cells **(Figure 4.5 B).** In contrast, Severe Cases had significantly higher frequencies of activated $CD4^+$ ($p = 0.0224$) and $CD8^+$ T cells ($p = 0.0170$) when compared with mild and fatal LF. In Survivors a slight trend towards higher $CD8^+$ T-cell activation in the blood in relation to increased AST levels and viremia was observed, while in Fatals CD8+ T-cell activation decreased with increased AST levels and viremia **(Supplemental Figure 8.1)**. These findings suggested that disease severity and T-cell activation correlate. In Survivors T-cell activation may increase in response to viral replication, while in Fatals strongly increased levels of viral replication and inflammation may cause especially in $CD8^+$ T-cells reduced activation and dysfunction.

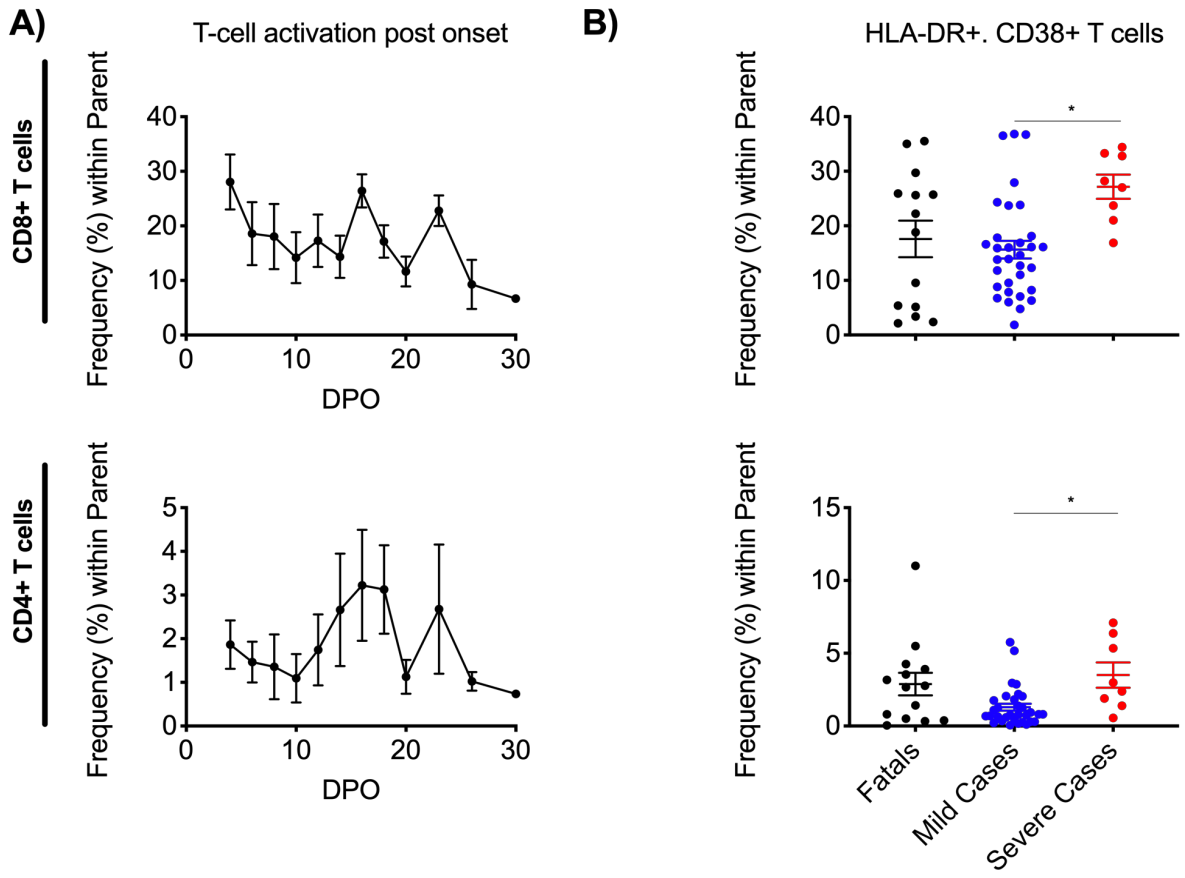

Figure 4.5: T-cell activation. Longitudinal co-expression of CD38 and HLA-DR was analyzed by flow cytometry of $CD4^+$ and $CD8^+$ T cells in relation to time post self-reported onset (A), samples were grouped in two-day intervals. Frequency (%) within parent is depicted. Activation was analyzed for different outcome groups (B). Fatals (N = 14) = black, Mild Cases (N = 32) = blue and Severe Cases (N = 8) = red. Graphs are presented with mean and SEM. Statistical significance was determines using Kruskal-Wallis test, followed by Dunn's multiple comparisons test. Significance levels are presented as follows: ns = $p > 0.05$; * = $p \leq 0.05$; ** = $p \leq 0.01$; *** = $p \leq 0.001$; **** = $p \leq 0.0001$. Abbreviations: DPO, days post-onset.

4.2.2 THE ACTIVATED T-CELL POPULATION COMPRISES LASSA-SPECIFIC AND BYSTANDER T CELLS

The finding that T-cell activation differed between outcome groups led to the question if the activated compartment was comprised of majorly LASV-specific T cells or if bystander responses were involved, as has been shown for other viral infections (Murali-Krishna et al., 1998; Rivino et al., 2015; Sckisel et al., 2014). Antigen-specific T cells can be identified via flow cytometry through staining with fluorescent tetramers. Tetramers are comprised of four MHC molecules bound to a specific antigen peptide, coupled together by streptavidin-biotin bonds and coupled with a fluorophore. The MHC/peptide complex can then be used to identify antigen-specific T cells with specificity for the selected peptide. Previous work has shown that fluorescent MHC-peptide tetramer complexes can be used in flow cytometry to identify LASV-specific T cells (McElroy et al., 2017).

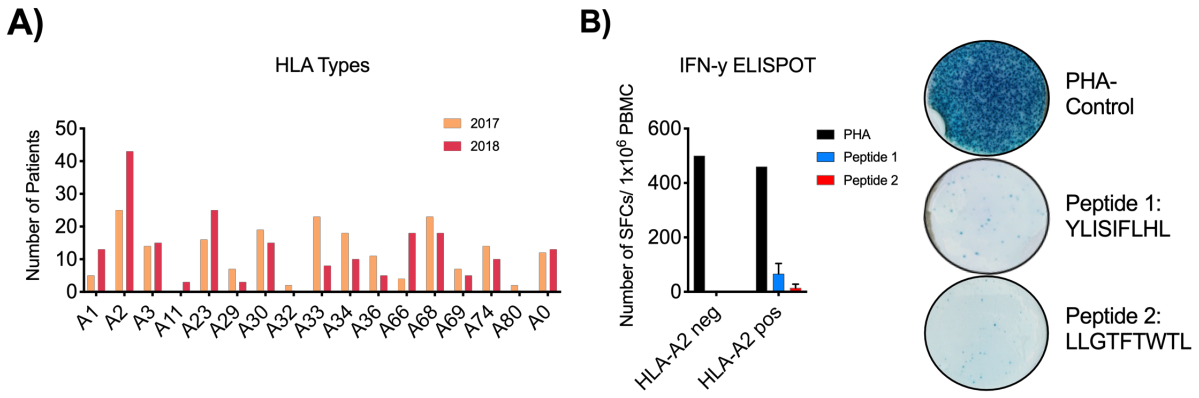

Figure 4.6: Development of LASV-specific tetramers. Using PCR based methodology, the HLA-A locus was genotyped for patients from the 2017 (yellow) and 2018 (pink) cohort to identify patients suitable for tetramer analysis (A). Number of patients is reported for each allele. An IFN-γ ELISPOT was used on HLA-A2 negative (N = 2) and positive (N = 2) patient samples collected after viral clearance to confirm immunogenicity of the selected peptides. Single Focus Forming Cells (SFCs) per 1 x 10^6 PBMCs are depicted. Representative wells are shown for each condition. Abbreviations: PHA, Polyhydroxyalkanoate; HLA, Human Leukocyte Antigen; IFN-χ, interferon χ. ELISPOT, Enzyme Linked Immuno Spot Assay; PBMC, Peripheral Blood Mononuclear Cells; SFC, Single Focus Forming Cells.

Thus, with the goal of characterizing LASV-specific T cells in our patient cohort, Flex-T tetramer methodology (Biolegend) was used to generate peptide-bound tetramers. PCR based methodology was utilized to HLA-type the 2017 and 2018 LF patient cohorts recruited at ISTH **(Figure 4.6 A)**. Alleles HLA-A2, A23, A33 and A68 were most commonly identified. Previous work has highlighted specifically two potential $CD8^+$ T-cell epitopes to be presented in the context of HLA-A2 (peptide 1 = YLISIFLHL; peptide 2 = LLGTFTWTL) (Botten et al.,

2006; McElroy et al., 2017). Using IFN-γ ELISPOT, it was verified that both peptides were able to stimulate T-cell responses with high specificity **(Figure 4.6 B)**. While both, HLA-A2 negative and positive convalescent LF-patient T cells responded to the chemical stimulant PHA, response to the peptide stimulus was only observed for HLA-A2 positive donors.

Tetramers were therefore generated for both peptides using UV-enabled exchange of signal peptides. To determine, if the generated tetramers were able to identify LASV-specific T cells, both were tested using flow-cytometry **(Figure 4.7 A/B)**. Only the tetramer generated with the LLGTFTWTL peptide showed a clearly defined double positive population, which was not present in both the healthy HLA-A2$^+$ and the LASV$^+$ HLA-A2$^-$ controls. Peptide 1 generated background signal in the LASV$^+$ HLA-A2$^-$ control and failed to stain a double positive population in the LASV$^+$ HLA-A2$^+$ sample.

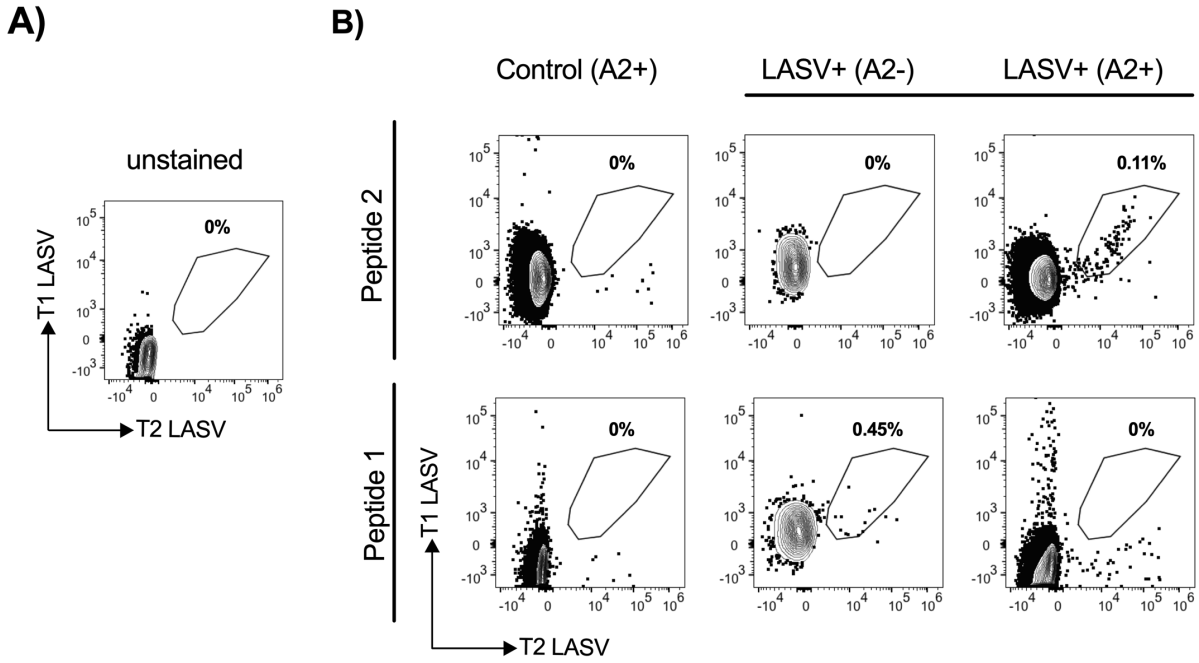

Figure 4.7: Identification of LASV-specific CD8$^+$ T cells. HLA-A2 tetramers were generated in-house and labeled in two fluorochrome colors (T1 and T2). CD8$^+$ T cells were identified by flow-cytometry. To identify background noise in the tetramer gate, gating was performed on unstained cells (A). Tetramers generated from both peptides were tested against HLA-A2$^+$ healthy controls, LASV patients either expressing HLA-A2 (A2$^+$) or not (A2$^-$). Representative plots are shown. Abbreviations: HLA, Human Leukocyte Antigen; LASV, Lassa virus.

The LLGTFTWTL-tetramer was used to determine the kinetics and phenotype of LASV-specific CD8$^+$ T cells in three patients during the acute phase of LF and after discharge. As the overall cell number in the samples was low, samples from multiple time-points during the acute phase were concatenated. In accordance with data published by McElroy et al., 2018,

low frequency of LASV-specific CD8+ T cells was detected during acute phase of infection (representative patient = 0.11 %), and increased amounts after discharge (0.26 %) **(Figure 4.8 A)**. However, when looking at the activated compartment within the $CD8^+$ T-cell population, the overall frequency of activated $CD8^+$ T cells was higher during the acute phase of disease and reduced in convalescence **(Figure 4.8 C)**. These results strongly suggested that, within the bulk of activated T cells in the acute phase of LF, there were both LASV-specific and non-specific (bystander) $CD8^+$ T cells.

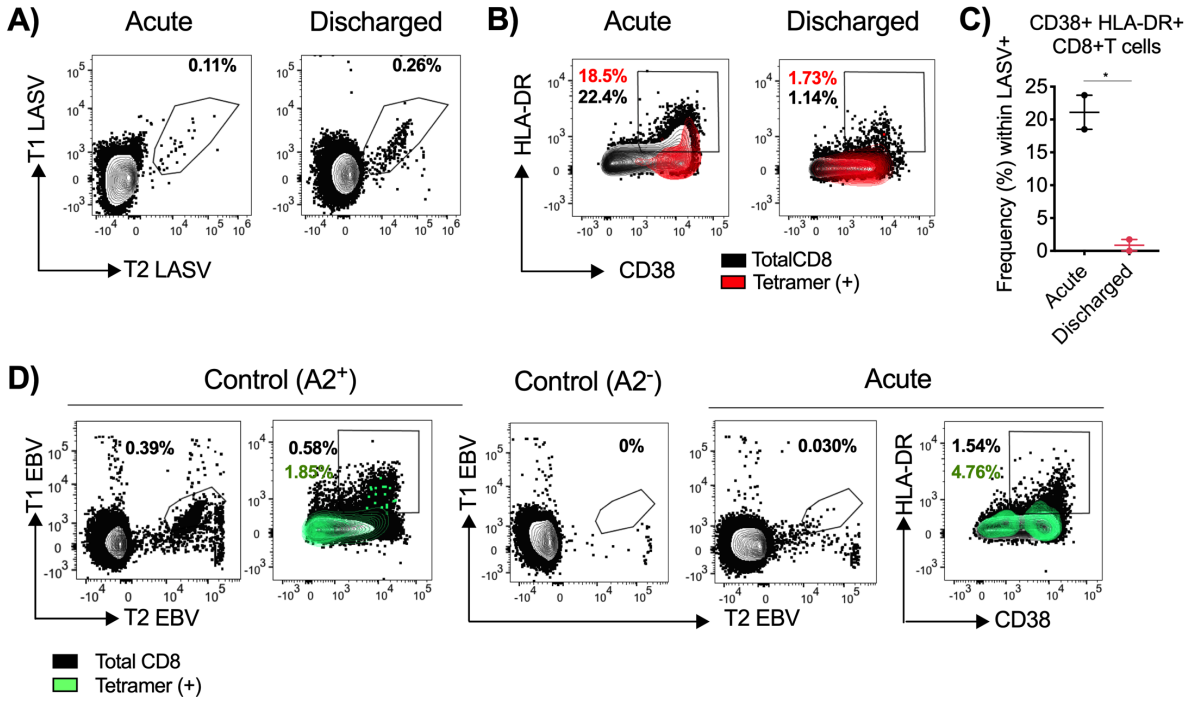

Figure 4.8 Appearance and activation profile of LASV-specific and bystander T cells. HLA-A2 tetramers were generated in-house and labeled in two fluorochrome colors (T1 and T2). $CD8^+$ T cells were identified by flow-cytometry. Frequency of LASV-specific T cells was investigated during acute phase (pooled samples) and after discharge (A). Activation status of LASV-specific T cells was compared with total $CD8^+$ T cells (B) and frequency of activated LASV-specific T cells was compared during acute phase and after discharge. EBV-specific T cells, as surrogate for bystander T cells, were identified in controls ($A2^+$) and ($A2^-$) and in acute LF patients. There activation profile was equally analyzed (D). Representative plots are show. Abbreviations: HLA, Human Leukocyte Antigen; LASV, Lassa virus; EBV, Epstein-Barr virus. Statistical significance was determines using unpaired t-test. Significance levels are presented as follows: ns = $p > 0.05$; * = $p \leq 0.05$; ** = $p \leq 0.01$; *** = $p \leq 0.001$; **** = $p \leq 0.0001$.

To study the putative involvement of bystander T cells, the strategy was to generate tetramers that would allow us to identify $CD8^+$ T cells specific for common epitopes not related with LASV. To this end, tetramers were generated against an HLA-A2-restricted

Epstein-Barr-Virus (EBV) peptide (GLCTLVAML), a common antigen in humans (Hjalgrim, Friborg, and Melbye, 2007). Tetramer staining of $CD8^+$ T cells in a EBV^+ healthy control was used to verify tetramer binding **(Figure 4.8 D)**. Interestingly, activated EBV-specific $CD8^+$ T cells were detected in LF patients during the acute phase of disease **(Figure 4.8 D)**. These results demonstrated that the activation of $CD8^+$ T cells in the acute phase of LF was comprised of LASV-specific T cells as well as bystander T cells.

4.2.3 A DISCRETE POPULATION OF BYSTANDER T CELLS IS ACTIVATED UPON INFECTION *IN VIVO*

We next sought to determine whether activation of bystander T cells was a general feature of LF reproducible in an animal model of disease. To this end, we used a chimeric mouse model previously developed in our laboratory which was based on transplantation of wildtype (WT) bone marrow progenitor cells into $IFNAR^{KO}$ recipient mice (hereafter referred to as IFNAR) (Oestereich, Lüdtke et al., 2016). To study the impact of LASV infection on the activation of bystander T cells, IFNAR mixed bone marrow chimeras were generated by transplantation of progenitor cells from WT and OT-1 donor mice in a 1:1 ratio. (**Figure 4.9 A)**. OT-1 mice are genetically modified to constitutively express only one T-cell receptor specific for the ovalbumin (OVA)-derived MHC class I-restricted peptide SIINFEKL (Clarke et al., 2000). Thus, after repopulation of the hematopoietic system, these mixed bone marrow chimeras harbor WT $CD8^+$ T cells which may respond specifically to LASV as well as non-specific traceable OT-1 $CD8^+$ T cells, which function as surrogate bystanders.

These mixed chimeric mice were infected with 1000 focus forming units (FFU) LASV intranasally (i.n.) and the T-cell response was analyzed on day 9 post infection. Infection resulted in different activation profiles in $CD8^+$ effector T cells. Effector T cells were characterized by loss of the lymphoid homing marker CD62L and expression of CD44 (Bajnok, Ivanova, Rigó, and Toldi, 2017; Pihlgren et al., 1995). WT T cells showed significantly increased effector phenotype ($CD44^+$ $CD62L^-$) compared to OT-1 T cells after infection, however OT-1 effector T cells frequency did also increase compared to the baseline (**Figure 4.9 B/C)**. To characterize the activation status of the effector subsets, expression of CD25, a marker for late T-cell activation, and CD69, a marker for early T-cell activation (Reddy, Eirikis, Davis, Davis, and Prabhakar, 2004) was utilized. Expression of activation markers CD69 and CD25 were significantly different in wildtype T cells and OT-1 effector T cells. Wildtype T cells expressed increased CD25, while expression of CD69 was significantly increased on bystander OT-1 T cells (**Figure 4.9 D)**. This implies a different activation kinetic for both subsets, in which bystander activation may be delayed. Taken

together, this provides preliminary evidence in an *in vivo* system that further indicate that bystander CD8$^+$ T cells are involved during LASV infection. Bystander T cells were characterized by increased effector phenotype, though magnitude of activation was significantly increased in LASV-specific T cells.

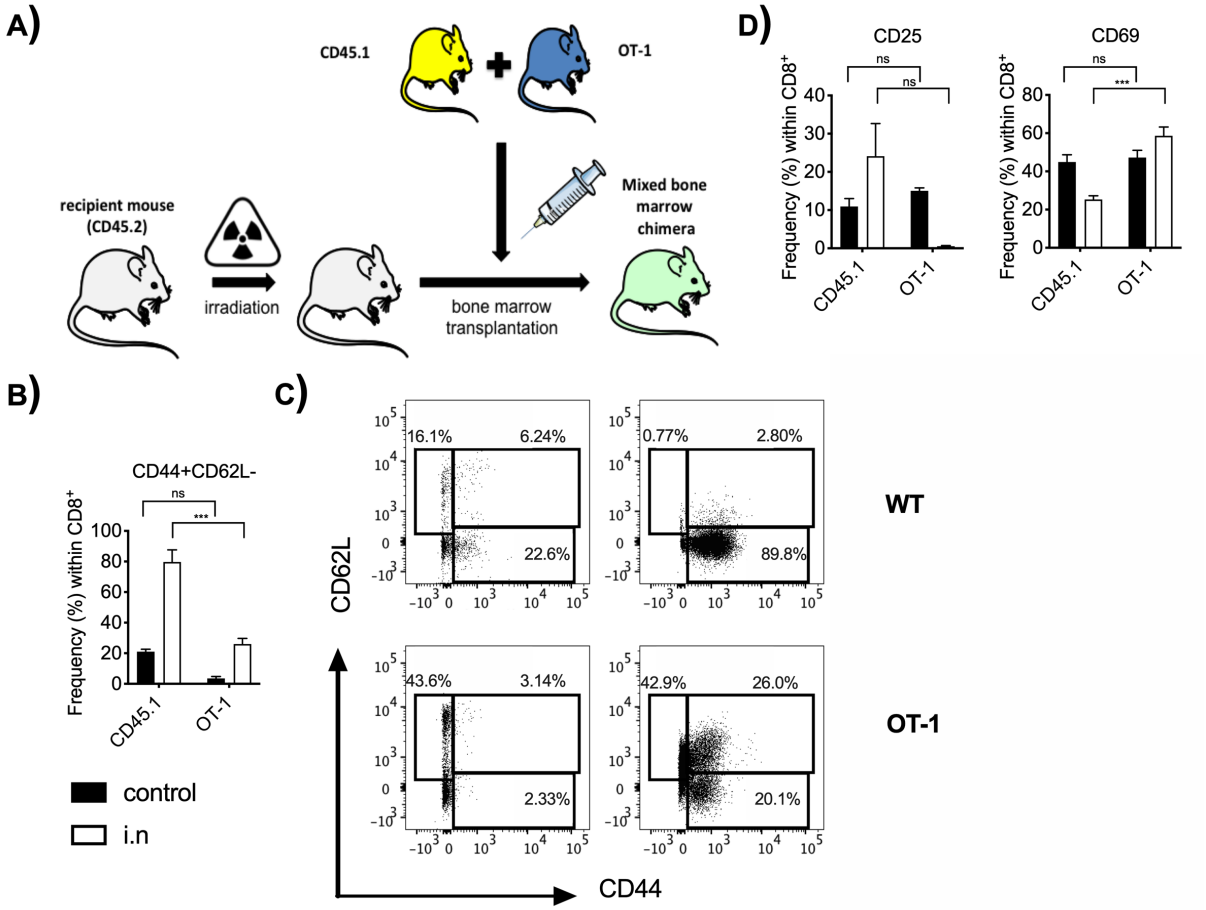

Figure 4.9: Bystander activation *in vivo*. Mixed bone marrow chimeras were generated by irradiation and transplantation of bone marrow harvested from wildtype (WT) CD45.1 and OT-I mice (A) and infected i.n. with 1000 FFU of LASV (N = 3). Uninfected mice served as control (N = 3). Frequency (%) of effector cells (CD44$^+$ CD62L$^-$) is shown for CD8$^+$ T cells (B). Exemplary plots are shown (C). Expression frequency (%) of activation markers CD25 and CD69 is depicted for infection (right) and control (left) (D). Mean and SEM are shown. Statistical significance was determines using ordinary two-way ANOVA, followed by Sidak's multiple comparison test. Significance levels are presented as follows: ns = $p > 0.05$; * = $p \leq 0.05$; ** = $p \leq 0.01$; *** = $p \leq 0.001$; **** = $p \leq 0.0001$. Abbreviations: WT, wildtype; i.n., intranasal; FFU, focus forming units.

4.2.4 ACTIVATION OF EFFECTOR FUNCTION IS OBSERVED IN A SUBSET OF PATIENTS

Next, as LASV-specific T cells were detected during the acute phase of LF, the functional capacity of T cells to respond to LASV-specific stimulus was evaluated. Effective cytotoxic T-cell responses rely on production of cytokines and degranulation. While in one previous

study of a human patient LASV-specific T-cell cytokine responses were detected also during the acute phase (McElroy et al., 2017), *in vitro* data also suggested that T-cell responses may be suppressed or dysfunctional (Baize et al., 2009). It was hypothesized that T-cell responses between patients differ, which may be linked to disease severity. To this end, first, re-stimulation of patient T cells with a LASV-specific peptide pool and, second, inactivated virus was employed to analyze cytokine production and degranulation upon stimulus.

Based on computational prediction, a LASV NP (based on a circulating Nigerian LASV strain Nig-08 and strain Ba366) peptide pool was generated for stimulation of cytotoxic T cells. Peptides were designed for presentation in the context of MHC I and to cover over 95 % of the HLA alleles previously described for West African cohorts (https://www.ebi.ac.uk/ipd/imgt/hla/). PBMCs were isolated from patients (N = 26) at different time points during acute infection. Directly at ISTH, cells were stimulated with the peptide pool and intracellular cytokine staining (ICS) was utilized to determine expression of IFN-γ and TNF-α, as readout of T-cell activation. In addition, expression of, LAMP-1/CD107a, a surrogate marker of degranulation, was also evaluated **(Figure 4.10 A)**. TNF-α production above background was observed in less than half (38.5 %) of analyzed samples, while slightly more responded with increased IFN-γ release (46.3 %) and CD107a up-regulation (42.3 %) **(Figure 4.10 B)**. The cytokine production and degranulation pattern observed amongst responders was diverse. While some (14.81 %) showed no detectable increase in IFN-γ, TNF-α or CD107a, similarly often the response was characterized by only IFN-γ (14.81 %), TNF-α (18.52 %) or CD107a (14.81 %) production. Polyfunctional responses were also observed in some samples. When T cells responded to NP peptide stimulation, the magnitude of response ranged quite considerably, with some samples showing strong and robust responses **(Figure 4.10 C/D).**

To clarify if the magnitude of response was linked to disease severity, next, the relationship of in IFN-γ, TNF-α and CD107a with AST level and viremia was characterized. For all three markers no or very limited response was demonstrated in samples from patients with corresponding high AST levels > 200 U/L. and low LASV PCR cycle threshold (Ct) values (< 25), which correlates to high viremia. Interestingly, while not significant, the greatest IFN-γ response was noted in samples from patients with intermediate AST levels and Ct values, while TNF-α or CD107a expression was highest in samples from patients with very low AST levels (< 50) and high Ct.

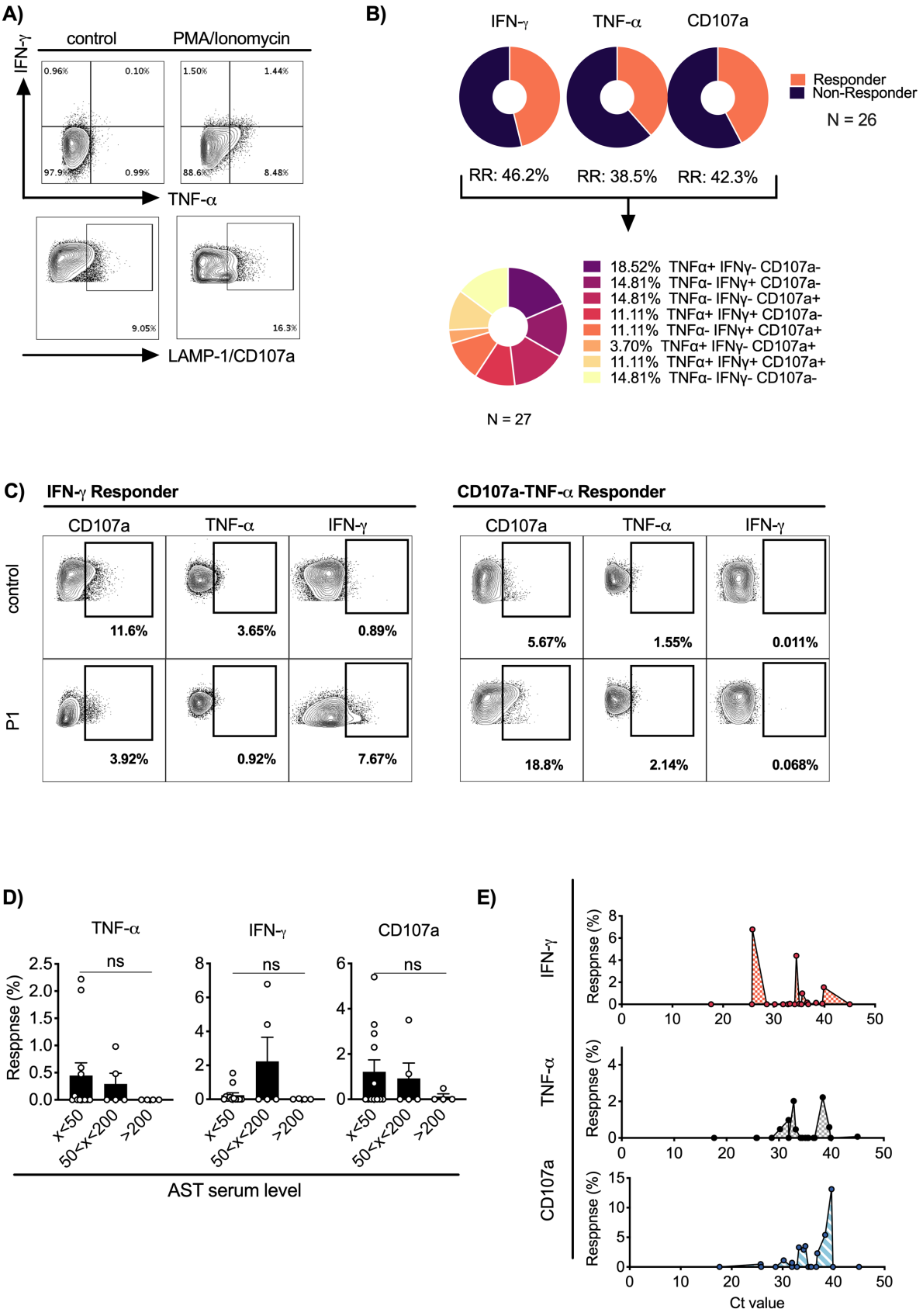
A)
control
PMA/Ionomycin
IFN-γ
0.96%
0.10%
97.9%
0.99%
1.50%
1.44%
88.6%
8.48%
TNF-α
9.05%
16.3%
LAMP-1/CD107a
B)
IFN-γ
TNF-α
CD107a
Responder
Non-Responder
N = 26
RR: 46.2%
RR: 38.5%
RR: 42.3%
18.52% TNFα+ IFNγ- CD107a-
14.81% TNFα- IFNγ+ CD107a-
14.81% TNFα- IFNγ- CD107a+
11.11% TNFα+ IFNγ+ CD107a-
11.11% TNFα- IFNγ+ CD107a+
3.70% TNFα+ IFNγ- CD107a+
11.11% TNFα+ IFNγ+ CD107a+
14.81% TNFα- IFNγ- CD107a-
N = 27
C)
IFN-γ Responder
CD107a-TNF-α Responder
CD107a
TNF-α
IFN-γ
control
P1
11.6%
3.65%
0.89%
3.92%
0.92%
7.67%
5.67%
1.55%
0.011%
18.8%
2.14%
0.068%
D)
TNF-α
IFN-γ
CD107a
ns
Resppnse (%)
x<50
50<x<200
>200
AST serum level
E)
IFN-γ
TNF-α
CD107a
Resppnse (%)
Ct value

Figure 4.10: Ex vivo stimulation of T cells with LASV peptides. CD8+ T-cell responses were analyzed after ex vivo stimulation with LASV specific peptides (N = 26). Cytokine production was measured by flow cytometry. Representative plots depicting the gating based on negative and positive control are shown (A). Frequency of CD8+ T cells producing IFN-γ, TNF-α or LAMP-1/CD107a was compared after peptide stimulation. Patients were separated into Responders and Non-Responders and response rate amongst all samples was calculated (B). Polyfunctionality of response is depicted (N = 27). Pie wedge colors refer to each respective combination as shown by legend on the right. Representative strong responses to LASV peptide stimulus are shown (C). Magnitude of response (% above background) is depicted in relation to patient AST level (U/L) for IFN-γ, TNF-α and LAMP-1/CD107a (D). Single samples are represented (dots), as is mean and SEM. Magnitude of response (% above background) is depicted in relation to viremia, represented by Ct value of RT-PCR (E). Single samples are represented (dots). If response magnitude was below background, response (%) was set to null. Statistical significance was determines using Kruskal-Wallis test, followed by Dunn's multiple comparison test. Significance levels are presented as follows: ns = $p > 0.05$; * = $p \leq 0.05$; ** = $p \leq 0.01$; *** = $p \leq 0.001$; **** = $p \leq 0.0001$. Abbreviations: IFN-γ, interferon γ, TNF-α, tumor necrosis factor α; RR, response rate; P1, peptide pool 1; AST, serum level aspartate transaminase.

For multiple patient samples collected during the acute phase, it was possible to, additionally, investigate the T-cell responses to inactivated complete LASV (N = 7). This was performed on thawed cells inside the BSL-4 containment at BNITM. To ensure a close match of T-cell specificity and virus epitopes, a LASV isolated from serum of a 2018 patient, was utilized for stimulation. Virus was heat inactivated and the $CD4^+$ and $CD8^+$ T-cell response was determined by TNF-α and IFN-γ cytokine release. In agreement with peptide stimulation, across patients neither $CD4^+$ nor $CD8^+$ T cells showed significant cytokine responses to stimulation compared with $LASV^-$ healthy controls. However noteworthy, also here it was observed that singular patients showed robust T-cell responses with above background levels of both IFN-γ and TNF-α **(Figure 4.11 A)**. The phenotype of these T cells was further characterized. Responder $CD8^+$ T cells expressed very low levels of CCR7 combined with both low and high levels of CD45RA, identifying them as T_{EM} and T_{eff}, respectively **(Figure 4.11 B)**. Interestingly, also α4 integrin and β1 integrin, makers of homing capacity to inflamed tissue and activation, were highly expressed. Decreased CCR7 and increased α4 integrin and β1 integrin expression was also observed in $CD4^+$ T cells that responded to stimulus **(Supplemental Figure 8.2 B)**.

In summary, using stimulation with NP peptides and fully inactivated virus, LASV-specific T-cell responses were observed in a subset of survivors that showed a mild course of LF. Conversely, in samples from severe and fatal cases T-cell stimulation failed to produce effector T-cell response. These data indicate that T-cell dysfunctionality is correlated to disease severity and may be a result of increased viral load or inflammation.

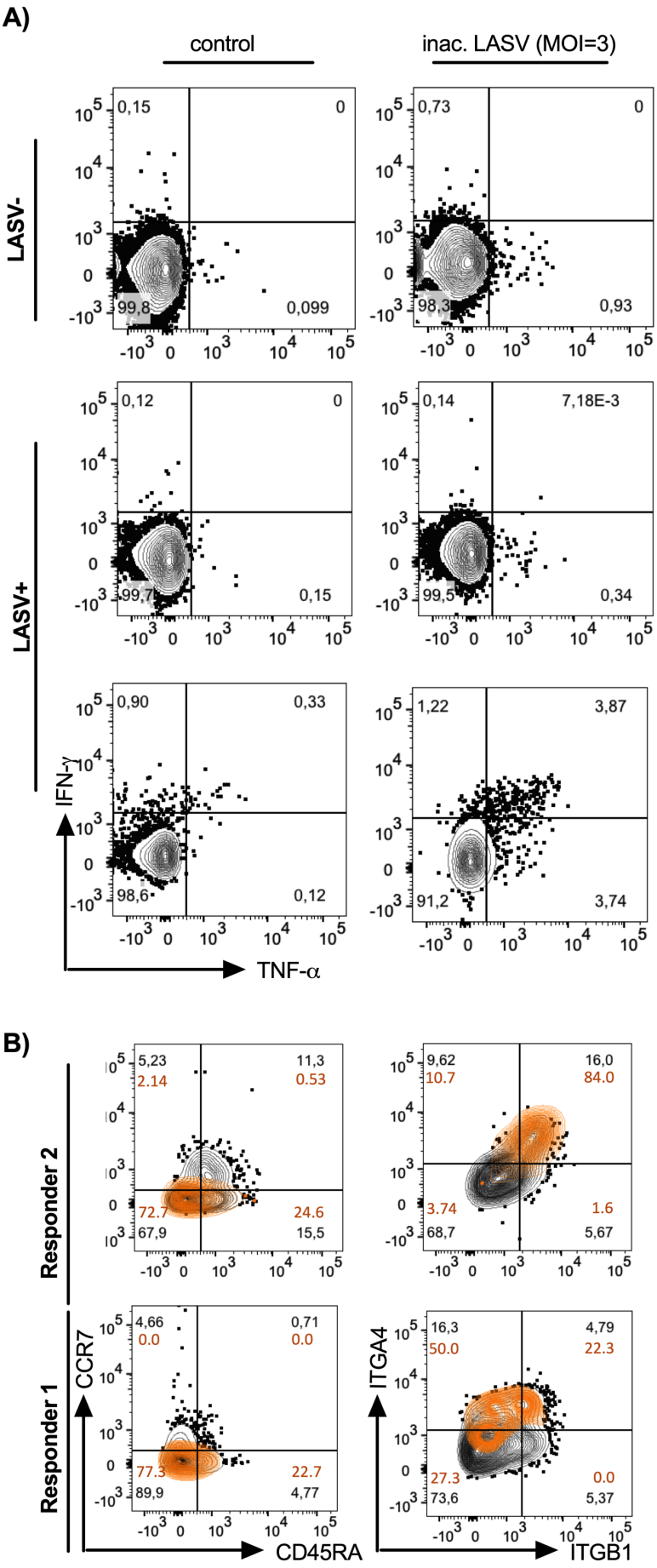

Figure 4.11: *Ex-vivo* stimulation of T cells with full LASV. T-cell responses were analyzed after *ex-vivo* stimulation. T cells producing IFN-γ, TNF-α or combination was compared after stimulation in patients (N = 7) and controls (N = 5) (A). Representative $CD8^+$ T-cell responses to LASV are shown for two patients and one control. Effector phenotype and inflammatory homing capacity of both IFN-γ and TNF-α producing $CD8^+$ T cells was analyzed, and representative overlay plots are shown (B). Total population of $CD8^+$ T cells is shown in black, cytokine producing fraction in orange. Abbreviations: IFN-γ, interferon γ, TNF-α, tumor necrosis factor α; LASV, Lassa virus; CCR7, chemokine receptor 7; ITGB1, integrin β1; ITGA4, integrin α4.

4.2.5 SEVERE LASSA FEVER IS ACCOMPANIED BY AN INCREASE IN CLONAL EXPANSION OF T CELLS, FATAL OUTCOME BY INCREASED DIVERSITY

In the steady state, the T-cell repertoire is comprised mostly of a multitude of T-cell clones with similar but relatively small frequency. Antigen encounter breaks homeostasis by driving T-cell expansion of responding clones, which dominate the response during the effector phase. As differences in the T-cell responsiveness to LASV in relation to disease severity were observed, it was perceived that this could also lead to differences in antigen-driven T-cell expansion, hence changes of the repertoire, which could further help differentiate between patient responses.

To investigate T-cell expansion during acute LF, the highly variable CDR3 region of the TCRβ chain was sequenced in 38 acute LF patients with different outcomes. Inverse Simpson Index was used as a measurement of diversity based on the abundance of each sequenced clonotype found within the total TCR repertoire of each sample. Gini Index indicated if the repertoire is skewed towards expression of specific clonotypes. No significant difference existed between Mild Cases and Severe Cases and Fatals based on TCR diversity and skewedness, as measured by Inverse Simpson Index and Gini Index, respectively **(Figure 4.12 A/B).**

This analysis of diversity and skewedness was performed cross-sectionally for samples collected at early time points after self-reported onset. Next, the longitudinal changes in the homeostasis were investigated. For longitudinal analysis additional 142 samples were analyzed. Longitudinal analysis revealed that while no early difference existed between patient groups in TCR diversity, Severe Cases showed a trend towards increased clonal hyperexpansion with time while homeostasis remained constant in Mild Cases **(Figure 4.12 C)**. Interestingly, the response in Fatals was characterized by decrease of clonal hyperexpansion, which means increased diversity, over time and, compared with Survivors, early clonal space in Fatals showed an increased proportion occupied by large and hyperexpanded clonotypes **(Figure 4.12 D)**. In contrast, Mild Cases showed highest frequency of rare or small clonotypes. Similarity between TCR repertoires of patients can indicate commonly recognized epitopes and, as such, if the T-cell response is driven in a particular direction. To measure similarity in the clonotypes present in each patient groups clonal overlap, represented by number of shared clonotypes between sets of two patients, was visualized **(Figure 4.13)**.

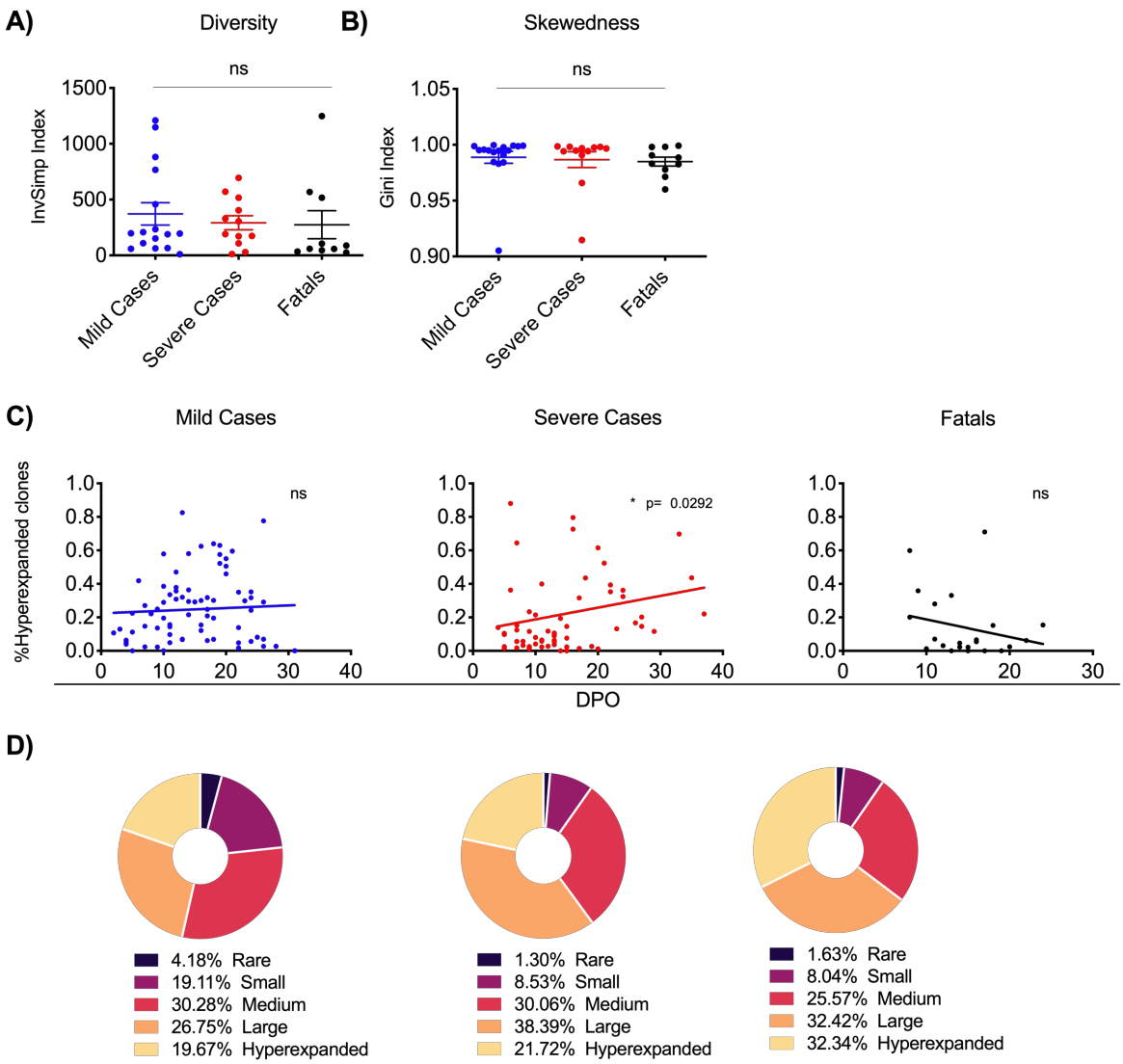

Figure 4.12: TCR diversity and homeostasis in human LF. Next generation sequencing of the TCRβ chain CDR3 region was utilized to analyze the TCR repertoire on mRNA level. Diversity of repertoire (measured by inverse Simpson Index) and skewness of response (measured by Gini Index) are shown for Fatals (black), Mild Cases (blue) and Severe Cases (red) at a cross-sectional early time point (A/B). Longitudinal sampling was executed and hyperexpansion of clones (%) analyzed for all three outcome groups (C) and individual samples and trend lines are shown. Complete clonal space was compared at early time point cross-sectionally (D). Pie wedge colors refer to each respective clone fraction as shown by legend below. Clones were defined as Rare: 0<x<=1e-05; Small: 1e-05<x<=1e-04; Medium: 1e-04<y<=0.001; Large: 0.001<x<=0.01; Hyperexpanded: 0.01<x<=0.1. Statistical significance was determines using Kruskal-Wallis test, followed by Dunn's multiple comparisons test, or Spearman correlation analysis. Significance levels are presented as follows: ns = $p > 0.05$; * = $p \leq 0.05$; ** = $p \leq 0.01$; *** = $p \leq 0.001$; **** = $p \leq 0.0001$. Abbreviations: DPO, days post-onset.

Interestingly, even though diversity measurement suggested that no difference in TCR repertoire existed, at early time points between Mild and Severe Cases, clonal overlap analysis revealed that Mild Survivors have increased amounts of shared clonotypes compared to Severe Survivors. Curiously, observation of shared clonotypes in Fatals was

peculiar. Whilst two Fatals had shared clonotypes with most other patients in this group, these clonotypes were not shared amongst the other Fatals themselves, suggesting that these two Fatals share different subsets of clonotypes with each of the other patients. Lastly, to further determine if the T-cell response is driven towards selection of specific TCR, the v-gene usage was analyzed across patient groups. While multiple v-genes showed variations of usage, only TCRBV4-1 was significantly more frequent in Fatals compared to Survivors (including Mild and Severe Cases) **(Figure 8.3)**.

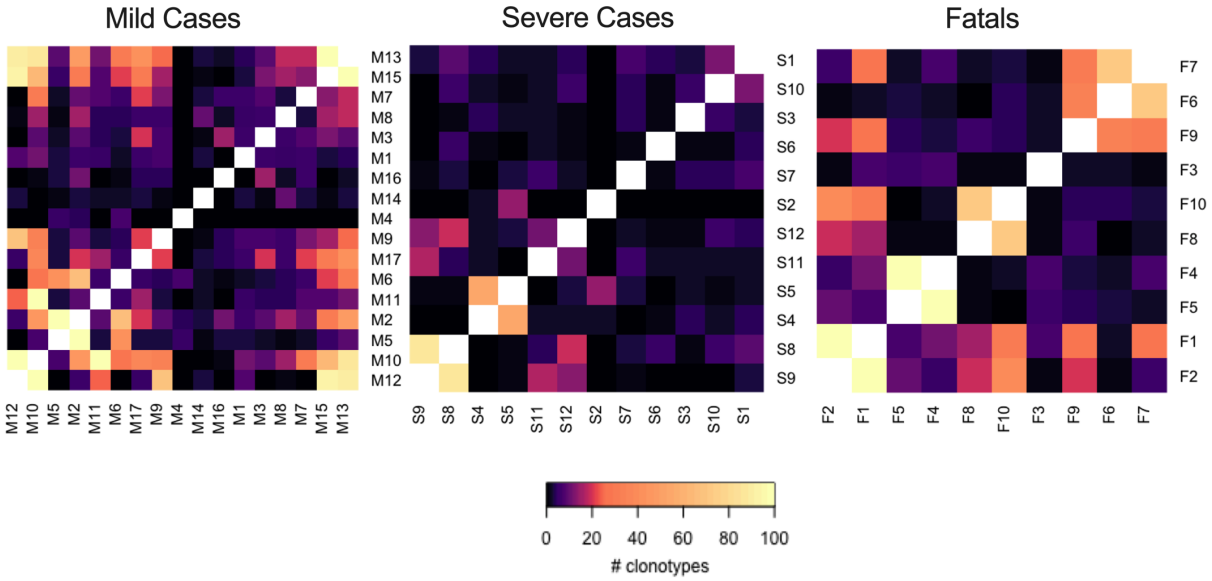

Figure 4.13: Clonal overlap in LF patients. Cross-sectional analysis of clonal overlap in each outcome group was employed to visualize the shared clonal repertoire. Heatmaps indicate the number of shared clonotypes for each combination of two patients according to legend bar below. Abbreviations: M, Mild Cases; S, Severe Case; F, Fatal.

In summary, while the early T-cell response was not significantly different in diversity and skewedness in the different groups of LF, differences in T-cell responses over time could be observed. Mild Cases were characterized by no observable changes in T-cell repertoire diversity over time and a high frequency of rare and small clonotypes. In contrast, Severe Cases share little antigen overlap early on but mounted a directed response characterized by clonal expansion over time. Conversely, in Fatals the opposite trend was observed characterized by reduced frequencies of hyperexpanded clones, implicating increased levels of diversity.

4.3 CHARACTERIZATION OF T-CELL HOMING IN ACUTE HUMAN LASSA FEVER

Depending on the homing markers expressed on their surface, T cells preferentially home to different tissues. While certain homing makers are more universal, others have been described to specifically target T cells to organs such as gut, lung and skin during steady-state and during inflammation. In the latter case, migration to specific tissues depends on the site of first antigen encounter. We hypothesized, that, based on the epidemiological data collected, multiple potential routes of infection existed in LF and this variability would be reflected also in different T-cell homing signatures. As differences in T-cell responsiveness to stimulus existed between patients, it was hypothesized further, that the ability of T cells to migrate to infected tissues might be affected and that a link between T-cell homing and LF severity might exist.

4.3.1 DIFFERENT HOMING SIGNATURES EXIST IN HUMAN LASSA FEVER

Even though restricted by the limitations of employing bench-top flow cytometry in a field setting, it was possible to analyze various homing markers on freshly isolated cytotoxic T cells during the 2018 Lassa outbreak in Nigeria. Using co-expression of CD38 and HLA-DR, activated CD8+ T cells were identified **(Figure 4.14 A)**. Using three different antibody panels on respective cohorts (N = 16, N = 25, N = 61), it was possible to measure frequency of expression of two chemokine receptors, CCR3, previously described as a homing marker for the upper airways (Danilova et al., 2015) and CCR5, a marker of inflammation and liver homing (Kunkel et al., 2002), skin homing selectin CLA (Babi et al., 1995), and integrins α4, β1 and β7. Integrin α4 can form a homodimeric structure with either the β1 or β7 subunit. Integrin α4β1 has been previously described to target T cells to inflamed tissues, irrespective of organ tissue, while integrin α4β7 specifically functions as a homing marker for the intestine. It has been described that expression of β1 integrin normally is excluded from intestinally homing T cells, unless in the context of active inflammation (Denucci, Mitchell, and Shimizu, 2009).

As expected, the frequency of activated cytotoxic T cells from acute LF patients expressing inflammatory homing receptor β1 integrin was high (71.44 %) **(Figure 4.14 B/C).** In contrast, the frequency of T cells expressing either CCR3 (1.79 %) or CCR5 (7.65 %) was quite low within the activated compartment. Cutaneous homing marker CLA was expressed more commonly, but also at rather low frequencies (9.36 %). Interestingly, also more than half of activated T cells expressed the intestinal marker β7 integrin (57.57 %). Overall, β1, β7 and α4 integrins were significantly higher expressed than CLA, CCR3 and CCR5.

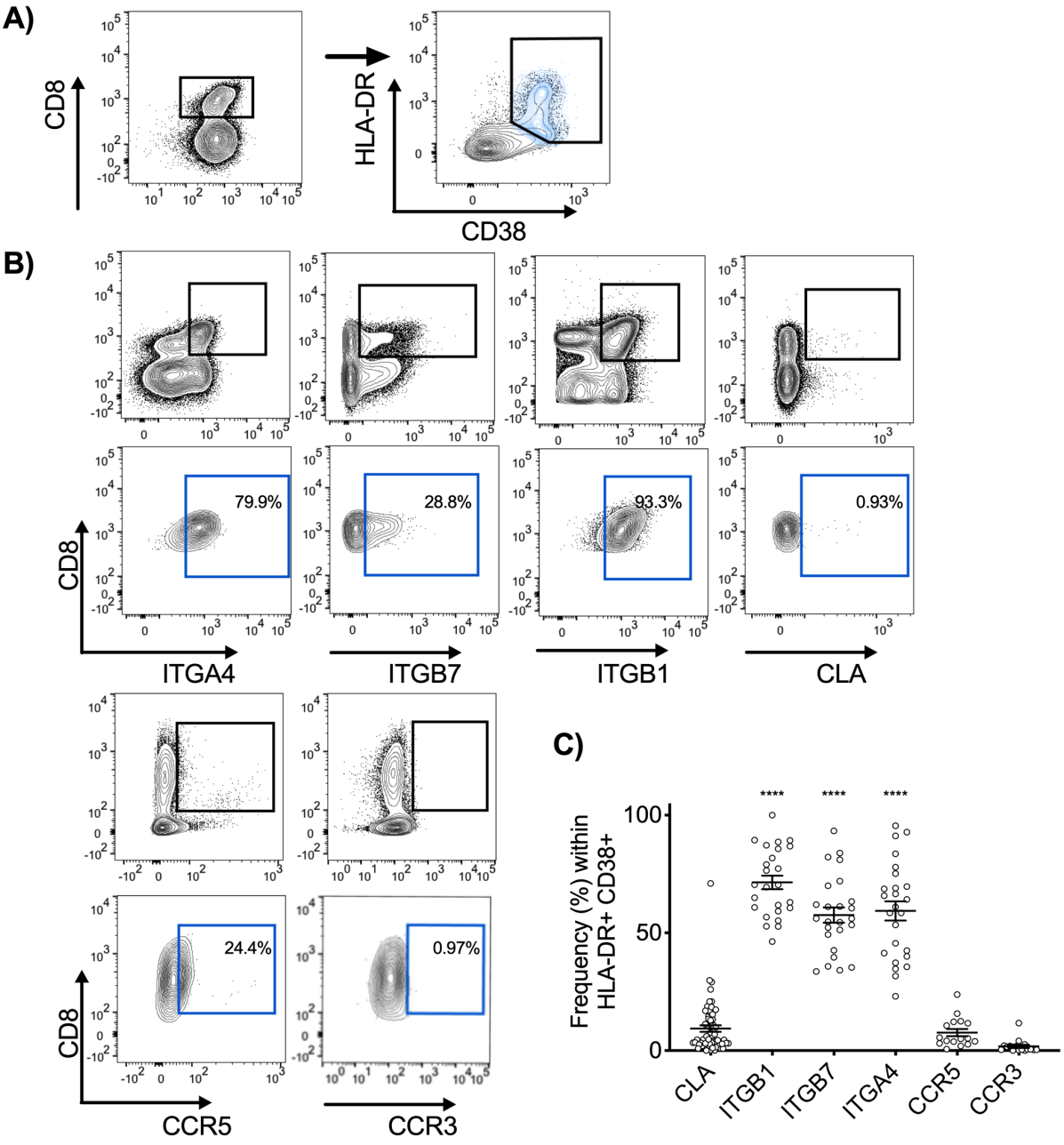

Figure 4.14: Analyses of homing marker expression during the 2018 outbreak. Using bench-top 8 -color flow cytometry expression of homing markers was analyzed on activated CD8⁺ T cells on patient samples collected during the 2017/2018 LF outbreaks at Irrua specialist Teaching Hospital, Nigeria. PBMCs were isolated from whole blood and cells stained for analysis immediately. Activation was determined by co-expression of CD38 and HLA-DR (A). Gating was performed on total T-cell compartment (black) and exemplary plots (blue) for each investigated marker on activated CD8⁺ T cells are shown (B). Frequency (%) within the activated CD8⁺ compartment was analyzed for each marker. Mean and SEM are depicted in plot (C). Statistical significance was determines using Kruskal-Wallis test, followed by Dunn's multiple comparisons test. Significance levels are presented as follows: ns = $p > 0.05$; * = $p \leq 0.05$; ** = $p \leq 0.01$; *** = $p \leq 0.001$; **** = $p \leq 0.0001$. Abbreviations: ITGB7, β7 integrin; ITGB1, β1 integrin; ITGA4, α4 integrin; CCR, chemokine receptor; CLA, cutaneous lymphocyte antigen.

As the analysis of multiple markers was restricted due to the field setup, attention was further focused on the potential interplay between the investigated integrins. While it could be expected to observe both T cells expressing either α4β1 integrin or α4β7 integrin, it was of note, that nearly 10 % of T cells expressed both integrin dimers simultaneously **(Figure 4.15)**.

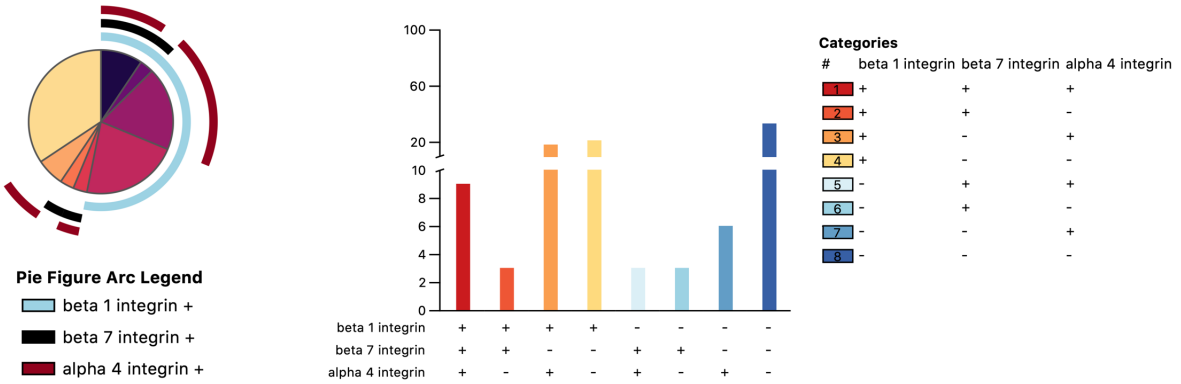

Figure 4.15: Co-expression of integrin homing markers: Bench-top flow cytometry was employed to evaluate homing marker expression levels and co-expression of integrins was analyzed. SPLICE plots visualized co-expression pattern of α4, β1 und β7 integrins.

As variability was observed amongst patients, it was of further interest to investigate the interplay between various homing markers in more detail. To this end, an in depth-multiparametric flow-cytometry analysis was conducted at BNITM using cryopreserved patient samples. Both $CD4^+$ and $CD8^+$ T-cell phenotypes were investigated. After performing sample quality analysis, 54 high quality samples from 23 patients could be phenotyped **(Figure 4.16 A)**. No significant difference was observed between outcome of disease and days post-onset of sample collection **(Figure 4.16 B)**.

Based on the findings made in the field cohort and on order to increase the analysis of tissue specific homing markers, expression analysis of CLA (skin), α4 and β7 integrin (intestine) and CCR3 (airways) was broadened to include chemokine receptors CCR4, which facilitates entry to skin and airway epithelium (Campbell, Brightling, et al., 2001; Kunkel et al., 2002). Additionally, also CCR7, vital for lymphoid tissue homing (Förster et al., 2008), integrin αE (CD103), a marker of residency, and α1 integrin (CD49a), also a marker of residency and inflammatory mucosal homing (Amsen, van Gisbergen, Hombrink, and van Lier, 2018; Sandoval et al., 2013; Stanley Cheuk et al., 2017), were studied. As CCR5 and β1 integrin

have been described as markers for general inflammation, they were excluded from further analysis.

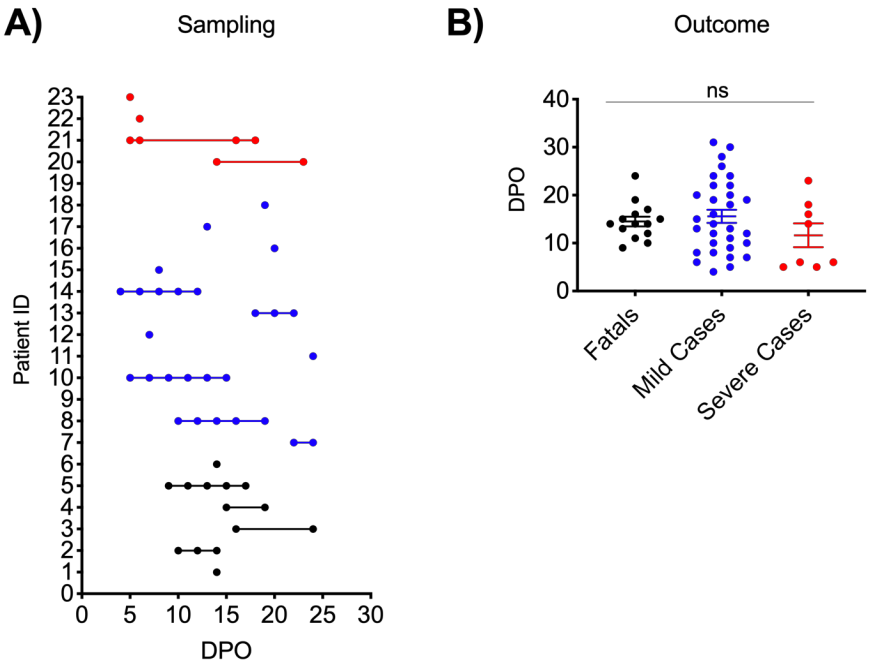

Figure 4.16: Sampling scheme. After quality analysis, 54 samples from 23 patients at various time point during the acute phase and early convalescence were analyzed (A). Outcome specific relation to days post-onset is shown in (B). Fatals (black) Mild Cases (blue), Severe Cases (red). Abbreviations: DPO, self-reported days post-onset. Statistical significance was determines using Kruskal-Wallis test, followed by Dunn's multiple comparisons test. Significance levels are presented as follows: ns = $p > 0.05$; * = $p \leq 0.05$; ** = $p \leq 0.01$; *** = $p \leq 0.001$; **** = $p \leq 0.0001$.

To first characterize the kinetics of T-cell homing during acute LF, longitudinal analysis was performed. Interestingly, CLA, CCR4, CCR3 and β7 integrin showed no significant change in expression in either $CD4^+$ or $CD8^+$ activated compartments over time **(Figure 4.17 A)**. Only α1 integrin and α4 integrin expression increased with time in both T-cell subsets significantly, which implies an increased inflammatory mucosal homing and tissue retention ability. CCR7 expression decreased in $CD4^+$ T cells, suggesting a loss of recruitment to the lymphoid organs.

As tissue-specific homing markers CLA, CCR4, CCR3 and β7 integrin showed no significant change in expression over time, this allowed cross-sectional analysis of the tissue-specific signatures. An analysis of different patients, based on first available sample of each patient and limited to collection time points < 16 days post self-reported onset showed that homing marker expression varied considerably between patients **(Figure 4.17 B)**. As described, the

activated compartment of both CD4$^+$ and CD8$^+$ T cells was analyzed. Skin, intestine and respiratory homing marker expression differed between CD4+ and CD8+ T cells but, in concordance with longitudinal analysis, no time-based clustering was observed even at these early time points.

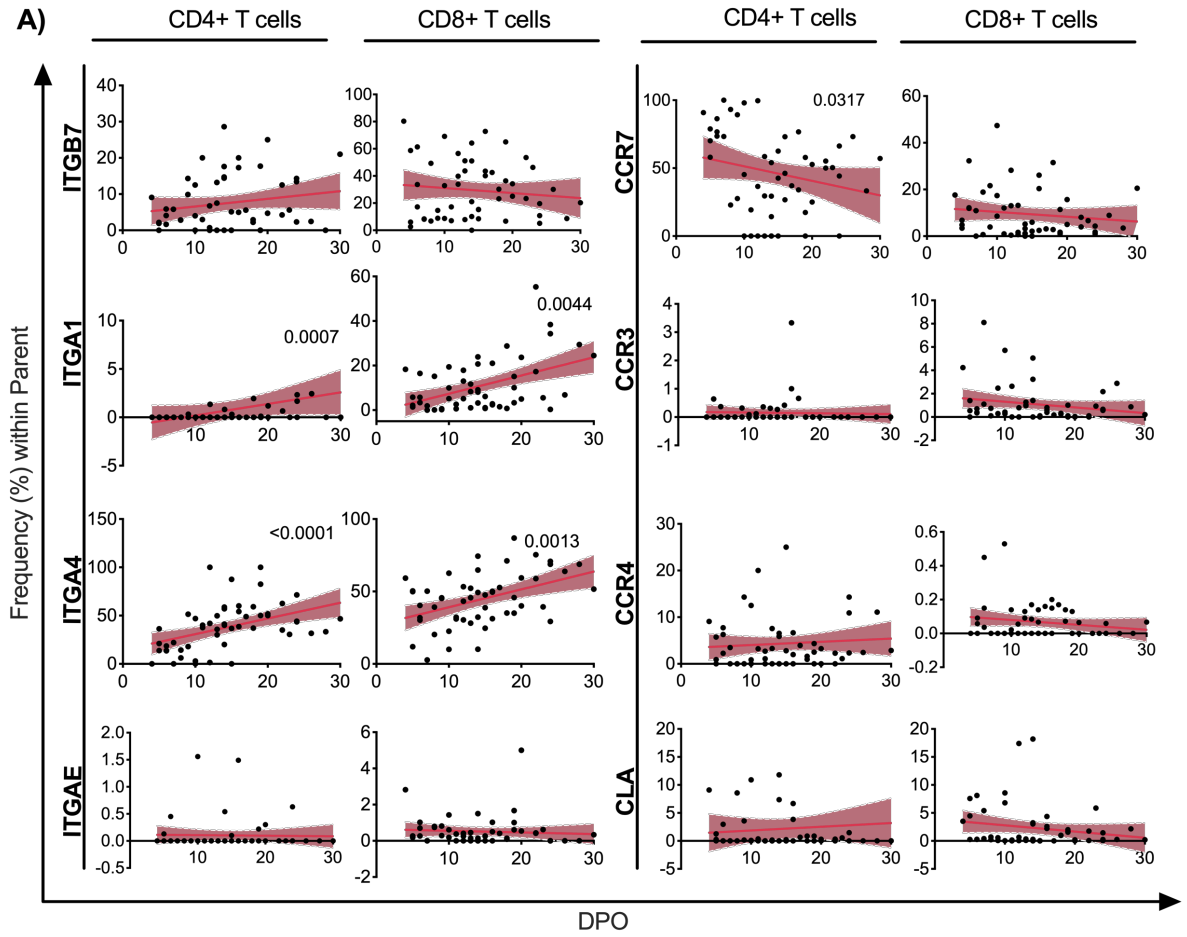

Figure 4.17: T-cell homing signatures in LF. Using multiparametric flow-cytometry, homing markers for skin, intestine and lung were phenotyped in the HLA-DR$^+$ CD38$^+$ compartments of CD4$^+$ and CD8$^+$ T cells. Longitudinal analysis was performed on CD4 and CD8 homing marker expression in the respective activated compartments (A). Trendlines and 95 % confidence intervals (CIs) are depicted in red; if significant, p-value is indicated (Spearman correlation analysis). Early cross-sectional analysis is depicted in (B). Data was normalized, and expression level is depicted according to color key. DPO 1-9 = black, DPO 10-16 = blue. Dendrogram clustering is shown for patients. Abbreviations: DPO, days post-onset; ITGB7, β7 integrin; ITGA1, α1 integrin; ITGA4, α4 integrin; ITGAE, αE integrin; CCR, chemokine receptor; CLA, cutaneous lymphocyte antigen.

4.3.2 T-CELL HOMING DIFFERENTIATES FATAL OUTCOME AND SURVIVAL

As the cross-sectional analysis of signatures implied a separation of patients based on homing signatures, a principal component analysis (PCA) was performed to further illuminate this observation. PCA allows dimensional reduction of multi-parametric data and visualization of strong patterns amongst samples. PCA was performed on cross-sectional and longitudinal samples on the homing and residency markers expressed in the activated $CD38^+$ $HLA\text{-}DR^+$ $CD4^+$ and $CD8^+$ compartments **(Figure 4.18 A)**. Using unsupervised hierarchical clustering, 4 main clusters were determined. Multiple observations were made based on the clustering results and the homing marker expression driving those clusters.

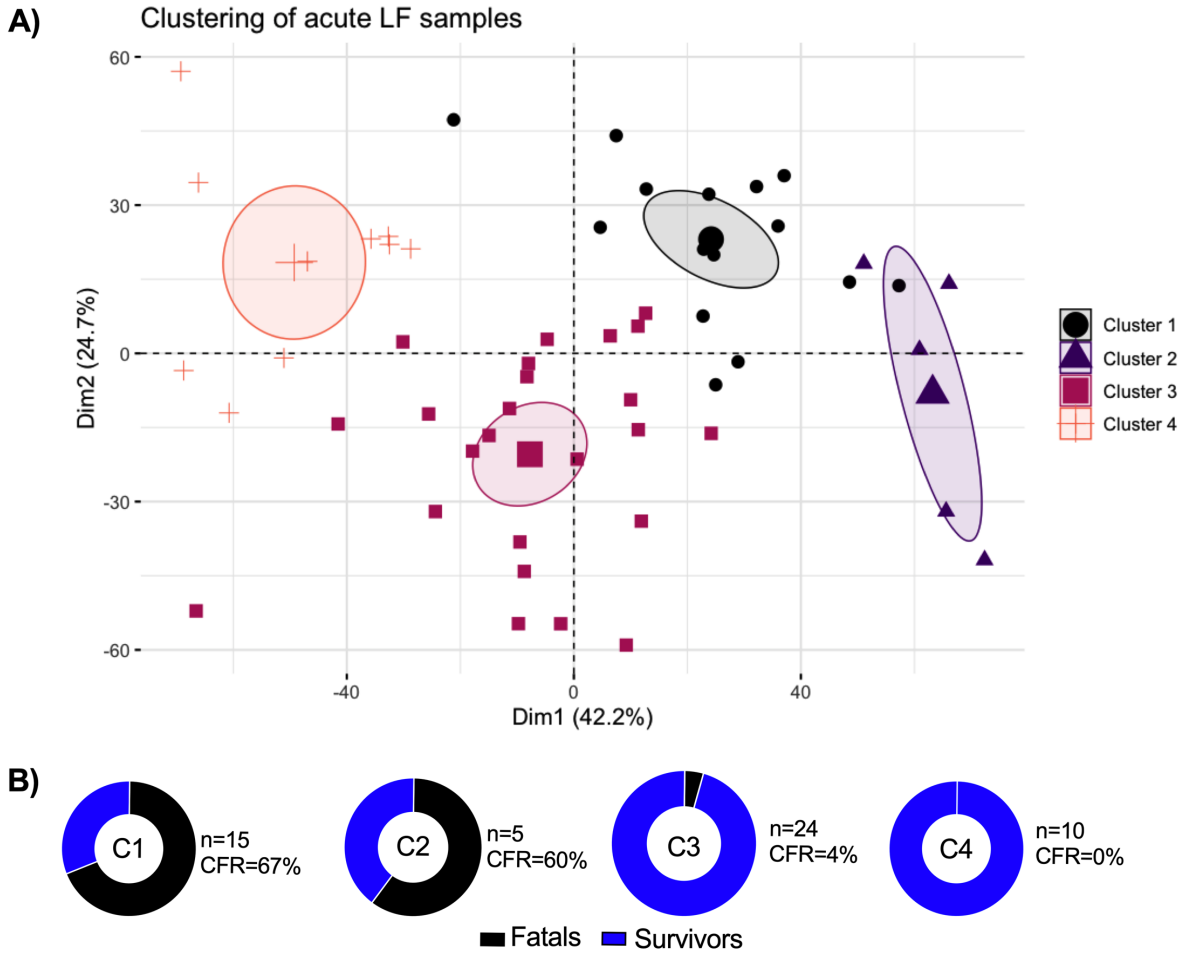

Figure 4.18: Clustering of LF patients based on homing signature: Multi-parametric flow cytometry was utilized to analyze homing markers expressed on both activated $CD4^+$ and $CD8^+$ T cells in human acute LF (N = 54). Activation was determined by co-expression of CD38 and HLA-DR. Principle component analysis was performed on homing marker expression (A). Clustering of samples was based on hierarchical analysis to identify main subsets. CFR for each cluster was calculated based on outcome of disease of the corresponding patient linked to each sample (B). Abbreviations: Dim, dimension; C, cluster; CFR, case fatality ratio.

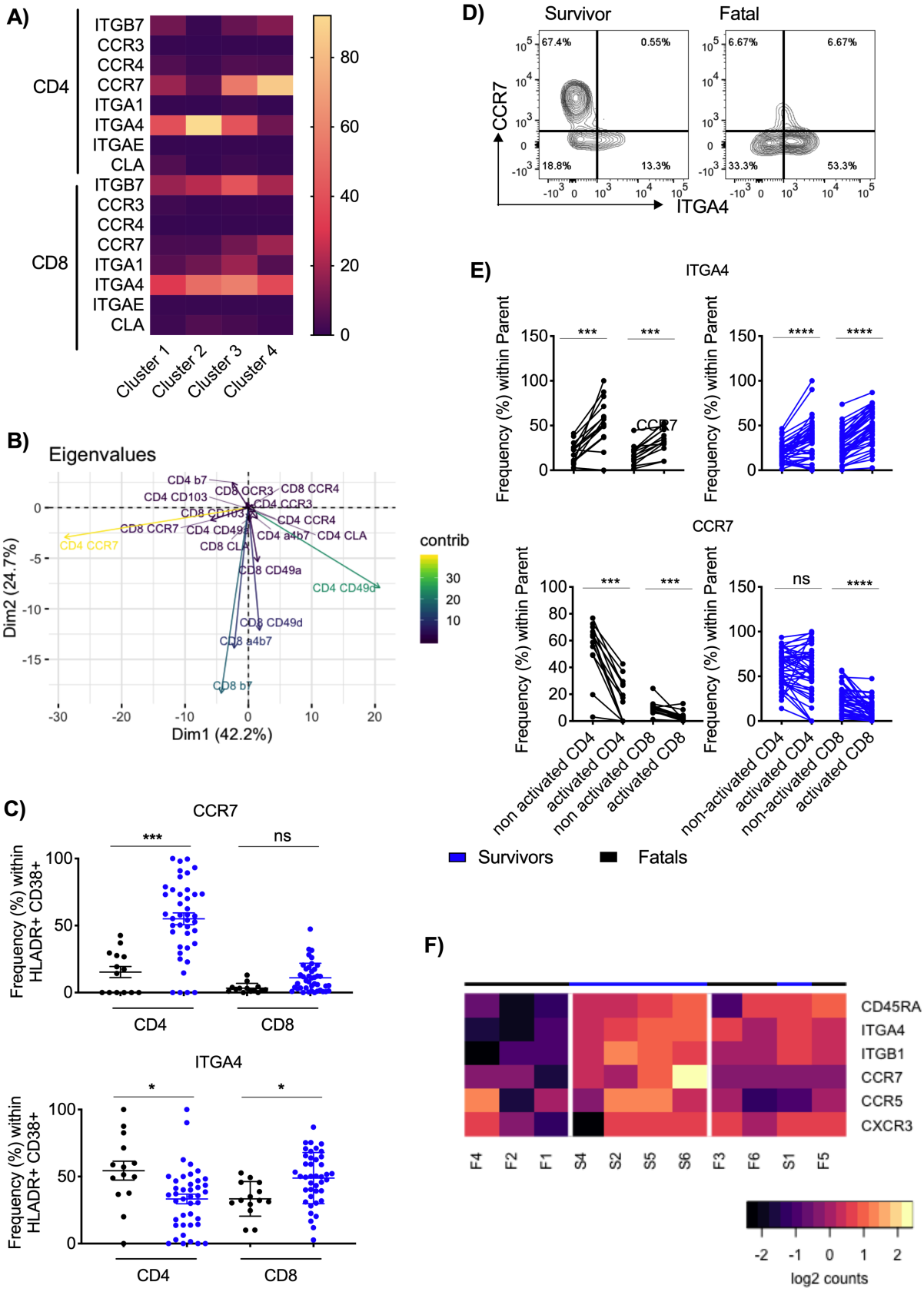
A)
CD4
CD8
ITGB7
CCR3
CCR4
CCR7
ITGA1
ITGA4
ITGAE
CLA
80
60
40
20
0
Cluster 1
Cluster 2
Cluster 3
Cluster 4
B)
Eigenvalues
CD4 b7
CD8 CCR3
CD8 CCR4
CD4 CD103
CD4 CCR3
CD8 CD103
CD4 CCR4
CD8 CCR7
CD4 CD49d
CD4 a4b7
CD4 CLA
CD4 CCR7
CD8 CLA
CD8 CD49a
CD4 CD49d
CD8 CD49d
CD8 a4b7
CD8 b7
contrib
30
20
10
Dim2 (24.7%)
Dim1 (42.2%)
C)
CCR7
***
ns
Frequency (%) within HLADR+ CD38+
CD4
CD8
ITGA4
*
*
D)
Survivor
Fatal
CCR7
ITGA4
67.4%
0.55%
18.8%
13.3%
6.67%
6.67%
33.3%
53.3%
E)
ITGA4
CCR7
Frequency (%) within Parent
***
****
ns
non activated CD4
activated CD4
non activated CD8
activated CD8
non-activated CD4
Survivors
Fatals
F)
CD45RA
ITGA4
ITGB1
CCR7
CCR5
CXCR3
F4
F2
F1
S4
S2
S5
S6
F3
F6
S1
F5
-2
-1
0
1
2
log2 counts

Figure 4.19: Impact of homing markers on clustering. Mean expression level for each homing marker in activated $CD4^+$ or $CD8^+$ T cells is depicted for each cluster determined through hierarchical clustering and PCA (A). Coloring of the Heatmap refers to color bar on the right. Eigenvalues for each homing marker are shown (B), contribution to dimension 1 and 2 is indicated according to color bar on the right. Expression of CCR7 and α4 integrin was compared between Fatals and Survivors (C) and representative plots of activated $CD4^+$ T cells are shown (D). Expression of both markers was compared between the activated and non-activated T-cell compartments (E). Nanostring transcriptomic analysis was utilized to investigate mRNA expression of homing markers in PBMCs for selected inflammatory and lymphoid markers, also including CD45RA (F). Patients were clustered based on expression profile and log2 counts of genes are depicted. White line indicates clusters, colors refer to color bar below. Fatals are shown in black, Survivors in blue. Statistical significance was determines using Mann-Whitney test. Significance levels are presented as follows: ns = $p > 0.05$; * = $p \leq 0.05$; ** = $p \leq 0.01$; *** = $p \leq 0.001$; **** = $p \leq 0.0001$. Abbreviations: Dim, dimension; ITGA4, α4 integrin; CCR, chemokine receptor; LASV, Lassa virus; ITGB1, β1 integrin.

First, it became evident that fatal outcome and survival were not evenly distributed **(Figure 4.18 B).** Clusters 1 (N = 15) and the notably smaller cluster 2 (N = 5) grouped together samples from fatal cases, with respective case fatality ratios (CFR) of 67 % and 60 %. In contrast, clusters 3 (N = 24) and 4 (N = 10), were comprised mostly of samples from patients that survived (CFR = 4 % and 0 %, respectively). Second, only selected homing markers drove this separation. The frequency of expression for each homing marker was considered for each cluster. Of note, expression of lymphoid marker CCR7 was increased in clusters 3 and 4 **(Figure 4.19 A)**. Highest expression of α4 integrin was observed in cluster 2 for $CD4^+$ T cells and, conversely, in cluster 3 for $CD8^+$ T cells. In fact, $CD4^+$ T-cell expression of CCR7 and α4 integrin contributed to explain most of the variance from dimension 1 **(Figure 4.19 B).** Moreover, Survivors had significantly higher expression of CCR7 amongst activated $CD4^+$ T cells compared with Fatals, a trend that is mirrored in activated $CD8^+$ T cells, however not significant **(Figure 4.19 C/D)**. Expression of α4 integrin also showed significant overall difference between Fatals and Survivors. As expected from the cluster analysis, Fatals expressed higher frequency of α4 integrin in the activated $CD4^+$ compartment, Survivors did so in the activated $CD8^+$ compartment **(Figure 4.19 C/D)**. It is thought that T cells downregulate CCR7 expression when they become activated and effector type cells (Campbell, Murphy, et al., 2001). As expected, when considering all outcomes, CCR7 expression frequency decreased in activated $CD4^+$ T cells compared to the non-activated compartment. Particularly interesting though, when separated by outcome, CCR7 expression frequency was not significantly decreased in Mild Cases and Severe Cases, but even increased in some cases. In Fatals, however, a sharp decrease in expression was observed **(Figure 4.19 E**). In comparison, α4 integrin expression was increased in all outcome groups

significantly in both CD4$^+$ and CD8$^+$ T cells. Especially in CD4$^+$ T cells magnitude of expression was higher in Fatals compared with Survivors.

Using nanostring-based transcriptomic analysis of gene expression in a small sample cohort RNA extracted from PBMCs was analyzed **(Figure 4.19 F)**. In support of the phenotypical flow cytometry data, CCR7 gene expression was also elevated in Survivors compared to Fatals. Also, in concordance with the clustering results of the PCA, expression of α4 integrin was elevated in some Fatals (corresponding to cluster 2) and low in others (corresponding to innermost edge of cluster 1). This group of Fatals identified in the transcriptomics analysis, also showed decreased levels of expression of CCR5, CXCR3 and β1 integrin, indicating low homing potential to inflamed mucosae.

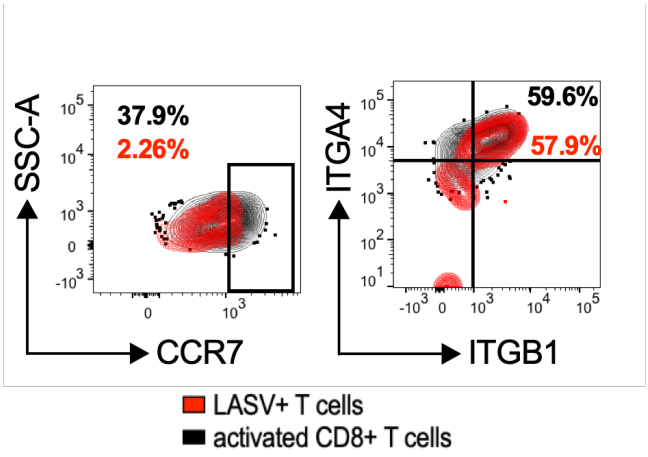

Figure 4.20: Homing profile of LASV-specific T cells. Expression of CCR7 and α4 integrin was analyzed for LASV-specific T cells identified by tetramer staining. Representative overlay plots are shown, activated CD8+ T cells are shown in black, LASV-specific T cells in red. Abbreviations: ITGA4, α4 integrin; CCR, chemokine receptor; ITGB1, β1 integrin; SSC-A, sideward scatter area.

Additionally, the antigen specificity of the CD8$^+$ T cells expressing CCR7 and α4 integrin was investigated. LASV-specific T cells showed equal amounts of α4 expression as the total activated population. In contrast, CCR7 expression in LASV-specific T-cells was notably absent **(Figure 4.20)**. This pattern was, interestingly, a match to the previously shown homing profile after re-stimulation with inactivated virus, which also demonstrated the same findings for CD4$^+$ T cells. This data suggests, that the T-cell response in survivors might be dominated by recently activated effector T-cells that still retain their lymphoid homing capacity, while in Fatals the CD4$^+$ T-cell response is characterizes by increased recruitment to inflammation, which could drive pathogenesis. Interestingly, tetramer analysis and phenotypical analysis after stimulation demonstrated that LASV-specific T cells do not retain lymphoid homing capacity and are strongly expressing inflammatory-homing signatures. This suggests that LASV-specific CD4$^+$ T-cell recruitment to inflammation might be involved to an increased degree in the response seen in Fatals, while the response in Survivors might rely more on tissue-recruitment of LASV-specific CD8$^+$ T cells.

While particularly expression of β7 integrin, followed by α4 and α1 integrins in the CD8+ T cells drove variance in dimension 2, this did not contribute significantly to the separation of fatal outcome and survival (data not shown). However, particularly clusters 3 and 4, including mostly samples from Survivors, were affected by differences of those markers. Distribution of samples from Mild and Severe Cases in cluster 3 and 4 was not equal **(Figure 4.19 B).** After dimensional reduction only 66.6 % of the variation between samples was explained by the first 2 new dimension (Dim1 and 2), implicating also that additional relevant differences existed in the homing signatures which contributed to variability but where not evident on this level. To better understand the differences between Mild and Severe Cases, we sought to determine whether smaller subpopulations of T cells could exist with specific phenotypes that were unique to each outcome group, but not sizeable enough in number to lead to statistical significance.

One tool to identify and analyze such unique subpopulations is t-distributed Stochastic Neighbor Embedding (tSNE). Based on the original flow cytometric expression data for each included marker tSNE analysis will generate a 2-dimensional map distributing single cells according to their phenotypical similarities, hence creating an “geographic” atlas of each single phenotype that exists within the population under investigation. As described, co-expression of HLA-DR and CD38 was used to identify the activated T-cell compartment. For further analysis, activated $CD8^+$ and $CD4^+$ T cells were combined across all samples, respectively and tSNE dimensional reduction and analysis was performed on the total population of activated T cells. tSNE was calculated on homing marker expression CLA, CCR3, CCR4, CCR7, α4 and β7 integrin, including also residency markers αE integrin, α1 integrin and CD45RA for further identification of effector and memory status. Hence an atlas of each single homing-related phenotype a T cell can express during acute LF was generated **(Figure 4.21 A; Supplemental Figure 8.5).**

The geographical distribution of activated $CD8^+$ T cells was mapped using the newly calculated tSNE dimensions **(Figure 4.21 B).** Cells originating from the three different outcome groups inhabited different regions and 18 clusters were identified, comprising cells originating to > 80 % from only one outcome group **(Figure 4.21 C)**. Interestingly, 4 of the clusters identified as unique T-cell populations occurring in Fatals had high expression of CCR7, expression of CCR3 combined with varying levels of α4 integrin, but absent expression of other homing markers and of CD45RA. In the context of the overall CCR7 expression observed in Fatals, this suggests that a unique activated $CD8^+$ T-cell population exists with T_{CM} phenotype and homing potential to the respiratory tract (**Figure 4.21 D/E)**.

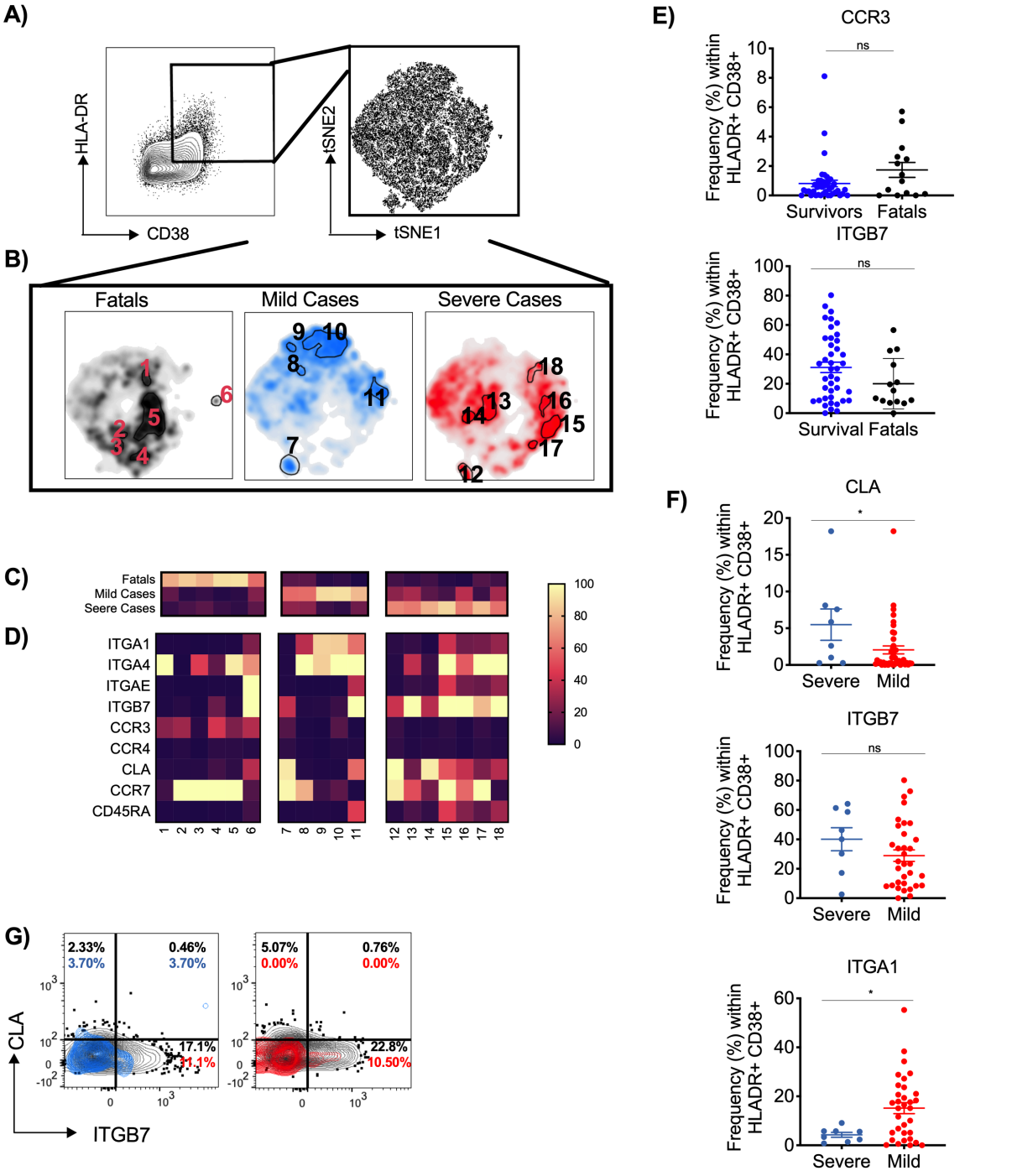
A)
HLA-DR
CD38
tSNE2
tSNE1
B)
Fatals
Mild Cases
Severe Cases
C)
Fatals
Mild Cases
Seere Cases
D)
ITGA1
ITGA4
ITGAE
ITGB7
CCR3
CCR4
CLA
CCR7
CD45RA
E)
CCR3
Frequency (%) within HLADR+ CD38+
ns
Survivors
Fatals
ITGB7
Survival
F)
CLA
Severe
Mild
G)
2.33%
3.70%
0.46%
3.70%
17.1%
21.1%
5.07%
0.00%
0.76%
0.00%
22.8%
10.50%
CLA
ITGB7

Figure 4.21: Unique CD8⁺ T-cell populations in Lassa Fever. Activated (CD38⁺ HLA-DR⁺) CD8⁺ T cells were concatenated across all patient samples. Input across outcome groups was normalized. tSNE was calculated on homing marker expression CLA, CCR3, CCR4, CCR7, α4 and β7 integrin, including also residency markers αE integrin, α1 integrin and CD45RA for further identification of effector and memory status. (A). Populations unique for each outcome were identified by automated density-based gating. (B). For each identified population, percentage (%) of contribution from each outcome was verified (C) and expression frequency (%) of each marker is shown according to color bar on the right (D). Frequency of expression was compared between Fatals (black), Mild Cases (blue) and Severe Cases (red) for selected homing markers (E/F). Representative plots show overlay of LASV-specific T cells (colored) on total of activated CD8⁺ T cells (black) for one Mild and one Severe Survivor depicting expression of homing markers (G). Abbreviations: ITGB7, β7 integrin; ITGA1, α1 integrin; ITGA4, α4 integrin; ITGAE, αE integrin; CCR, chemokine receptor; CLA, cutaneous lymphocyte antigen; tSNE, t-distributed stochastic neighbor embedding. Statistical significance was determines using Mann-Whitney test. Significance levels are presented as follows: ns = $p > 0.05$; * = $p \leq 0.05$; ** = $p \leq 0.01$; *** = $p \leq 0.001$; **** = $p \leq 0.0001$.

Different populations of activated CD8⁺ T cells were enriched in Mild Cases compared to Severe Cases. Of note, 4 populations identified as unique to Mild Cases express high levels of α1 integrin, while unique populations identified in Severe Cases are characterized by expression of CLA, β7 integrin. As nearly all unique clusters in Mild and Severe Cases were characterized by expression of the above-mentioned markers, overall expression of these homing markers was compared between survivors. Interestingly, it was confirmed that Mild Cases expressed significantly more α1 integrin, while Severe Cases expressed significantly more CLA and a trend towards higher expression of β7 integrin was confirmed (**Figure 4.21 F)**. The unique populations in Severe Cases were additionally expressing CCR7 and CD45RA, implicating that these are T_{eff} with homing potential to both the intestine and skin. Using LASV-specific tetramer staining CLA and β7 integrin expression in survivors was compared between activated T cells and LASV-specific T cells (**Figure 4.21 G)**. A subset of LASV-specific T cells could be demonstrated to express also CLA or β7 integrin, suggesting that the homing marker expression is representative for LASV-specific and bystander T cells involved in the response.

Similar analysis was executed for activated CD4⁺ T cells. Here, geographic distribution of cells differed less intensely as compared of CD8⁺ T cells. Only 12 unique populations could be identified with >50 % unique origin from one of that outcome groups **(Figure 4.22; Supplemental Figure 8.6)**. Interestingly, the populations identified as enriched in Fatals showed no noteworthy homing marker expression besides α4 integrin combined with a T_{EM} phenotype ($CCR7^-$ $CD45RA^-$) while enriched populations in both Mild and Severe Cases expressed CLA and showed medium to high frequency of CCR7. As CD45RA expression was absent, these populations would classically be identified as T_{CM}.

In summary, these data demonstrate a relationship between LF severity and T-cell homing. While the differences between fatal outcome and survival were driven by expression of lymphoid homing marker CCR7 in Survivors and α4 integrin on $CD4^+$ T cells in Fatals, multiple small population of $CD8^+$ T cells could be identified, which were uniquely enriched in each disease outcome group. Especially of interest, Severe Cases were characterized by increased expression of skin homing marker CLA and intestinal marker β7 integrin, while Mild Cases showed increased expression of α1 integrin. This suggests that severe disease involves increased recruitment of cytotoxic T cells to the gut and, partially, to the skin, while mild disease is characterized by cytotoxic T cells with increased potential for tissue retention.

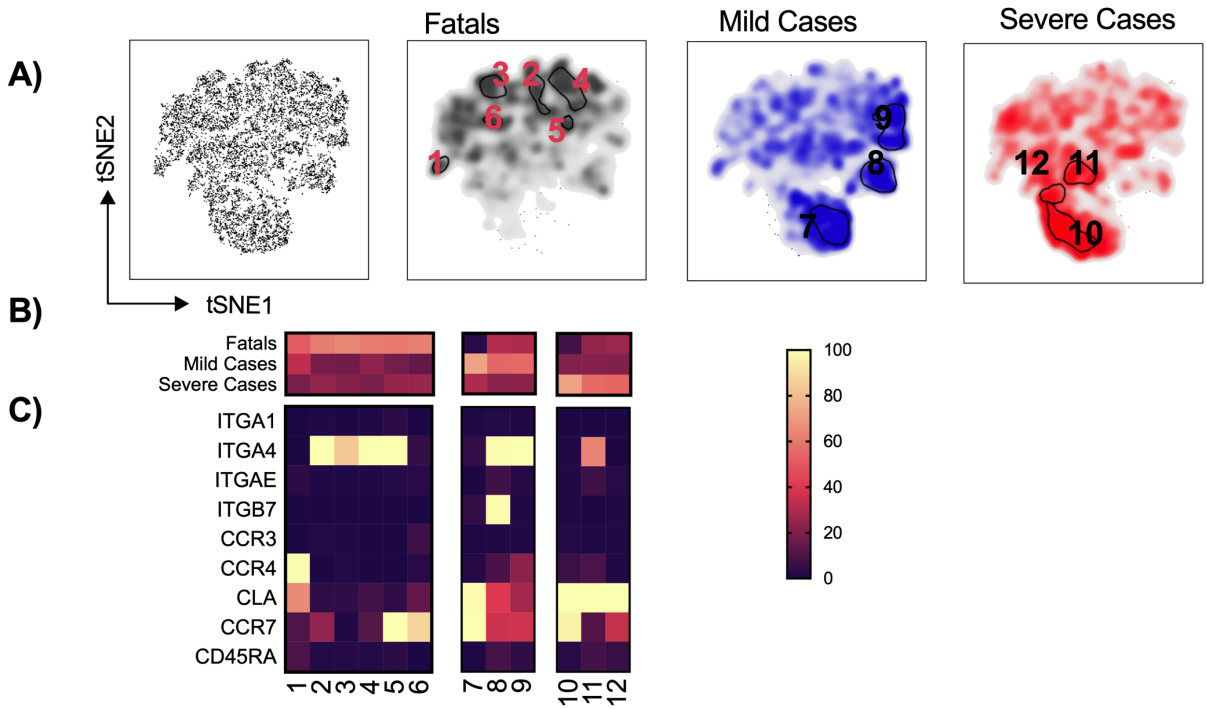

Figure 4.22: Unique $CD4^+$ T-cell populations in LF. Activated ($CD38^+$ $HLA\text{-}DR^+$) $CD4^+$ T cells were concatenated across all patient samples. Input across outcome groups was normalized. tSNE was calculated on homing marker expression CLA, CCR3, CCR4, CCR7, α4 and β7 integrin, including also residency markers αE integrin, α1 integrin and CD45RA for further identification of effector and memory status. Populations unique for each outcome were identified by automated density-based gating. (A). For each identified population, percentage (%) of contribution from each outcome was verified (B) and expression frequency (%) of each marker is shown according to color bar on the right (C). Abbreviations: ITGB7, β7 integrin; ITGA1, α1 integrin; ITGA4, α4 integrin; ITGAE, αE integrin; CCR, chemokine receptor; CLA, cutaneous lymphocyte antigen; tSNE, t-distributed stochastic neighbor embedding.

4.3.3 T-CELL HOMING IN RELATION TO DISEASE BIOMARKERS

Based on the findings of the PCA and tSNE analysis, relationships of selected homing markers and disease parameters were further analyzed **(Figure 4.23).** Viremia, measured as RNA copies/mL, and AST serum level have previously been described as indicators for disease severity. Analysis was performed only on samples were both clinical parameters were available. In this study cohort, AST levels, as described, were significantly higher in Severe Cases and Fatals, as compared to Mild Cases. This observation was also made with respect to viremia **(Figure 4.23 A).** And, as expected both parameters showed a highly significant positive correlation.

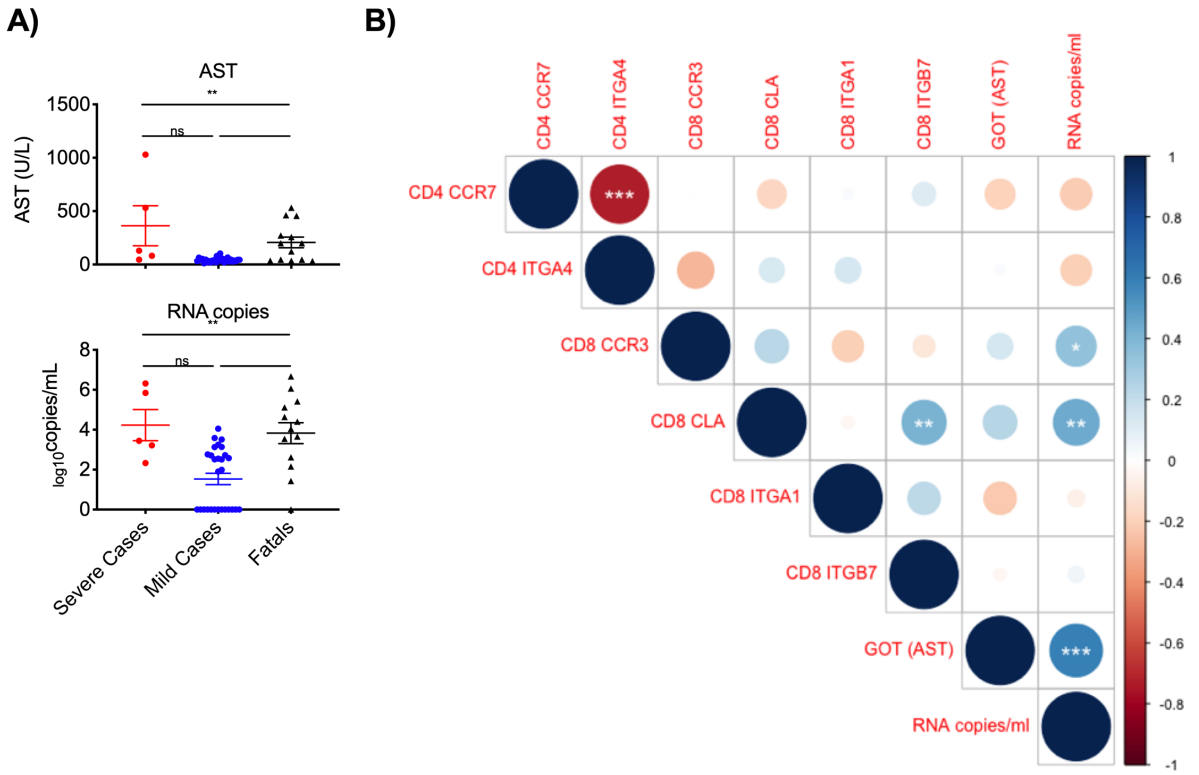

Figure 4.23 Correlation of Homing markers and clinical parameters. AST (U/L) and viremia (RNA copies/ml whole blood) were measured for study participants (A). Using multi-parametric flow cytometry homing marker expression was analyzed on $CD4^+$ and $CD8^+$ T cells during acute LF. Correlation is visualized by size of circle according to R^2 legend on the right and significance level is indicated. Relationship with RNA copies/mL and AST, indicators of disease severity, is depicted (B). Analysis was performed only on subset of samples were both measurements were available (N = 47). Statistical significance was determines using Kruskal-Wallis test, followed by Dunn's multiple comparisons test, or Spearman correlation analysis. Significance levels are presented as follows: ns = $p > 0.05$; * = $p \leq 0.05$; ** = $p \leq 0.01$; *** = $p \leq 0.001$; **** = $p \leq 0.0001$. Abbreviations: ITGB7, β7 integrin; ITGA1, α1 integrin; ITGA4, α4 integrin; ITGAE, αE integrin; CCR, chemokine receptor; CLA, cutaneous lymphocyte antigen; AST, serum level aspartate transaminase.

As expected, a highly significant negative correlation existed between CCR7 and α4 integrin in activated $CD4^+$ T cells **(Figure 4.23 B).** Interestingly, CCR7 in $CD4^+$ T cells expression showed a negative correlation trend also with AST and LASV RNA copies in the blood, confirming that CCR7 expression in $CD4^+$ T cells is higher in individuals with lower disease severity. CCR3 expression in $CD8^+$ T cells was positively correlated with LASV RNA copy number, which fit with the observation of an enrichment of activated $CCR3^+$ $CD8^+$ T cells in Fatals with high viremia. Interestingly, expression of CLA strongly correlated to expression of β7 integrin, which matched the observation of unique populations of $CD8^+$ T cells co-expressing both in Severe Cases. However, only expression of CLA in $CD8^+$ T cells correlated positively and significantly with RNA copies, not β7 integrin. Even though enrichment of T_{CM} was observed in Mild Cases expressing α1 integrin, only a non-significant negative trend with both disease parameters was noted.

4.4 NATURAL ROUTES OF EXPOSURE AND INFECTION AND THE RELATED T-CELL RESPONSE

Characterization of T-cell activation, antigen-specific response and homing in acute human LF suggested a relationship between disease severity and T-cell homing. To further investigate this relationship, we went back to the animal models to study the patterns of T-cell homing in mice infected via different routes.

4.4.1 IFNAR BONE MARROW CHIMERIC MICE ARE SUSCEPTIBLE TO NATURAL ROUTES OF INFECTION

Previous work in animal models has relied only on applications through intraperitoneal (i.p.) or subcutaneous (s.c.) infection (Carrion et al., 2007; Oestereich, et al., 2016; Yun and Walker, 2012). The mouse model established by Oestereich et al., has been demonstrated to be highly susceptible to i.p. exposure and to undergo systemic infection after infection with non-adapted LASV. We used this mouse model to investigate whether infection through respiratory, oral and skin in these mice induced different disease manifestations and outcome.

IFNAR chimeras were generated by irradiation of recipient $IFNAR^{KO}$, followed by bone marrow transplantation from immunologically fully functional wild type donors **(Figure 4.24 A).** Exposure to LASV through the respiratory mucosa was mimicked by i.n. inoculation. Application of the virus through a feeding needle into the esophagus, per os (p.o.), was

utilized to mimic oral exposure and exposure through small skin lesions was imitated by intradermal (i.d.) inoculation **(Figure 4.24 B).** In all three routes mice were exposed to 1000 FFU of LASV (recombinant BA366), which was previously published as 100 % lethal in this model (Oestereich, et al., 2016). To evaluate morbidity and mortality, measurements of body temperature and weight were taken daily. Viremia and serum AST levels were determined in blood at day 3, 7 and 10 post infection. An additional measurement was taken at the experimental endpoint.

Mice exposed to LASV through the respiratory mucosa (i.n. infection), developed systemic infection. Animals showed significant weight loss starting at day 6 post infection **(Figure 4.24 C)** and increased temperature starting also from day 6 post infection **(Figure 4.24 D).** Virus was detectable at day 7 post infection in the blood **(Figure 4.24 E)** which coincided with elevated AST serum levels, which increased significantly over time. In comparison, oral exposure resulted also in high lethality (60 %) but the time-of-death was delayed with respect to i.n. infection. After oral exposure mice showed increased temperatures at day 8 post infection, which coincided with first sign of weight loss. A severe drop in temperature was observed shortly before death. Mice also showed blood viremia at day 7 post-infection and elevated AST levels. Interestingly, AST levels at day 7 were higher compared to i.n. infection but remained at this level or decreased with time. In contrast, exposure through skin (i.d. infection) resulted in the mildest course of LF in the model. Significant losses of weight and body temperature were observed early on, but mice recovered starting from day 9 post-infection. Viremia could be observed in some animals at day 10 post exposure at low levels and serum AST was only minimally above control mice on day 3 and 10 post infection. However, 25 % of mice succumbed to disease, with day of death varying between days 10 and 12.

To further characterize the disease pathogenicity of the three exposure routes, virus titers in organs were determined for brain, lung, liver, kidney heart and small intestine for animals that succumbed to disease **(Figure 4.24 H)**. At the experimental endpoint, mice that died after i.d. infection overall had lower organ titers compared to i.n. and p.o. infection, even though virus was present in the blood and animals showed signs of disease. Comparing i.n. and p.o. infection, organ viral titers were higher in lung, brain, heart and kidney after i.n. infection. Interestingly, p.o. infection showed higher titers in kidney and, as expected, small intestine.

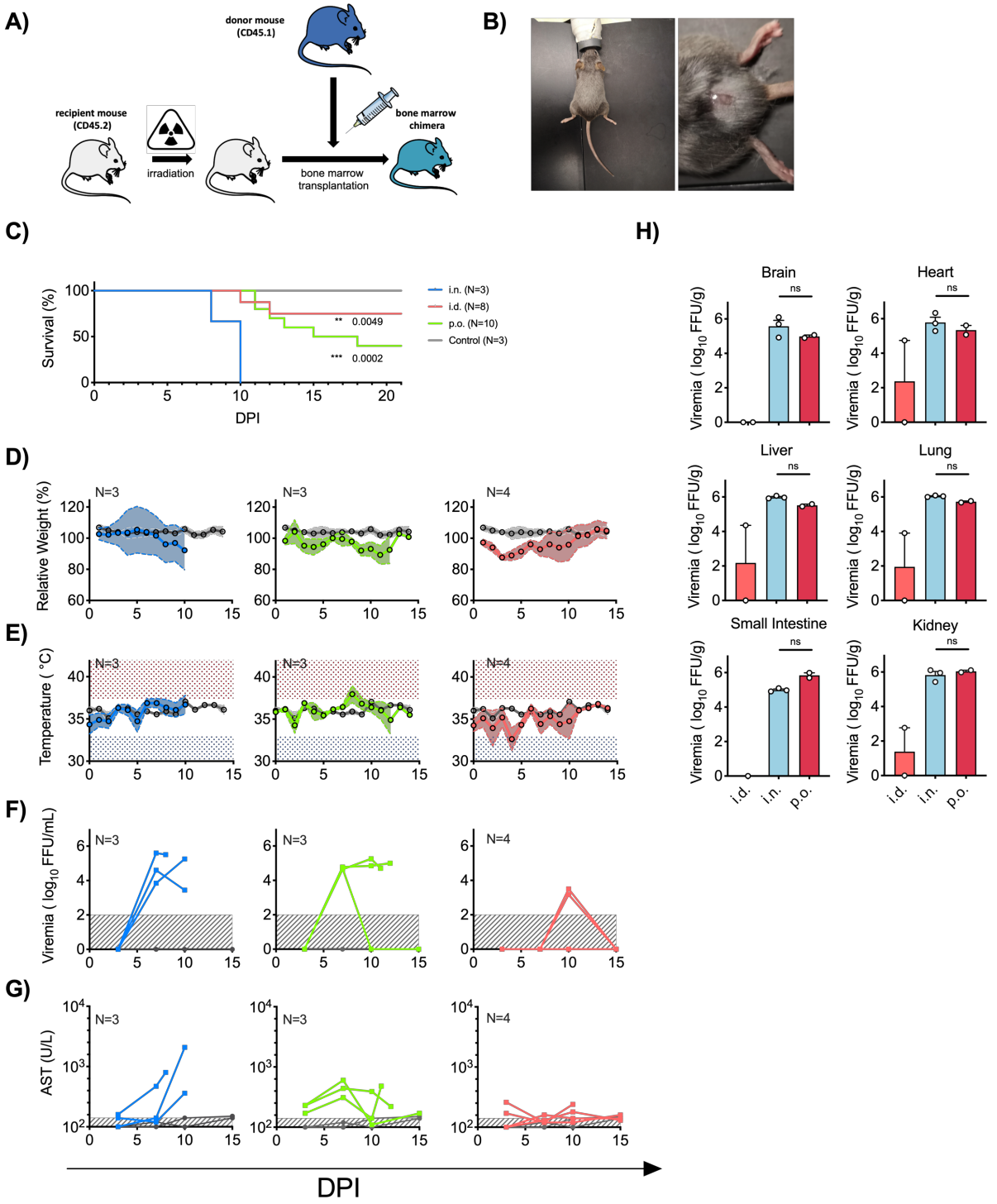

Figure 4.24: Susceptibility of IFNAR chimeras to natural routes of exposure. Chimeras were generated by irradiation and transplantation of bone marrow (A) infected either i.n., p.o. or i.d. with 1000 FFU of LASV. To mimic skin lesions, mice were shaved at the base of the tail and scratched with sandpaper prior to infection (B). Temperature, weight and general well-being was monitored daily post infection (C/D). Cut-off for extreme body temperature (fever) is are shaded in red and blue. Uninfected mice served as control (grey). Viremia and ASTs were determined at selected time points (E/F). The normal range for AST and the limit of detection for viremia are shaded in grey. Mean and SEM are shown, unless individual data points are depicted. Organ viral titers were determined at day of death (H) for i.n. (N = 3), p.o. (N = 2) and i.d. (N = 2) exposure. Abbreviations: DPI, days post infection; AST, aspartate transaminase; i.n., intranasal, p.o., per os; i.d., intradermal.

In summary, this indicates that exposure through especially respiratory and intestinal mucosae and partially through skin lesions can lead to lethal infection in IFNAR chimeras. Importantly however, susceptibility and disease progression varied, and higher resistance was observed against oral and especially intradermal infection. This suggests, that pathogenesis is linked to the route of infection. As T-cell involvement in disease severity and pathogenesis is indicated, it was of further interest to clarify the impact of exposure route on the resulting T-cell response.

4.4.2 T-CELL ACTIVATION AND MEMORY DEPEND ON ROUTE OF EXPOSURE

To further characterize the impact the exposure route has on the cellular immune response, T-cell effector phenotype and activation was analyzed by flow cytometry at day 9 post infection in the blood **(Figure 4.25 A).** In mice, effector T cells are characterized by expression of CD44 and absence of CD62L surface expression.

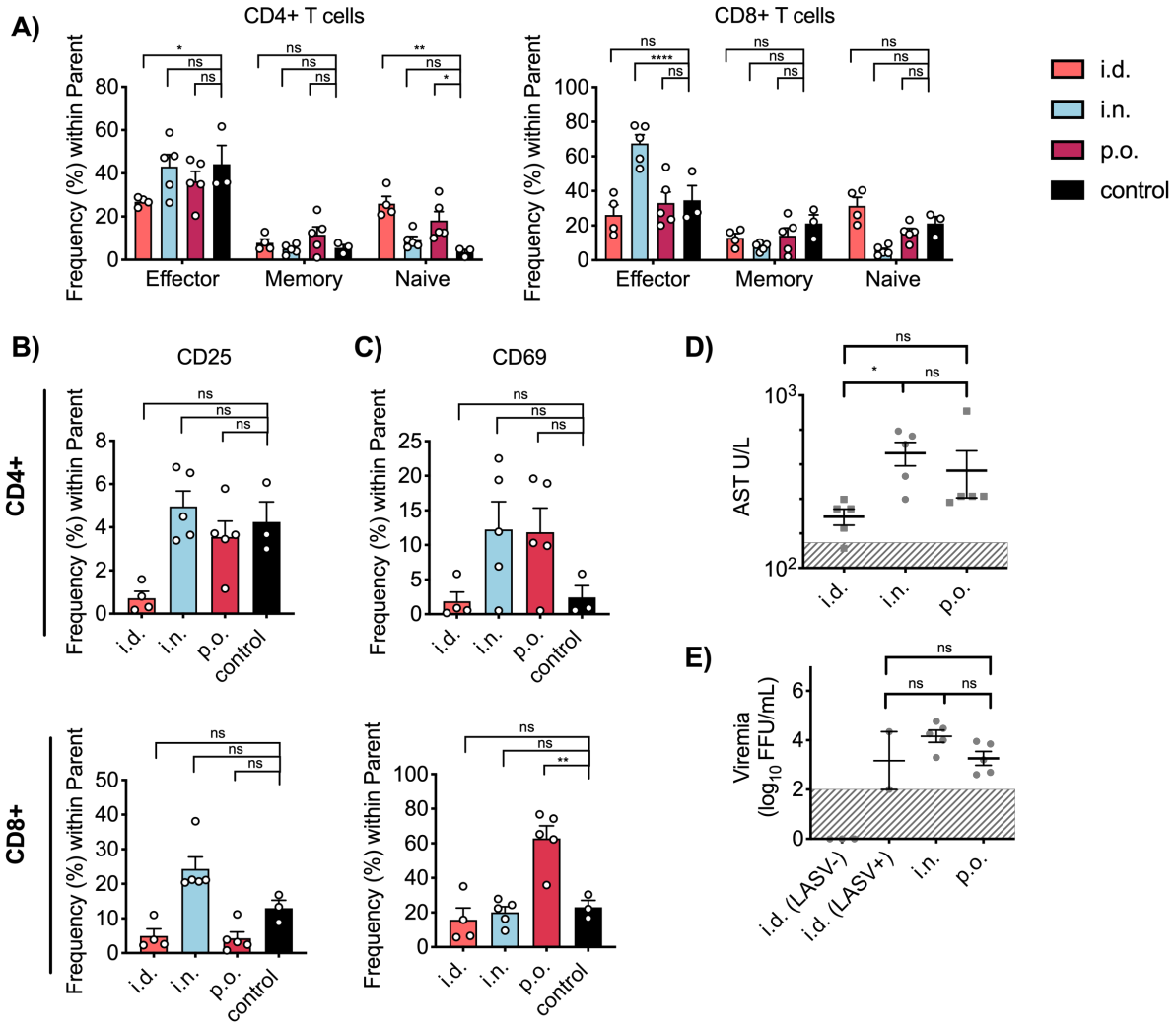

Figure 4.25: T-cell activation and effector phenotype in natural routes of exposure. IFNAR chimeras were infected either i.n., p.o. or i.d. with 1000 FFU of LASV and T-cell activation and effector phenotype in the blood analyzed by flow-cytometry 9 days post infection. Uninfected mice served as control. Frequency (%) of effector cells ($CD44^+$ $CD62L^-$), memory T cells ($CD44^+$ $CD62L^+$) and naïve cells ($CD44^-$ $CD62L^+$) is shown for botch $CD4^+$ and $CD8^+$ compartments (A). Exposure routes are color coded according to legend on the right. Expression frequency (%) of activation markers CD25 and CD69 is depicted for each route (B and C). Mean and SEM are shown. For reference, corresponding AST levels (D) and viremia (E) are shown. The normal range for AST and the limit of detection for viremia are shaded in grey. Mean and SEM are shown, unless individual data points are depicted. For clarification, data was split for i.d. exposure to differentiate between animals that showed systemic infections and those, that did not. Statistical significance was determined either by using Kruskal-Wallis test, followed by Dunn's multiple comparisons test, or ordinary two-way ANOVA, followed by Dunnett's multiple comparison test. Significance levels are presented as follows: ns = $p > 0.05$; * = $p \leq 0.05$; ** = $p \leq 0.01$; *** = $p \leq 0.001$; **** = $p \leq 0.0001$. Abbreviations: i.n., intranasal, p.o., per os; i.d., intradermal.

Memory T cells express both $CD44^+$ and $CD62L^+$, while naïve T cells are $CD62L^+$ and $CD44^-$ (Bajnok et al., 2017; Pihlgren et al., 1995; Swain and Bradley, 1992). No significant differences were observed in the memory T-cell compartment for any of the exposure routes as compared to uninfected mice. After i.d. infection the frequency of effector $CD4^+$ T cells decreased significantly, coinciding with a significant increase of naïve $CD4^+$ T cells which suggested increased thymic output after infection (Permar et al., 2003). Also p.o. infection was characterized by a significant increase of naïve $CD4^+$ T cells. In contrast, i.n. infection was characterized by a significant increase in effector $CD8^+$ T cells.

To characterize the activation status of the effector subsets, expression of CD25, a marker for late T-cell activation, and CD69, a marker for early T-cell activation (Reddy et al., 2004) was utilized **(Figure 4.25 B)**. While not significant. CD25 was higher expressed after i.n. infection, a trend more readily demonstrated in $CD8^+$ T cells. CD69 was upregulated on effector T cells after p.o. infection in the $CD8^+$ compartment significantly. This coincided with high viral titers and AST levels after i.n. exposure compared to p.o. **(Figure 4.25 C/D).** In the context of the observed differences of disease progression this suggests that T-cell response after oral exposure is delayed compared to respiratory exposure.

4.4.3 DIFFERENT EXPOSURE ROUTES TO LASV IMPRINT SPECIFIC HOMING SIGNATURES

As described, T-cell homing is a consequence of antigen encounter and priming by DCs in different draining lymph nodes, which enforces organ specific homing marker expression. As such, differently expression profiles of homing markers could be expected following different routes of LASV exposure. However, it has not been shown for any VHF that presents with multiple naturally occurring exposure routes, if this impacts the resulting homing signature.

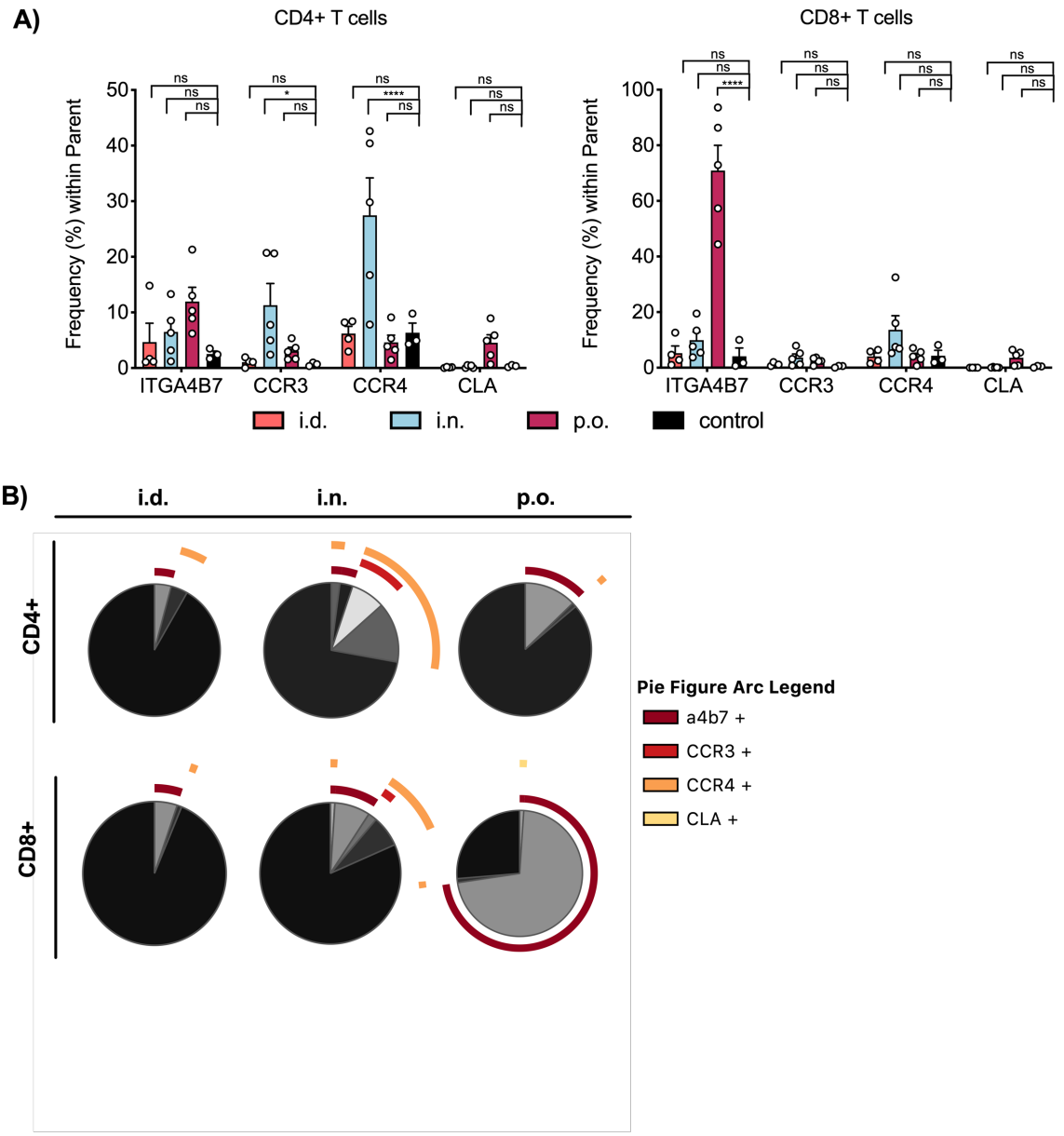

Figure 4.26: T-cell homing signatures after natural routes of exposure. IFNAR chimeras were infected either i.n., p.o. or i.d. with 1000 FFU of LASV and T-cell homing in the blood analyzed by flow-cytometry 9 days post infection. Uninfected mice served as control. Frequency (%) within effector cells ($CD44^+$ $CD62L^-$) expressing homing markers) is shown for botch $CD4^+$ and $CD8^+$ compartments (A). Exposure routes are color coded according to legend on the right. Mean and SEM are shown. Combination gates were generated, and SPLICE plots were utilized to visualize co-expression pattern after each exposure route (B). Pie arc is color coded according to legend on the right. Abbreviations: ITGA4B7, α4β7 integrin; CCR, chemokine receptor; CLA, cutaneous lymphocyte antigen; i.n., intranasal, p.o., per os; i.d., intradermal. Statistical significance was determines using Kruskal-Wallis test, followed by Dunn's multiple comparisons test. Significance levels are presented as follows: ns = $p > 0.05$; * = $p \leq 0.05$; ** = $p \leq 0.01$; *** = $p \leq 0.001$; **** = $p \leq 0.0001$.

After mimicking natural exposure through the respiratory mucosa (i.n.), skin (i.d.) and intestinal mucosa (p.o.) in IFNAR chimeras homing marker expression was analyzed 9 days post exposure on effector T cells, defined by $CD44^+$ $CD62L^-$ expression. To investigate if

respiratory, intestinal or skin homing capacity was induced, tissue specific homing markers CCR3 (respiratory), $\alpha4\beta7$ integrin (intestinal), CLA (skin) and CCR4 (skin/respiratory) were selected for analysis as representatives of each organ tissue **(Figure 4.26 A).**

After i.d. exposure to LASV, effector T cells were not characterized by significantly increased frequency of expression in homing. Against expectations, neither skin homing markers CLA nor CCR4 showed increase in frequency compared to unexposed mice. After i.n. exposure $CD4^+$ effector T cells expressed increased levels of CCR3 and significantly more CCR4. This trend was also observed in $CD8^+$ effector T cells, but to a lesser degree and without significance. In contrast, both effector $CD4^+$ and $CD8^+$ T cells upregulated $\alpha4\beta7$ integrin expression after p.o. exposure, in the $CD8^+$ compartment significantly. Importantly, these signatures were unique to both routes, respectively.

As especially the homing signature after respiratory an oral exposure was comprised of more than one marker, co-expression patterns were of interest to confirm gut or lung-specific imprinting **(Figure 4.26 B).** Co-expression of respiratory markers was observed after i.n. exposure. Expression of CCR3 coincided with simultaneous expression of CCR4 but did not overlap with the population of effector T cells characterized by $\alpha4\beta7$ integrin expression. The signature after p.o. exposure was dominated by high expression of $\alpha4\beta7$ integrin. Interestingly, CLA, which is thought to be imprinted only by skin DCs was also observed after p.o. exposure on a small subset of both $CD4^+$ and $CD8^+$ effector T cells. Interestingly, CLA was both co-expressed with $\alpha4\beta7$ integrin and appeared only in single expression. In summary, this strongly implies that respiratory exposure lead to imprinting lung-tropic ($CCR3^+$ $CCR4^+$) T cells, while oral exposure lead to the generation gut-tropic T cells. The observation of $\alpha4\beta7$ integrin-expressing T cells after i.n. exposure suggested that this infection route also resulted in the generation of T cells with gut homing signatures.

As the homing signatures varied between exposure routes, further analysis of organ-specific T-cell populations was conducted for the small intestine, lung, spleen, skin and brain **(Figure 4.27 A**. Frequencies of memory T cells remained without significant change. No significant increase of effector T cells was observed in brain, skin or spleen for any route. After i.n. and p.o. exposure significantly increased frequencies of effector $CD4^+$ T cells were demonstrated in the small intestine. Both routes also showed significantly higher frequencies of effector T cells, and decreased frequencies of naïve T cells in the lung, an observation that was even stronger after i.n. exposure. It can be assumed that T-cell infiltration into inflamed tissues may contribute to LF pathogenesis. In this context it would be important to observe, if the

unique homing signatures observed in blood are also represented on the tissue-resident populations and are predicative of organ infiltration. To differentiate between T cells that have actually infiltrated the organ tissue and those in circulation in residual blood is impossible especially for organs with high blood circulation such as the lung. To circumvents this issue, i.v. staining with anti-CD3 antibodies prior to death can be utilized. Antibodies circulate with the blood flow but are unable to enter the tissue. Hence, this allows for labelling of all circulating $CD3^+$ T cells, while infiltrating resident populations remain unlabeled (Pitsillides et al., 2011).

First, the fraction of infiltrating T cells for each organ was investigated within the effector population **(Figure 4.27 B).** As expected, the fraction of infiltrating T cells was highest in the skin after skin exposure. Concordantly, oral application of the virus led to highest frequency of infiltrating T cells in the small intestine, which matched the observed intestinal homing signature. Interestingly, however, while i.n. infection significantly increased the frequency of effector T cells, it did now lead to increased frequency of the resident population in the lung. The highest frequency of infiltrating effector T cells here was also observed after oral exposure. Interestingly, in support of the observation that oral exposure was connected to the appearance of CLA^+ effector T cells, increased infiltration of the skin was observed compared to respiratory exposure. Next, the homing signatures of infiltrating effector T cells was analyzed. Interestingly, in the lung, as a representative organ, homing marker expression allowed clustering of mice according to route of exposure, indicating that the unique signatures observed in blood are also represented on the resident populations **(Figure 4.27 C).**

Taken together, these data showed that different exposure routes, especially respiratory and oral exposure, not only led to different disease progressions, but also imprinted different T-cell homing signatures which were observable in blood, and also in organs. Interestingly, the homing signature observed after oral exposure comprising intestinal and skin recruitment was reminiscent of the observations made in Severe Cases of human LF. The frequency of effector T cells and T-cell infiltration into the organs also differed in mice depending on the exposure route, however, also aberrant of-target homing and infiltration was observed. In the context of the increased inflammatory non-specific homing signatures seen especially in Fatals, aberrant homing and tissue infiltration may also contribute to pathogenesis in humans.

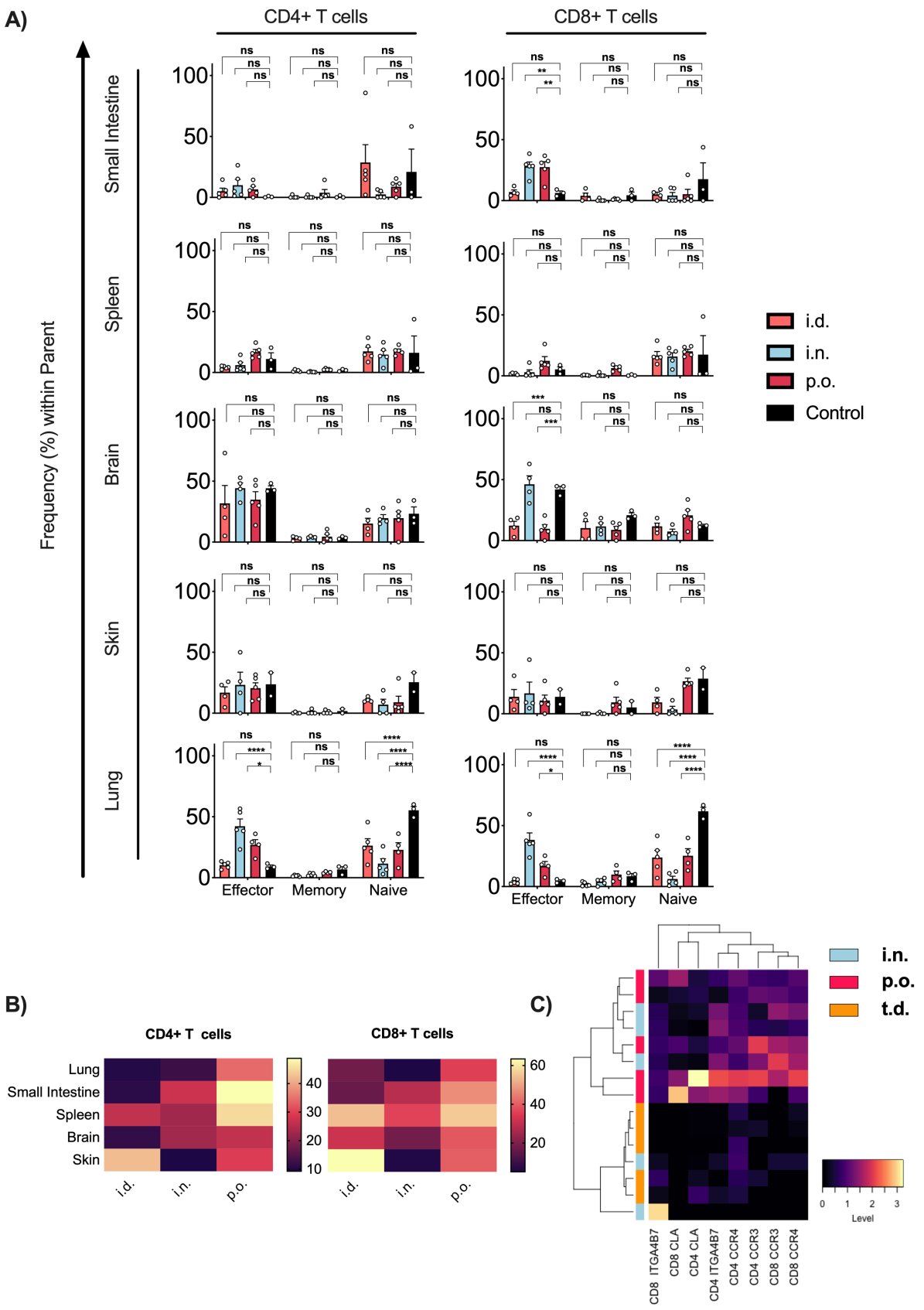
A)
CD4+ T cells
CD8+ T cells
Frequency (%) within Parent
Small Intestine
Spleen
Brain
Skin
Lung
Effector
Memory
Naive
i.d.
i.n.
p.o.
Control
B)
CD4+ T cells
CD8+ T cells
Lung
Small Intestine
Spleen
Brain
Skin
i.d.
i.n.
p.o.
C)
i.n.
p.o.
t.d.
Level
CD8 ITGA4B7
CD8 CLA
CD4 CLA
CD4 ITGA4B7
CD4 CCR4
CD4 CCR3
CD8 CCR3
CD8 CCR4

Figure 4.27: T-cell response in organ tissues after natural routes of infection. IFNAR chimeras were infected either i.n., p.o. or i.d. with 1000 FFU of LASV and T-cell homing in the blood analyzed by flow-cytometry 9 days post infection. Uninfected mice served as control. Frequency (%) of effector cells (CD44+ CD62L-), memory T cells ($CD44^+$ $CD62L^-$) and naïve T cells ($CD44^-$ $CD62L^+$) is shown for botch $CD4^+$ and $CD8^+$ compartments in selected organs (A). Exposure routes are color coded according to legend on the right. Mean and SEM are shown. Using i.v. antibody staining to mark circulating lymphocytes, frequency of resident effector T cells was determined (B). Heatmap colors visualize frequency (%) in selected organs according to color bar below. Representative, homing marker expression on resident effector T cells is shown as a heatmap for the lung (C). Dendrograms are based on hierarchical clustering. Expression frequency was normalized for each marker. Heatmap colors are according to color bar below. Exposure route corresponding to each sample is indicated on row colors. Statistical significance was determines using 2-way ANOVA test, followed by Dunnette's multiple comparisons test. Significance levels are presented as follows: ns = $p > 0.05$; * = $p \leq 0.05$; ** = $p \leq 0.01$; *** = $p \leq 0.001$; **** = $p \leq 0.0001$. Abbreviations: ITGA4B7, α4β7 integrin; CCR, chemokine receptor; CLA, cutaneous lymphocyte antigen; i.n., intranasal, p.o., per os; i.d., intradermal.

5 DISCUSSION

LASV, the etiological agent of LF, causes each year seasonal epidemics in West African countries with case-fatality rates of up to 20 % in hospitalized patients. So far, no vaccine or specific treatments are licensed for LF. Previous studies indicate a dual role of T-cell immunity in LF. Early activation of T cells is important for survival (Baize et al., 2009; Flatz et al., 2010; Yun and Walker, 2012) but aberrant T-cell responses may also drive immunopathology (Flatz et al., 2010; Oestereich, et al., 2016). However, due to the geographical limitation of LF outbreaks and the difficulties accessing these areas, human LF remains understudied.

One part of T-cell immunology that has not previously been investigated in LF is whether T-cell recruitment into different organ tissues influences disease severity. The goal of this thesis was to investigate the role of T cells in LF pathophysiology paying special attention to the role of T-cell homing. I also sought to determine the putative role of T-cell homing signatures as biomarkers of LASV severity and transmission.

5.1 T-CELL RESPONSES TO LASV INFECTION

5.1.1 ACTIVATION AND (DYS)FUNCTION

Co-expression of HLA-DR and CD38 was utilized to characterize T-cell activation in samples collected from acute LF patients. Strong early activation was observed in $CD8^+$ T cells, followed by two peaks of activation at days 15/16 and 23/24 post-onset. Activation peaked in the $CD4^+$ compartment from day 14 to day 18 post-onset and a second activation peak was observed at days 24/25 post-onset. These activation profiles support the data from McElroy et al, who previously described similar activation peaks in a LF patient treated in the US. Slight differences of activation kinetics and the early activation seen in the cytotoxic T cells could be due to inter-patient variance, which is more clearly observable in the data presented here, or inclusion of samples from patients with multiple disease severity, which presented with different activation levels. It is possible that the second peak of T-cell activation is a result of viral persistence (McElroy et al., 2017). In support of this hypothesis it could be shown that activation levels were increased in Severe Cases and that in all survivors a positive trend could be seen between activation of $CD8^+$ T cells, viremia and AST levels. Interestingly, in fatal outcome a strong negative correlation between viremia, AST and activation levels of $CD4^+$ T cells was seen instead, implicating that in fatal outcome high levels of viral replication and inflammation might lead to T-cell dysregulation.

Previous studies indicated, that dysfunctional T-cell responses are dominant in severe disease, while intact responses help control viral replication (Warner et al., 2018). Fatal outcome in NHP infected with LASV was correlated to decreased proliferation and cytokine production (Baize et al., 2009). *In vitro* studies have shown that LASV infection of APCs results in defective T-cell responses (Schaeffer et al., 2018). Interestingly, the findings presented in this thesis also corroborate the observation that high levels of activation of cytotoxic T cells may be related with diminished functional LASV-specific responses in humans (McElroy et al., 2017).

An 8-color benchtop flow cytometer was employed to analyze T-cell-specific effector responses to LASV during the 2017/2018 LF outbreaks in Nigeria in 26 patient samples. An NP-derived peptide pool was utilized for stimulation of patient peripheral blood cells, in agreement with the idea that NP-directed T cells are immunodominant (ter Meulen et al., 2000). In agreement with previously published data, a subset of LASV-specific T cells were polyfunctional, namely, they produced effector cytokines IFN-γ, TNF-α and expressed markers of degranulation LAMP-1/CD107a (a surrogate for granzyme B production) (McElroy et al., 2017). However, in a sizeable fraction of samples no response was observed, suggesting impairment of T-cell functionality during the acute phase. Evaluation of patient data indicated that, indeed, this functional impairment of T-cell immunity was linked to disease severity. Patients with mild disease mounted effective T-cell responses while severe and fatal cases did not. These findings suggested that increased viral infection and T-cell dysfunctionality may correlate.

Interestingly, this is in agreement with previous work in NHP, which has also suggested that the strongest T-cell responses to LASV-specific stimulus were linked to low viremia and disease severity (Baize et al., 2009). McElroy et al. has previously demonstrated that in one patient clinical symptoms of LF coincide with spontaneous degranulation and the $CD8^+$ T-cell activation peak observed during the third week of disease. Unfortunately, in the patient cohort investigated T-cell functional responses were only analyzed up to day 20 post-self-reported onset, and this observation could not be validated. However, data suggest that the early peak of cytotoxic T-cell activation (day14/15) during the acute phase may also be accompanied by increased spontaneous degranulation. This further supports the immune-mediated etiology suspected in LF pathogenesis (McElroy et al., 2017), however sample size needs to be increased in future experiments and studies in fatal patients need to be conducted to validate this observation further.

A detailed study of Dengue virus infection in humans demonstrated that also in this VHF the acute cytotoxic T-cell response is dysfunctional and only a small fraction of effector T cells responded with IFN-γ production to specific stimulus, while many only showed reaction to TCR-independent signal induction (Chandele et al., 2016). As suggested by the authors of this study for Dengue, the data presented here similarly implies that T cells during acute phase of LF in severe disease may exhibit a high activation level, but also exhibit exhaustion as seen in chronic viral infections or a “stunned” phenotype which has been described during acute infection with HIV, hepatitis and also EVD (Lechner et al., 2000; Ndhlovu et al., 2015; Ruibal et al., 2016). Interestingly, while not significant, we observed that in relation to ASTs in blood as a measure of severity, TNF-α responsiveness was diminished before IFN-γ, which is also reminiscent of observations made in chronic viral infections (Chandele et al., 2016; Wherry and Kurachi, 2015; Zajac et al., 1998) and supports the idea that T cells may suffer from exhaustion in acute LF in relation to disease severity.

5.1.2 T-CELL DIVERSITY AND EXPANSION

In the framework of this thesis observations made on T-cell diversity and expansion during the acute phase were able to describe a more comprehensive picture of T-cell responses in relation to disease severity. It was possible to analyze the TCR repertoires present during acute infection in LF patients with different outcomes. Severe Cases presented with increased clonal expansion over time, which implies preferentially expansion of specific clonotypes. Interestingly, in contrast in Fatals, the opposite trend was demonstrated, a loss of hyperexpanded clones, meaning an increase in TCR diversity. A similar effect was previously observed by us in the context of fatal EVD (Speranza et al., 2018). The early increase in hyperexpanded clones could be either explained by the assumption, that only the end of the virus-induced proliferation of responding T cells was observed or by proliferation of non-specific bystander memory cells due to inflammation (Goldrath et al., 2002; Min, Foucras, Meier-Schellersheim, and Paul, 2004; Speranza et al., 2018; Troy and Shen, 2003). The increase in diversity of the repertoire over time could be due to multiple reasons. Previously expanded clones could be lost due to apoptosis (Ch’en et al., 2008) or increased recruitment into the tissues and retention could reduce the number of expanded clones circulating in the blood. It is also feasible that increased activation and thymic output could lead to higher frequencies of new T-cell clones.

To clarify the mechanisms behind the observed changes in repertoire, especially in the context of fatal disease, it would be highly relevant to investigate changes in the T-cell repertoire in particular at very early time points after infection, which were not included in this

analysis. Furthermore, this study was not designed to investigate T-cell exhaustion in greater detail, which would be of interest especially in the context of severe disease and fatal outcome to validate if exhaustion and apoptosis affect the repertoire.

In contrast, Mild Survivors showed little to no change in T-cell diversity over time. In regard to the low levels of activation observed and reduced clinical manifestation of disease, this implies that T-cell responses in mild LF are carefully controlled and, in the end, successful. This would be supported by the observation that T cells from patients with AST levels close to or within physiological range and limited viremia, were functionally still most responsive. It remains unclear in how far the T-cell response may determine outcome of disease or if this response is itself a consequence of underlying mechanisms which are causative of outcome.

With the current limitations of peptide reconstruction from partial TCR sequences, it was not possible to determine if the observed changes in repertoire were due to LASV-specific or bystander T cells. However, tetramer technology was utilized to identify LASV-specific T cells and, in accord with previous data, LASV-specific T cells were demonstrated across the acute phase of LF at low frequencies (McElroy et al., 2017). It was demonstrated further, that these cells showed an activated phenotype characterized by strong expression of CD38, and partial co-expression of HLA-DR. Frequency of LASV-specific T cells increased after patient discharge from the treatment center, which coincided with strong reduction of the frequency of activated T cells. McElroy et al. hypothesized that the frequency of LASV-specific T cells is limited during acute infection and increases during convalescence due to increased T-cell recruitment into peripheral tissues before viral clearance is achieved. The observations made in this patient cohort would support this hypothesis further by demonstrating that both tetramer positive T cells and T cells responding to LASV-specific stimulus during the acute phase exhibited increased homing capacity to inflamed tissue combined with a loss of lymphoid homing. This would suggest increased tissue recruitment. However, the caveat must be given, that tissue recruitment does not necessitate retention of cells in peripheral tissues, and further studies are necessary to determine the role of tissue retention of T cells in humans.

Importantly, it was also possible to verify the activation of bystander T cells during acute LF by identification of HLA-DR$^+$ CD38$^+$ T cells specific for EBV. Bystander activation is not uncommon in viral infection and can occur through TCR-independent activation by the cytokine milieu (Zhang, Sun, Hwang, Tough, and Sprent, 1998), can include clonal expansion of these memory T cells and active recruitment to infected tissues (Ostler, Pircher, and Ehl, 2003; Sckisel et al., 2014; Kim et al., 2002). Interestingly, bystander T cells may still

interact with APCs and compete with naïve T cells for access to them. In LF, increased numbers of bystander T cells could limit the priming of naive LASV-specific T cells, as has previously been described (Gray, Reiner, Smith, Kaye, and Scott, 2006; L. R. Johnson, Weizman, Rapp, Way, and Sun, 2016). If this could be validated in further studies, then bystander T cells activated by inflammation may prevent maturation and expansion of LASV-specific T cells until inflammation is resolved.

The biological relevance of bystander activation is not necessary homogenous across viral infections (Ehl, Hombach, Aichele, Hengartner, and Zinkernagel, 1997; Fujinami, von Herrath, Christen, and Whitton, 2006). In viral infections such as herpes, HIV and LCMV bystander activation has been linked to both pathology and protection (Bangs, McMichael and Xu 2006; Kim et al., 2002). For another VHF virus, Hantavirus, it was demonstrated recently that $CD8^+$ T-cell bystander activation actually is relevant by supporting the viral response by bypassing PD-L1 and PD-L2 checkpoint inhibition (Raftery, Abdelaziz, Hofmann, and Schönrich, 2018), and bystander responses have been demonstrated also in Dengue infection as a response to the cytokine storm (Suwannasaen, Romphruk, Leelayuwat, and Lertmemongkolchai, 2010). It needs to be further qualified which impact bystander activation has on LF pathophysiology. It would be of interest to also investigate further the functional capacity of activated non-specific T cells and if a correlation between bystander activation and spontaneous T-cell cytokine release and degranulation exists.

5.2 T-CELL HOMING IN RELATION TO PATHOGENESIS

Targeted T-cell migration and organotropism increase the likelihood of T cells to encounter their antigen, which improves chances of successful viral clearance. To guide T cells towards inflammation, but also to specific peripheral organs, T-cell homing signatures are imprinted upon antigen encounter by APCs, in particular by DCs (Fu et al., 2016; Marelli-Berg et al., 2008). However, infiltration of T cells and the coinciding immune activation, cell damage and cytokine inflammation can also cause tissue damage and negatively impact outcome if the response is not modulated correctly. It has been shown that T-cell infiltration can negatively affect disease for different viral infections including Influenza A and LCMV, the prototypic arenavirus (Duan and Thomas, 2016). In LF, a detrimental effect of T cells was observed in mouse models (Flatz et al., 2010; Oestereich, et al., 2016) and infiltration of T cells has been shown to be related to LF-associated hearing loss (Mateer, Huang, Shehu, and Paessler, 2018; Yun et al., 2015).

LF is caused by multiple spillover events (Siddle et al., 2018; Grahn et al., 2018; McCormick et al., 1987), involving contact with rodents or their excreta (Bonwitt et al., 2017; Stephenson, Larson, and Dominik, 1984; Johnson et al., 1983). Therefore, at the beginning of our study, we hypothesized that humans could get in contact with LASV through multiple routes including skin, respiratory and oral mucosae. Thus, as opposed to Dengue or rotavirus infection where homing patterns are unique (Rivino et al., 2015; Rott et al., 1997; Jiang et al., 2008) I expected to encounter multiple T-cell homing signatures in LF. An 8-color bench top flow cytometer was employed during the 2017/2018 LF outbreaks in Nigeria to analyze T-cell homing signatures in the field. It was demonstrated that T-cell homing marker expression in LF is dominated by integrins referring mucosal and inflammatory recruitment. Only low to intermediate level expression of CLA and CCR5 were present in some patients, suggesting selected involvement of skin and liver recruitment (Grant et al., 2002; Kunkel et al., 2002; Rivino et al., 2015), respectively. The magnitude of CCR3 expression, indicating lung-tropism (Danilova et al., 2015), was very low. Interestingly, expression was high for both β1 integrin and β7 integrin. Physiologically, the alpha subunit α4 can dimerize with either beta unit, though it has been shown that β1 integrin suppresses the binding to β7 integrin and both integrin dimers fulfill different roles in the process of T-cell homing (Bertoni, Alabiso, Galetto, and Baldanzi, 2018). The co-expression of both integrin subunits observed in LF patients suggests homing to inflamed intestinal tissue.

Due to the outbreak-specific patient distribution, this analysis was mostly restricted to individuals that survived disease and presented with mild symptoms. To further clarify the role of T-cell homing, a more in-depth *ex vivo* analysis was conducted including a wider variety of homing markers and patient distribution on cryopreserved PBMCs. It was shown, that different disease outcome groups presented with characteristic up- or downregulation of selected markers, which allowed clustering of patients based on homing signatures. It was further revealed, that unique T-cell populations were enriched, especially in $CD8^+$ T cells, depending on the disease severity.

5.2.1 T-CELL HOMING SIGNATURES IN SURVIVAL

Observations made on T-cell homing capacity during LASV infection in patients that present with mild disease and survived, further supported the above described low-level activation and minimal recruitment of effector T cells during the acute phase. Besides the above described high expression frequency of β7 integrin, activated T cells in survivors were characterized by expression of CCR7, a marker for T-cell homing to lymphoid tissue, which is generally lost upon antigen encounter (Förster, Davalos-Misslitz, and Rot, 2008; Campbell et

al., 2001; Sallusto, Lenig, et al., 1999; Dios-Esponera et al., 2019). This implies that the small compartment of activated T cells demonstrated in Mild Cases is comprised mainly of recently activated T cells, which have not lost their “naïve” phenotype with preferred homing potential to lymphoid tissue and to intestine associated lymphoid organs (DeNucci, Pagán, Mitchell, and Shimizu, 2010). As this signature enforcing egress from inflamed tissue, this could contribute to the observed minimal tissue damage in mild disease. It was demonstrated that during LASV infection also bystander T cells are recruited. At least partially, the expression of CCR7 also indicated the activation of central memory T cells, as confirmed by tSNE analysis, which shows that even in this low activation context, mild disease may involve recruitment of bystander T cells.

Interestingly, cytotoxic T cells unique to Mild Cases were enriched in expression of α1 integrin, which only can dimerize with β1 integrin, also referred to as VLA-1. Expression of this integrin negatively correlated with the AST levels, which suggests tissue recruitment and retention in mild disease increase once inflammation is reduced. Importantly, this integrin can facilitate positioning of effector T cells in the extracellular matrix after extravasation, which allows cells to migration to the site of viral replication (Kauffmann, Thomsen, and Christensen, 2006). It is upregulated on resident T cells, playing a role in tissue retention and formation of pathogen-specific tissue memory formation (Kumar et al., 2017; Stanley Cheuk et al., 2017). Up-regulation of α1 integrin during the course of disease could imply an increase in tissue retention or the beginning of tissue resident memory formation, which has been demonstrated before for virus-specific memory T cells in the airways after influenza infection or vaginal mucosa after herpes infection (Stanley Cheuk et al., 2017; Tang and Rosenthal, 2010). As it is suspected that infection with LASV confers immunity against re-infection, this T-cell memory formation process should be studied further mechanistically at the level of mucosal and non-mucosal periphery. Understanding this could inform future vaccine design strategies to maximize efficacy.

While β7 integrin expression was overall higher amongst survivors as compared to Fatals, in severe disease, a uniquely enriched population of β7 integrin$^+$ cytotoxic T cells was identified. This population showed varying levels of CCR7 and CD45RA expression, suggesting that this population is comprised of both naïve and T_{eff} cells (Sallusto et al., 1999). On naïve T cells this would support increased recruitment to the mesenteric lymph node and Peyer`s patches, which could be related with strong inflammation and virus replication in the intestinal mucosae (Bertoni et al., 2018; Denucci et al., 2009). The same signature on mature T cells also supports intestinal tropism. In EVD it was shown that

significantly higher levels of β7 integrin were present in patients that succumbed to disease. This was thought to be linked to severity associated to Ebola virus replication in the gastrointestinal tract (Speranza et al., 2018). In our patient cohort many individuals reported gastrointestinal symptoms such as vomiting, abdominal pain, nausea and diarrhea. It has been demonstrated that the ligand of β7 integrin, MadCAM-1, is enhanced in the gut through the cytokine environment (Kraal, Schornagel, Streeter, Holzmann, and Butcher, 1995; Ogawa et al., 2005), especially TNF-α, which was shown in previous work (McElroy et al., 2017) and the work described in this thesis to be part of the T-cell response to LASV stimulus, and could further enhance recruitment and retention of T cells to the intestine.

Interestingly, in certain chronic infections the limitation of MadCAM-1 to the intestine is disturbed, leading to aberrant T-cell homing. MadCAM-1 expression was demonstrated for inflammatory bowel disease and diabetes in eyes, joints, skin and pancreas, as well as liver and linked to hepatic complications (Adams and Eksteen, 2006; Grant et al., 2002; Kraal et al., 1995). It could be suggested that, especially in Severe Cases of LF, increased expression β7 integrin could cause damaging T-cell infiltration into those of-target tissues and cause also hepatic complications. In fact, liver damage has been well described in LF and is an important correlate of disease severity (Winn et al., 1975). To further support the data gathered in humans, increased tissue infiltration of T cells was observed after oral exposure of mice to LASV, coinciding with strong expression of α4β7 integrin and early increased AST levels. It would be interesting to further investigate if off-target homing in Lassa occurs and if inflammation-based change of the endovascular ligands is responsible.

5.2.2 T-CELL HOMING SIGNATURES IN FATAL OUTCOME

In Fatals, expression of α4 integrin was observed on activated $CD4^+$ T cells, coinciding with massive downregulation of CCR7. tSNE revealed enrichment especially of T_{EM} cells. Interestingly, α4 integrin did not co-express with β7 integrin. No staining for β1 integrin was included in the analysis, however, data collected in the field would suggests this dimerization would occur instead. This implies that fatal LF is characterized by substantially increased homing of $CD4^+$ T cells to inflamed tissue in an non-specific manner (Bertoni et al., 2018). The increased expression of α4β1 integrin in fatal LF may also contribute to the neurological symptoms observed in some Fatals by increasing infiltration into the brain. Within the cohort studied in this thesis, we observed a subset of Severe Cases in which neurological symptoms were notable. These included seizures, changes in personality and coma at later stages of disease. During inflammation the vascular of the brain is expressing VCAM-1,

which allows entry of activated T cells expressing α4 integrin. α4 integrin expression has been shown to correlate with brain autoreactive T cells in multiple sclerosis and autoimmune encephalitis (Baron, Madri, Ruddle, Hashim, and Janeway, 1993; Steinman, 2005; Yednock et al., 1992) and it has been shown for $CD8^+$ T cells that antigen encounter in the cranial lymph node imprints α4β1 integrin (Calzascia et al., 2005; Denucci et al., 2009). Further studies would need to verify the role of infiltration of α4 $integrin^+$ activated $CD4^+$ T cells and their contribution to the neuropathogenesis of LF.

In addition to its above-described homing-function on activated mature T cells the result of α4 integrin expression has also additional consequences. If expressed in the context of TCR involvement, which was indicated in the cell population analyzed, α4 integrin has been demonstrated to increase activation-induced cell death of chronically stimulated $CD4^+$ T cells (Snow, Pandiyan, Zheng, Krummey, and Lenardo, 2010). In this context, high expression frequency of α4 integrin could support the hypothesis that T cells driven to exhaustion and cell death are biomarkers of fatal LF. It is possible that in Fatals a previous tissue-specific signature on $CD4^+$ T cells was overwritten by recruitment of $CD4^+$ T cells to sites of inflammation. It has been showed previously that excess of β1 integrin will decrease binding of α4 integrin to β7 integrin (DeNucci et al., 2010), which would reduce gut-specific recruitment of T cells and favor inflammation driven tissue infiltration, which could increase pathogenesis notably.

Of note, an enrichment of activated $CCR3^+$ $CD8^+$ T cells was also observed in Fatals implicating T-cell recruitment to the upper respiratory tract (Shono et al., 2019). These cell partially were of central memory phenotype, which could imply recruitment of bystander memory T cells from previous respiratory infections (Schmidt and Varga, 2018; Wu et al., 2014). Here, the caveat must be given, that CCR3 has also been implicated in infections outside the respiratory system and plays a role as an inflammatory cytokine receptor (Miranda et al., 2017; Sallusto, Kremmer, et al., 1999; Shono et al., 2019). Further clarification of the function of these cells is necessary.

5.2.3 IMPLICATIONS: T-CELL HOMING AS BIOMARKERS OF DISEASE

The data presented here indicates that T-cell migration and homing contribute to pathophysiology. It was also observed that not one common homing signature existed across patients. Additionally, data suggests that T-cell homing observed includes recruitment of bystander T cells with similar organotropism to inflamed tissues. Hence, it was hypothesized

that homing capacity and behavior might not just differ between patients but varies depending on disease severity and different signatures were identified to be specific for different patient outcome groups. The findings presented in this thesis suggest that a potential exists to employ homing markers also as biomarkers of disease in LF **(Figure 5.1**). Homing markers have also been suggested as biomarkers of disease in other infections and, interestingly, in another VHF, EVD, differences of T-cell homing were demonstrated previously for different disease outcomes (Speranza et al., 2018).

Figure 5.1: Proposed model of T-cell activation, changes in repertoire and homing. Schematic summary of viremia, AST levels, indicating liver damage and disease severity, T-cell activation measured by co-expression of HLA-DR and CD38, T-cell diversity and expansion, and T-cell homing markers unique to disease outcome groups.

As described, clear differences existed between outcome groups. Mild survival with low levels of virus and AST in the blood was characterized by upregulation of CCR7 on activated $CD4^+$ T cells and a T_{CM} phenotype. Within activated $CD8^+$ T cells a phenotype comprising expression of $\alpha 1$ integrin and a T_{EM} profile was enriched. In contrast, unique signatures of $\beta 7$ integrin and CLA were observed on T_{eff} in severe survival, patients in which viremia and AST

levels were significantly higher. It was shown in EVD that significantly higher levels of mucosal homing factors were present in fatal outcome (Speranza et al., 2018) while CLA has been proposed as a biomarker for skin diseases (Czarnowicki et al., 2017). In Mycosis Fungoides and Sézary Syndrome CCR3 was linked to poor prognosis (Shono et al., 2019). In Fatals, however, CCR3 was found on uniquely enriched activated $CD8^+$ T cells, which would imply respiratory involvement and recruiting. CCR3 expression has been linked to chronic cardiomyopathy in Chagas disease (Miranda et al., 2017). Fatals also showed significantly high expression of $\alpha 4$ integrin, which was demonstrated on effector memory $CD4^+$ T cells.

5.3 T-CELL HOMING IN RELATION TO ROUTE OF INFECTION

In humans, studies of the impact of transmission routes and exposure on disease are difficult, but mimicry of exposure routes in mouse models has been utilized for other viruses (Oyoshi et al., 2011; Jiang et al., 2008; Rai et al., 1997; Kugelberg et al., 2005). Previously, a lethal mouse model for LASV was developed in our lab, which supported systemic infection mimicking signs of disease in humans (Oestereich et al., 2016).

Epidemiological data collected throughout multiple West African cohorts and studies on virus ecology suggest that transmission of LASV into humans may occur indirectly or directly through contact with the rodent reservoir, *Mastomys natalensis* (Bonwitt et al., 2017; Monath et al., 1974). The majority of interviewed patients reported to have eaten uncooked or uncovered food before symptoms onset. This supports the hypothesis that oral infection might occur through consumption of contaminated food items. Data collected from our patient cohort also suggested that patients handled dead *M. natalensis* and came into contact with potentially infectious rat body fluids on their bare skin. It is thought that LASV infection through the skin barrier, if it occurs, is possible through small skin lesions, wounds or rat bites. In regard to respiratory exposure risks, a sizeable number of patients reported to have swiped the floor, which creates abundance of dust particles and aerosols. Accordingly, to confer exposure through the intestine in mice, also including esophagus and passage through the stomach, oral exposure was executed through application of the virus through a feeding needle placed into the esophagus. To mimic transmission through skin lesions a i.d. infection route was designed based on studies for dermatophytosis and bacterial infections amongst other skin infections which does not rely on the use of needles (Kugelberg et al., 2005). This allows surface level exposure without breaking through the dermis by scraping of the upper epidermal layer by sandpaper, which causes multiple small lesions but no

breakage of the vasculature. Mimicry of respiratory exposure was conducted through i.n. application of virus. It was possible to characterize T-cell activation and homing signatures in relation to the described infection routes and the resulting disease phenotype. To limit noise, analysis was restricted to the effector T-cell compartment, as defined by $CD44^+$ $CD62L^-$ expression. The data presented here suggests that the putative exposure risks through damaged skin barrier, respiratory mucosae and through the intestinal mucosae are in fact feasible and can lead to systemic infection *in vivo*. However, distinct differences presented themselves for each exposure route.

5.3.1 SKIN EXPOSURE

Compared to respiratory exposure skin exposure presented with limited systemic viral spread, morbidity and mortality. No trend of T-cell activation, measured by CD25 and CD69 surface expression on effector T cells, was observed after skin exposure. It has been demonstrated that skin homing is characterized by expression of CLA and CCR4 expression and was imprinted by infection with another hemorrhagic fever virus, Dengue (Mikhak et al., 2013; Rivino, 2018). However, the experiments conducted here demonstrated that skin exposure to LASV did not imprint an observable skin-specific homing signature on T cells. Considering that many animals did not succumb to disease and also no increase in effector T cells and activation was observed, skin-homing T cells still may have been imprinted but their frequency was below limit of detection. This suggests that most likely the skin barrier, even though physically damaged and the epidermis abraded, still confers protection and immunological involvement remains at low level systemically. This could be due to the immunological environment being different in these three barrier tissues. As LASV affects cells of the innate system as early targets, the different distribution of subsets of APCs in the initial exposure site could affect viral spread as has been suggested for skin infection with Ebola virus previously conducted in this mouse model (Lüdtke et al., 2017). The high level of infiltrating effector T cells would indicate active involvement of the immune response after i.d. infection on a local level. For further clarification, also studies employing additional markers suggested to play a role in targeting T cells to the skin could assist. CCR6, CCR8 and CCR10, as well as other P an E-selectins could be involved (Cochez et al., 2017; Ebert, Meuter, and Moser, 2006; Soler, Humphreys, Spinola, and Campbell, 2003). However, taking together low morbidity and mortality observed in the mouse studies and the lack of observable T-cell response systemically after i.d. exposure, would suggest that this route of exposure is least relevant in the context of human disease and skin exposure might not convey lasting immunity.

5.3.2 RESPIRATORY AND ORAL EXPOSURE

Respiratory exposure through i.n. infection induced 100 % lethality, disease developing day 6 onwards with systemic viral spread and high viremia, concluding in death by day 11 post infection. In contrast, oral exposure presented with a delayed presentation of symptoms (weight loss, changes in temperature) and death, however accompanied by early increase in ASTs. Interestingly, some animal survived disease after oral exposure.

While oral application as performed in the context of the experiments described here also may expose surfaces of the esophagus, it is expected that virus first replicates in the stomach before entering the intestine. This is supported by previous work demonstrating successful oral exposure through intragastric (i.g.) inoculation in mice and NHPs with LCMV, which is often used as the model virus of this family. After i.g. inoculation of mice with LCMV, the stomach was identified as the primary site of infection, followed by virus spread to the intestine and other organs (Rai et al., 1997). Work in NHPs i.g. inoculated with LCMV has supported that oral exposure with arenaviruses presents with less severe disease. Animal infected i.g. did not develop hemorrhagic fever as compared to an i.v. infected group (Lukashevich et al., 2002). Our observations of reduced mortality and delayed symptoms after oral exposure with LASV would support that this hypothesis also hold true for LF. Interestingly, this study proposed that the observed reduction in disease severity is either due to viral reduction, viral attenuation though mucosal immunity or due to increased protective immune responses, as ingestion of arenaviruses or antigens has been shown to protect from lethal challenge (Djavani et al., 2001; Djavani et al., 2000; Pauza et al., 1993).

The data presented here demonstrates that exposure through the gastrointestinal mucosae, as compared to the respiratory mucosae, presents with overall similar levels of systemic viral replication but decreased amounts of virus in organs other than the intestine itself and kidneys at day of death. However, due to small sample size this could not be demonstrated to be significant. Coinciding with lower AST serum levels and viremia after oral exposure, it was observed that T cells were expressing higher levels of early activation marker CD69 as compared to higher expression of late activation marker CD25 after i.n. exposure 9 days post infection. The low frequency of effector T cells in the blood at day 9 after oral exposure would also indicate a delay or downregulation of the systemic T-cell response. As T-cell activation is a consequence of antigen presentation and interaction with APCs in the draining lymph nodes, this indicates that spread of virus to lymph nodes might be delayed after p.o. infection as has been suggested to occur after i.g. infection of LCMV in mice before (Rai et al., 1997). However, considering this delay, this also implies that it is not the resulting T-cell response that decreases viral spread to organs after oral infection.

Conversely, i.n. infection was linked to high expression of respiratory markers CCR3 and CCR4 (Danilova et al., 2015; Mikhak et al., 2013), especially on $CD4^+$ T cells. Both markers also showed significant co-expression, implicating a strong respiratory-homing capacity. It was demonstrated that T-cell effector frequencies differed between organs, and that i.n. infection recruited highest number of effector T cells to the lung, in accordance to the observed homing signature, and also to a certain degree the small intestine. Interestingly, it was identified, that those T cells were temporarily circulating and not robustly infiltrated into the lung tissue. In contrast, p.o. infection, as expected, was characterized by high expression of $\alpha4\beta7$ integrin, especially on $CD8^+$ T cells, which would imprint intestinal tropism onto these effector cells and has been described previously after oral exposure for rotavirus infection (Rott et al., 1997). In contrast, oral exposure was linked to higher frequencies of temporarily resident effector T cells in the small intestine, but also lung and spleen. Of note in this context is, however, that recently CD69 expression, which was shown here to be upregulated at this time point in orally exposed animals, has been demonstrated to also play a role in T-cell migration and tissue retention and acquisition of effector phenotype (Cibrián and Sánchez-Madrid, 2017). This could suggest, that during later acute phase of disease T-cell infiltration and retention in organs is increased after oral exposure and intestinal imprinting

This demonstrates that both exposure routes of LASV imprint corresponding T-cell homing signatures especially for these target tissues. However, further data suggest that these homing signatures might not be equally equipped to combat systemic disease. These observations are limited by the fact that data was only collected at one cross-sectional time point and it remains possible that the observed differences in T-cell infiltration are due to differences in T-cell activation kinetics.

5.3.3 IMPLICATIONS OF T-CELL HOMING FOR LASV TRANSMISSION IN HUMANS

Taken together this data heavily implies that LASV-specific T cells are imprinted with different homing signatures depending on the exposure route. It was previously demonstrated that homing signatures are not virus-specific but rely on the site of antigen encounter and exposure route. It was shown that rotavirus-specific homing signatures could be modified by change of the exposure route (Jiang et al., 2008). I hypothesized that also for Lassa the route of transmission determined the observable homing signature, not the virus itself. It was demonstrated here, that the signature imprinted on T cells during LF is subject to variation and that this is a consequence of the exposure route **(Figure 5.2)**.

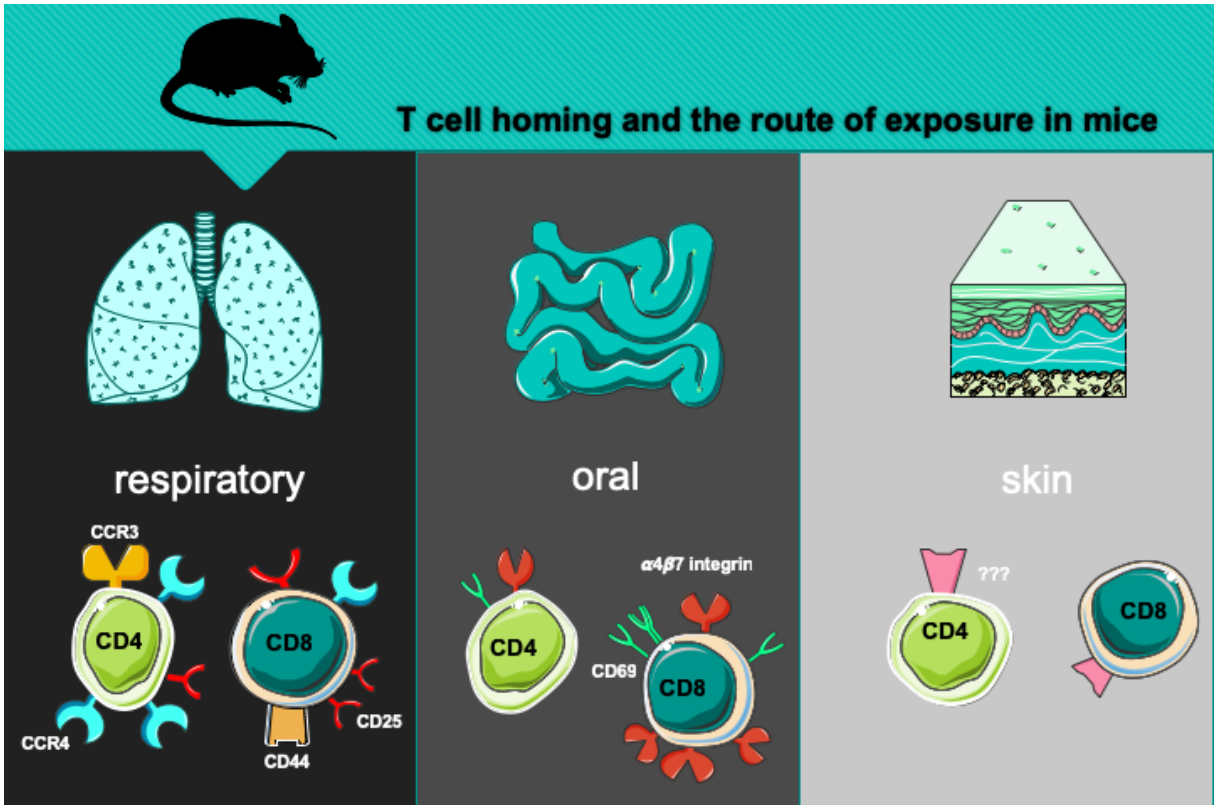

Figure 5.2: Exposure route dependent T-cell homing and activation in mice. Cross-sectional analysis of activation marker CD25 and CD69 is depicted for respiratory, oral and skin exposure with LASV in mice. Key differences in homing marker expression are summarized.

Respiratory or intestinal mucosae-imprinted T cells were identified, which matched the route of exposure. Signatures were clearly different between these two investigated mucosal exposure routes, which would allow for retroactive determination of exposure route based on the homing signature. It remains unclear if the imprinted homing signatures also would remain expressed long term. It would rely on identification of LASV-specific memory T cells, which could be achieved through tetramer technology. However, so far, no such tetramer is commercially available, and development has proven challenging in our hands due to off target effects. Additionally, further clarification is needed, if the T cells observed in this study are solely LASV-specific or if bystander activation is involved. Unfortunately, the herein used model is mostly lethal and characterized by strong inflammation which could mask LASV-specific responses and generation of a robust survivor cohort is only possible through drug administration (Oestereich, Rieger, et al., 2016). To cleanly define transmission dependent homing without the backdrop of systemic inflammation more artificial systems could also be employed such as a recombinant virus expressing OVA, which then could be tracked by OT1-T cells, which has been shown previously for example with yellow fever and murine CMV (McAllister, Arbetman, Mandl, Peña-Rossi, and Andino, 2000).

Interestingly, a circumstantial link has been suggested between gastrointestinal mucosal immunity and suspected asymptomatic infections with LASV by individuals living in close contact with rodents (Lukashevich, Clegg, and Sidibe, 1993; Lukashevich et al., 2002; Bonwitt et al., 2016). In the context of the epidemiological data gathered in our survey and the $\alpha 4\beta 1$ and $\alpha 4\beta 7$ integrin dominated homing signatures observed in human patients, the observations made in this mouse model would support that oral exposure risks are most common in the population we investigated, but that such exposure might not always lead to symptomatic disease and might favor, if symptomatic, survival.

Based on the T-cell phenotype observed in fatal LF in humans and the lethality, strong and fast immune activation and disease severity observed in mice after respiratory exposure it could be hypothesized that this infection route in humans might also be more likely to cause fatal outcome. Further work is necessary to determine if this hypothesis is correct and in respiratory infection does in fact also in mice reproduce other aspects of the dysfunctional and inflammation-driven T-cell response we described in fatal human cases.

While clear differences in homing and T-cell activation were observed depending on the exposure route in mice, verification of these in humans is strife with complications. Based on the observations that bystander T-cell involvement occurs it is possible that LASV-specific homing in humans to the site of antigen encounter is masked due to increased levels of inflammation, which overrides the organ-specific signatures. This would be supported by the observation, that T-cell infiltration occurs in the mouse model into various organs disregarding or even in spite of the non-matched homing markers expressed by those T cells. One solution to better mimic the human response would be adaptation of the model system. The immune memory of humans and lab-bred mice is not comparable. It can be expected, that LF patients have previously encountered acute and chronic infections, which shaped their immune system prior to infection with LASV. However, mice were housed in clean environments and husbandry was kept specific pathogen free, which has been reported to affect the immune system (Huggins, Jameson, and Hamilton, 2019; Mestas and Hughes, 2004; Tao and Reese, 2017) and has effect on the responses of bystander T cells to infection. For example, herpes infection has been shown to affect challenge with unrelated new viruses (Reese et al., 2016). In this context also co-infections must be considered, which cannot be ruled out for our human cohort, and which can alter unrelated memory or even T-cell activation and proliferation, as shown in the context of helminth infection in mice on virus-specific T cells (Osborne et al., 2014). Various comparative work have shown that mice with exposure to various pathogens present with enhanced interferon and effector/memory lymphocyte signatures more similar to adult humans (Beura et al., 2016; Kugelberg et al.,

2005; Tao and Reese, 2017). To more correctly mimic natural exposure routes and the homing signatures they imprint, it might be interesting in the future to repeat this study in mice, which were gradually reintroduced to a selection of pathogens before exposure to LASV occurs.

5.4 OUTLOOK: IMPLICATIONS FOR TREATMENT AND VACCINE DEVELOPMENT

The present studies described for the first time T-cell homing signatures during acute LF in a human cohort. It was shown that in humans, not only do different signatures exist, but also that severity of disease and outcome are differentiated by homing marker expression and may be due to differences of initial exposure to the virus. This has implication for both future treatment and vaccine developments

5.4.1 TREATMENT

If additional data could be generated to support the role of intestinal and inflammatory $\alpha4$ and $\beta7$ integrin mediated homing in LF in pathogenesis, this would allow for consideration of treatment options especially in the case of severe and fatal disease. Previously, treatment by antibodies targeted towards $\alpha4\beta7$ integrin has been used in multiple diseases with various levels of clinical success. Ulcerative colitis has been positively affected by such treatment (Feagan et al., 2005) and anti-$\alpha4\beta7$ antibodies have also been tried against Crohn`s disease (Bertoni et al., 2018; Feagan et al., 2008). Interestingly, treatment with such antibodies has also been proposed in HIV to ameliorate gut damage and decrease recruitment of susceptible T-cell to infection (Cao, Jiang, Zhang, Kondza, and Woodrow, 2018; Perciani et al., 2018). Vedolizumab, a monoclonal anti-$\alpha4\beta7$ antibody that blocks binding to MadCam-1, has also been used in humans to counteract severe intestinal acute graft-versus-host disease (Danylesko et al., 2019). If anti-$\alpha4\beta7$ treatment could reduce severity of symptoms due to reduced T-cell infiltration and pathogenesis should be further investigated applying Vedolizumab treatment especially after oral exposure in mice.

If in fatal outcome $CD4^+$ T cells, characterized by $\alpha4$ integrin expression, are demonstrated to be causative of pathogenesis and a direct negative effect of these cells could be attributed further, also here treatment with anti-$\alpha4$ integrin antibodies could be utilized to reduce immune-mediated pathology. Natalizumab is a humanized antibody against only the $\alpha4$ integrin subunit, which has been used against multiple sclerosis and Crohn's disease (Feagan et al., 2008; Polman et al., 2006). In an NHP simian immunodeficiency virus model

treatment with anti-α4 antibodies conferred blocking of virus form the brain and gut, which also protected from injury in the central nervous system (Campbell et al., 2014). Once the role of integrins in LF has been even more determined, such antibody treatments could be proposed and tested.

5.4.2 VACCINE DEVELOPMENT

If a slowly developing but robust α1 integrin supported mucosal signature is naturally associated with mild disease and survival, this could inform future vaccine developments. It should then be taken into consideration, whether potential vaccine candidates impress similar behavior on the T cells generated. In this context also, it needs to be further clarified if intestinal homing, as observed in some survivors, is necessary to combat disease or a part of aberrant T-cell behavior and pathology. If the former, it might be worth considering also for the vaccine design. Interestingly, modification of the homing potential though variation of inoculation route or through direct targeting of T-cell priming an imprinting milieu have been used in other disease to increase vaccine efficiency. This has especially focused on involvement of mucosal homing capacity and increase thereof (Mwanza-Lisulo et al., 2018; Sackstein et al., 2017; Sandoval et al., 2013). In this context it would be interesting to further see, if increased mucosal homing capacity confers protection from disease.

5.5 OUTLOOK: IMPLICATIONS FOR PUBLIC HEALTH

The work presented here also characterized differences in homing behavior after natural exposure routes in mice, which allows speculation on the more prevalent infection risks in humans. As our data suggest that different exposure risks may also be potentially linked to differences in disease severity, this is highly relevant and could inform future public health policies. Clearly the caveat must be given, that while in mice exposure routes clearly presented with differences in T-cell homing, these were difficult in humans to ascertain in the context of overall activation and inflammation. As of now, the T-cell homing signatures may provide information towards the potential exposure route but more work in necessary to fully identify if, also in humans, retrospective identification of the infection route through analysis of T cells is accurate.

Placed in the epidemiological context, homing data might suggest that exposure routes through the intestinal mucosae are most prevalent. If this could be further confirmed, it would entail future implications for public health management. As no vaccine and LASV-specific treatment are available currently, minimizing exposure risk to LASV is key to combat LF.

Especially since the last outbreaks in Nigeria, public health awareness measures and public knowledge on disease have noticeably increased. However, as our epidemiological survey confirms, awareness of oral exposure through contaminated food items does not carry over into actually protection by non-consumption of uncooked or uncovered food. If additional studies in humans and model animals could support our putative link between respiratory exposure and fatal outcome this would be highly relevant and more protective measures could be advised to protect people from inhalation of contaminated particles.

Hence, if a more concise link between T-cell homing signatures and exposure route in humans could be confirmed this could allow for identification and confirmation of the suspected exposure risks on a patient cohort or outbreak-specific level. These findings could then be utilized to not only inform general future public health policies but to specifically design more directed public awareness measured to minimizes the specific risks for each unique population exposed to LASV.

6 MATERIALS

6.1 GENERAL PLASTIC CONSUMABLES

General consumables were obtained from Eppendorf, Sarstedt, Greiner Bio One, Qiagen, Thermo Scientific, Miltenyi, Sigma-Aldrich, Carl Roth and StemCell Technologies. Specific equipment is listed below:

MATERIAL	MANUFACTURER
Syringe 1 mL	Braun
Syringe 5 mL	Braun
Insulin Syringe	Braun
Needles	Braun
Tuberculin syringe	Braun
Surgical Blades (Carbon Steel Sterile No. 11)	Swann-Morton
Sterile cellulose swabs Pur-Zellin	Hartmann
Microvette z-Gel tubes	Sarstedt
Microvette LiHep-Gel tubes	Sarstedt
EDTA tubes	Sarstedt

6.2 REAGENTS, CHEMICALS AND KITS

ITEM	MANUFACTURER
HLA-A low resolution screening kit	Olerup
Agarose	Bio & Sell
Agencout AMPure XP reagent	Beckman Coulter
Baytril	Bayer
BSA	Sigma-Aldrich
Collagenase D	Thermo Fisher Scientific
CompBeads	BD
custom Flex-T™ MHC Tetramer kit	Biolegend
Cytofix/Cytoperm	BD
D-Biotin	Invitrogen
dH2O	Ampuwa
Direct-zol™ RNA Miniprep Plus	Zymo
DMEM	Gibco
DMSO	Sigma-Aldrich
DNAse I	Thermo Fisher Scientific
DNeasy Blood and Tissue kit	Qiagen
dNTPs	Roth

ITEM	MANUFACTURER
Ethanol	Roth
Ethidiumbromid	Roth
FCS	Gibco
Formaldehyde solution 37%	Roth
Fuji DRI-CHEM AST(GOT8) test chips	Fujifilm
GenerRuler 1kb DNA ladder	Thermo Fisher Scientific
GolgiStopTM	BD
Illumina Nextera XT index kit	Illumina
Isoflurane	Baxter
Isopropanol	Roth
L-Glutamin	Gibco
Lymphoprep/SepMate	Stemcell Technologies
Lysing matrix D	MP Biomedicals
Methanol	Roth
Methylcellulose	Sigma-Aldrich
Multiplex PCR kit	Qiagen
NaN_3	Sigma-Aldrich
NP-40	Sigma-Aldrich
Oligonucleotide	Sigma-Aldrich
Paraformaldehyd	Roth
PBS	Gibco
Penicillin	Gibco
Peracidic Acid	Roth
PermWash solution	BD
PHA-L	Merck
PMA/ionomycin	Sigma-Aldrich
QIAamp® Viral RNA Mini Kit	Qiagen
random primers	Roth
RBC Lysis Buffer	Biolegend
RealStar® Lassa Kit 1.0	Altona Diagnostics
Red blood cell lysis buffer	Biolegend
RPMI	Gibco
Strep-HRP	Dako
Streptomycin	Gibco
streptavidin labelling kits	Biolegend
SuperScript III reaction kit	Thermo Fisher Scientific
TAE-Buffer	Merck
TMB substrate	Mikrogen Diagnostic
TMB substrate Elispot	MabTech
TRIzol™ Reagent	Invitrogen
TrypLE™ Express	Gibco
Tween-20	Roth

ITEM	MANUFACTURER
Zombie Aqua™ Fixable Viability Kit	Biolegend
Zombie Nir™ Fixable Viability Kit	Biolegend
Zombie Yellow™ Fixable Viability Kit	Biolegend

6.3 MEDIA AND SOLUTIONS

NAME	COMPOSITION	VOLUME
Cell culture medium with 5 % FCS	DMEM FCS Penicillin/Streptomycin (100x) L-Glutamine (100x)	500 mL 25 mL 5 mL 5 mL
T-cell medium with 10 % serum	RPMI-1640 or CO_2-free medium FCS or HS Penicillin/Streptomycin (100x) L-Glutamine (100x)	500 mL 50 mL 5 mL 5 mL
Titration medium with 2 % FCS	DMEM FCS Penicillin/Streptomycin (100x) L-Glutamine (100x)	500 mL 25 mL 5 mL 5 mL
Methylcellulose solution for overlay media	Methylcellulose dH_2O autoclaved; stirred for 24 hours	16.8 g 600 mL
Overlay medium for immunofocus assays	Cell culture media with 10% FCS Methylcellulose solution	400 mL 200 mL
Collagenase D stock solution (20 mg/mL)	Collagenase D 1x HBSS	20 mg 1 mL
DNaseI stock solution (5 mg/mL)	DNase I 1x HBSS	5 mg 1 mL
Tetramer peptide exchange blocking solution	50 mM D-Biotin 10 % (w/v) NaN3 PBS	1.6 µL 6 µL 192.4 µl

6.4 PRIMERS, PEPTIDES AND ANTIBODIES

PRIMERS

TCR sequencing primers were designed according to literature (Robins et al., 2009). Two sets were used, either with or without nextera adapter sequences.

Table 6.1: TCR sequencing primers

OLIGO-	SEQUENCE (5‘-3‘)
TRBV2-gDNA-For	TCAAATTTCACTCTGAAGATCCGGTCCACAA
TRBV3-1-gDNA-For	GCTCACTTAAATCTTCACATCAATTCCCTGG
TRBV4-1-gDNA-For	CTTAAACCTTCACCTACACGCCCTGC
TRBV4-2+-gDNA-For	CTTATTCCTTCACCTACACACCCTGC

OLIGO-	SEQUENCE (5‘-3‘)
TRBV5-1-gDNA-For	GCTCTGAGATGAATGTGAGCACCTTG
TRBV5-3-gDNA-For	GCTCTGAGATGAATGTGAGTGCCTTG
TRBV5-4+-gDNA-For	GCTCTGAGCTGAATGTGAACGCCTTG
TRBV6-1-gDNA-For	TCGCTCAGGCTGGAGTCGGCTG
TRBV6-2+-gDNA-For	GCTGGGGTTGGAGTCGGCTG
TRBV6-4-gDNA-For	CCCTCACGTTGGCGTCTGCTG
TRBV6-5-gDNA-For	GCTCAGGCTGCTGTCGGCTG
TRBV6-6-gDNA-For	CGCTCAGGCTGGAGTTGGCTG
TRBV6-7-gDNA-For	CCCCTCAAGCTGGAGTCAGCTG
TRBV6-8-gDNA-For	CACTCAGGCTGGTGTCGGCTG
TRBV6-9-gDNA-For	CGCTCAGGCTGGAGTCAGCTG
TRBV7-1-gDNA-For	CCACTCTGAAGTTCCAGCGCACAC
TRBV7-2-gDNA-For	CACTCTGACGATCCAGCGCACAC
TRBV7-3-gDNA-For	CTCTACTCTGAAGATCCAGCGCACAG
TRBV7-4-gDNA-For	CCACTCTGAAGATCCAGCGCACAG
TRBV7-6-gDNA-For	CACTCTGACGATCCAGCGCACAG
TRBV7-7-gDNA-For	CCACTCTGACGATTCAGCGCACAG
TRBV7-8-gDNA-For	CCACTCTGAAGATCCAGCGCACAC
TRBV7-9-gDNA-For	CACCTTGGAGATCCAGCGCACAG
TRBV9-gDNA-For	GCACTCTGAACTAAACCTGAGCTCTCTG
TRBV10-1-gDNA-For	CCCCTCACTCTGGAGTCTGCTG
TRBV10-2-gDNA-For	CCCCCTCACTCTGGAGTCAGCTA
TRBV10-3-gDNA-For	CCTCCTCACTCTGGAGTCCGCTA
TRBV11-1+-gDNA-For	CCACTCTCAAGATCCAGCCTGCAG
TRBV11-2-DNA-For	CTCCACTCTCAAGATCCAGCCTGCAA
TRBV12-3+-gDNA-For	CCACTCTGAAGATCCAGCCCTCAG
TRBV13-gDNA-For	CATTCTGAACTGAACATGAGCTCCTTGG
TRBV14-gDNA-For	CTACTCTGAAGGTGCAGCCTGCAG
TRBV15-gDNA-For	GATAACTTCCAATCCAGGAGGCCGAACA
TRBV16-gDNA-For	CTGTAGCCTTGAGATCCAGGCTACGA
TRBV17-gDNA-For	CTTCCACGCTGAAGATCCATCCCG
TRBV18-gDNA-For	GCATCCTGAGGATCCAGCAGGTAG
TRBV19-gDNA-For	CCTCTCACTGTGACATCGGCCC
TRBV20-1-gDNA-For	CTTGTCCACTCTGACAGTGACCAGTG
TRBV23-1-gDNA-For	CAGCCTGGCAATCCTGTCCTCAG
TRBV24-1-gDNA-For	CTCCCTGTCCCTAGAGTCTGCCAT
TRBV25-1-gDNA-For	CCCTGACCCTGGAGTCTGCCA
TRBV27-gDNA-For	CCCTGATCCTGGAGTCGCCCA
TRBV28-gDNA-For	CTCCCTGATTCTGGAGTCCGCCA
TRBV29-1-gDNA-For	CTAACATTCTCAACTCTGACTGTGAGCAACA
TRBV30-gDNA-For	CGGCAGTTCATCCTGAGTTCTAAGAAGC
TRBJ1-1-gDNA-Rev	TTACCTACAACTGTGAGTCTGGTGCCTTGTCCAAA
TRBJ1-2-gDNA-Rev	ACCTACAACGGTTAACCTGGTCCCCGAACCGAA
TRBJ1-3-gDNA-Rev	ACCTACAACAGTGAGCCAACTTCCCTCTCCAAA
TRBJ1-4-gDNA-Rev	CCAAGACAGAGAGCTGGGTTCCACTGCCAAA
TRBJ1-5-gDNA-Rev	AGGATGGAGAGTCGAGTCCCATCACCAAA
TRBJ1-6-gDNA-Rev	CTGTCACAGTGAGCCTGGTCCCGTTCCCAAA
TRBJ2-1-gDNA-Rev	CGGTGAGCCGTGTCCCTGGCCCGAA
TRBJ2-2-gDNA-Rev	CCAGTACGGTCAGCCTAGAGCCTTCTCCAAA
TRBJ2-3-gDNA-Rev	ACTGTCAGCCGGGTGCCTGGGCCAAA
TRBJ2-4-gDNA-Rev	AGAGCCGGGTCCCGGCGCCGAA
TRBJ2-5-gDNA-Rev	GGAGCCGCGTGCCTGGCCCGAA
TRBJ2-6-gDNA-Rev	GTCAGCCTGCTGCCGGCCCCGAA
TRBJ2-7-gDNA-Rev	GTGAGCCTGGTGCCCGGCCCGAA
TRBV2-Nextera-gDNA-For	TCGTCGGCAGCGTCAGATGTGTATAAGAGACAGTCAAATTTCACTCTGAAGATCCGGTCCAC AA
TRBV3-1-Nextera-gDNA-For	TCGTCGGCAGCGTCAGATGTGTATAAGAGACAGGCTCACTTAAATCTTCACATCAATTCCCT GG
TRBV4-1-Nextera-gDNA-For	TCGTCGGCAGCGTCAGATGTGTATAAGAGACAGCTTAAACCTTCACCTACACGCCCTGC
TRBV4-2+Nextera-gDNA-For	TCGTCGGCAGCGTCAGATGTGTATAAGAGACAGCTTATTCCTTCACCTACACACCCTGC
TRBV5-1-Nextera-gDNA-For	TCGTCGGCAGCGTCAGATGTGTATAAGAGACAGGCTCTGAGATGAATGTGAGCACCTTG
TRBV5-3-Nextera-gDNA-For	TCGTCGGCAGCGTCAGATGTGTATAAGAGACAGGCTCTGAGATGAATGTGAGTGCCTTG
TRBV5-4+Nextera-gDNA-For	TCGTCGGCAGCGTCAGATGTGTATAAGAGACAGGCTCTGAGCTGAATGTGAACGCCTTG
TRBV6-1-Nextera-gDNA-For	TCGTCGGCAGCGTCAGATGTGTATAAGAGACAGTCGCTCAGGCTGGAGTCGGCTG
TRBV6-2+Nextera-gDNA-For	TCGTCGGCAGCGTCAGATGTGTATAAGAGACAGGCTGGGGTTGGAGTCGGCTG
TRBV6-4-Nextera-gDNA-For	TCGTCGGCAGCGTCAGATGTGTATAAGAGACAGCCCTCACGTTGGCGTCTGCTG

OLIGO-	SEQUENCE (5‘-3‘)
TRBV6-5-Nextera-gDNA-For	TCGTCGGCAGCGTCAGATGTGTATAAGAGACAGGCTCAGGCTGCTGTCGGCTG
TRBV6-6-Nextera-gDNA-For	TCGTCGGCAGCGTCAGATGTGTATAAGAGACAGCGCTCAGGCTGGAGTTGGCTG
TRBV6-7-Nextera-gDNA-For	TCGTCGGCAGCGTCAGATGTGTATAAGAGACAGCCCCTCAAGCTGGAGTCAGCTG
TRBV6-8-Nextera-gDNA-For	TCGTCGGCAGCGTCAGATGTGTATAAGAGACAGCACTCAGGCTGGTGTCGGCTG
TRBV6-9-Nextera-gDNA-For	TCGTCGGCAGCGTCAGATGTGTATAAGAGACAGCGCTCAGGCTGGAGTCAGCTG
TRBV7-1-Nextera-gDNA-For	TCGTCGGCAGCGTCAGATGTGTATAAGAGACAGCCACTCTGAAGTTCCAGCGCACAC
TRBV7-2-Nextera-gDNA-For	TCGTCGGCAGCGTCAGATGTGTATAAGAGACAGCACTCTGACGATCCAGCGCACAC
TRBV7-3-Nextera-gDNA-For	TCGTCGGCAGCGTCAGATGTGTATAAGAGACAGCTCTACTCTGAAGATCCAGCGCACAG
TRBV7-4-Nextera-gDNA-For	TCGTCGGCAGCGTCAGATGTGTATAAGAGACAGCCACTCTGAAGATCCAGCGCACAG
TRBV7-6-Nextera-gDNA-For	TCGTCGGCAGCGTCAGATGTGTATAAGAGACAGCACTCTGACGATCCAGCGCACAG
TRBV7-7-Nextera-gDNA-For	TCGTCGGCAGCGTCAGATGTGTATAAGAGACAGCCACTCTGACGATTCAGCGCACAG
TRBV7-8-Nextera-gDNA-For	TCGTCGGCAGCGTCAGATGTGTATAAGAGACAGCCACTCTGAAGATCCAGCGCACAC
TRBV7-9-Nextera-gDNA-For	TCGTCGGCAGCGTCAGATGTGTATAAGAGACAGCACCTTGGAGATCCAGCGCACAG
TRBV9-Nextera-gDNA-For	TCGTCGGCAGCGTCAGATGTGTATAAGAGACAGGCACTCTGAACTAAACCTGAGCTCTCTG
TRBV10-1-Nextera-gDNA-For	TCGTCGGCAGCGTCAGATGTGTATAAGAGACAGCCCCTCACTCTGGAGTCTGCTG
TRBV10-2-Nextera-gDNA-For	TCGTCGGCAGCGTCAGATGTGTATAAGAGACAGCCCCCTCACTCTGGAGTCAGCTA
TRBV10-3-Nextera-gDNA-For	TCGTCGGCAGCGTCAGATGTGTATAAGAGACAGCCTCCTCACTCTGGAGTCCGCTA
TRBV11-1+Nextera-gDNA-For	TCGTCGGCAGCGTCAGATGTGTATAAGAGACAGCCACTCTCAAGATCCAGCCTGCAG
TRBV11-2-Nextera-DNA-For	TCGTCGGCAGCGTCAGATGTGTATAAGAGACAGCTCCACTCTCAAGATCCAGCCTGCAA
TRBV12-3+Nextera-gDNA-For	TCGTCGGCAGCGTCAGATGTGTATAAGAGACAGCCACTCTGAAGATCCAGCCCTCAG
TRBV13-Nextera-gDNA-For	TCGTCGGCAGCGTCAGATGTGTATAAGAGACAGCATTCTGAACTGAACATGAGCTCCTTGG
TRBV14-Nextera-gDNA-For	TCGTCGGCAGCGTCAGATGTGTATAAGAGACAGCTACTCTGAAGGTGCAGCCTGCAG
TRBV15-Nextera-gDNA-For	TCGTCGGCAGCGTCAGATGTGTATAAGAGACAGGATAACTTCCAATCCAGGAGGCCGAACA
TRBV16-Nextera-gDNA-For	TCGTCGGCAGCGTCAGATGTGTATAAGAGACAGCTGTAGCCTTGAGATCCAGGCTACGA
TRBV17-Nextera-gDNA-For	TCGTCGGCAGCGTCAGATGTGTATAAGAGACAGCTTCCACGCTGAAGATCCATCCCG
TRBV18-Nextera-gDNA-For	TCGTCGGCAGCGTCAGATGTGTATAAGAGACAGGCATCCTGAGGATCCAGCAGGTAG
TRBV19-Nextera-gDNA-For	TCGTCGGCAGCGTCAGATGTGTATAAGAGACAGCCTCTCACTGTGACATCGGCCC
TRBV20-1-Nextera-gDNA-For	TCGTCGGCAGCGTCAGATGTGTATAAGAGACAGCTTGTCCACTCTGACAGTGACCAGTG
TRBV23-1-Nextera-gDNA-For	TCGTCGGCAGCGTCAGATGTGTATAAGAGACAGCAGCCTGGCAATCCTGTCCTCAG
TRBV24-1-Nextera-gDNA-For	TCGTCGGCAGCGTCAGATGTGTATAAGAGACAGCTCCCTGTCCCTAGAGTCTGCCAT
TRBV25-1-Nextera-gDNA-For	TCGTCGGCAGCGTCAGATGTGTATAAGAGACAGCCCTGACCCTGGAGTCTGCCA
TRBV27-Nextera-gDNA-For	TCGTCGGCAGCGTCAGATGTGTATAAGAGACAGCCCTGATCCTGGAGTCGCCCA
TRBV28-Nextera-gDNA-For	TCGTCGGCAGCGTCAGATGTGTATAAGAGACAGCTCCCTGATTCTGGAGTCCGCCA
TRBV29-1-Nextera-gDNA-For	TCGTCGGCAGCGTCAGATGTGTATAAGAGACAGCTAACATTCTCAACTCTGACTGTGAGCAACA
TRBV30-Nextera-gDNA-For	TCGTCGGCAGCGTCAGATGTGTATAAGAGACAGCGGCAGTTCATCCTGAGTTCTAAGAAGC
TRBJ1-1-Nextera-gDNA-Rev	GTCTCGTGGGCTCGGAGATGTGTATAAGAGACAGTTACCTACAACTGTGAGTCTGGTGCCTTGTCCAAA
TRBJ1-2-Nextera-gDNA-Rev	GTCTCGTGGGCTCGGAGATGTGTATAAGAGACAGACCTACAACGGTTAACCTGGTCCCCGAACCGAA
TRBJ1-3-Nextera-gDNA-	GTCTCGTGGGCTCGGAGATGTGTATAAGAGACAGACCTACAACAGTGAGCCAACTTCCCTCT

OLIGO-	SEQUENCE (5'-3')
Rev	CCAAA
TRBJ1-4-Nextera-gDNA-Rev	GTCTCGTGGGCTCGGAGATGTGTATAAGAGACAGCCAAGACAGAGAGCTGGGTTCCACTGCCAAA
TRBJ1-5-Nextera-gDNA-Rev	GTCTCGTGGGCTCGGAGATGTGTATAAGAGACAGAGGATGGAGAGTCGAGTCCCATCACCAAA
TRBJ1-6-Nextera-gDNA-Rev	GTCTCGTGGGCTCGGAGATGTGTATAAGAGACAGCTGTCACAGTGAGCCTGGTCCCGTTCCCAAA
TRBJ2-1-Nextera-gDNA-Rev	GTCTCGTGGGCTCGGAGATGTGTATAAGAGACAGCGGTGAGCCGTGTCCCTGGCCCGAA
TRBJ2-2-Nextera-gDNA-Rev	GTCTCGTGGGCTCGGAGATGTGTATAAGAGACAGCCAGTACGGTCAGCCTAGAGCCTTCTCCAAA
TRBJ2-3-Nextera-gDNA-Rev	GTCTCGTGGGCTCGGAGATGTGTATAAGAGACAGACTGTCAGCCGGGTGCCTGGGCCAAA
TRBJ2-4-Nextera-gDNA-Rev	GTCTCGTGGGCTCGGAGATGTGTATAAGAGACAGAGAGCCGGGTCCCGGCGCCGAA
TRBJ2-5-Nextera-gDNA-Rev	GTCTCGTGGGCTCGGAGATGTGTATAAGAGACAGGGAGCCGCGTGCCTGGCCCGAA
TRBJ2-6-Nextera-gDNA-Rev	GTCTCGTGGGCTCGGAGATGTGTATAAGAGACAGGTCAGCCTGCTGCCGGCCCCGAA
TRBJ2-7-Nextera-gDNA-Rev	GTCTCGTGGGCTCGGAGATGTGTATAAGAGACAGGTGAGCCTGGTGCCCGGCCCGAA

LASV-SPECIFIC PEPTIDES

Peptides were generated using the immune epitope data base (IEDB) prediction tool utilizing an artificial neural network prediction method (ANN) for MHC-I binding prediction. (http://tools.immuneepitope.org/mhci/). Peptides were predicted for all common HLA-A and HLA-B alleles to cover > 95 % of the Nigerian population. Only peptides with a predicted IC_{50} < 100 nmol were selected. Peptide prediction was performed for LASV strain Ba366 (GU830839.1), which is a commonly used lab strain and a field isolated strain Nig-08-A47 (Irrua, Nigeria 2008) (ADU56631.1). A peptide pool was generated comprising peptides found in both sequences to increase likelihood of sequence conservation.

https://www.ncbi.nlm.nih.gov/nuccore/GU830839.1

https://www.ncbi.nlm.nih.gov/protein/ADU56631.1

Table 6.2: Predicted LASV peptides: with affinity for the indicated HLA-A or B alleles. IC_{50}=halve maximal inhibitory concentration (nM). Only peptides predicted for Ba366 (black) and Nig 08-A47 (blue) were included in the generation of a peptide pool.

ALLELE	START POSITION IN NP	PEPTIDE	PREDICTED IC_{50}
HLA-A*32:01	8	KSFLWTQSL	11.18
HLA-A*32:01	8	KSFLWTQSL	11.18
HLA-B*15:03	8	KSFLWTQSL	16.31
HLA-B*15:03	8	KSFLWTQSL	16.31
HLA-B*57:01	8	KSFLWTQSL	56.71
HLA-B*57:01	8	KSFLWTQSL	56.71
HLA-B*58:01	8	KSFLWTQSL	74.08
HLA-B*58:01	8	KSFLWTQSL	74.08
HLA-A*31:01	9	SFLWTQSLR	17.58
HLA-A*31:01	9	SFLWTQSLR	17.58
HLA-A*33:01	9	SFLWTQSLR	27.05
HLA-A*33:01	9	SFLWTQSLR	27.05
HLA-A*68:01	44	FSEVSNVQR	23.64

ALLELE	START POSITION IN NP	PEPTIDE	PREDICTED IC_{50}
HLA-A*68:01	44	FSEVSNVQR	23.64
HLA-B*40:01	45	SEVSNVQRL	102.10
HLA-A*02:03	66	RLRDLNQAV	13.62
HLA-A*02:03	66	RLRDLNQAV	13.62
HLA-A*30:01	66	RLRDLNQAV	27.78
HLA-A*30:01	66	RLRDLNQAV	27.78
HLA-A*11:01	73	AVNNLVELK	12.02
HLA-A*11:01	73	AVNNLVELK	12.02
HLA-A*11:01	82	STQQKSILR	71.59
HLA-A*31:01	82	STQQKSILR	68.43
HLA-A*68:01	82	STQQKSILR	98.16
HLA-A*02:06	94	LTSDDLLTL	19.33
HLA-A*01:01	95	TSDDLLILA	89.63
HLA-A*01:01	95	TSDDLLTLA	88.79
HLA-A*11:01	100	LILAADLEK	84.94
HLA-A*11:01	100	LTLAADLEK	51.94
HLA-A*02:01	101	ILAADLEKL	52.22
HLA-A*02:03	101	ILAADLEKL	18.60
HLA-A*02:03	101	TLAADLEKL	27.70
HLA-A*02:06	101	ILAADLEKL	65.68
HLA-A*30:01	110	KTKVTRTER	14.56
HLA-A*30:01	110	KSKVIRTER	51.68
HLA-A*31:01	110	KTKVTRTER	4.59
HLA-A*31:01	110	KSKVIRTER	4.38
HLA-A*30:01	113	VTRTERPLS	84.49
HLA-B*07:02	118	RPLSAGVYM	12.19
HLA-B*07:02	118	RPLSSGVYM	13.94
HLA-A*02:01	139	ALLNMIGMV	18.92
HLA-A*02:03	139	ALLNMIGMV	9.53
HLA-A*02:06	139	ALLNMIGMV	20.99
HLA-A*02:03	142	NMIGMVGGA	6.54
HLA-A*02:03	145	GMNGGNQGV	19.66
HLA-A*11:01	159	GVVRVWDVK	81.96
HLA-A*11:01	159	GVVRVWDVK	81.96
HLA-B*15:01	171	LLNNQFGTM	21.46
HLA-B*15:01	171	LLNNQFGTM	21.46
HLA-A*02:06	174	NQFGTMPSL	11.07
HLA-A*02:06	174	NQFGTMPSL	11.07
HLA-A*02:03	177	GTMPSLTLA	29.49
HLA-A*02:03	177	GTMPSLTLA	29.49
HLA-A*02:06	177	GTMPSLTLA	20.99
HLA-A*02:06	177	GTMPSLTLA	20.99
HLA-B*07:02	179	MPSLTLACL	67.99
HLA-B*07:02	179	MPSLTLACL	67.99
HLA-B*35:01	179	MPSLTLACL	39.75
HLA-B*35:01	179	MPSLTLACL	39.75
HLA-B*53:01	179	MPSLTLACL	84.33
HLA-B*53:01	179	MPSLTLACL	84.33
HLA-A*02:06	191	GQVDLNDAV	8.30
HLA-A*02:06	191	GQVDLNDAV	8.30
HLA-A*30:02	205	LGLIYTAKY	76.55
HLA-A*30:02	205	LGLIYTAKY	76.55
HLA-B*15:03	205	LGLIYTAKY	66.64
HLA-B*15:03	205	LGLIYTAKY	66.64
HLA-B*15:03	211	AKYPNTSDL	21.29
HLA-B*15:03	211	AKYPNSSDL	24.99
HLA-B*15:03	223	AQSHPILNM	11.51
HLA-B*15:03	223	SQSHPILNM	11.46
HLA-A*68:02	224	QSHPILNMI	35.40
HLA-A*68:02	224	QSHPILNMV	12.64
HLA-B*08:01	231	MIDTKKSSL	84.22
HLA-A*30:02	236	KSSLNISGY	28.11
HLA-A*30:02	236	KSSLNISGY	28.11
HLA-B*15:03	236	KSSLNISGY	76.13
HLA-B*15:03	236	KSSLNISGY	76.13
HLA-A*02:01	240	NISGYNFSL	80.37
HLA-A*02:01	240	NISGYNFSL	80.37
HLA-A*30:01	251	AVKAGACML	40.73
HLA-A*30:01	251	AVKAGACML	40.73
HLA-A*02:01	257	CMLDGGNML	99.67
HLA-A*02:03	257	CMLDGGNML	94.04
HLA-A*02:06	257	CMLDGGNML	68.45
HLA-B*15:03	257	CMLDGGNML	69.27
HLA-B*07:02	271	SPQTMDGIL	32.76

ALLELE	START POSITION IN NP	PEPTIDE	PREDICTED IC_{50}
HLA-A*32:01	287	RTLGMFVSD	31.81
HLA-A*68:01	292	FVSDTPGER	15.39
HLA-A*68:01	292	FVSDTPGER	15.39
HLA-A*26:01	295	DTPGERNPY	59.74
HLA-A*26:01	295	DTPGERNPY	59.74
HLA-A*23:01	302	PYENILYKI	43.42
HLA-A*23:01	302	PYENILYKI	43.42
HLA-A*24:02	302	PYENILYKI	289.38
HLA-A*24:02	302	PYENILYKI	289.38
HLA-A*33:01	315	DGWPYIASR	18.95
HLA-A*33:01	315	DGWPYIASR	18.95
HLA-A*02:01	319	YIASRTSIV	95.75
HLA-A*02:03	319	YIASRTSIT	36.97
HLA-A*02:03	319	YIASRTSIV	3.13
HLA-A*02:06	319	YIASRTSIV	81.46
HLA-A*68:02	319	YIASRTSIV	97.87
HLA-A*31:01	321	ASRTSITGR	9.91
HLA-A*31:01	321	ASRTSIVGR	8.90
HLA-B*57:01	323	RTSITGRAW	13.80
HLA-B*57:01	323	RTSIVGRAW	11.27
HLA-B*58:01	323	RTSITGRAW	38.01
HLA-B*58:01	323	RTSIVGRAW	12.56
HLA-A*03:01	346	KVGTAGSNK	67.73
HLA-B*15:01	356	LQSAGFTAG	53.13
HLA-A*68:02	357	QSAGFTAGL	6.57
HLA-A*68:02	357	QSAGFPTGL	50.58
HLA-B*15:01	359	AGFTAGLTY	97.44
HLA-B*15:01	359	AGFPTGLTY	67.57
HLA-A*68:02	361	FTAGLTYSQ	81.17
HLA-B*35:01	361	FPTGLTYSQ	20.15
HLA-B*53:01	361	FPTGLTYSQ	62.42
HLA-A*02:03	365	LTYSQLMTL	69.03
HLA-A*02:03	365	LTYSQLMTL	69.03
HLA-A*02:06	365	LTYSQLMTL	52.33
HLA-A*02:06	365	LTYSQLMTL	52.33
HLA-B*15:03	365	LTYSQLMTL	32.17
HLA-B*15:03	365	LTYSQLMTL	32.17
HLA-A*02:03	372	TLKDAMLQL	17.64
HLA-A*02:03	372	TLKDSMMQL	9.94
HLA-A*02:01	376	SMMQLDPSA	37.62
HLA-A*02:03	376	SMMQLDPSA	70.58
HLA-A*02:06	376	SMMQLDPSA	87.91
HLA-A*31:01	385	KTWMDIEGR	29.25
HLA-A*31:01	385	KTWIDIEGR	31.99
HLA-B*15:03	398	VEIALYQPM	96.21
HLA-B*40:01	398	VEIALYQPM	21.25
HLA-B*44:02	398	VEIALYQPM	39.67
HLA-B*44:03	398	VEIALYQPM	97.47
HLA-A*30:02	402	LYQPSSGCY	40.97
HLA-A*30:02	402	LYQPMSGCY	33.12
HLA-A*02:06	403	YQPSSGCYI	19.33
HLA-A*02:06	403	YQPMSGCYI	15.34
HLA-B*15:03	403	YQPSSGCYI	12.06
HLA-B*15:03	403	YQPMSGCYI	11.79
HLA-B*35:01	404	QPSSGCYIH	87.11
HLA-B*35:01	404	QPMSGCYIH	30.65
HLA-A*23:01	406	MSGCYIHFF	36.42
HLA-B*15:03	406	SSGCYIHFF	79.43
HLA-B*15:03	406	MSGCYIHFF	46.26
HLA-B*58:01	406	MSGCYIHFF	35.93
HLA-A*31:01	407	SGCYIHFFR	5.64
HLA-A*31:01	407	SGCYIHFFR	5.64
HLA-A*33:01	407	SGCYIHFFR	75.72
HLA-A*33:01	407	SGCYIHFFR	75.72
HLA-A*68:01	407	SGCYIHFFR	22.52
HLA-A*68:01	407	SGCYIHFFR	22.52
HLA-A*30:02	421	KQFKQDAKY	50.80
HLA-A*30:02	421	KQFKQDAKY	50.80
HLA-B*15:01	421	KQFKQDAKY	91.67
HLA-B*15:01	421	KQFKQDAKY	91.67
HLA-B*15:03	421	KQFKQDAKY	3.33
HLA-B*15:03	421	KQFKQDAKY	3.33
HLA-B*15:03	427	AKYSHGIDV	24.23
HLA-B*15:03	427	AKYSHGIDV	24.23

ALLELE	START POSITION IN NP	PEPTIDE	PREDICTED IC_{50}
HLA-B*35:01	439	FPAQPGLTS	37.67
HLA-A*02:03	441	AQPGLTSAV	19.95
HLA-A*02:03	441	AQPGLTSAV	19.95
HLA-A*02:06	441	AQPGLTSAV	12.40
HLA-A*02:06	441	AQPGLTSAV	12.40
HLA-A*02:01	444	GLTSAVIEA	99.58
HLA-A*02:01	444	GLTSAVIEA	99.58
HLA-A*02:03	444	GLTSAVIEA	42.35
HLA-A*02:03	444	GLTSAVIEA	42.35
HLA-A*68:02	445	LTSAVIEAL	13.84
HLA-A*68:02	445	LTSAVIEAL	13.84
HLA-B*08:01	451	EALPRNMVL	126.51
HLA-A*03:01	469	KLLESQGRK	18.54
HLA-A*03:01	480	KLIDIALSK	28.90
HLA-A*03:01	480	KLIDIALSK	28.90
HLA-A*11:01	480	KLIDIALSK	12.71
HLA-A*11:01	480	KLIDIALSK	12.71
HLA-A*30:01	480	KLIDIALSK	89.73
HLA-A*30:01	480	KLIDIALSK	89.73
HLA-B*44:02	494	YENAVWDQY	42.29
HLA-B*44:03	494	YENAVWDQY	35.56
HLA-A*68:01	509	HTGVVVEKK	33.40
HLA-A*68:01	509	HTGVVVEKK	33.40
HLA-B*40:01	523	EEMTPHCAL	42.06
HLA-B*40:01	523	EEITPHCAL	42.21
HLA-B*44:02	523	EEMTPHCAL	76.77
HLA-A*26:01	524	EITPHCALM	87.40
HLA-B*15:03	529	CALMDCIMF	30.50
HLA-B*15:03	529	CALMDCIMY	61.00
HLA-B*35:01	529	CALMDCIMF	69.53
HLA-B*35:01	529	CALMDCIMY	20.96
HLA-A*02:01	531	LMDCIMFDA	26.12
HLA-A*02:01	531	LMDCIMYDA	34.29
HLA-A*02:06	531	LMDCIMFDA	70.02
HLA-A*03:01	558	MVFRTSTPK	11.55
HLA-A*03:01	558	MVFRTSSPK	8.59
HLA-A*11:01	558	MVFRTSTPK	8.90
HLA-A*11:01	558	MVFRTSSPK	8.28
HLA-A*30:01	558	MVFRTSTPK	6.90
HLA-A*30:01	558	MVFRTSSPK	5.70
HLA-A*31:01	558	MVFRTSTPK	44.96
HLA-A*31:01	558	MVFRTSSPK	55.13
HLA-A*68:01	558	MVFRTSTPK	6.28
HLA-A*68:01	558	MVFRTSSPK	5.73

ANTIBODIES

REACTIVITY	ANTIBODY	CONJUGATED FLUOROPHORE	CLONE	COMPANY
α-human	Integrin α 1 /CD49a	APC	TS2/7	Biolegend
α-human	Integrin α 4 /CD49d	PE/Dazzle 594	9F10	Biolegend
α-human	Integrin α 4 /CD49d	APC	9F10	Biolegend
α-human	Integrin α E /CD103	BV711	Ber-ACT8	BD Biosciences
α-human	Integrin α E /CD103	BUV395	Ber-ACT8	BD Biosciences
α-mouse	CD103	PerCP/Cy5.5	2E7	Biolegend
α-human	CD14	APC/Cy7	HCD14	Biolegend
α-human	CD16	APC/Cy7	3G	Biolegend
α-human	CD183(CXCR3)	BUV395	1C6/CXCR3	BD Biosciences
α-human	CD19	Alexa Fluor 700	HIB19	Biolegend
α-human	CD193 (CCR3)	APC/Cy7	Clone5E8	Biolegend
α-human	CD193 (CCR3)	PerCP/Cy5.5	Clone5E8	Biolegend
α-human	CD193 (CCR3)	PE	Clone5E8	Biolegend
α-mouse	CD193 (CCR3)	APC FireTM 750	J073E5	Biolegend

REACTIVITY	ANTIBODY	CONJUGATED FLUOROPHORE	CLONE	COMPANY
α-human	CD194 (CCR4)	BV605	L291H4	Biolegend
α-mouse	CD194(CCR4)	PE/Cy7	2G12	Biolegend
α-human	CD195(CCR5)	BV421	HEK/1/85a	Biolegend
α-human	CD197(CCR7)	BV421	G043H7	Biolegend
α-human	CD197(CCR7)	BV711	G043H7	Biolegend
α-mouse	CD25	APC	3C7	Biolegend
α-human	CD3	BV421	OKT3	Biolegend
α-human	CD3	BV510	OKT3	Biolegend
α-mouse	CD3	FITC	17A2	Biolegend
α-human	CD38	PerCP/Cy5.5	HIT2	Biolegend
α-human	CD38	BV510	HIT2	Biolegend
α-mouse	CD3ε	PE/Dazzle 594	145-2C11	Biolegend
α-human	CD4	PerCP/CY5.5	SK3	BD Biosciences
α-human	CD4	BUV737	SK3	BD Biosciences
α-human	CD4	BV711	SK3	Biolegend
α-mouse	CD4	BUV737	GK1.5	BD Biosciences
α-mouse	CD44	BV395	IM7	BD Biosciences
α-mouse	CD45.2	PE	104	eBioscience
α-mouse	CD45.1	APC	A20	Biolegend
α-mouse	CD45.1	FITC	A20	Biolegend
α-mouse	CD45.2	Alexa Fluor 700	104	Biolegend
α-human	CD45RA	BV711	HI100	Biolegend
α-mouse	CD49a	BV711	Ha31/8	BD Biosciences
α-human	CD56	APC/Cy7	HCD56	Biolegend
α-human	CD56	BV510	HCD56	Biolegend
α-human	CD56 (NCAM)	Alexa Fluor 700	5.1H11	Biolegend
α-human	CD56 (NCAM)	Alexa Fluor 700	5.1H11	Biolegend
α-mouse	CD62L	BV785	MEL-14	Biolegend
α-mouse	CD69	BV605	H1.2F3	Biolegend
α-human	CD8a	FITC	RPA-T8	Biolegend
α-human	CD8a	BV510	RPA-T8	Biolegend
α-human	CD8a	PE/CY7	RPA-T8	Biolegend
α-human	CD8a	BV650	RPA-T8	Biolegend
α-mouse	CD8a	BV650	53-6.7	Biolegend
α-human/mouse	CLA	PE	HECA-452	BD Pharmingen
α-human	CLA	FITC	HECA-452	Biolegend
α-human	HLA-DR	PE/Cy7	L243	Biolegend
α-human	HLA-DR	PerCP/Cy5.5	L243	Biolegend
α-human	HLA-DR	FITC	L243	Biolegend
α-human	IFN-γ	APC	4S.B3	Biolegend
α-human	Integrin β 1 / CD29	PE/Cy7	TS2/16	Biolegend
α-human	Integrin β 1 / CD29	Alexa Fluor 700	TS2/16	Biolegend
α-human/mouse	Integrin β 7	PE	FIB27	Biolegend
α-human/mouse	Integrin β 7	PerCP/Cy5.5	FIB27	Biolegend
α-human	LAMP-1 /CD107a	PE/CY7	H4A3	Biolegend

REACTIVITY	ANTIBODY	CONJUGATED FLUOROPHORE	CLONE	COMPANY
α-mouse	LPAM-1/ α4β7 Integrin	BV421	DATK32	BD Biosciences
α-mouse	Mouse OVA H-2Db/SIINFEKL	PE	TETRAMER	Immudex
α-human	TNF-α	BV785	MAb11	Biolegend
α-human	TNF-α	PE	MAb11	Biolegend

IMMUNOFOCUS ASSAY AND ELISPOT ANTIBODIES

REAGENT	MANUFACTURER
Mouse α-LASV mAb 2F1	BNITM, Virology
Sheep Anti-Mouse IgG peroxidase-conjugated	Jackson Immuno Research
Goat Anti-Mouse IgG FITC-conjugated	Jackson Immuno Research
Anti-human INF-γ mAb 7-B6-1 biotinylated	MabTech
Anti-human INF-γ mAb 1-DIk purified	MabTech

6.5 INSTRUMENTS

INSTRUMENT	MANUFACTURER
Accu-Jet® pro	Brand
animal rack	Tecniplast
bioanalyzer 2100	Agilent
biosafety animal changing station	Tecniplast
Cell counter LUNA-FL	Logos Biosystems
Centrifuge 541SC	Eppendorf
CKX41 microscope	Olympus
Clini Tray	KLINIKA Medical
DRI-CHEM NX500 Chemistry Analyzer	Fuji
Autoclave (bench-top)	Tuttnauer Systec
Class 2 safety cabinet	Kojair
Electrophoresis power supply EV231 Consort	Sigma Aldrich
F1-ClipTip (10-100µl)/(30-300µl)	Thermo Fisher Scientific
Fast-Prep-24 - Tissue homogenator	mpbio
FlowSafe® C-[MaxPro]³-130 safety cabinet	Berner
Fortessa flow cytometer	BD
freezer (-20°C)	Bosch
freezer (-20°C) profi line	Liebherr
fridge	Bosch
fridge	Liebherr
FUJIFILM NX 500 chemical analyzer	Fujifilm
Glovebox	GS Glovebox Systemtechnik GmbH
Guava® easyCyte™	Merck, Millipore
Heracell 150 incubator	Thermo Fisher Scientific
Innova CO-170 incubator	New Brunswick Scientific
IKA® Vortex 3	IKA

INSTRUMENT	MANUFACTURER
infrared light	HT instruments
Isoflurane vaporizer Univentor 410 and inhalation chamber	UNO BV
LSR II flow cytometer	BD
Microwave	Sharp
Mini Start table centrifuge	VWR
MiSeq	Illumina
NanoDrop	Thermo Fisher Scientific
PCR cycler T100	Bio Rad
PCR cycler MJ Mini	Bio Rad
PCR cycler Rotorgene	Qiagen
Photo scanner Reflection V550	Epson
Pipet Filler S1	Thermo Fisher Scientific
Pipette (1-2µl)/-20µL)/(20-200µL)/(100-1000µL)	Gilson
plate shaker 3006	GFL
precision scale PCB	Kern
Qubit	Thermo Fisher Scientific
Red Tube Tailveiner® Restrainer	Braintree Scientific
Refrigerated centrifuge; swing buckets 15 & 50 mL (Rotina 420R)	Hettich
Refrigerated centrifuge;1.5 - 2 mL (5417R)	Eppendorf
SpotChem	Axonlab
Thermocouple with rectal probe (BIO-TK8851 & BIO-BRET-3)	Bioseb
Thermomixer 5436	Eppendorf
ThermoMixer C	Eppendorf
TwinGuard freezer	PHCBI
vortex-genie2	Scientific Industries
Waterbath M20	Lauda

6.6 SOFTWARE

NAME	MANUFACTURER
FlowJo Version 10	BD/ FlowJo LLC
GraphPad Prism Version 6,7,8	GraphPad
Microsoft Excel 16	Microsoft
Microsoft Word 16	Microsoft
Microsoft PowerPoint 16 (with material from https://smart.servier.com/)	Microsoft
R and RStudio	R Core Team Babraham Bioinformatics
FastDC	MiLaboratory
MiXCR	BD
FACS Diva	Mendeley
Mendeley	

6.7 VIRUSES

Most infection experiments were carried out using a recombinant wild-type Lassa virus (LASV Ba366; Accession: KP339063.1). Generally, viruses were stored at -80 °C and harvested from infected Vero E6 cell supernatant. In one experiment Nigerian isolate from the 2018 outbreak (**ISTH-2018-013_NGA-Imo_Hs_2018**) was used. This virus was isolated from patient plasma and grown on Vero FM cells. Both viruses were provided for use in the described experiments by the virology department, BNITM, and had previously been amplified.

6.8 CELL LINES

Vero E6 cells 76 or FM were utilized for virus amplification and focus formation assays.

6.9 MOUSE COLONIES

Mouse strains C57BL/6, C57BL/6_Ly5.1, IFNAR^{KO}and OT-I were used for the described experiments. All mouse colonies were maintained in the animal housing facility at BNITM, Hamburg. Breeding pairs were obtained from Jackson Laboratories, through Charles River supplier.

7 METHODS

7.1 STUDY SITES AND RESEARCH FRAMEWORK

7.1.1 CLINICAL RESEARCH STUDY SITE IN NIGERIA

All samples were obtained in the period between January 2017 and April 2018 from acute and convalescent LF patients that were diagnosed and treated at Irrua Specialist Teaching Hospital (ISTH) in Edo state, South-West Nigeria. This university hospital is located at KM 87 Benin Auchi Rd, in Irrua, close to Benin city. It houses a nationally recognized Lassa diagnostic lab and a quarantine ward. Diagnostic samples were received from across Nigeria. Patients were diagnosed for LASV using whole blood samples collected in ethylendiamintetraacetate (EDTA) tubes and a commercially available reverse transcriptase PCR kit. Study and analysis were performed with approval of the ISTH Research and Ethics Committee (**Table 7.1**) and the Ethics Committee of the Medical Association of Hamburg (PV3186).

Lassa fever patients were enrolled in the study “Clinical manifestation and pathogenesis of Lassa fever in Edo State, Nigeria” at earliest convenience post arrival. Patients were administered ribavirin treatment post arrival to the hospital. Every second day EDTA and heparin whole blood samples were collected from enrolled patients by ISTH staff until patients were released from the quarantine ward.

Table 7.1: Study Ethics

NAME STUDY	APPROVAL STUDY NUMBER	DATE APPROVAL
Follow-up of survivors of Lassa Fever in Edo State, Nigeria: study of viral persistence, correlates of immunity and sequelae (version 02)	ISTH/HREC/20171208/44	Original: 14/12/2017 Renewal:14/12/2018 to 13/12/2019
Clinical manifestation and pathogenesis of Lassa fever in Edo State, Nigeria	ISTH/HREC/20171208/43	Original: 14/12/2017 Renewal: 14/12/2018 to 13/12/2019
Use of de-identified Leftover Specimens and Related Data from Diagnostic Service of ILFRC and Lassa Fever Patients Treated at ISTH	ISTH/HREC/20171208/45	Original: 16/01/2018 Renewal: 02/12/2018 to 01/12/2019

7.1.2 SAMPLE HANDLING AND INACTIVATION

LASV is classified in Germany as a category 4 high-risk pathogens and therefore infectious material must be handled within BSL-4 containment. Samples were stored at -80°C on study

site at ISTH or under BSL-4 containment at BNITM, Hamburg, Germany. Transport of samples was conducted on dry ice under constant temperature monitoring following Category A regulations. Experiments with infectious samples and animals were performed in the BSL-4 laboratory at BNITM, Hamburg. If removal from BSL-4 containment was required for further analysis, samples were inactivated. Methods of inactivation are referred to in the corresponding sections. Inactivated samples were removed from the BSL-4 laboratory through decontamination by 2-3 % peracidic acid. At the partner sites in West Africa, infectious samples were handled within a glovebox. Decontamination of potentially infectious surfaces was achieved through incubation for 15 min in a 0.5 % chlorine atmosphere or submersion in 0.5 % chlorine solution.

7.2 CLINICAL PARAMETERS

Clinical patient management was performed by staff doctors and nurses at ISTH. Sampling of patients and sample preparation for analysis of clinical chemistry and viremia were performed by ISTH staff scientists.

7.2.1 DETERMINATION OF VIREMIA

For determination of viremia EDTA blood was used. All steps were performed at room temperature (RT). RNA was extracted using the QIAamp® Viral RNA Mini Kit (Qiagen) according to the manufacturer's protocol. Briefly, carrier RNA, suspended in AVE buffer, was added to AVL buffer for a final concentration of 10 µg/mL. For sample lysis and inactivation 140 µL of separated plasma was added to AVL–carrier RNA and mixed by pulse-vortexing. As a nucleic acid extraction control, samples were spiked with internal control (IC) RNA provided by Altona diagnostics. IC was added at 10 % elution buffer volume (6 µL). 560 µL of ethanol (96–100 %) were added and again mixed by pulse-vortexing for 15 s. 630 µL of the solution were added to QIAamp Mini columns and centrifuged at 6,000 x g for 1 min. Samples were washed once with 500 µL AW1, followed by two washes with 500 µL AW2. Samples were eluded in 60 µL AVE buffer. Samples were incubated at RT for 10 min, before centrifugation at 6,000 x g for 1 min. Viremia determination was performed through reverse transcriptase (RT)-PCR measurement of the viral RNA copies using the RealStar® Lassa Kit 1.0 (Altona Diagnostics) following the manufacturer's protocol. The IC provided by the manufacturer was used as a RT-PCR inhibition control and nucleic acid preparation control. LASV-specific RNA was detected in the FAM™, IC RNA in the JOE™ channel, respectively. Reverse transcription was performed at 55°C for 20 min. Acquisition of fluorescence was recorded during annealing at 55°C.

7.2.2 CLINICAL CHEMISTRY

For determination of clinical chemistry parameters including AST levels, whole blood was collected in heparin tubes. Samples were separated by centrifugation at 25,000 x g for 15 min, plasma removed and inactivated with 2 % NP40 by mixing 6 µL of NP40 with 300 µL plasma. Samples were mixed by vortexing and disseverment of NP40 verified. Inactivated plasma was removed from glovebox containment and transferred to SpotChem tubes. A SpotChem machine was used for analysis.

7.2.3 EPIDEMIOLOGICAL DATA COLLECTION

For epidemiological data collection, a cross-sectional questionnaire survey was carried out. The questionnaire was given to hospitalized patients at earliest convenience and was designed based on previously published findings in West Africa (Bonwitt et al., 2017; McCormick, Webb, et al., 1987). Epidemiological data was collected with MS Excel 16. To complete the survey, 18 questions were asked. Questions covered details about the patient's living conditions, the ongoing acute LASV infection, history of LASV infection in their environment and details on possible exposure routes and contact with rodents. The answer formal was either single- or multiple-choice. ISTH staff members familiar with local dialects and customs were instructed to interview patients at earliest convenience after collection of consent. Records were excluded, if data was incomplete. Answers purposefully left open were not included in the analysis. Downstream analysis was performed with GraphPad Prism and R statistical software, which were also used to generate graphs. To determine geographic distribution of the patient cohort, patients provided place of residence and local government area (LGA). Geographic coordinates were matched to each location and longitude and latitude filed using MS Excel 16. If no match could be found for the address provided, data was excluded from analysis. Spatial mapping was performed in R using ggplot2 package for visualization. Shapefiles were obtained from (https://data.humdata.org/dataset/nga-administrative-boundaries) and applied using the rgdal package function.

7.3 MOUSE MODELS

7.3.1 ANIMAL HOUSING

Animal experiments were conducted according to the guidelines of the German animal protection law and under approvals 31/17, 92/18 and 28/19. Animals were bred and reared in the animal facilities of the BNITM. One week before the start of the experiment, mice were

transferred in individually ventilated cages (IVCs) into the BSL-4 laboratory with pellet chow and water ad libitum. On a weekly basis, cages were changed.

7.3.2 IFNAR^{B6} BONE MARROW CHIMERAS (IFNAR CHIMERAS)

ISOLATION OF MURINE BONE MARROW STEM CELLS

8-12-week-old C57BL/6J_Ly5.1 mice were euthanized according to the animal committee's approved protocols mentioned above. Mice were sprayed with 70 % ethanol and an incision was made to remove the skin from the lower extremities. Legs were separated by carefully dislocating the acetabulum from the hip joint and the muscles were removed. Tibia and femur were separated, taking care to not break the bones and leave the ends. Bones were placed in sterile phosphate buffered saline (PBS) and kept on ice. Under sterile conditions bones were sterilized with 70 % ethanol and placed into a petri dish containing culture medium (Dulbecco's Modified Eagle Medium (DMEM)). The epiphyses were cut off on each end. Using a 25-guage needle and a 12 cc syringe filled with culture medium, bones were flushed from both ends until visibly blanched. Bones were scraped with the needle if necessary, to remove all cells. Media containing cells was filtered through a 100 µm strainer, centrifuged for 5 min at 500 x g at RT. The pellet was resuspended in 5 mL 1x red blood cell (RBC) lysis buffer for 5 min (10x RBC buffer diluted 1:10 (v/v) in distilled (d)H_2O). Cells were washed with culture medium and counted. Cells were pelleted, resuspended in PBS and then used directly for transplantation.

GENERATION OF CHIMERIC MICE

8-10-week-old B6(Cg)-Ifnar1tm1.2Ees/J recipient mice were lethally irradiated with 4 Rad in a self-shielded Cs-137 irradiator. To minimize the stress for the animals from this procedure, irradiation was split into two rounds with a 4 h break in-between. One day after irradiation recipient mice are were transplanted 3 x 10^6 bone marrow stem cells from B6.SJL-Ptprca Pepcb/BoyJ (Ly5.1/ CD45.1) mice in 50 µL sterile PBS intravenously (i.v.) via the retro orbital sinus. Mice were anesthetized using isoflurane and placed on their ventral side on a heating pad (37 - 38°C) To avoid injection injures of the experimenter the head was fixed carefully using padded forceps. A tuberculin syringe with little resistance and 30 G-cannula was carefully inserted through the cornea at the inner canthus at a 20 - 40° degree until the retro orbital sinus. 50 µL sterile solution was applied. Mice were monitored and drinking water was supplied with antibiotics (Baytril, 0.01 % (v/v)) for 4 weeks post transplantation. Engraftment of donor cells in the recipient mice was analyzed at 5-6 weeks post transplantation. 25 - 50 µL of peripheral blood was drawn via tail vein puncture. The use of CD45.1 and CD45.2

alleles of the hematopoietic marker CD45 allows for the separation of cells into populations belonging to either the donor (CD45.1) or recipient (CD45.2). Mice with less than 80 % CD45.1 cells within all single positive CD45.1 and CD45.2 fraction were excluded from experiments.

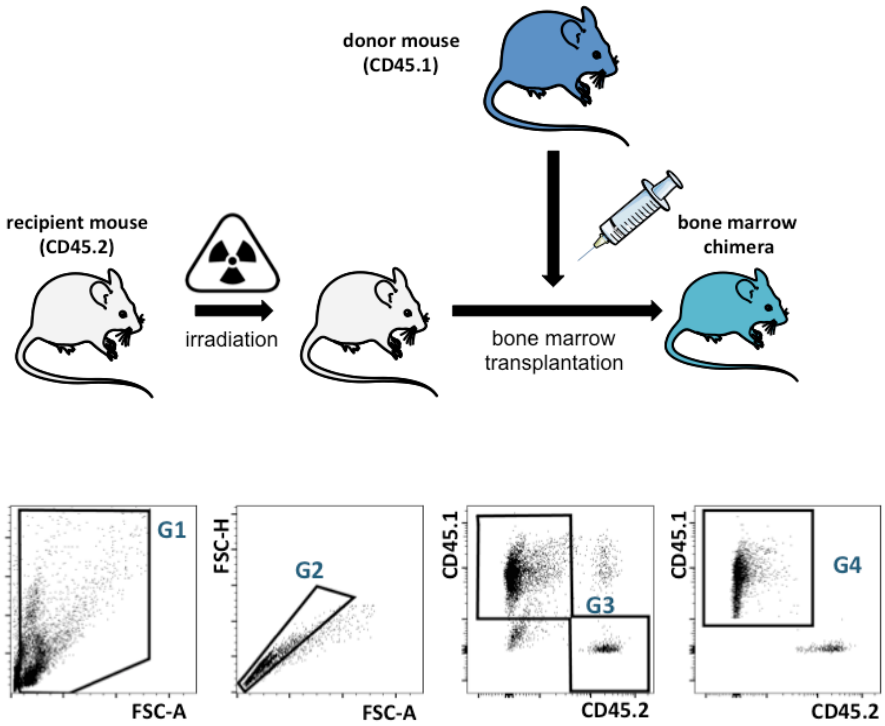

Figure 7.1:Schematic of IFNAR^{B6} generation. Recipient (CD45.2) IFNAR^{KO} mice were irradiated with 4 R, then transplanted with bone marrow stem cells isolated from donor mice (CD45.1). Transplantation efficiency was investigated by flow cytometry, gating on all PBMCs (G1), singlets (G2), single positive CD45.1 or CD45.2 cells (G3). Frequency of CD45.1 cells is recorded (G4).

IFNAR$^{B6/OT-1}$ MIXED BONE MARROW CHIMERA

Irradiation of 8-10-week-old B6(Cg)-Ifnar1tm1.2Ees/J recipient mice was conducted as described. One day after irradiation, recipient mice were transplanted i.v. via the retro orbital sinus under isoflurane anesthesia with a total of 3 x 10^6 bone marrow stem cells from B6.SJL-Ptprca Peb/BoyJ (Ly5.1) mice and OT-1 (Ly45.2) mice at a ratio of 1:1 in 50 µL sterile PBS. OT-I mice express a genetically modified TCR receptor on CD8$^+$ T cells. These CD8$^+$ T cells specifically recognize ovalbumin peptide (OVA). Mice were monitored and drinking water was supplied with antibiotics (Baytril, 0.01 % (v/v) for 4 weeks post transplantation. The use of CD45.1 and CD45.2 combined with dextramer staining for OVA-specific T-cells allowed separation of cells into populations belonging to the donor (CD45.1) wildtype and OT-1 (dextramer$^+$) and recipient (CD45.2).

7.4 *IN VIVO* INFECTION EXPERIMENTS

7.4.1 INFECTION ROUTES

To mimic natural routes of infection, mice were infected either intranasally (i.n.), intradermally (i.d.) or per os (p.o.). Bone marrow chimeras were generated as described above. Mice were infected with 1000 FFU LASV (recombinant Ba366 strain) 6 weeks after transplantation in a volume of sterile PBS fitted to the infection route, as described below.

INTRANASAL (I.N.)

Mice were anesthetized using isoflurane, and then placed on their backs on a heating mat (37°C). Using a pipette, 25 µL liquid (either virus or PBS alone) was administered through small drops (ca. 5. µL) into the nasal cavity. Mice were then turned on their side and monitored until fully awake.

ORAL (PER OS, P.O.)

To administer virus or PBS orally, a sterile buttoned cannula (22 G), 3 cm in length and 1.25 mm in diameter, with a 1 ml tuberculin syringe was used. The cannula was inserted with care, the angle and depth controlled and breathing pattern of the mice observed. If breathing was correct, 100 µL solution were applied. The cannula was removed slowly, taking care not to damage the teeth.

INTRADERMAL (I.D.)

Mice were anesthetized using isoflurane and placed on their ventral side on a heating pad (37-38°C), attached to continuous isoflurane source over the nose. Using an electric shaver, fur was shaved off in a 1x1 to 2x2 cm area on the back of the mouse, just above the tail base. Hairs were brushed aside, and the skin was gently scratched using UV sterilized sandpaper (P150 to P400 granularity). On the scratched surface 10 µL sterile solution were pipetted and distributed evenly. After application mice were kept under anesthesia for 15 min. Afterwards, the skin area was dried off with a sterile tissue to remove residual liquid.

7.4.2 MONITORING AND SCORING

Mice were sacrificed 9 days post infection or when termination criteria were met, for analysis of immune cell populations in blood and organs, as well as AST serum levels, viremia and virus titer in different organs. Throughout experiments, mice were monitored daily and weight, temperature and appearance (score) was noted. Temperature was measured

through a rectal probe. Mice were euthanized if termination criteria were met by isoflurane overdose, followed by cervical dislocation.

7.4.3 ANALYSIS OF MOUSE SAMPLES

BLOOD PROCESSING

To collect small volumes of blood during experiments through the tail vain, mice were placed under infra-red light for 5 min to increase vascular flow and visibility. Mice were restrained in a mouse restrainer and blood was collected by pressure applied to the base of the tail with two fingers. The tail was disinfected, and the lateral vein was punctured with a small scalpel and 2 - 3 blood drops were collected. Bleeding was stopped by application of pressure with a sterile tissue. After sacrifice, blood was collected through heart puncture using 1 mL U-100 insulin syringes. For flow cytometry analysis, blood was collected in EDTA tubes. Blood was transferred into 2 mL Eppendorf tubes containing 1 mL 1x RBC lysis buffer, incubated for 10 min at RT. The lysis reaction was stopped by PBS and cells were washed twice, spinning down at 500 x g for 5 min. The cell pallet was resuspended as required. For measurement of AST levels and viremia, blood was collected in heparin tubes. 20 µL of whole blood were diluted 1:20 (v/v) with DMEM and frozen at -20°C for later viremia measurement. Heparin tubes were centrifuged at 15,000 x g for 5 min and also frozen at -20°C for later AST analysis.

7.4.4 ORGAN PROCESSING

Lung, spleen, liver, kidney, small intestine, heart, skin, lymph nodes and brain were harvested. Organs were distributed in each experiment for further analysis including virus titration and flow cytometry. For virus titration, organs were stored at -80°C. Organs were thawed, weighted and whole organs or pieces (< 0.25 g) were transferred to Lysing matrix D tubes prefilled with 1 mL of DMEM. Organs were homogenized with a FastPrep homogenizer (3 x 30 sec, level 5). Tubes were centrifuged at 5,000 x g and then stored at -80°C. For flow cytometry, organs were transferred to 2 mL Eppendorf tubes containing 1 mL of PBS with collagenase D (2 mg/mL) and DNAse I (50 µg/mL). Organs were cut into small pieces manually and incubated for 30 min at 37°C, 650 rpm, on a ThermoMixer C (Eppendorf) thermoblock. Skin pieces were incubated for 75 min. Organ pieces were poured and mashed through a 70 nm cell strainer into a 50 mL falcon tube, creating a single cell suspension. Cell strainers were washed once with 15 mL PBS to increase yield. Cells were centrifuged at 500 x g for 5 min, followed by erythrocyte lysis for all organs excluding brain, skin, gut and lymph nodes. Erythrocyte lysis was performed in 1 mL 1x RBC lysis buffer for 1 min at RT and

stopped with PBS. Cells were washed twice with PBS at 500 x g for 5 min, and the cell pellet was resuspended in PBS or culture medium as required.

7.4.5 MEASUREMENT OF AST LEVELS IN SERUM

Levels of AST in serum were analyzed with a commercial kit and using a Fujifilm machine. Sera were diluted 1:10 or higher with a 0.9 % saline solution (v/v). The normal range of AST in bone marrow chimeric mice has been determined as < 200 U/L.

7.4.6 FOCUS FORMATION ASSAY

To quantify viral titers of cell cultures, blood or tissues from infected animals, focus formation assays were employed for LASV. 1 x 10^6 Vero E6 (76) cells were seeded in a 24-well plate one day prior to viral titration. The next day samples were thawed, and a logarithmic dilution was prepared in DMEM in a 96-well u-bottom plate. Blood was pre-diluted 1:20 in DMEM. Culture medium was removed from the seeded cells and 200 µL of each dilution was transferred to the cells. Cells were incubated for 1 h at 37℃ and 5 % CO_2. The inoculum was removed. 1 mL of overlay medium (2/3 DMEM with 10 % FCS and 1/3 methylcellulose medium) was added to each well and cells were incubated for 5 days, at 37℃ and 5 % CO_2. Overlay medium was removed and cells were fixated and inactivated for BSL-4 removal by submersion of the whole plate in 4 % formaldehyde in PBS (v/v) for 45 min at RT. Plates were then removed from the BSL-4 laboratory. Cells were thoroughly rinsed under running H_2O, and then permeabilized with PBS containing 0.5 % Triton X-100 for 30 min at RT. Cells were washed with H_2O, followed by blocking with 5 % FCS in PBS for 1 hour at RT. Blocking solution was removed and cells were incubated with primary anti-LASV antibody (2F1, monoclonal anti-LASV antibody,1:20 in PBS with 5 % FCS) for 1 hour at RT or overnight at 4°C. Plates were rinsed with H_2O and incubated with the HRP (horseradish peroxidase) coupled secondary anti-mouse antibody (1:1000 in PBS with 5 % FCS (v/v)) for 1 hour at RT. For detection of foci cells were washed with H_2O and incubated with TMB substrate (3,3',5,5'-Tetramethylbenzidine). Blue foci were counted manually. Viral titer was calculated based on dilution factors.

7.5 *EX VIVO* ANALYSIS OF T-CELL PHENOTYPE

7.5.1 PBMC ISOLATION FROM WHOLE BLOOD

HUMAN PBMC

Human peripheral blood mononuclear cells (PBMCs) were isolated from whole blood samples using the Lymphoprep gradient and SepMate systems (Stemcell Technologies). Whole blood was diluted at equal volume with PBS. Depending on blood volume, a 15 mL or 50 mL SepMate falcon was used for separation. Lymphoprep was layered into the separation tube at described volume; 5 mL or 15 mL, respectively, Diluted blood was carefully layered on top. Tubes were centrifuged at 800 x g at RT for 20 min. If older blood samples were processed, centrifugation was prolonged to 30 min. Plasma layer and mononuclear cell layer were decanted and washed twice with PBS (10 % FCS). For washing, samples were centrifuged at 500 x g for 6 min. Human PBMCs were either directly used for analysis in the field or cryopreserved in 90 % heat inactivated FCS and 10 % Dimethyl Sulfoxide (DMSO) for later analysis.

MURINE PBMC

Murine PBMCs were processed by first performing RBC lysis and thorough washing with PBS after. 1x RBC Lysis Buffer (Biolegend) was prepared by dilution with dH_20. Samples were mixed with 5 x volume of buffer and incubated at RT for 5 – 10 min until lysis was observed. The lysis reaction was stopped by the addition of an equal volume of PBS and the cells were then washed and centrifuged at 500 x g for 6 min. This method was also utilized if field conditions did not allow for gradient isolation due to too small sample volume or electrical shortages, which restricted use of lab equipment.

7.5.2 GENERATION OF DEXTRAMERS FOR ANTIGEN-SPECIFIC T-CELL IDENTIFICATION

Tetramers were selected based on previously published human HLA-A2 Lassa virus specific peptide sequences (Botten et al., 2006; McElroy et al., 2017) (H-YLISIFLHL-OH and H-LLGTFTWTL-OH). Sequences were confirmed to match current virus found in Nigeria by positive alignment with virus isolated from Irrua, Nigeria in 2018 (http://virological.org/t/2018-lasv-sequencing/180). Tetramers were generated using the Custom Flex-T™ MHC Tetramer kit (BioLegend) using the same signal peptides according to the manufacturer's instructions.
Peptide exchange was performed on ice; all reagents were thawed on ice. Stock solutions of peptides of choice were diluted to 400 µM with PBS. 20 µL diluted peptide and 20 µL conditional Flex-T™ monomer (200 µg/mL) were mixed in one well of a 96-well u-bottom

plate, which was sealed and centrifuged at 3,300 x g for 2 min at 4°C. After seal was removed, plated were placed back on ice and illuminated at a distance of 2 - 5 cm with UV light (254 nm wavelength) for 30 min. Plates were resealed and incubated in the dark at 37°C for 30 min. 15 µL of peptide-exchanged monomer were transferred into a new plate and 1.72 µL of antibody-conjugated streptavidin was added and mixed. Plates were incubated on ice in a 4°C room in the dark for 30 min. Tetramers were labeled with either PE or APC fluorochromes (Biolegend). Blocking solution was prepared by adding 1.6 µL 50 mM D-Biotin and 6 µL 10% (w/v) NaN_3 to 192.4 µL PBS. Blocking solution was vortexed and 2.4 µL of blocking solution was added to conjugated tetramers. Plates were sealed and incubated on ice for 30 min in the dark. Tetramers were used directly for cell straining.

7.5.3 PHENOTYPING OF CELLS WITH FLOW CYTOMETRY

CELL PREPARATION

All washing steps were performed by adding 200 µL of PBS or PBS (2 % FCS) and centrifugation at 500 x g for 6 min, followed by removal of supernatant. Cells were either stained in 2 mL Eppendorf tubes or 96-well v-bottom plates. Cells were stained either directly after isolation, or after cryopreservation. Cryopreserved human cells were thawed in pre-warmed RPMI medium (10 % human serum, 1x Streptomycine, 1x Peniciline, 1x L-Glutamine) in the presence of 50 µg/mL DNAse I. For human samples all further staining steps until fixation were performed in the presence of DNase I. Murine cells were always stained directly after isolation.

CELL STAINING

All following staining steps were performed at RT and in the dark. Centrifugation was performed at 500 x g for 6 min. Specific antibody combinations are detailed in section 7.9. If antigen specific T cells were stained for, cells were first incubated with a dextramer for 30 min in 50 µL PBS (10 % FCS). If self-generated tetramers were used, 1 µL of Flex-T™ complex of each color was used per sample for staining in 100 µL and incubated on ice in the dark for 30 min. After washing with PBS, cells were stained using a live/dead staining for 20 min (1/1000) in 100 µL PBS (Zombie dyes, Biolegend). Samples were washed with PBS (2 % FCS), then Fc-receptor was blocked. Cells were stained extracellularly in 50 µL PBS (2 % FCS) for 45 min.

FIXATION, INACTIVATION AND INTRACELLULAR STAINING

For fixation of cells and inactivation of infectious material all samples were washed, and then treated with Cytofix/Cytoperm (BD) containing additional 4 % formaldehyde solution for a minimum of 30 min in 400 µL. If staining for intracellular epitopes was required, samples were washed twice with 1x PermWash solution (BD) diluted in dH_20 and stained for 30 min with intracellular antibodies in 50 µL PermWash solution. Samples were washed with PBS (2 % FCS) twice and resuspended for acquisition.

ACQUISITION AND ANALYSIS

Samples were either acquired using a bench top Guava (Millipore) cytometer on site at ISTH or a Fortessa (BD) cytometer at BNITM. Compensation matrices were generated using CompBeads (BD) and if necessary, manually adapted using FlowJo software (TreeStar). Files generated using the Guava cytometer were run through preliminary analysis on InSight Software (Millipore). For analysis, quality of samples was controlled. First, samples, that had abnormally low cell numbers, were disregarded as this signifies low quality. Next, samples with aberrant staining artifacts, due to low quality, were removed. Gating strategies and panel design for complex panels is shown in section 7.9.

7.6 DNA AND RNA-BASED ANALYSIS

7.6.1 DNA ISOLATION

DNA isolation from PBMCs was performed using the DNeasy Blood and Tissue kit (Qiagen) according to the manufacturer's instructions. Briefly, for human LASV patient samples approx. 1 x 10^5 PBMCs were frozen in 50 µL PBS and stored at -80°C. Cells were pelleted and resuspended in 200 µL PBS. 2 µL proteinase K were added to each sample. 200 µL of AL buffer were added for lysis, then samples were mixed by vortexing thoroughly and incubated for complete inactivation at 56°C for 30 min. 200 µL ethanol (96–100 %) were added and samples were mixed thoroughly by vortexing. If required, samples were removed from BSL-4 containment at this step. Samples were added to a DNeasy Mini spin column placed in a 2 mL collection tube. Samples were centrifuged at 6,000 x g for 1 min, and the flow-through and collection tube was discarded. Columns were placed into a new collection tube and samples were washed with 500 µL AW1 buffer at the same speed. The flow-through and collection tubes were discarded. Columns were placed into a new collection tube and samples were washed with 500 µL AW2 buffer and centrifuged for 3 min at 20,000 x g. Columns were transferred to a new 1.5 mL microcentrifuge tube and the DNA was eluted into 200 µL DNase/RNase-free water. Columns were incubated for 1 min at RT before

elution at 6,000 x g for 1 min. DNA was either used for downstream applications immediately or stored at -20°C for short term, at -80°C for long term storage.

7.6.2 RNA ISOLATION

Isolated PBMCs (approx. 1 x 10^5 cells) were lysed in 50 µL PBS and inactivated in 1 mL of TRIzol™ Reagent (Invitrogen) and stored at -80°C. RNA was isolated using the Direct-zol™ RNA Miniprep Plus kit (Zymo) according to the manufacturer's instructions. All extraction steps were performed at RT. Centrifugations were performed at 16,000 x g for 30 s, unless specified otherwise. Briefly, samples were thawed and mixed with an equal volume of ethanol (95-100 %). Mixture was transferred to the provided Zymo-Spin™ IIICG Column, placed into a collection tube and centrifuged. Flow through was discarded, columns placed into a new collection tube and samples treated with DNase I after washing with 400 µL RNA Wash Buffer. Samples were incubated with 5 µL DNase I (6 U/µL) in 75 µL DNA Digestion Buffer for 15 min. Samples were washed twice with 400 µL Direct-zol™ RNA PreWash. Samples were washed with 700 µL RNA Wash Buffer. Centrifugation time was elongated to for 2 min to ensure complete removal of the wash buffer. Columns were transferred to RNase free tubes and RNA was eluted into 50 µL of DNase/RNase-free water. RNA was either used for downstream applications immediately or stored at -20°C for short term, at -80°C for long-term storage.

7.6.3 DETERMINATION OF PATIENT'S HLA TYPES

DNA was used for PCR based genotyping using an HLA-A low resolution screening kit (OLERUP SPP) according to the manufacturer's instructions. The primer set contained 5'- and 3'-primers for grouping the HLA-A*01:01 to A*80:03 alleles into the corresponding serological groups A1 to A80. Analysis was performed in a 24 reaction PCR plate pre-prepared with required primers. Negative control primers were included, amplifying Olerup SSP® HLA Class I, DRB, DQB1, DPB1 and DQA1 amplicons, as well as all the amplicons generated by the control primer pairs matching the human growth hormone gene. The PCR reaction mix was prepared at RT. The provided reaction mix was vortexed briefly and 81 µL were removed for each typing. Sample DNA concentrations were determined using a Nanodrop machine, and 60 ng were added to the reaction mix in 186.8 µL dH_20. Lastly, 2.2 µL Taq polymerase was added (5 U/µL). The mixture was then vortexed and spun down. 10 µL were added to each well of the 24-reaction PCR plate. Plates were sealed, and PCR reaction performed on a commercial PCR cycler. HLA-allele-specific amplification was achieved through initial denaturation for 2 min at 94°C, followed by 10 cycles with 10 s

denaturation at 94°C and 60 s annealing and extension at 65°C. Additional 20 cycles were performed with 10 s denaturation at 94°C, 50 s annealing at 50°C and extension for 30 s at 72°C.

HLA-specific PCR product sizes ranged from 75 to 200 base pairs. PCR results were analyzed by agarose-gel electrophoresis using gels of 2 % (w/v) agarose in 1x tris-acetate EDTA buffer (TAE) buffer at 100 V with a 45 min run-time. Band size was verified against the GenerRuler 1kb DNA ladder. Results were confirmed against the PCR product generated by the positive control primer pair included in each reaction. Results were analyzed with the corresponding software proved by the manufacturer. If results were unclear, PCR was repeated. If result remained undefined, most likely combination of alleles was assumed based on software

7.6.4 TRANSCRIPTOMIC ANALYSIS BY NANOSTRING

Gene expression was analyzed through nanoString technology at a core facility in Essen, Germany, using the company designed nCounter® human immunology code-set for general immunology.
(https://www.nanostring.com/products/gene-expression-panels/ncounter-immunology-panels).
RNA was diluted in dH_20 at a concentration between 8 - 20 ng/µL and shipped on dry ice. Counts were analyzed using nSolver Advance Analysis Software v3.0 to compile counts tables and perform cartridge quality control checks. Gene expression was normalized against the expression of several housekeeping genes included in the code set. Data was then exported as a csv file for further analysis. Log2counts were calculated and genes sorted for significance in difference between patient groups by adjusted p-value. Alternatively, genes of interest were specifically selected for manually. Heatmaps were generated on Log2counts with heatmap.2 function in R; “ward.D2” agglomeration method for clustering and euclidean measure to obtain distance matrix were applied.

7.6.5 ANALYSIS OF T-CELL RECEPTOR REPERTOIRE

CDNA GENERATION

cDNA was generated using the SuperScript III reaction kit (Thermofisher) as recommended by the manufacturer. Briefly, for each sample 5 µL RNA, 6 µL dH_20, 1 µL random primers and 1 µL 10 mM dNTPs were mixed well and incubated at 65°C for 3 min on a commercial PCR cycler. Samples were removed, chilled on ice and spun down. To each reaction 4 µL 5

x First Strand Buffer, 1 µL 0.1 mM DTT, 1 µL RNAse Out (400 U/µL) and 1 µL SuperScript III enzyme were added and mixed well. cDNA synthesis was performed at 25°C for 5 min, followed by 50°C for 60 min and stopped at 70°C for 15 min.

TCR AMPLIFICATION

First, the sequence-specific TCR locus was amplified from cDNA. A combination of 45 forward primers and 13 reverse primers was used to amplify all potential V and J gene regions (Robins et al., 2009). Primers used are listed in 0. A second set of primers was generated including Illumina Nextera adapter sequences.

Forward overhang: 5' TCGTCGGCAGCGTCAGATGTGTATAAGAGACAG-[locus-specific sequence]
Reverse overhang: 5' GTCTCGTGGGCTCGGAGATGTGTATAAGAGACAG-[locus-specific sequence]

For amplification both primer sets were used. All 45 forward primers (0.22 µM each) were pooled at a final concentration of 10 µM; all 13 reverse primers (0.77 µM each) were equally pooled at 10 µM final concentration. Primer pools with Nextera overhang were generated similarly. PCR amplification of the CDR3 region was performed using a Multiplex PCR kit (QIAGEN). PCR amplification was performed at a reduced 25 µL reaction volume with a final primer concentration of 0.2 µM of forward and reverse primer mixes, respectively, and 1 µM for the nextera adapter primers mixes each. Q solution (2.5 µL) was used to increase reaction efficiency. 1 µL of DNA template was added. The PCR run included a 15 min HotStart at 95°C, 30 s denaturation at 94°C and annealing for 90 s applying a touchdown gradient from 69°C to 59°C (1°C each cycle) and extension at 72°C for 90 s. Additional 30 amplification cycles were performed at 59°C annealing temperature. Final extension was performed for 10 min at 72°C. PCR products were purified and cleaned immediately or stored at 4°C.

PCR PRODUCT CLEANING AND SIZE SELECTION

PCR products were selected for the correct size and then cleaned using the Agencout AMPure XP reagent. Beads were removed from 4°C storage 30 min before usage and all reaction steps were performed at RT. Beads were vortexed before use. PCR product was mixed with beads at a 1:1.8 ratio, then vortexed and spun down briefly and incubated at RT for 5 min. Samples were either prepared for cleaning in 0.5 mL reaction tubes or 96-well u-

bottom plates. Tubes or plates were placed into a magnetic rack until the solution became visibly clear. Supernatant was removed, and DNA bound beads washed twice with either 500 µL or 200 µL freshly prepared 70 % ethanol by incubating for 35 s and rotating against the magnetic pole to facilitate better cleaning. Supernatant was removed completely. Samples were air-dried at RT for maximum of 5 min to remove residues. Samples were removed from the magnetic field and resuspended in 20 µL H_2O. Samples were vortexed for 10 s to remove DNA from beads and tubes placed into the magnetic field to clear supernatant. Supernatant was transferred into a clean reaction tube. Success of template purification was verified by agarose gel electrophoreses using a gel at 1.5 % (w/v) agarose in 1x TAE buffer running at 100 V voltage. Template size was confirmed against a GeneRuler 1kb marker at approx. 300 bp.

LIBRARY PREPARATION

To generate the sequencing library, primers from the Illumina Nextera XT index kit were used to amplify and index the cleaned PCR products utilizing the same Qiagen Multiplex PCR Kit. Each sample was labeled with a specific pair of forward and reverse primers from this kit using a reduced 25 µL reaction volume with 2.5 µL of each primer and 5 µL of DNA template. Amplification was achieved through a HotStart of 15 min at 95°C, followed by 15 cycles of 30 s denaturation at 95°C, annealing of 30 s at 55°C and extension of 30 s at 72°C, concluded by a final extension of 5 min at 72°C. Adapter labeled amplicons were purified as described above through Agencout beads.

SAMPLE QUANTIFICATION AND SEQUENCING

Sample quantification and sequencing was performed at the sequencing core facility at Heinrich-Pette-Institute, Hamburg. Samples were pooled according to concentration after quality and quantity assessment through Qubit and Agilent Bioanalyzer 2100 with the DNA 1000 kit measurement. Samples were analyzed using the Illumina MiSeq chemistry V2 and a paired end 2x150 cycle run was performed following the manufacturer's instructions. The pooled and denatured library was diluted to a final concentration of 12 pM and a PhiX control of 5% spike-in was used.

BIOINFARMATIC ANALYSIS

First, FastQC (v0.11.5) was used to assess the overall quality of the sequenced reads. Next, overlapping paired end sequences were merged and the obtained sequences were aligned to reference V, D and J genes of T-cell receptors in order to identify the genes present in the

samples. Identical CDR3 sequences were identified and grouped into clonotypes and finally exported into a human readable, tab-delimited text file. For all these steps MiXCR (v1.8.1) was employed. Afterwards, the R package tcR was used for advanced data analysis on the files obtained from MiXCR. Files were parsed into the R environment. Simpson inverse diversity was calculated using repDiversity function based on read proportion. Clonal overlap was analyzed using repOverlap function and visualized using ggplot2 package and heatmap.2 function at default settings. Clonal expansion was calculated using clonal.space.homeostasis function defining clones as Rare (0 < X <= 1e-05), Small (1e-05 < X <= 1e-04), Medium (1e-04 < X <= 0.001), Large (0.001 < X <= 0.01) and Hyperexpanded (0.01 < X <= 1). Gene usage was calculated using geneUsage function.

7.7 *EX VIVO* CHARACTERIZATION OF T-CELL FUNCTIONALITY

7.7.1 ENZYME-LINKED IMMUNO-SPOT (ELISPOT) ASSAY

The assay was performed under BSL-3 containment using cryopreserved human PBMCs. Peptide and peptide-pool responses by T cells were measured using an IFN-γ based ELISPOT assay. ELISPOT was performed according an in-house modified protocol as follows:

COATING OF PLATE AND PREPARATION OF EFFECTOR CELLS

Coating of plates and T-cell stimulation was performed under sterile conditions. 96-well ELISPOT plates were activated by adding 25 µL 35 % ethanol to each well. Immediately, plates were emptied, and residues removed by patting on paper towels. Plates were washed three times with 100 µL sterile PBS. 100 µL capture Ab (IFN-γ Mab 1-D1K) (1 mg/mL) was diluted in 10 mL PBS and 100 µL added per well and incubated overnight at 4°C. Human PBMCs were thawed in pre-warmed RPMI medium (10 % human serum, 1x Streptomycine, 1x Penicillin, 1x L-Glutamine) in the presence of 50 µg/mL DNase I, washed twice in DNase free RPMI. The cell count was determined, and cells were resuspended at a desired concentration of 2.5 x 10^6 cells/mL. The cells were incubated overnight at 37℃ and 5 % CO_2.

T-CELL STIMULATION

The coated plates were emptied and washed with 150 µL/well sterile PBS. In each well 150 µL RPMI (10 % HS) were added and incubated for 30 min at RT to block against unspecific reactions. PBMCs were washed and then the live cell count was determined. The cells were resuspended at 2.5 x 10^6 cells/mL in RPMI (10 % HS). Plates were emptied, pat dry and

immediately 100 µL RPMI (0 % HS + stimulus) was added to each well. Single peptides were used for stimulation at a final concentration of 1 mg/mL. Phytohaemagglutinin (PHA)-L was used as a positive control with a final concentration of 1 µg/mL. 100 µL cell suspension (250,000 cells per well) were added slowly. Plates were incubated for 20 h at 37℃ and 5 % CO_2.

DEVELOPMENT

Plates were emptied and pat dry, washed twice with 150 µL/well dH_2O and incubated for 5 min at RT. Plates were emptied and pat dry, then washed 4 x with 150 µL/well PBS-0,05% Tween and once with PBS. Plates were pat dry again and 100 µL detection Ab (IFN-γ Mab 1-D1K 7-B6-1 biotin) in PBS-0,05% Tween-0,5 BSA was added. Plates were incubated for 2 min at RT, then washed 5 x with 150µL/well PBS-0,05% and once with PBS. 100 µL streptavidin solution (1 µL Strep-HRP (Dako) in 10 mL PBS-0,5% BSA) were added in each well. Plates were incubated for 1 h at room temperature. Substrate buffer was removed from 4°C storage 10 min before use to reach room temperature. Plates were washed 4 x with 150 µL/well PBS-0,05% Tween and 2 x with PBS. 100 µL filtered TMB substrate was added per well and plates incubated for 30 min at RT until spot formation was observed. Plates were flushed with water thoroughly, then dried 1 h under laminal flow. Plates were analyzed manually as removal from BSL-3 containment was impossible.

7.7.2 INTRACELLULAR STIMULATION (ICS) OF T CELLS AND MEASUREMENT OF CYTOKINE RESPONSE

STIMULATION OF T CELLS IN THE FIELD WITH LASV-SPECIFIC PEPTIDE POOL

All steps until inactivation were performed in a glovebox. Human PBMCs were isolated freshly as described in 7.5.1, cell count was determined with a Guava cytometer and cells were resuspended in CO_2-free medium (10 % HS, 1x Streptomycin, 1x Penicillin, 1x L-Glutamine) at desired the concentration of 2.5 x 10^6 cells/mL. Cells were transferred to a 96-well v-bottom plate at approx. 2.5 x 10^5 cell per well (100 µL) and mixed with 100 µL fresh CO_2-free medium (10% HS, 1x Streptomycin, 1x Penicillin, 1x L-Glutamine) containing additional stimulus. All conditions were performed in duplicate. Cells were stimulated with a LASV specific peptide pool (see 6.4) at concentration of 1 µg/mL for each individual peptide. As peptides were diluted in DMSO, maximum final concentration of DMSO was also added to the negative control. PMA/ionomycin (50 ng/mL/ 2.5 µM/mL) was used as a positive stimulation control. To maintain containment, a small portable CO_2-free incubator was placed

into the glovebox. PBMCs were incubated with stimulus for 6 h at 37°C. To prevent cytokine release into the medium, cells were treated with GolgiStop™ (BD) protein transport inhibitor (1/1000 dilution) for the last 5 h. Plates were sealed airtight and placed at 4°C overnight. Cells were stained for flow cytometry after ICS; all steps until fixation were performed in the presence of GolgiStop™ (1:1000 dilution).

STIMULATION OF T CELLS WITH INACTIVATED LASV

Cryopreserved human PBMCs were used and the assay was performed under BSL-4 containment. Cells were thawed in pre-warmed RPMI medium (10 % HS, 1x Streptomycin, 1x Penicillin, 1x L-Glutamine) in the presence of 50 µg/mL DNase I, washed twice in DNase free RPMI, cell count was determined, and the cells were resuspended at the desired concentration of 2.5 x 10^6 cells/mL. If required, cells were incubated overnight at 37°C for resting. Cells were transferred to a 96-well v-bottom plate at 2.5 x 10^5 cell per well (100 µL) and mixed with 100 µL fresh RPMI medium (10 % HS, 1x Streptomycin, 1x Penicillin, 1x L-Glutamine) containing additional stimulus. All conditions were performed in duplicate. Cells were stimulated with heat inactivated LASV (field isolated virus strain, Nigeria 2018, inactivation for 45 min at 56°C) at MOI of 3. PMA/ionomycin (50 ng/mL/ 2.5 µM/mL) was used as a positive stimulation control. PBMCs were incubated with stimulus for 6 h. To prevent cytokine release into the medium, cells were treated with GolgiStop™ (BD) protein transport inhibitor (1/1000 dilution) for the last 5 h. Plates were sealed airtight and placed at 4°C overnight. Cells were stained for flow cytometry after ICS; all steps until fixation were performed in the presence of GolgiStop™ (1:1000 dilution).

7.8 STATISTICAL ANALYSIS

7.8.1 SINGLE-PARAMETRIC DATA ANALYSIS

Visualization of data was performed using R statistical software environment and GraphPad Prism, as were analyses of statistical significance. Non-parametric testing was applied using Wilcoxon and Kruskal-Wallis tests, followed by Dunn's multiple comparison test. Survival curves were analyzed using LogRank (Mantel-Cox) test. The levels of significance were interpreted as follows: NS (not significant) $p>0,05$, *$p\leq0,05$, **$p\leq0,01$, ***$p\leq0,001$, and ****$p\leq0,0001$.

7.8.2 MULTI-PARAMETRIC DATA ANALYSIS

Visualization of data was performed using R statistical software environment and GraphPad Prism, as were analyses of statistical significance. Non-parametric testing was applied using two-way ANOVA tests, followed by Dunnette's or Silak's multiple comparison test. Correlation were analyzed using linear regression to generate trend lines for visualization and Spearman's correlation analysis for independent variables. The levels of significance were interpreted as follows: NS (not significant) $p>0,05$, *$p\leq0,05$, **$p\leq0,01$, ***$p\leq0,001$, and ****$p\leq0,0001$. In addition, analysis of data was performed in R statistical software using gplots, mclust, corrplot and factoextra packages. Heatmaps were generated with heatmap.2 function, defaulting to euclidean measurement of distance and "ward.D2" agglomeration method for clustering. Correlation matrices were visualized with corrplot function ordering the variables based on angular order of the eigenvectors. Principal component analysis was performed on correlation matrices and unscaled original variables. Cluster number was chosen manually based on hierarchical clustering of samples by hclust function by "ward.D2" agglomeration method for clustering and euclidean measure to obtain distance matrix.

7.9 FLOW CYTOMETRY PANELS AND GATING

Panel design for flow-panels employed in the field (Guava) and at BNITM (Fortessa) is listed in Table 7.2. For complex 16-color panels the main gating strategies are depicted in Figure 7.2 and Figure 7.3. Antibodies were diluted 1:200 (v/v) unless otherwise indicated. Zombie dies were diluted 1:1000 (v/v).

tSNE DIMENSION REDUCTION OF FLOW CYTOMETRIC DATA

For T-Distributed Stochastic Neighbor Embedding (tSNE) analyses, the population of cells of interest was selected and concatenated across all samples for each pre-defined category respectively using FlowJo software plugins. These pools were then downsized based on the least abundant population and then merged again to generate one FSC file on which tSNE analysis was performed using the tSNE plugin at default settings. Populations were gated manually based on density and clustering. Contribution of cells originating from the outcome pools and expression frequency of cell surface markers were identified for each population.

BOOLEAN GATING AND VISUALIZATION OF CO-EXPRESSION PATTERN IN SPICE

Boolean gating was performed through FlowJo software after applying manual gating to determine markers of interest. Data was recorded using csv format and analyzed using SPICE V6 software.

Table 7.2: Flow cytometry panels. * = 1/100 dilution; ** = 1/50 dilution

MACHINE	LASER (EXCITATIO	DETECTOR/FILTER	FLIOROCHROME	PANEL 1	PANEL 2	PANEL 3	PANEL 4	
Guava	Violet Laser (405 nm)	Blue 488/50	BV421	CD3	CCR5*	CD3	CCR7*	
		Green 525/30	BV510	CD8	CD38	CD8	CD3	
		Yellow 583/26	BV570			empty		
		Red 695/50	BV711	CD4	CD4	ITGAE/ CD103*	CD45RA	
	Blue Laser (488 nm)	Green 525/30	FITC	CLA*	CD8	HLA DR	CD8	
		Yellow 583/26	PE	ITGB7*	CD38	ITGB7*	TNFα**	
		Red 695/50	PerCp/Cy5.5	CD38	CCR3*	CD38	CD4	
		NIR 785/70	PE Cy7	HLA DR	HLA DR	CD29/ ITGB1*	LAMP-1/ CD107a**	
	Red Laser (640 nm)	Red 661/15	APC	ITGA4/ CD49d*	empty	ITGA4/ CD49d*	IFNγ**	
		NIR 785/70	APC Cy7		Zombie NIR, CD16, CD19, CD56			

				PANEL 1	PANEL 2	PANEL 3	MOUSE PANEL 1	MOUSE PANEL 2
Fortessa	UV-Laser (355 nm)	740/35 650	BUV737	CD4	CD4	CD4	CD4	CD4
		380/14	BUV395	ITGAE/ CD103*	empty	empty	CD44	CD44
	Yellow/Green Laser (561 nm)	780/60 750	PE Cy7	CD8	CD38	LAMP-1/ CD107a**	CCR4*	CCR4*
		670/30 635	PE Cy5	empty	empty	empty	empty	empty
		610/20 600	PE-Texas Red	ITGA4/ CD49d*	ITGA4/CD49d*	ITGA4/ CD49d*	CD3*	CD3*
		586/15	PE	ITGB7*	Tetramer 2	CCR3*	CLA*	Tetramer OT-1**
	Violet Laser (405 nm)	780/60 735	BV785	HLA DR	HLA DR	TNFα**	CD62L	CD62L
		710/40 670	BV711	CD45RA	CCR7*	CD45RA	ITGA1/ CD49a	ITGA1/ CD49a
		675/50 635	BV650	empty	CD8	CD8	CD8	CD8
		610/20 600	BV605	CCR4**	CCR4**	CCR4**	CD69	CD69
		586/15 570	BV570	Zombie Yellow	empty	empty	empty	empty
		525/50 505	BV510	CD3	Zombie Aqua, CD56*, CD19*	CD3	Zombie Aqua	Zombie Aqua
		450/50	BV421	CCR7*	CD3	CCR7*	ITGA4B7*	ITGA4B7*
	Red Laser (640 nm)	780/60 750	APC Cy7	CCR3*	CCR3*	Zombie NIR	CCR3*	CCR3*
		730/45 690	AlexaFluor 700	CD56/* CD19*	CD29/ ITGB1*	CD29/ ITGB1*	CD45*	CD45.1*
		670/14	APC	ITGA1/ CD49a*	Tetramer 1	IFNγ**	CD25	CD25
	Blue Laser (488 nm)	710/40 685	PerCP-Cy5.5	CD38	ITGB7*	ITGB7*	ITGAE/ CD103*	ITGAE/ CD103*
		530/30 595	FITC	CLA*	CLA*	CLA*	CD3 (i.v.)	CD45.2

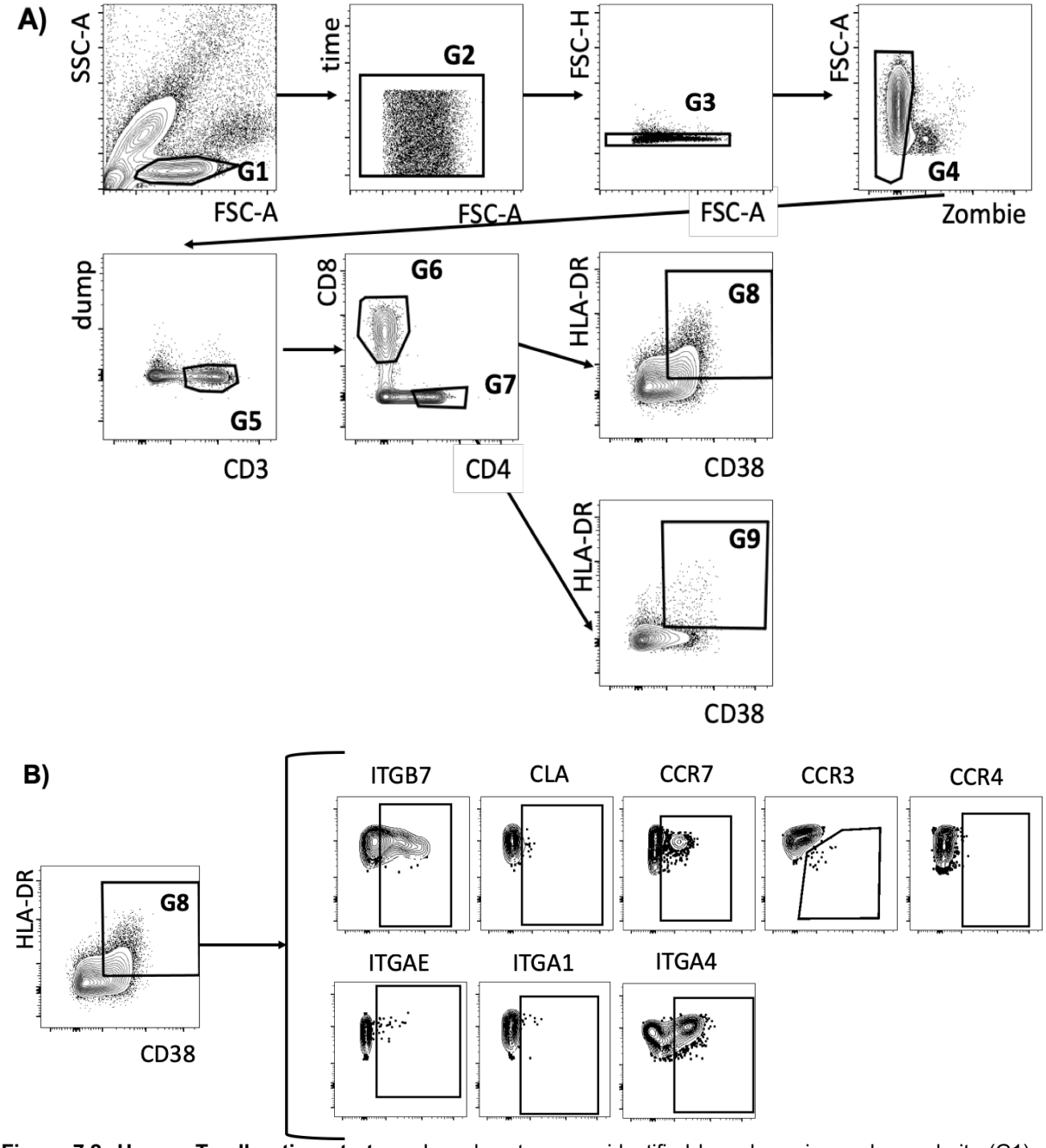

Figure 7.2: Human T-cell gating strategy. Lymphocytes were identified based on size and granularity (G1). Flow artifacts were excluded (G2) and single cells selected (G3). Zombie viability dye was used to identify living cells (G4) and T cells were selected based on expression of CD3 (G5) and absence of dump-channel markers (CD56/CD19). T cells were separated into CD8 (G6) and CD4 cells (G7) and the activated population in each through co-expression of CD38 and HLA-DR (G8/G9) (A). Exemplary patient plots are shown for gating on each homing marker of interest (B). For continuous populations, gating was performed based on fluorescence-minus-one (FMO) or isotype controls.

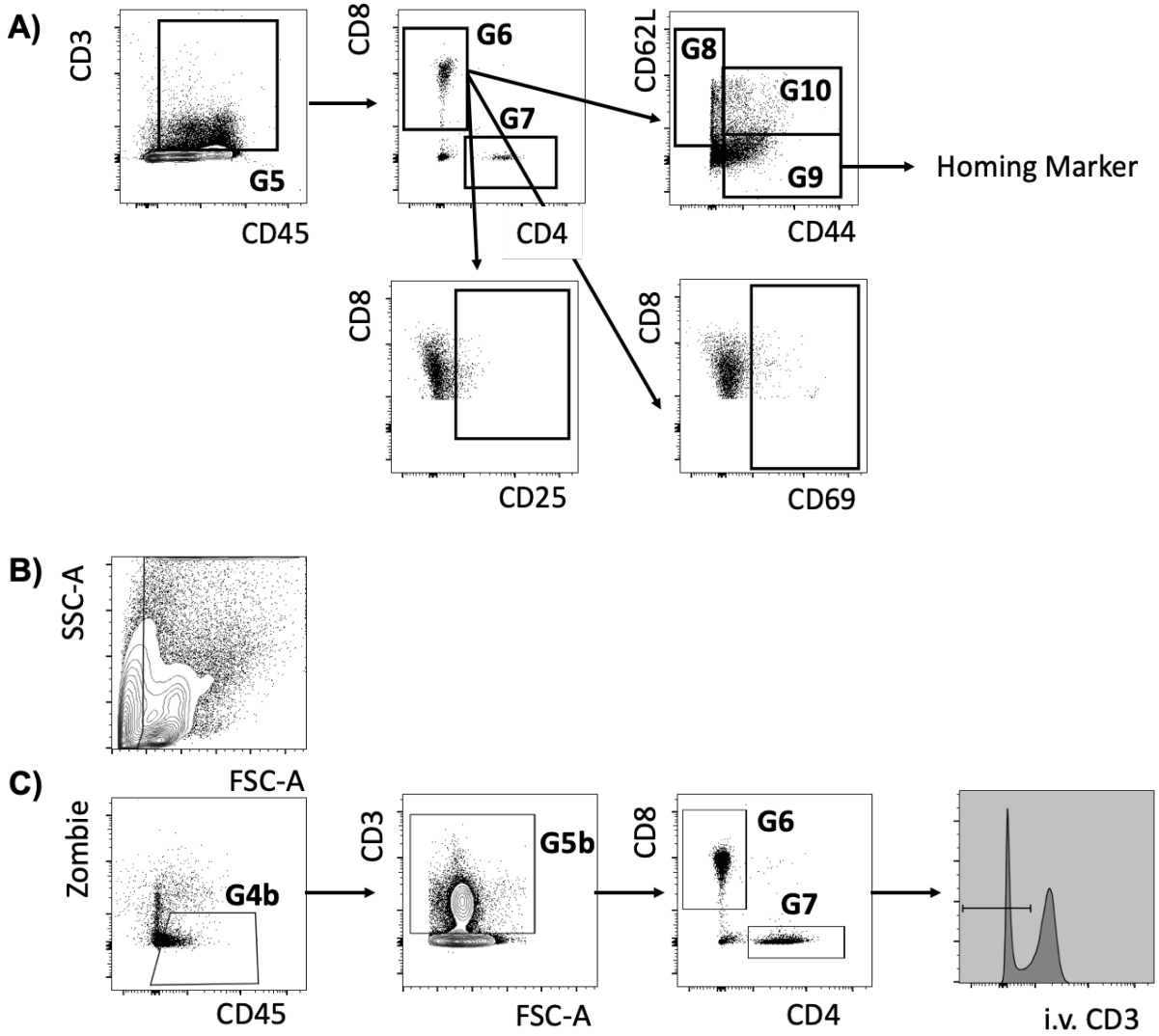

Figure 7.3: Mouse T-cell gating strategy. Lymphocytes were identifies as described for human samples. T cells were identified using expression of CD45 and CD3 (G5). T cells were separated into CD8 (G6) and CD4 cells (G7) and the memory (G10), naïve (G8) and effector (G9) compartment in each through CD44 and CD62L expression (A). Expression of activation markers CD25 and CD69 was performed on total population of CD4/CD8 cells. Homing marker analysis was performed on effector T cells. For continuous populations, gating was performed based on fluorescence-minus-one (FMO) or isotype controls. For organ analysis, the lymphoid gate was adapted to include all cells (B) and the identification though CD45 and CD3 expression was separated for clarification of populations (G4b and G5b) (C). Resident T cells were identified through i.v. application of anti-CD3 antibody and gating performed on the corresponding histogram.

8 SUPPLEMENTAL DATA

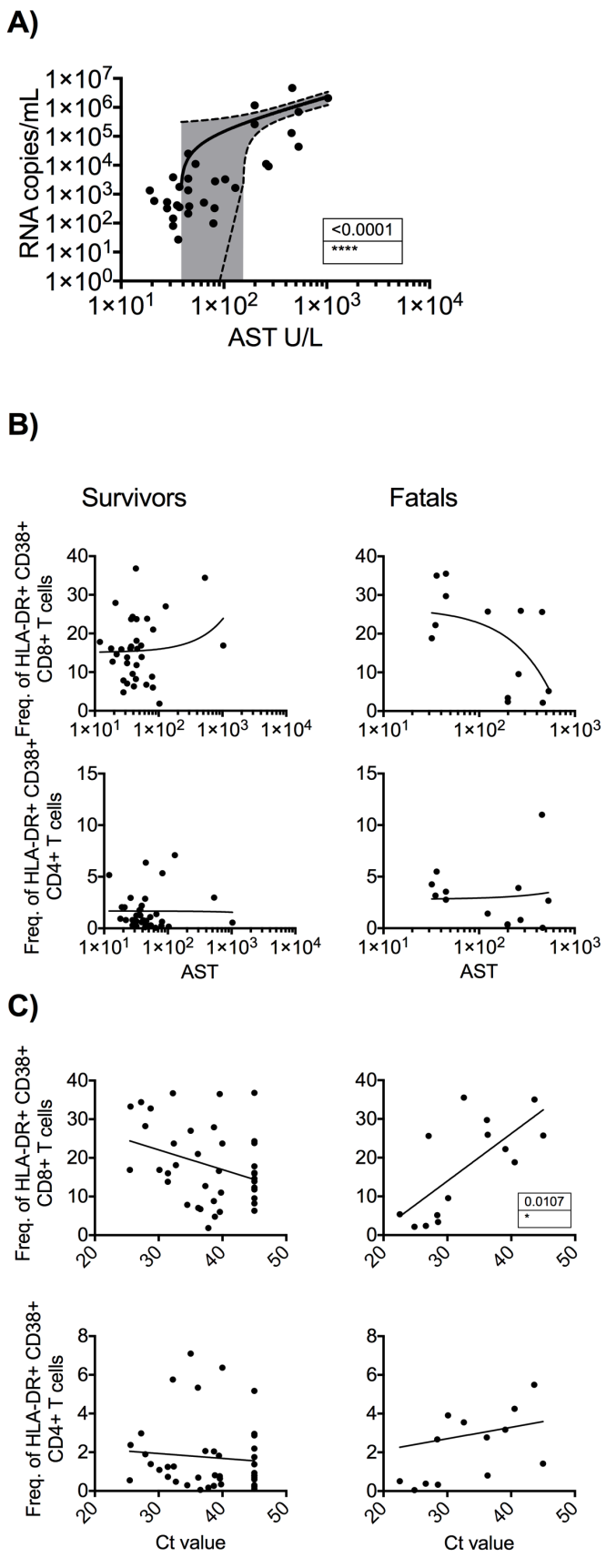

Figure 8.1: Relationship between AST (U/L) and viremia (RNA copies/mL, based on Ct value of the Altona RT-PCR for LASV) was analyzed. P-value and significance of correlation is indicated (A). Co-expression of CD38 and HLA-DR was analyzed by flow cytometry of $CD4^+$ and $CD8^+$ T cells in relation to AST levels (U/L) (B) and viremia (Ct-value) (C). Frequency (%) within parent is depicted. Activation was analyzed for Fatals and Survivors. Graphs are presented with correlation line. Statistical significance was determines using Spearman correlation analysis. Significance levels are presented as follows: ns = $p > 0.05$; * = $p \leq 0.05$; ** = $p \leq 0.01$; *** = $p \leq 0.001$; **** = $p \leq 0.0001$. Abbreviations: AST, serum level aspartate aminotransaminase; Ct, cycle threshold.

A)

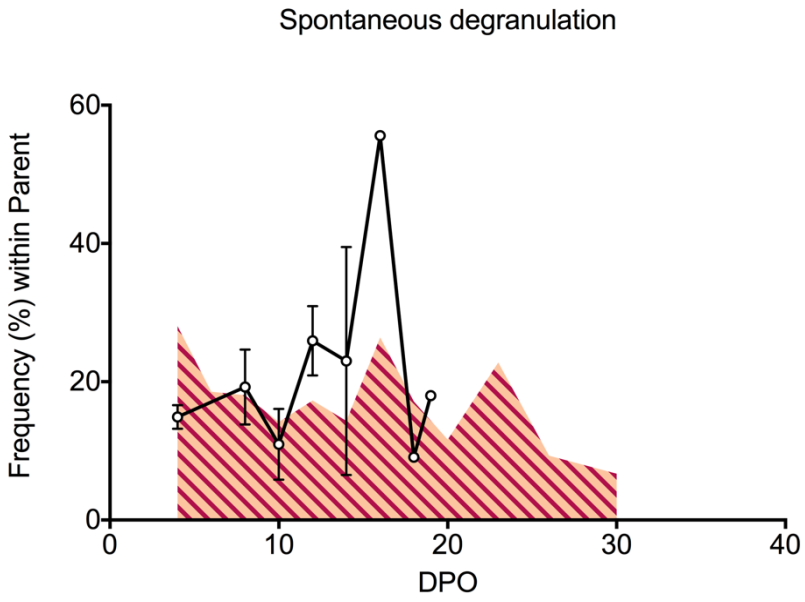

B)

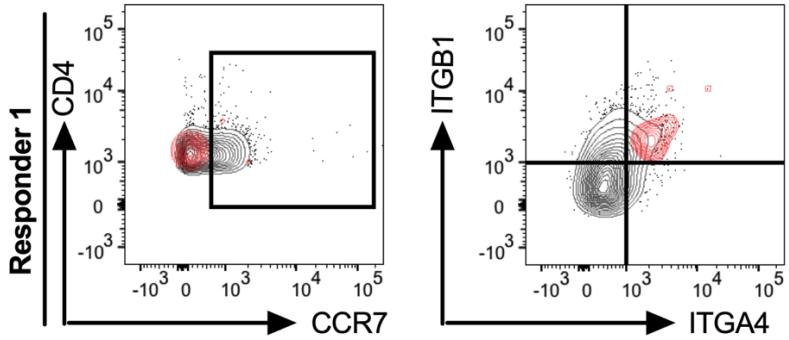

Figure 8.2: T-cell responses to stimulation. $CD8^+$ T-cell spontaneous degranulation was analyzed after *ex vivo* stimulation with no stimulus (N=26) (A). Frequency of $CD8^+$ T cells producing LAMP-1/CD107a is shown (black line, depicting mean and SEM) in relation to time and activation level associated with time (N=54) (HLA-DR^+ $CD38^+$ expression) (red area under the curve). T-cell responses were analyzed after *ex-vivo* stimulation with inactivated LASV and lymphoid and inflammatory homing capacity of both IFN-γ and TNF-α producing $CD4^+$ T cells was analyzed, and representative overlay plots are shown (B). Total population of $CD8^+$ T cells is shown in black, cytokine producing fraction in red. Abbreviations: LASV, Lassa virus; CCR7, chemokine receptor 7; ITGB1, integrin β1; ITGA4, integrin α4; DPO, days post-onset.

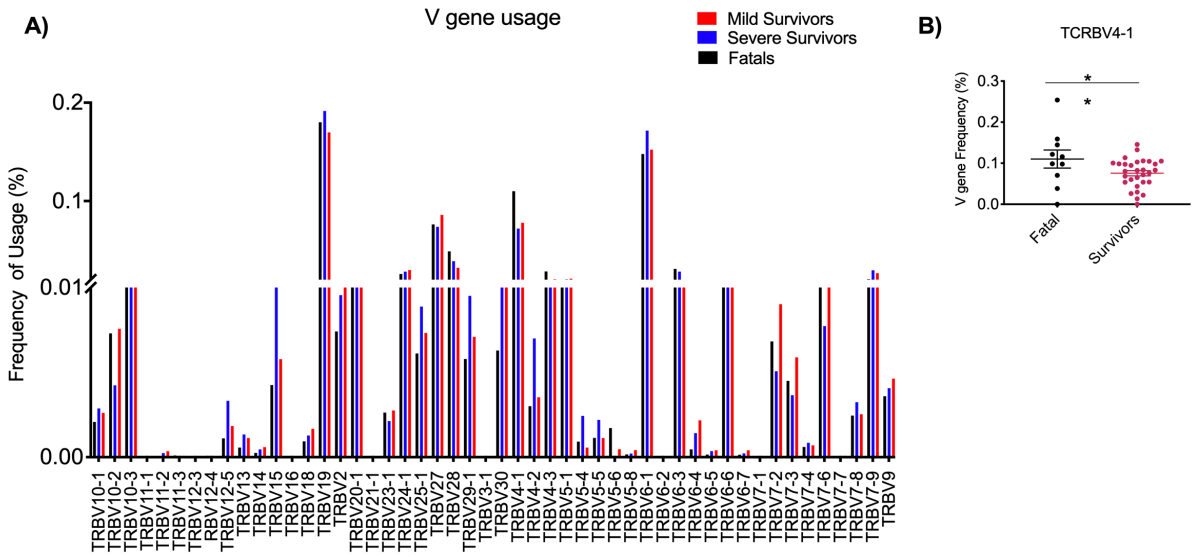

Figure 8.3: V-gene Usage in acute human LF. Based on sequencing results of the V-gene region of the TCRβ-chain frequency of use (%) for each v-gene was calculated for the TCR repertoires found in Fatals (black), Mild Survivors (Blue) and Severe Survivors (Red) (A). Frequency (%) of usage for TCRBV4-1 gene is depicted for Fatals and all Survivors (B). Abbreviations: TCRBV, T-cell receptor beta chain v gene. Statistical significance was determines using unpaired Mann-Whitney test. Significance levels are presented as follows: ns = $p > 0.05$; * = $p \leq 0.05$; ** = $p \leq 0.01$; *** = $p \leq 0.001$; **** = $p \leq 0.0001$.

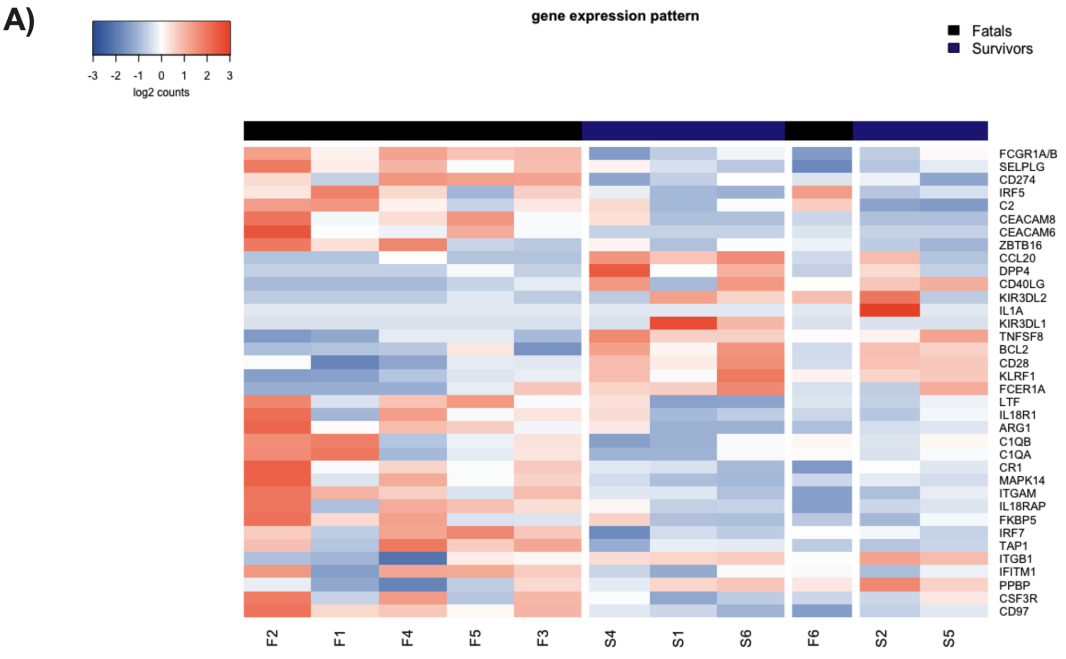

Figure 8.4: Top variable genes. Nanostring transcriptomic analysis was utilized to investigate mRNA expression during acute human LF in 6 patients with fatal outcome (black) and 5 survivors (blue). Heatmap depicts expression level (log2counts) of top differentially expressed genes according to color bar on left. Genes were selected based on adjusted p-values.

A)

HLA-DR+ CD38+ CD8+ T cells

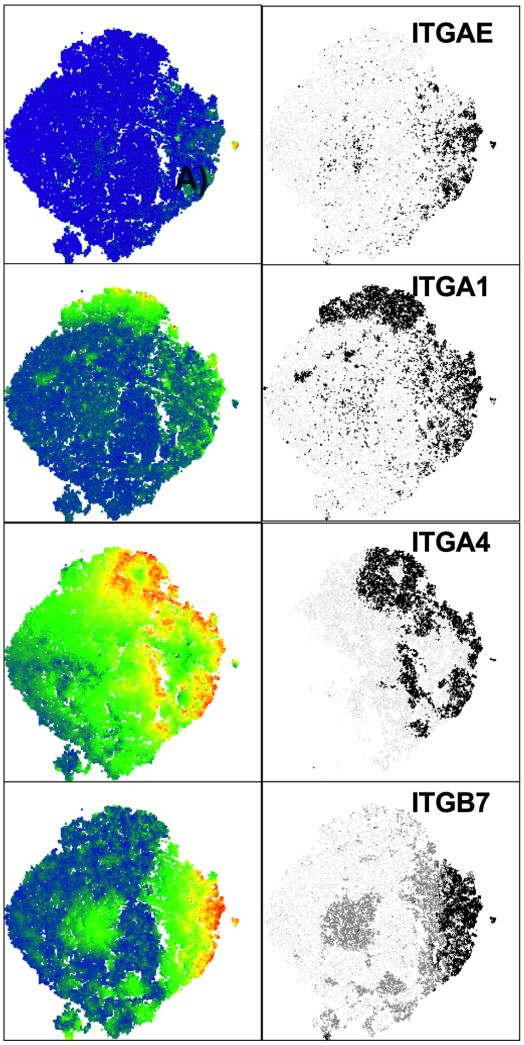

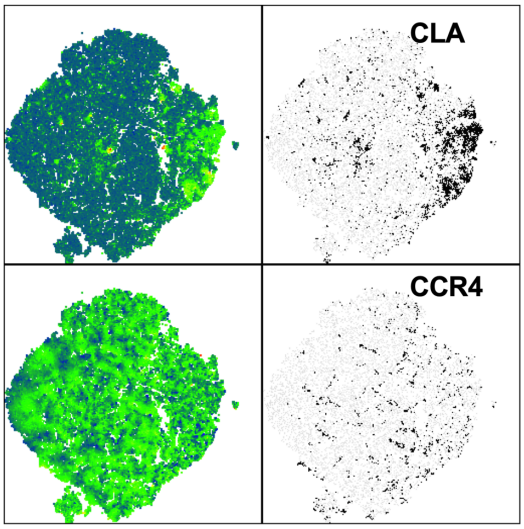

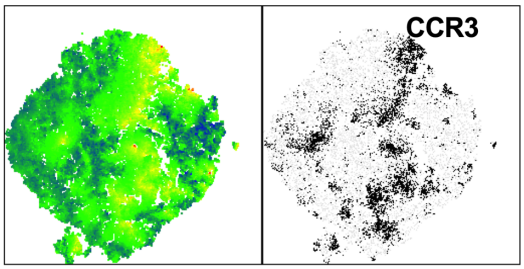

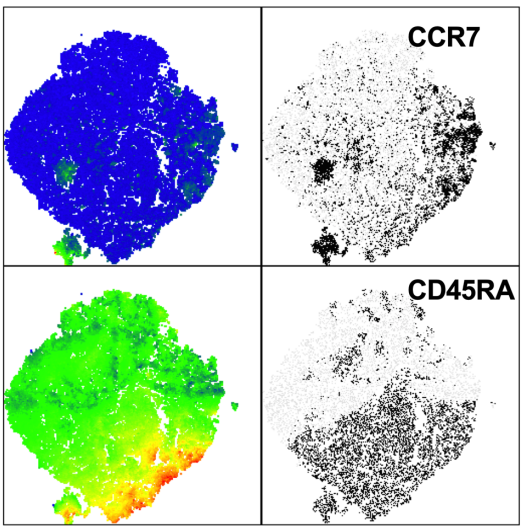

B)

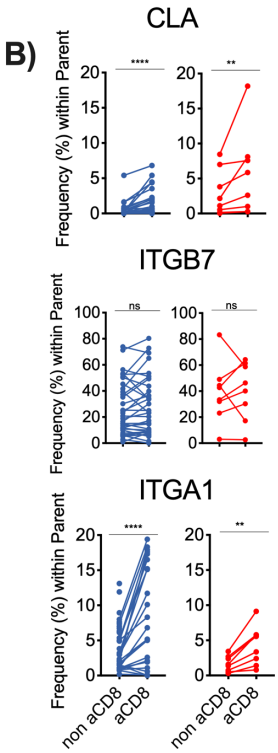

HLA-DR+ CD38+ CD4+ T cells

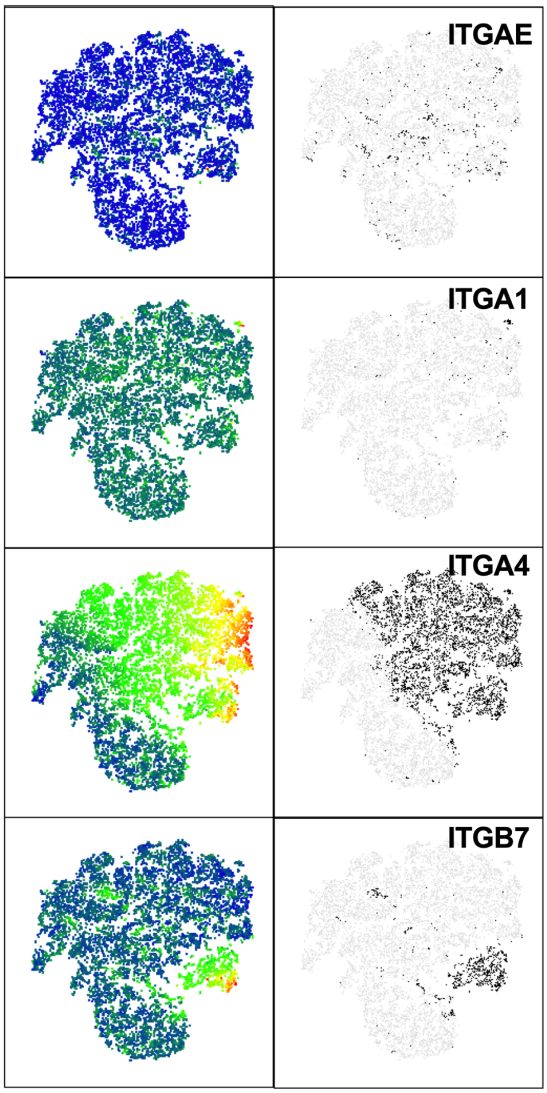

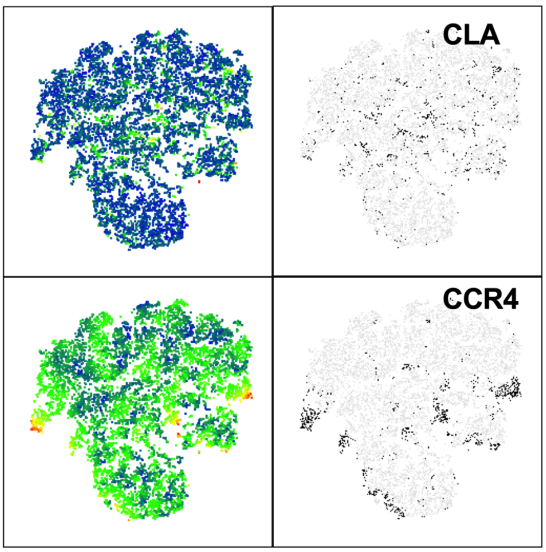

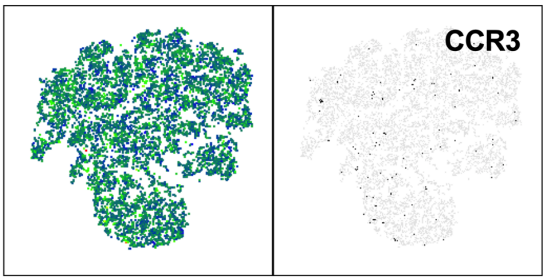

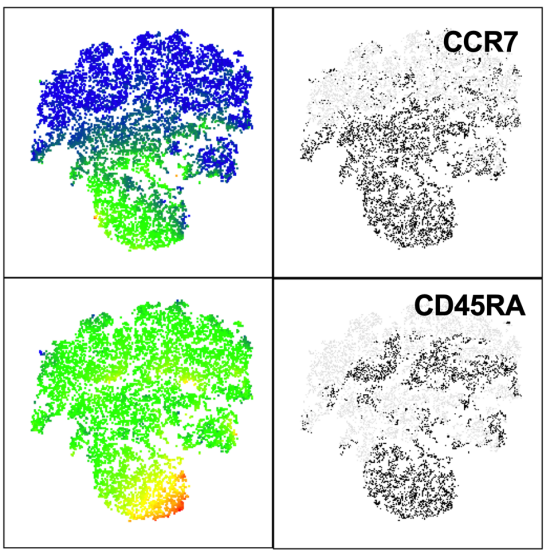

Figure 8.5: Activated ($CD38^+$ $HLA\text{-}DR^+$) $CD8^+$ T cells were concatenated across all patient samples. Input across outcome groups was normalized. tSNE was calculated on homing marker expression CLA, CCR3, CCR4, CCR7, α4 and β7 integrin, including also residency markers αE integrin, α1 integrin and CD45RA for further identification of effector and memory status. (A). Density of expression is depicted for each marker (green = low, red = high) in each respective left panel; right panels show in black the positively gated population for each marker. Frequency of expression was compared between Mild Cases (blue) and Severe Cases (red) for selected homing markers (B) comparing the expression in the activated compartment and the non-activated compartment. Abbreviations: ITGB7, β7 integrin; ITGA1, α1 integrin; ITGA4, α4 integrin; ITGAE, αE integrin; CCR, chemokine receptor; CLA, cutaneous lymphocyte antigen; HLA, human leukocyte antigen; tSNE, t-distributed stochastic neighbor embedding; a, activated; non a, non-activated. Statistical significance was determines using Mann-Whitney test. Significance levels are presented as follows: ns = $p > 0.05$; * = $p \leq 0.05$; ** = $p \leq 0.01$; *** = $p \leq 0.001$; **** = $p \leq 0.0001$.

Figure 8.6: Activated ($CD38^+$ $HLA\text{-}DR^+$) $CD4^+$ T cells were concatenated across all patient samples. Input across outcome groups was normalized. tSNE was calculated on homing marker expression CLA, CCR3, CCR4, CCR7, α4 and β7 integrin, including also residency markers αE integrin, α1 integrin and CD45RA for further identification of effector and memory status. (A). Density of expression is depicted for each marker (green = low, red = high) in each respective left panel; right panels show in black the positively gated population for each marker. Abbreviations: ITGB7, β7 integrin; ITGA1, α1 integrin; ITGA4, α4 integrin; ITGAE, αE integrin; CCR, chemokine receptor; CLA, cutaneous lymphocyte antigen; HLA, human leukocyte antigen; tSNE, t-distributed stochastic neighbor embedding.

9 REFERENCES

Abad-Fernández, M., Gutiérrez, C., Madrid, N., Hernández-Novoa, B., Díaz, L., Muñoz-Fernández, M., … Vallejo, A. (2015). Expression of gut-homing β7 receptor on T cells: surrogate marker for microbial translocation in suppressed HIV-1-infected patients? *HIV Medicine*, *16*(1), 15–23. https://doi.org/10.1111/hiv.12167

Adams, D. H., & Eksteen, B. (2006). Aberrant homing of mucosal T cells and extra-intestinal manifestations of inflammatory bowel disease. *Nature Reviews Immunology*, *6*(3), 244–251. https://doi.org/10.1038/nri1784

Ager, A., Watson, H. A., Wehenkel, S. C., & Mohammed, R. N. (2016). Homing to solid cancers: a vascular checkpoint in adoptive cell therapy using CAR T-cells. *Biochemical Society Transactions*, *44*(2), 377–385. https://doi.org/10.1042/BST20150254

Amsen, D., van Gisbergen, K. P. J. M., Hombrink, P., & van Lier, R. A. W. (2018). Tissue-resident memory T cells at the center of immunity to solid tumors. *Nature Immunology*, *19*(6), 538–546. https://doi.org/10.1038/s41590-018-0114-2

Ariotti, S., Hogenbirk, M. A., Dijkgraaf, F. E., Visser, L. L., Hoekstra, M. E., Song, J.-Y., … Schumacher, T. N. (2014). Skin-resident memory CD8 $^{+}$ T cells trigger a state of tissue-wide pathogen alert. *Science*, *346*(6205), 101–105. https://doi.org/10.1126/science.1254803

Armstrong, L. R., Zaki, S. R., Goldoft, M. J., Todd, R. L., Khan, A. S., Khabbaz, R. F., … Peters, C. J. (1995). Hantavirus Pulmonary Syndrome Associated with Entering or Cleaning Rarely Used, Rodent-Infested Structures. *Journal of Infectious Diseases*, *172*(4), 1166–1166. https://doi.org/10.1093/infdis/172.4.1166

Asogun, D. A., Adomeh, D. I., Ehimuan, J., Odia, I., Hass, M., Gabriel, M., … Günther, S. (2012). Molecular Diagnostics for Lassa Fever at Irrua Specialist Teaching Hospital, Nigeria: Lessons Learnt from Two Years of Laboratory Operation. *PLoS Neglected Tropical Diseases*, *6*(9), e1839. https://doi.org/10.1371/journal.pntd.0001839

Baekkevold, E. S., Wurbel, M.-A., Kivisäkk, P., Wain, C. M., Power, C. A., Haraldsen, G., & Campbell, J. J. (2005). A role for CCR4 in development of mature circulating cutaneous T helper memory cell populations. *The Journal of Experimental Medicine*, *201*(7), 1045–1051. https://doi.org/10.1084/jem.20041059

Baize, S., Marianneau, P., Loth, P., Reynard, S., Journeaux, A., Chevallier, M., … Contamin, H. (2009). Early and Strong Immune Responses Are Associated with Control of Viral Replication and Recovery in Lassa Virus-Infected Cynomolgus Monkeys. *Journal of Virology*, *83*(11), 5890–5903. https://doi.org/10.1128/JVI.01948-08

Baize, Sylvain, Kaplon, J., Faure, C., Pannetier, D., Georges-Courbot, M.-C., & Deubel, V. (2004). Lassa virus infection of human dendritic cells and macrophages is productive but fails to activate cells. *Journal of Immunology (Baltimore, Md. : 1950)*, *172*(5), 2861–2869. https://doi.org/ 10.4049/jimmunol.172.5.2861

Bajnok, A., Ivanova, M., Rigó, J., & Toldi, G. (2017). The Distribution of Activation Markers and Selectins on Peripheral T Lymphocytes in Preeclampsia. *Mediators of Inflammation*, *2017*, 1–7. https://doi.org/10.1155/2017/8045161

BANGS, S., MCMICHAEL, A., & XU, X. (2006). Bystander T cell activation – implications for HIV infection and other diseases. *Trends in Immunology*, *27*(11), 518–524. https://doi.org/10.1016/j.it.2006.09.006

Baron, J. L., Madri, J. A., Ruddle, N. H., Hashim, G., & Janeway, C. A. (1993). Surface expression of alpha 4 integrin by CD4 T cells is required for their entry into brain parenchyma. *Journal of Experimental Medicine*, *177*(1), 57–68. https://doi.org/10.1084/jem.177.1.57

Bauer, M., Brakebusch, C., Coisne, C., Sixt, M., Wekerle, H., Engelhardt, B., & Fässler, R. (2009). β1 integrins differentially control extravasation of inflammatory cell subsets into the CNS during autoimmunity.

Proceedings of the National Academy of Sciences, *106*(6), 1920–1925. https://doi.org/10.1073/pnas.0808909106

Bausch, D. G., Demby, A. H., Coulibaly, M., Kanu, J., Goba, A., Bah, A., … Rollin, P. E. (2001). Lassa Fever in Guinea: I. Epidemiology of Human Disease and Clinical Observations. *Vector-Borne and Zoonotic Diseases*, *1*(4), 269–281. https://doi.org/10.1089/15303660160025903

Bertoni, A., Alabiso, O., Galetto, A. S., & Baldanzi, G. (2018). Integrins in T Cell Physiology. *International Journal of Molecular Sciences*, *19*(2). https://doi.org/10.3390/ijms19020485

Beura, L. K., Hamilton, S. E., Bi, K., Schenkel, J. M., Odumade, O. A., Casey, K. A., … Masopust, D. (2016). Normalizing the environment recapitulates adult human immune traits in laboratory mice. *Nature*, *532*(7600), 512–516. https://doi.org/10.1038/nature17655

Bono, M., Tejon, G., Flores-Santibañez, F., Fernandez, D., Rosemblatt, M., & Sauma, D. (2016). Retinoic Acid as a Modulator of T Cell Immunity. *Nutrients*, *8*(6), 349. https://doi.org/10.3390/nu8060349

Bonwitt, J., Kelly, A. H., Ansumana, R., Agbla, S., Sahr, F., Saez, A. M., … Fichet-Calvet, E. (2016). Rat-atouille: A Mixed Method Study to Characterize Rodent Hunting and Consumption in the Context of Lassa Fever. https://doi.org/10.1007/s10393-016-1098-8

Bonwitt, J., Sáez, A. M., Lamin, J., Ansumana, R., Dawson, M., Buanie, J., … Brown, H. (2017). At Home with Mastomys and Rattus: Human-Rodent Interactions and Potential for Primary Transmission of Lassa Virus in Domestic Spaces. *Am. J. Trop. Med. Hyg*, *96*(4), 935–943. https://doi.org/10.4269/ajtmh.16-0675

Botten, J., Alexander, J., Pasquetto, V., Sidney, J., Barrowman, P., Ting, J., … Buchmeier, M. J. (2006). Identification of protective Lassa virus epitopes that are restricted by HLA-A2. *Journal of Virology*, *80*(17), 8351–8361. https://doi.org/10.1128/JVI.00896-06

Bowen, M. D., Peters, C. J., & Nichol, S. T. (1997). Phylogenetic Analysis of the Arenaviridae:Patterns of Virus Evolution and Evidence for Cospeciation between Arenaviruses and Their Rodent Hosts. *Molecular Phylogenetics and Evolution*, *8*(3), 301–316. https://doi.org/10.1006/MPEV.1997.0436

Briese, T., Paweska, J. T., McMullan, L. K., Hutchison, S. K., Street, C., Palacios, G., … Lipkin, W. I. (2009). Genetic detection and characterization of Lujo virus, a new hemorrhagic fever-associated arenavirus from southern Africa. *PLoS Pathogens*, *5*(5), e1000455. https://doi.org/10.1371/journal.ppat.1000455

Bromley, S. K., Mempel, T. R., & Luster, A. D. (2008). Orchestrating the orchestrators: chemokines in control of T cell traffic. *Nature Immunology*, *9*(9), 970–980. https://doi.org/10.1038/ni.f.213

Buchmeier, M., Peters, C. J., & De la Torre, C. (2007). *Arenaviridae: the virus and their replication*. *Fields Virology* (Vol. 2).

Buckley, S. M., & Casals, J. (1970). Lassa fever, a new virus disease of man from West Africa. 3. Isolation and characterization of the virus. *The American Journal of Tropical Medicine and Hygiene*, *19*(4), 680–691. https://doi.org/10.4269/ajtmh.1970.19.680

Calzascia, T., Masson, F., Di Berardino-Besson, W., Contassot, E., Wilmotte, R., Aurrand-Lions, M., … Walker, P. R. (2005). Homing Phenotypes of Tumor-Specific CD8 T Cells Are Predetermined at the Tumor Site by Crosspresenting APCs. *Immunity*, *22*(2), 175–184. https://doi.org/10.1016/j.immuni.2004.12.008

Campbell, J. H., Ratai, E.-M., Autissier, P., Nolan, D. J., Tse, S., Miller, A. D., … Williams, K. C. (2014). Anti-α4 Antibody Treatment Blocks Virus Traffic to the Brain and Gut Early, and Stabilizes CNS Injury Late in Infection. *PLoS Pathogens*, *10*(12), e1004533. https://doi.org/10.1371/journal.ppat.1004533

Campbell, J. J., Brightling, C. E., Symon, F. A., Qin, S., Murphy, K. E., Hodge, M., … Wardlaw, A. J. (2001). Expression of chemokine receptors by lung T cells from normal and asthmatic subjects. *Journal of Immunology (Baltimore, Md. : 1950)*, *166*(4), 2842–2848. https://doi.org/10.4049/JIMMUNOL.166.4.2842

Campbell, J. J., Murphy, K. E., Kunkel, E. J., Brightling, C. E., Soler, D., Shen, Z., … Wu, L. (2001). CCR7 expression and memory T cell diversity in humans. *Journal of Immunology (Baltimore, Md. : 1950)*, *166*(2),

877–884. https://doi.org/10.4049/jimmunol.166.2.877

Candia, E., Reyes, P., Covian, C., Rodriguez, F., Wainstein, N., Morales, J., … Fierro, J. A. (2017). Single and combined effect of retinoic acid and rapamycin modulate the generation, activity and homing potential of induced human regulatory T cells. https://doi.org/10.1371/journal.pone.0182009

Cao, S., Jiang, Y., Zhang, H., Kondza, N., & Woodrow, K. A. (2018). Core-shell nanoparticles for targeted and combination antiretroviral activity in gut-homing T cells. *Nanomedicine: Nanotechnology, Biology and Medicine*. https://doi.org/10.1016/J.NANO.2018.06.005

Cao, W., Henry, M. D., Borrow, P., Yamada, H., Elder, J. H., Ravkov, E. V, … Oldstone, M. B. (1998). Identification of alpha-dystroglycan as a receptor for lymphocytic choriomeningitis virus and Lassa fever virus. *Science (New York, N.Y.)*, *282*(5396), 2079–2081. http://doi.org/ 10.1126/science.282.5396.2079

Carrion, R., Brasky, K., Mansfield, K., Johnson, C., Gonzales, M., Ticer, A., … Patterson, J. (2007). Lassa virus infection in experimentally infected marmosets: liver pathology and immunophenotypic alterations in target tissues. *Journal of Virology*, *81*(12), 6482–6490. https://doi.org/10.1128/JVI.02876-06

Cerwenka, A., Morgan, T. M., & Dutton, R. W. (1999). Naive, effector, and memory CD8 T cells in protection against pulmonary influenza virus infection: homing properties rather than initial frequencies are crucial. *Journal of Immunology (Baltimore, Md. : 1950)*, *163*(10), 5535–5543. httos://doi.org/ 163 (10) 5535-5543

Ch'en, I. L., Beisner, D. R., Degterev, A., Lynch, C., Yuan, J., Hoffmann, A., & Hedrick, S. M. (2008). Antigen-mediated T cell expansion regulated by parallel pathways of death. *Proceedings of the National Academy of Sciences of the United States of America*, *105*(45), 17463–17468. https://doi.org/10.1073/pnas.0808043105

Chandele, A., Sewatanon, J., Gunisetty, S., Singla, M., Onlamoon, N., Akondy, R. S., … Murali-Krishna, K. (2016). Characterization of Human CD8 T Cell Responses in Dengue Virus-Infected Patients from India. *Journal of Virology*, *90*(24), 11259–11278. https://doi.org/10.1128/JVI.01424-16

Chen, X., Tu, C., Qin, T., Zhu, L., Yin, Y., & Yang, Q. (2016). Retinoic acid facilitates inactivated transmissible gastroenteritis virus induction of CD8+ T-cell migration to the porcine gut. *Scientific Reports*, *6*(1), 24152. https://doi.org/10.1038/srep24152

Childs, J. E., Cheek, J. E., Rollin, P. E., Enscore, R. E., Maupin, G. O., Glass, G. E., … Sarisky, J. (1995). A Household-Based, Case-Control Study of Environmental Factors Associated with Hantavirus Pulmonary Syndrome in the Southwestern United States. *The American Journal of Tropical Medicine and Hygiene*, *52*(5), 393–397. https://doi.org/10.4269/ajtmh.1995.52.393

Cibrián, D., & Sánchez-Madrid, F. (2017). CD69: from activation marker to metabolic gatekeeper. *European Journal of Immunology*, *47*(6), 946–953. https://doi.org/10.1002/eji.201646837

Clarke, S. Rm., Barnden, M., Kurts, C., Carbone, F. R., Miller, J. F., & Heath, W. R. (2000). Characterization of the ovalbumin-specific TCR transgenic line OT-I: MHC elements for positive and negative selection. *Immunology and Cell Biology*, *78*(2), 110–117. https://doi.org/10.1046/j.1440-1711.2000.00889.x

Cochez, P. M., Michiels, C., Hendrickx, E., Dauguet, N., Warnier, G., Renauld, J.-C., & Dumoutier, L. (2017). Ccr6 Is Dispensable for the Development of Skin Lesions Induced by Imiquimod despite its Effect on Epidermal Homing of IL-22-Producing Cells. *The Journal of Investigative Dermatology*, *137*(5), 1094–1103. https://doi.org/10.1016/j.jid.2016.12.023

Colangelo, P., Verheyen, E., Leirs, H., Tatard, C., Denys, C., Dobigny, G., … Lecompte, E. (2013). A mitochondrial phylogeographic scenario for the most widespread African rodent, *Mastomys natalensis*. *Biological Journal of the Linnean Society*, *108*(4), 901–916. https://doi.org/10.1111/bij.12013

Cox, D., Brennan, M., & Moran, N. (2010). Integrins as therapeutic targets: lessons and opportunities. *Nature Reviews Drug Discovery*, *9*(10), 804–820. https://doi.org/10.1038/nrd3266

Cummins, D, Fisher-Hoch, S. P., Walshe, K. J., Mackie, I. J., McCormick, J. B., Bennett, D., … Machin, S. J.

(1989). A plasma inhibitor of platelet aggregation in patients with Lassa fever. *British Journal of Haematology*, *72*(4), 543–548. https://doi.org/ 10.1111/j.1365-2141.1989.tb04321.x

Cummins, David, McCormick, J. B., Bennett, D., Samba, J. A., Farrar, B., Machin, S. J., & Fisher-Hoch, S. P. (1990). Acute Sensorineural Deafness in Lassa Fever. *JAMA: The Journal of the American Medical Association*, *264*(16), 2093. https://doi.org/10.1001/jama.1990.03450160063030

Czarnowicki, T., Santamaria-Babí, L. F., & Guttman-Yassky, E. (2017). Circulating CLA $^{+}$ T cells in atopic dermatitis and their possible role as peripheral biomarkers. *Allergy*, *72*(3), 366–372. https://doi.org/10.1111/all.13080

Danilova, E., Skrindo, I., Gran, E., Hales, B. J., Smith, W. A., Jahnsen, J., … Baekkevold, E. S. (2015). A role for CCL28–CCR3 in T-cell homing to the human upper airway mucosa. *Mucosal Immunology*, *8*(1), 107–114. https://doi.org/10.1038/mi.2014.46

Danylesko, I., Bukauskas, A., Paulson, M., Peceliunas, V., Gedde-Dahl d.y, T., Shimoni, A., … Nagler, A. (2019). Anti-α4β7 integrin monoclonal antibody (vedolizumab) for the treatment of steroid-resistant severe intestinal acute graft-versus-host disease. *Bone Marrow Transplantation*, *54*(7), 987–993. https://doi.org/10.1038/s41409-018-0364-5

Davila, S. J., Olive, A. J., & Starnbach, M. N. (2014). Integrin α4β1 Is Necessary for CD4+ T Cell-Mediated Protection against Genital Chlamydia trachomatis Infection. *The Journal of Immunology*, *192*(9), 4284–4293. https://doi.org/10.4049/jimmunol.1303238

Denucci, C. C., Mitchell, J. S., & Shimizu, Y. (2009). Integrin function in T-cell homing to lymphoid and nonlymphoid sites: getting there and staying there. *Critical Reviews in Immunology*, *29*(2), 87–109. Retrieved from http://www.ncbi.nlm.nih.gov/pubmed/19496742

DeNucci, C. C., Pagán, A. J., Mitchell, J. S., & Shimizu, Y. (2010). Control of α4β7 Integrin Expression and CD4 T Cell Homing by the β1 Integrin Subunit. *The Journal of Immunology*, *184*(5), 2458–2467. https://doi.org/10.4049/JIMMUNOL.0902407

Dios-Esponera, A., Melis, N., Subramanian, B. C., Weigert, R., & Samelson, L. E. (2019). Pak1 Kinase Promotes Activated T Cell Trafficking by Regulating the Expression of L-Selectin and CCR7. *Frontiers in Immunology*, *10*, 370. https://doi.org/10.3389/fimmu.2019.00370

Djavani, M, Yin, C., Lukashevich, I. S., Rodas, J., Rai, S. K., & Salvato, M. S. (2001). Mucosal immunization with Salmonella typhimurium expressing Lassa virus nucleocapsid protein cross-protects mice from lethal challenge with lymphocytic choriomeningitis virus. *Journal of Human Virology*, *4*(2), 103–108. Retrieved from http://www.ncbi.nlm.nih.gov/pubmed/11437313

Djavani, Mahmoud, Yin, C., Xia, L., Lukashevich, I. S., Pauza, C. D., & Salvato, M. S. (2000). Murine immune responses to mucosally delivered Salmonella expressing Lassa fever virus nucleoprotein. *Vaccine*, *18*(15), 1543–1554. https://doi.org/10.1016/S0264-410X(99)00439-9

Downs, W. G., Anderson, C. R., Spence, L., Aitken, T. H. G., & Greenhall, A. H. (1963). Tacaribe virus, a new agent isolated from Artibeus bats and mosquitoes in Trinidad, West Indies. *The American Journal of Tropical Medicine and Hygiene*, *12*, 640–646. https://doi.org/ 10.4269/ajtmh.1963.12.640

Duan, S., & Thomas, P. G. (2016). Balancing Immune Protection and Immune Pathology by CD8+ T-Cell Responses to Influenza Infection. *Frontiers in Immunology*, *7*, 25. https://doi.org/10.3389/fimmu.2016.00025

Dzutsev, A., Hogg, A., Sui, Y., Solaymani-Mohammadi, S., Yu, H., Frey, B., … Berzofsky, J. A. (2017). Differential T cell homing to colon vs. small intestine is imprinted by local CD11c+ APCs that determine homing receptors. *Journal of Leukocyte Biology*, *102*(6), 1381–1388. https://doi.org/10.1189/jlb.1A1116-463RR

Ebert, L. M., Meuter, S., & Moser, B. (2006). Homing and function of human skin gammadelta T cells and NK cells: relevance for tumor surveillance. *Journal of Immunology (Baltimore, Md. : 1950)*, *176*(7), 4331–4336. https://doi.org/10.4049/JIMMUNOL.176.7.4331

Ehl, S., Hombach, J., Aichele, P., Hengartner, H., & Zinkernagel, R. M. (1997). Bystander activation of cytotoxic T cells: studies on the mechanism and evaluation of in vivo significance in a transgenic mouse model. *The Journal of Experimental Medicine*, *185*(7), 1241–1251. https://doi.org/10.1084/jem.185.7.1241

Farber, D. L., Yudanin, N. A., & Restifo, N. P. (2014). Human memory T cells: generation, compartmentalization and homeostasis. *Nature Reviews Immunology*, *14*(1), 24–35. https://doi.org/10.1038/nri3567

Feagan, B. G., Greenberg, G. R., Wild, G., Fedorak, R. N., Paré, P., McDonald, J. W. D., … Parikh, A. (2008). Treatment of Active Crohn's Disease With MLN0002, a Humanized Antibody to the α4β7 Integrin. *Clinical Gastroenterology and Hepatology*, *6*(12), 1370–1377. https://doi.org/10.1016/j.cgh.2008.06.007

Feagan, B. G., Greenberg, G. R., Wild, G., Fedorak, R. N., Paré, P., McDonald, J. W. D., … Vandervoort, M. K. (2005). Treatment of Ulcerative Colitis with a Humanized Antibody to the $\alpha_4\beta_7$ Integrin. *New England Journal of Medicine*, *352*(24), 2499–2507. https://doi.org/10.1056/NEJMoa042982

Fehling, S. K., Lennartz, F., & Strecker, T. (2012). Multifunctional nature of the arenavirus RING finger protein Z. *Viruses*, *4*(11), 2973–3011. https://doi.org/10.3390/v4112973

Fichet-Calvet, E., Lecompte, E., Koivogui, L., Soropogui, B., Doré, A., Kourouma, F., … Meulen, J. Ter. (2007). Fluctuation of Abundance and Lassa Virus Prevalence in *Mastomys natalensis* in Guinea, West Africa. *Vector-Borne and Zoonotic Diseases*, *7*(2), 119–128. https://doi.org/10.1089/vbz.2006.0520

Fichet-Calvet, E., & Rogers, D. J. (2009). Risk Maps of Lassa Fever in West Africa. *PLoS Neglected Tropical Diseases*, *3*(3), e388. https://doi.org/10.1371/journal.pntd.0000388

Fisher-Hoch, S P, Hutwagner, L., Brown, B., & McCormick, J. B. (2000). Effective vaccine for lassa fever. *Journal of Virology*, *74*(15), 6777–6783. https://doi.org/10.1128/jvi.74.15.6777-6783.2000

Fisher-Hoch, S P, Tomori, O., Nasidi, A., Perez-Oronoz, G. I., Fakile, Y., Hutwagner, L., & McCormick, J. B. (1995). Review of cases of nosocomial Lassa fever in Nigeria: the high price of poor medical practice. *BMJ (Clinical Research Ed.)*, *311*(7009), 857–859. https://doi.org/10.1136/bmj.311.7009.857

Fisher-Hoch, Susan P., McCormick, J. B., Sasso, D., & Craven, R. B. (1988). Hematologic dysfunction in Lassa fever. *Journal of Medical Virology*, *26*(2), 127–135. https://doi.org/10.1002/jmv.1890260204

Flatz, L., Rieger, T., Merkler, D., Bergthaler, A., Regen, T., Schedensack, M., … Pinschewer, D. D. (2010). T Cell-Dependence of Lassa Fever Pathogenesis. *PLoS Pathogens*, *6*(3), e1000836. https://doi.org/10.1371/journal.ppat.1000836

Förster, R., Davalos-Misslitz, A. C., & Rot, A. (2008). CCR7 and its ligands: balancing immunity and tolerance. *Nature Reviews Immunology*, *8*(5), 362–371. https://doi.org/10.1038/nri2297

Fu, H., Wang, A., Mauro, C., & Marelli-Berg, F. (2013). T lymphocyte trafficking: molecules and mechanisms. *Frontiers in Bioscience (Landmark Edition)*, *18*, 422–440. Retrieved from http://www.ncbi.nlm.nih.gov/pubmed/23276933

Fu, H., Ward, E. J., & Marelli-Berg, F. M. (2016). Mechanisms of T cell organotropism. *Cellular and Molecular Life Sciences : CMLS*, *73*(16), 3009–3033. https://doi.org/10.1007/s00018-016-2211-4

Fujinami, R. S., von Herrath, M. G., Christen, U., & Whitton, J. L. (2006). Molecular mimicry, bystander activation, or viral persistence: infections and autoimmune disease. *Clinical Microbiology Reviews*, *19*(1), 80–94. https://doi.org/10.1128/CMR.19.1.80-94.2006

Gaide, O., Emerson, R. O., Jiang, X., Gulati, N., Nizza, S., Desmarais, C., … Kupper, T. S. (2015). Common clonal origin of central and resident memory T cells following skin immunization. *Nature Medicine*, *21*(6), 647–653. https://doi.org/10.1038/nm.3860

Gallaher, W. R., DiSimone, C., & Buchmeier, M. J. (2001). The viral transmembrane superfamily: possible divergence of Arenavirus and Filovirus glycoproteins from a common RNA virus ancestor. *BMC Microbiology*, *1*, 1. Retrieved from http://www.ncbi.nlm.nih.gov/pubmed/11208257

Gálvez-Cancino, F., López, E., Menares, E., Díaz, X., Flores, C., Cáceres, P., … Lladser, A. (2018). Vaccination-

induced skin-resident memory CD8+ T cells mediate strong protection against cutaneous melanoma. *Oncoimmunology*, *7*(7), e1442163. https://doi.org/10.1080/2162402X.2018.1442163

Girard, J.-P., Moussion, C., & Förster, R. (2012). HEVs, lymphatics and homeostatic immune cell trafficking in lymph nodes. *Nature Reviews Immunology*, *12*(11), 762–773. https://doi.org/10.1038/nri3298

Goddeeris, M. M., Wu, B., Venzke, D., Yoshida-Moriguchi, T., Saito, F., Matsumura, K., … Campbell, K. P. (2013). LARGE glycans on dystroglycan function as a tunable matrix scaffold to prevent dystrophy. *Nature*, *503*(7474), 136–140. https://doi.org/10.1038/nature12605

Goedhart, M., Gessel, S., van der Voort, R., Slot, E., Lucas, B., Gielen, E., … Nolte, M. A. (2019). CXCR4, but not CXCR3, drives CD8 T-cell entry into and migration through the murine bone marrow. *European Journal of Immunology*. https://doi.org/10.1002/eji.201747438

Goldrath, A. W., Sivakumar, P. V., Glaccum, M., Kennedy, M. K., Bevan, M. J., Benoist, C., … Butz, E. A. (2002). Cytokine Requirements for Acute and Basal Homeostatic Proliferation of Naive and Memory CD8 $^{+}$ T Cells. *The Journal of Experimental Medicine*, *195*(12), 1515–1522. https://doi.org/10.1084/jem.20020033

González, J. C., Kwok, W. W., Wald, A., McClurkan, C. L., Huang, J., & Koelle, D. M. (2005). Expression of Cutaneous Lymphocyte–Associated Antigen and E-selectin Ligand by Circulating Human Memory CD4 $^{+}$ T Lymphocytes Specific for Herpes Simplex Virus Type 2. *The Journal of Infectious Diseases*, *191*(2), 243–254. https://doi.org/10.1086/426944

Gonzalo-Asensio, J., Portevin, D., Fisch, P., Latorre, I., Fernández-Sanmartín, M. A., Muriel-Moreno, B., … Joan Despí, S. (2019). Study of CD27 and CCR4 Markers on Specific CD4 + T-Cells as Immune Tools for Active and Latent Tuberculosis Management. *Frontiers in Immunology | Www.Frontiersin.Org*, *1*, 3094. https://doi.org/10.3389/fimmu.2018.03094

Gorfu, G., Rivera-Nieves, J., & Ley, K. (2009). *Role of β 7 integrins in intestinal lymphocyte homing and retention*. https://doi.org/10.2174/156652409789105525

Grahn, A., Bråve, A., Tolfvenstam, T., & Studahl, M. (2018). Absence of Nosocomial Transmission of Imported Lassa Fever during Use of Standard Barrier Nursing Methods. *Emerging Infectious Diseases*, *24*(6), 978–987. https://doi.org/10.3201/eid2406.172097

Grant, A. J., Lalor, P. F., Salmi, M., Jalkanen, S., & Adams, D. H. (2002). Homing of mucosal lymphocytes to the liver in the pathogenesis of hepatic complications of inflammatory bowel disease. *The Lancet*, *359*(9301), 150–157. https://doi.org/10.1016/S0140-6736(02)07374-9

Gray, P. M., Reiner, S. L., Smith, D. F., Kaye, P. M., & Scott, P. (2006). Antigen-Experienced T Cells Limit the Priming of Naive T Cells during Infection with *Leishmania major*. *The Journal of Immunology*, *177*(2), 925–933. https://doi.org/10.4049/jimmunol.177.2.925

Griffith, J. W., Sokol, C. L., & Luster, A. D. (2014). Chemokines and Chemokine Receptors: Positioning Cells for Host Defense and Immunity. *Annual Review of Immunology*, *32*(1), 659–702. https://doi.org/10.1146/annurev-immunol-032713-120145

Gryseels, S., Baird, S. J. E., Borremans, B., Makundi, R., Leirs, H., & Goüy de Bellocq, J. (2017). When Viruses Don't Go Viral: The Importance of Host Phylogeographic Structure in the Spatial Spread of Arenaviruses. *PLOS Pathogens*, *13*(1), e1006073. https://doi.org/10.1371/journal.ppat.1006073

Gunther, S. (2000). Imported Lassa Fever in Germany: Molecular Characterization of a New Lassa Virus Strain. *Emerging Infectious Diseases*, *6*(5), 466–476. https://doi.org/10.3201/eid0605.000504

Günther, S, Kühle, O., Rehder, D., Odaibo, G. N., Olaleye, D. O., Emmerich, P., … Schmitz, H. (2001). Antibodies to Lassa virus Z protein and nucleoprotein co-occur in human sera from Lassa fever endemic regions. *Medical Microbiology and Immunology*, *189*(4), 225–229. https://doi.org/10.1007/s004300100061

Günther, Stephan, & Lenz, O. (2004). Lassa Virus. *Critical Reviews in Clinical Laboratory Sciences*, *41*(4), 339–390. https://doi.org/10.1080/10408360490497456

Haller, O., Kochs, G., & Weber, F. (2006). The interferon response circuit: Induction and suppression by pathogenic viruses. *Virology*, *344*(1), 119–130. https://doi.org/10.1016/j.virol.2005.09.024

Han, T., Abdel-Motal, U. M., Chang, D.-K., Sui, J., Muvaffak, A., Campbell, J., … Marasco, W. A. (2012). Human Anti-CCR4 Minibody Gene Transfer for the Treatment of Cutaneous T-Cell Lymphoma. *PLoS ONE*, *7*(9), e44455. https://doi.org/10.1371/journal.pone.0044455

Hastie, K. M., King, L. B., Zandonatti, M. A., & Saphire, E. O. (2012). Structural basis for the dsRNA specificity of the Lassa virus NP exonuclease. *PloS One*, *7*(8), e44211. https://doi.org/10.1371/journal.pone.0044211

Hastie, K. M., Zandonatti, M. A., Kleinfelter, L. M., Heinrich, M. L., Rowland, M. M., Chandran, K., … Saphire, E. O. (2017). Structural basis for antibody-mediated neutralization of Lassa virus. *Science*, *356*(6341). https://doi.org/10.1126/science.aam7260

Hensel, M. T., Peng, T., Cheng, A., De Rosa, S. C., Wald, A., Laing, K. J., … Koelle, D. M. (2017). Selective Expression of CCR10 and CXCR3 by Circulating Human Herpes Simplex Virus-Specific CD8 T Cells. *Journal of Virology*, *91*(19). https://doi.org/10.1128/JVI.00810-17

Hjalgrim, H., Friborg, J., & Melbye, M. (2007). *The epidemiology of EBV and its association with malignant disease*. *Human Herpesviruses: Biology, Therapy, and Immunoprophylaxis*. Cambridge University Press. https://doi.org/10.3390/v4112766

Huggins, M. A., Jameson, S. C., & Hamilton, S. E. (2019). Embracing microbial exposure in mouse research. *Journal of Leukocyte Biology*, *105*(1), 73–79. https://doi.org/10.1002/JLB.4RI0718-273R

Ii, W. A. F., & Wohl, D. A. (2017). Moving Lassa Fever Research and Care Into the 21st Century. *The Journal of Infectious Diseases The Journal of Infectious Diseases ®*, *215*, 1779–1781. https://doi.org/10.1093/infdis/jix206

Ikushima, H., Negishi, H., & Taniguchi, T. (2013). The IRF family transcription factors at the interface of innate and adaptive immune responses. *Cold Spring Harbor Symposia on Quantitative Biology*, *78*(0), 105–116. https://doi.org/10.1101/sqb.2013.78.020321

Illick, M. M., Branco, L. M., Fair, J. N., Illick, K. A., Matschiner, A., Schoepp, R., … Guttieri, M. C. (2008). Uncoupling GP1 and GP2 expression in the Lassa virus glycoprotein complex: implications for GP1 ectodomain shedding. *Virology Journal*, *5*, 161. https://doi.org/10.1186/1743-422X-5-161

International Committee on Taxonomy of Viruses. Arenaviridae, Virus Taxonomy § (2012). Elsevier. https://doi.org/10.1016/B978-0-12-384684-6.00058-6

Jahrling, P. B., Frame, J. D., Rhoderick, J. B., & Monson, M. H. (1985). Endemic lassa fever in liberia. IV. Selection of optimally effective plasma for treatment by passive immunization. *Transactions of the Royal Society of Tropical Medicine and Hygiene*, *79*(3), 380–384. https://doi.org/10.1016/0035-9203(85)90388-8

Jahrling, P. B., Frame, J. D., Smith, S. B., & Monson, M. H. (1985). Endemic Lassa fever in Liberia. III. Characterization of Lassa virus isolates. *Transactions of the Royal Society of Tropical Medicine and Hygiene*, *79*(3), 374–379. https://doi.org/10.1016/0035-9203(85)90386-4

Jiang, J. Q., He, X.-S., Feng, N., & Greenberg, H. B. (2008). Qualitative and Quantitative Characteristics of Rotavirus-Specific CD8 T Cells Vary Depending on the Route of Infection. *Journal of Virology*, *82*(14), 6812–6819. https://doi.org/10.1128/JVI.00450-08

Jiang, X., Huang, Q., Wang, W., Dong, H., Ly, H., Liang, Y., & Dong, C. (2013). Structures of Arenaviral Nucleoproteins with Triphosphate dsRNA Reveal a Unique Mechanism of Immune Suppression. *Journal of Biological Chemistry*, *288*(23), 16949–16959. https://doi.org/10.1074/jbc.M112.420521

Johnson, K M, McCormick, J. B., Webb, P. A., Smith, E. S., Elliott, L. H., & King, I. J. (1987). Clinical virology of Lassa fever in hospitalized patients. *The Journal of Infectious Diseases*, *155*(3), 456–464. https://doi.org/10.1093/infdis/155.3.456

Johnson, Karl M., Webb, P. A., Smith, E., Keenlyside, R. A., Elliott, L., & McCormick, J. B. (1983). Case-Control

Study of Mastomys Natalensis and Humans in Lassa Virus-Infected Households in Sierra Leone *. *The American Journal of Tropical Medicine and Hygiene*, *32*(4), 829–837. https://doi.org/10.4269/ajtmh.1983.32.829

Johnson, L. R., Weizman, O.-E., Rapp, M., Way, S. S., & Sun, J. C. (2016). Epitope-Specific Vaccination Limits Clonal Expansion of Heterologous Naive T Cells during Viral Challenge. *Cell Reports*, *17*(3), 636–644. https://doi.org/10.1016/j.celrep.2016.09.019

Kafetzopoulou, L. E., Pullan, S. T., Lemey, P., Suchard, M. A., Ehichioya, D. U., Pahlmann, M., … Duraffour, S. (2019). Metagenomic sequencing at the epicenter of the Nigeria 2018 Lassa fever outbreak. *Science*, *363*(6422), 74–77. https://doi.org/10.1126/science.aau9343

Kauffmann, S. O., Thomsen, A. R., & Christensen, J. P. (2006). Role of Very Late Antigen-1 in T-cell-Mediated Immunity to Systemic Viral Infection. *Scandinavian Journal of Immunology*, *63*(4), 290–298. https://doi.org/10.1111/j.1365-3083.2006.01744.x

Khan, S. H., Goba, A., Chu, M., Roth, C., Healing, T., Marx, A., … Bausch, D. G. (2008). New opportunities for field research on the pathogenesis and treatment of Lassa fever. *Antiviral Research*, *78*(1), 103–115. https://doi.org/10.1016/J.ANTIVIRAL.2007.11.003

Kim, S.-K., Brehm, M. A., Welsh, R. M., & Selin, L. K. (2002). Dynamics of Memory T Cell Proliferation Under Conditions of Heterologous Immunity and Bystander Stimulation. *The Journal of Immunology*, *169*(1), 90–98. https://doi.org/10.4049/jimmunol.169.1.90

Kim, Y. K., Shin, J. S., & Nahm, M. H. (2016). NOD-Like Receptors in Infection, Immunity, and Diseases. *Yonsei Medical Journal*, *57*(1), 5–14. https://doi.org/10.3349/ymj.2016.57.1.5

Koelle, D. M., Huang, J., Hensel, M. T., & McClurkan, C. L. (2006). Innate Immune Responses to Herpes Simplex Virus Type 2 Influence Skin Homing Molecule Expression by Memory CD4+ Lymphocytes. *Journal of Virology*, *80*(6), 2863–2872. https://doi.org/10.1128/JVI.80.6.2863-2872.2006

Koszinowski, U. H., Reddehase, M. J., & Jonjic, S. (1991). The role of CD4 and CD8 T cells in viral infections. *Current Opinion in Immunology*, *3*(4), 471–475. https://doi.org/10.1016/0952-7915(91)90005-L

Koyama, S., Ishii, K. J., Coban, C., & Akira, S. (2008). Innate immune response to viral infection. *Cytokine*, *43*(3), 336–341. https://doi.org/10.1016/j.cyto.2008.07.009

Kraal, G., Schornagel, K., Streeter, P. R., Holzmann, B., & Butcher, E. C. (1995). Expression of the mucosal vascular addressin, MAdCAM-1, on sinus-lining cells in the spleen. *The American Journal of Pathology*, *147*(3), 763–771. Retrieved from http://www.ncbi.nlm.nih.gov/pubmed/7677187

Kugelberg, E., Norström, T., Petersen, T. K., Duvold, T., Andersson, D. I., & Hughes, D. (2005). Establishment of a Superficial Skin Infection Model in Mice by Using Staphylococcus aureus and Streptococcus pyogenes. *ANTIMICROBIAL AGENTS AND CHEMOTHERAPY*, *49*(8), 3435–3441. https://doi.org/10.1128/AAC.49.8.3435-3441.2005

Kumar, B. V, Ma, W., Miron, M., Granot, T., Guyer, R. S., Carpenter, D. J., … Farber, D. L. (2017). Human Tissue-Resident Memory T Cells Are Defined by Core Transcriptional and Functional Signatures in Lymphoid and Mucosal Sites. *Cell Reports*, *20*(12), 2921–2934. https://doi.org/10.1016/j.celrep.2017.08.078

Kunkel, E. J., Boisvert, J., Murphy, K., Vierra, M. A., Genovese, M. C., Wardlaw, A. J., … Campbell, J. J. (2002). Expression of the Chemokine Receptors CCR4, CCR5, and CXCR3 by Human Tissue-Infiltrating Lymphocytes. *The American Journal of Pathology*, *160*(1), 347–355. https://doi.org/10.1016/S0002-9440(10)64378-7

Laydon, D. J., Bangham, C. R. M., & Asquith, B. (2015). Estimating T-cell repertoire diversity: limitations of classical estimators and a new approach. *Philosophical Transactions of the Royal Society of London. Series B, Biological Sciences*, *370*(1675). https://doi.org/10.1098/rstb.2014.0291

Lechner, F., Wong, D. K. H., Dunbar, P. R., Chapman, R., Chung, R. T., Dohrenwend, P., … Walker, B. D. (2000). Analysis of Successful Immune Responses in Persons Infected with Hepatitis C Virus. *The Journal of Experimental Medicine*, *191*(9), 1499–1512. https://doi.org/10.1084/jem.191.9.1499

Lindgren, T., Ahlm, C., Mohamed, N., Evander, M., Ljunggren, H.-G., & Bjorkstrom, N. K. (2011). Longitudinal Analysis of the Human T Cell Response during Acute Hantavirus Infection. *Journal of Virology*, *85*(19), 10252–10260. https://doi.org/10.1128/JVI.05548-11

Lloyd, G., Barber, G. N., Clegg, J. C., & Kelly, P. (1989). Identification of Lassa fever virus infection with recombinant nucleocapsid protein antigen. *Lancet (London, England)*, *2*(8673), 1222. https://doi.org/10.1016/s0140-6736(89)91833-3

Loo, Y.-M., Gale, M., & Jr. (2011). Immune signaling by RIG-I-like receptors. *Immunity*, *34*(5), 680. https://doi.org/10.1016/J.IMMUNI.2011.05.003

Lüdtke, A., Ruibal, P., Wozniak, D. M., Pallasch, E., Wurr, S., Bockholt, S., … Muñoz-Fontela, C. (2017). Ebola virus infection kinetics in chimeric mice reveal a key role of T cells as barriers for virus dissemination. *Scientific Reports*, *7*, 43776. https://doi.org/10.1038/srep43776

Lukashevich, I S, Clegg, J. C., & Sidibe, K. (1993). Lassa virus activity in Guinea: distribution of human antiviral antibody defined using enzyme-linked immunosorbent assay with recombinant antigen. *Journal of Medical Virology*, *40*(3), 210–217. https://doi.org/10.1002/jmv.1890400308

Lukashevich, I S, Maryankova, R., Vladyko, A. S., Nashkevich, N., Koleda, S., Djavani, M., … Salvato, M. S. (1999). Lassa and Mopeia virus replication in human monocytes/macrophages and in endothelial cells: different effects on IL-8 and TNF-alpha gene expression. *Journal of Medical Virology*, *59*(4), 552–560. Retrieved from http://www.ncbi.nlm.nih.gov/pubmed/10534741

Lukashevich, Igor S, Djavani, M., Rodas, J. D., Zapata, J. C., Usborne, A., Emerson, C., … Salvato, M. S. (2002). Hemorrhagic fever occurs after intravenous, but not after intragastric, inoculation of rhesus macaques with lymphocytic choriomeningitis virus. *Journal of Medical Virology*, *67*(2), 171–186. https://doi.org/10.1002/jmv.2206

Lukens, M. V., Kruijsen, D., Coenjaerts, F. E. J., Kimpen, J. L. L., & van Bleek, G. M. (2009). Respiratory Syncytial Virus-Induced Activation and Migration of Respiratory Dendritic Cells and Subsequent Antigen Presentation in the Lung-Draining Lymph Node. *Journal of Virology*, *83*(14), 7235–7243. https://doi.org/10.1128/JVI.00452-09

Mahanty, S., Bausch, D. G., Thomas, R. L., Goba, A., Bah, A., Peters, C. J., & Rollin, P. E. (2001). Low Levels of Interleukin-8 and Interferon-Inducible Protein–10 in Serum Are Associated with Fatal Infections in Acute Lassa Fever. *The Journal of Infectious Diseases*, *183*(12), 1713–1721. https://doi.org/10.1086/320722

Malhotra, S., Yen, J. Y., Honko, A. N., Garamszegi, S., Caballero, I. S., Johnson, J. C., … Connor, J. H. (2013). Transcriptional Profiling of the Circulating Immune Response to Lassa Virus in an Aerosol Model of Exposure. *PLoS Neglected Tropical Diseases*, *7*(4), e2171. https://doi.org/10.1371/journal.pntd.0002171

Marcus, P. I., & Sekellick, M. J. (1977). Defective interfering particles with covalently linked [+/-]RNA induce interferon. *Nature*, *266*(5605), 815–819. https://doi.org/10.2217/fvl-2018-0021

Marcus, P. I., Svitlik, C., & Sekellick, M. J. (1983). Interferon Induction by Viruses. X. A Model for Interferon Induction by Newcastle Disease Virus. *Journal of General Virology*, *64*(11), 2419–2431. https://doi.org/10.1099/0022-1317-64-11-2419

Marelli-Berg, F. M., Cannella, L., Dazzi, F., & Mirenda, V. (2008). The highway code of T cell trafficking. *The Journal of Pathology*, *214*(2), 179–189. https://doi.org/10.1002/path.2269

Mateer, E. J., Huang, C., Shehu, N. Y., & Paessler, S. (2018). Lassa fever-induced sensorineural hearing loss: A neglected public health and social burden. *PLoS Neglected Tropical Diseases*, *12*(2), e0006187. https://doi.org/10.1371/journal.pntd.0006187

McAllister, A., Arbetman, A. E., Mandl, S., Peña-Rossi, C., & Andino, R. (2000). Recombinant yellow fever viruses are effective therapeutic vaccines for treatment of murine experimental solid tumors and pulmonary metastases. *Journal of Virology*, *74*(19), 9197–9205. https://doi.org/10.1128/jvi.74.19.9197-9205.2000

McCormick, J. B. (1986). Clinical, epidemiologic, and therapeutic aspects of Lassa fever. *Medical Microbiology and Immunology*, *175*(2–3), 153–155. https://doi.org/10.1007/BF02122438

McCormick, J B, & Fisher-Hoch, S. P. (2002). Lassa fever. *Current Topics in Microbiology and Immunology*, *262*, 75–109. https://doi.org/10.1007/978-3-642-56029-3_4

McCormick, J B, King, I. J., Webb, P. A., Johnson, K. M., O'Sullivan, R., Smith, E. S., … Tong, T. C. (1987). A case-control study of the clinical diagnosis and course of Lassa fever. *The Journal of Infectious Diseases*, *155*(3), 445–455. https://doi.org/ 10.1093/infdis/155.3.445

McCormick, J B, Walker, D. H., King, I. J., Webb, P. A., Elliott, L. H., Whitfield, S. G., & Johnson, K. M. (1986). Lassa virus hepatitis: a study of fatal Lassa fever in humans. *The American Journal of Tropical Medicine and Hygiene*, *35*(2), 401–407. Retrieved from http://www.ncbi.nlm.nih.gov/pubmed/3953952

McCormick, J B, Webb, P. A., Krebs, J. W., Johnson, K. M., & Smith, E. S. (1987). A prospective study of the epidemiology and ecology of Lassa fever. *The Journal of Infectious Diseases*, *155*(3), 437–444. https://doi.org/10.1093/infdis/155.3.437

McCormick, Joseph B., King, I. J., Webb, P. A., Scribner, C. L., Craven, R. B., Johnson, K. M., … Belmont-Williams, R. (1986a). Lassa fever. Effective therapy with ribavirin. *New England Journal of Medicine*, *314*(1), 20–26. https://doi.org/10.1056/NEJM198601023140104

McCormick, Joseph B., King, I. J., Webb, P. A., Scribner, C. L., Craven, R. B., Johnson, K. M., … Belmont-Williams, R. (1986b). Lassa Fever. *New England Journal of Medicine*, *314*(1), 20–26. https://doi.org/10.1056/NEJM198601023140104

McElroy, A. K., Akondy, R. S., Davis, C. W., Ellebedy, A. H., Mehta, A. K., Kraft, C. S., … Ahmed, R. (2015). Human Ebola virus infection results in substantial immune activation. *Proceedings of the National Academy of Sciences of the United States of America*, *112*(15), 4719–4724. https://doi.org/10.1073/pnas.1502619112

McElroy, A. K., Akondy, R. S., Harmon, J. R., Ellebedy, A. H., Cannon, D., Klena, J. D., … Spiropoulou, C. F. (2017). A Case of Human Lassa Virus Infection With Robust Acute T-Cell Activation and Long-Term Virus-Specific T-Cell Responses. *The Journal of Infectious Diseases*, *215*(12), 1862–1872. https://doi.org/10.1093/infdis/jix201

Mehand, M. S., Al-Shorbaji, F., Millett, P., & Murgue, B. (2018). The WHO R&D Blueprint: 2018 review of emerging infectious diseases requiring urgent research and development efforts. *Antiviral Research*. https://doi.org/10.1016/j.antiviral.2018.09.009

Mestas, J., & Hughes, C. C. W. (2004). Of Mice and Not Men: Differences between Mouse and Human Immunology. *The Journal of Immunology*, *172*(5), 2731–2738. https://doi.org/10.4049/jimmunol.172.5.2731

Meyer, B., & Ly, H. (2016). Inhibition of Innate Immune Responses Is Key to Pathogenesis by Arenaviruses. *Journal of Virology*, *90*(8), 3810–3818. https://doi.org/10.1128/JVI.03049-15

Mikhak, Z., Strassner, J. P., & Luster, A. D. (2013). Lung dendritic cells imprint T cell lung homing and promote lung immunity through the chemokine receptor CCR4. *The Journal of Experimental Medicine*, *210*(9), 1855–1869. https://doi.org/10.1084/jem.20130091

Miller, J. D., van der Most, R. G., Akondy, R. S., Glidewell, J. T., Albott, S., Masopust, D., … Ahmed, R. (2008). Human Effector and Memory CD8+ T Cell Responses to Smallpox and Yellow Fever Vaccines. *Immunity*, *28*(5), 710–722. https://doi.org/10.1016/j.immuni.2008.02.020

Min, B., Foucras, G., Meier-Schellersheim, M., & Paul, W. E. (2004). Spontaneous proliferation, a response of naive CD4 T cells determined by the diversity of the memory cell repertoire. *Proceedings of the National Academy of Sciences*, *101*(11), 3874–3879. https://doi.org/10.1073/pnas.0400606101

Miranda, M. B. de, Melo, A. S. de, Almeida, M. S., Marinho, S. M., Oliveira Junior, W., & Gomes, Y. de M. (2017). Ex vivo T-lymphocyte chemokine receptor phenotypes in patients with chronic Chagas disease. *Revista Da Sociedade Brasileira de Medicina Tropical*, *50*(5), 689–692. https://doi.org/10.1590/0037-8682-0025-2017

Miyasaka, M., & Tanaka, T. (2004). Lymphocyte trafficking across high endothelial venules: dogmas and enigmas. *Nature Reviews Immunology*, *4*(5), 360–370. https://doi.org/10.1038/nri1354

Monath, T. P., Newhouse, V. F., Kemp, G. E., Setzer, H. W., & Cacciapuoti, A. (1974). Lassa Virus Isolation from Mastomys natalensis Rodents during an Epidemic in Sierra Leone. *Science*, *185*(4147), 263–265. https://doi.org/10.1126/science.185.4147.263

Murali-Krishna, K., Altman, J. D., Suresh, M., Sourdive, D. J., Zajac, A. J., Miller, J. D., … Ahmed, R. (1998). Counting antigen-specific CD8 T cells: a reevaluation of bystander activation during viral infection. *Immunity*, *8*(2), 177–187. https://doi.org/10.1016/s1074-7613(00)80470-7

Mwanza-Lisulo, M., Chomba, M. S., Chama, M., Besa, E. C., Funjika, E., Zyambo, K., … Kelly, P. M. (2018). Retinoic acid elicits a coordinated expression of gut homing markers on T lymphocytes of Zambian men receiving oral Vivotif, but not Rotarix, Dukoral or OPVERO vaccines. https://doi.org/10.1016/j.vaccine.2018.04.083

Ndhlovu, Z. M., Kamya, P., Mewalal, N., Kløverpris, H. N., Nkosi, T., Pretorius, K., … Walker, B. D. (2015). Magnitude and Kinetics of CD8+ T Cell Activation during Hyperacute HIV Infection Impact Viral Set Point. *Immunity*, *43*(3), 591–604. https://doi.org/10.1016/j.immuni.2015.08.012

Ntranos, A., Ntranos, V., Bonnefil, V., Liu, J., Kim-Schulze, S., He, Y., … Casaccia, P. (2019). Fumarates target the metabolic-epigenetic interplay of brain-homing T cells in multiple sclerosis. *Brain*. https://doi.org/10.1093/brain/awy344

Oeckinghaus, A., & Ghosh, S. (2009). The NF- B Family of Transcription Factors and Its Regulation. *Cold Spring Harbor Perspectives in Biology*, *1*(4), a000034–a000034. https://doi.org/10.1101/cshperspect.a000034

Oestereich, L., Lüdtke, A., Ruibal, P., Pallasch, E., Kerber, R., Rieger, T., … Muñoz-Fontela, C. (2016). Chimeric Mice with Competent Hematopoietic Immunity Reproduce Key Features of Severe Lassa Fever. *PLoS Pathogens*, *12*(5), e1005656. https://doi.org/10.1371/journal.ppat.1005656

Oestereich, L., Rieger, T., Lüdtke, A., Ruibal, P., Wurr, S., Pallasch, E., … Günther, S. (2016). Efficacy of Favipiravir Alone and in Combination With Ribavirin in a Lethal, Immunocompetent Mouse Model of Lassa Fever. *Journal of Infectious Diseases*, *213*(6). https://doi.org/10.1093/infdis/jiv522

Ogawa, H., Binion, D. G., Heidemann, J., Theriot, M., Fisher, P. J., Johnson, N. A., … Rafiee, P. (2005). Mechanisms of MAdCAM-1 gene expression in human intestinal microvascular endothelial cells. *American Journal of Physiology-Cell Physiology*, *288*(2), C272–C281. https://doi.org/10.1152/ajpcell.00406.2003

Olayemi, A., Cadar, D., Magassouba, N., Obadare, A., Kourouma, F., Oyeyiola, A., … Fichet-Calvet, E. (2016). New Hosts of The Lassa Virus. *Scientific Reports*, *6*. https://doi.org/10.1038/srep25280

Osborne, L. C., Monticelli, L. A., Nice, T. J., Sutherland, T. E., Siracusa, M. C., Hepworth, M. R., … Artis, D. (2014). Virus-helminth coinfection reveals a microbiota-independent mechanism of immunomodulation. *Science*, *345*(6196), 578–582. https://doi.org/10.1126/science.1256942

Ostler, T., Pircher, H., & Ehl, S. (2003). "Bystander" recruitment of systemic memory T cells delays the immune response to respiratory virus infection. *European Journal of Immunology*, *33*(7), 1839–1848. https://doi.org/10.1002/eji.200323460

Oyoshi, M. K., Elkhal, A., Scott, J. E., Wurbel, M.-A., Hornick, J. L., Campbell, J. J., & Geha, R. S. (2011). Epicutaneous challenge of orally immunized mice redirects antigen-specific gut-homing T cells to the skin. *Journal of Clinical Investigation*, *121*(6), 2210–2220. https://doi.org/10.1172/JCI43586

Parra, M., Herrera, D., Calvo-Calle, J. M., Stern, L. J., Parra-López, C. A., Butcher, E., … Angel, J. (2014). Circulating human rotavirus specific CD4 T cells identified with a class II tetramer express the intestinal

homing receptors α4β7 and CCR9. *Virology*, *452–453*, 191–201. https://doi.org/10.1016/j.virol.2014.01.014

Paust, S., Blish, C. A., & Reeves, R. K. (2017). Redefining Memory: Building the Case for Adaptive NK Cells. *Journal of Virology*, *91*(20). https://doi.org/10.1128/JVI.00169-17

Pauza, C. D., Emau, P., Salvato, M. S., Trivedi, P., MacKenzie, D., Malkovsky, M., … Schultz, K. T. (1993). Pathogenesis of SIVmac251 after atraumatic inoculation of the rectal mucosa in rhesus monkeys. *Journal of Medical Primatology*, *22*(2–3), 154–161. Retrieved from http://www.ncbi.nlm.nih.gov/pubmed/8411107

Perciani, C. T., Jaoko, W., Farah, B., Ostrowski, M. A., Anzala, O., & MacDonald, K. S. (2018). αeβ7, α4β7 and α4β1 integrin contributions to T cell distribution in blood, cervix and rectal tissues: Potential implications for HIV transmission. *PLoS ONE*, *13*(2). https://doi.org/10.1371/journal.pone.0192482

Pérez-Girón, J. V, Belicha-Villanueva, A., Hassan, E., Gómez-Medina, S., Cruz, J. L. G., Lüdtke, A., … Muñoz-Fontela, C. (2014). Mucosal polyinosinic-polycytidylic acid improves protection elicited by replicating influenza vaccines via enhanced dendritic cell function and T cell immunity. *Journal of Immunology (Baltimore, Md. : 1950)*, *193*(3), 1324–1332. https://doi.org/10.4049/jimmunol.1400222

Permar, S. R., Moss, W. J., Ryon, J. J., Douek, D. C., Monze, M., & Griffin, D. E. (2003). Increased thymic output during acute measles virus infection. *Journal of Virology*, *77*(14), 7872–7879. https://doi.org/10.1128/jvi.77.14.7872-7879.2003

Pihlgren, M., Lightstone, L., Mamalaki, C., Rimon, G., Kioussis, D., & Marvel, J. (1995). Expressionin vivo of CD45RA, CD45RB and CD44 on T cell receptor-transgenic CD8+ T cells following immunization. *European Journal of Immunology*, *25*(6), 1755–1759. https://doi.org/10.1002/eji.1830250640

Pitsillides, C. M., Runnels, J. M., Spencer, J. A., Zhi, L., Wu, M. X., & Lin, C. P. (2011). Cell labeling approaches for fluorescence-based in vivo flow cytometry. *Cytometry. Part A : The Journal of the International Society for Analytical Cytology*, *79*(10), 758–765. https://doi.org/10.1002/cyto.a.21125

Polman, C. H., O'Connor, P. W., Havrdova, E., Hutchinson, M., Kappos, L., Miller, D. H., … AFFIRM Investigators. (2006). A Randomized, Placebo-Controlled Trial of Natalizumab for Relapsing Multiple Sclerosis. *New England Journal of Medicine*, *354*(9), 899–910. https://doi.org/10.1056/NEJMoa044397

Prescott, J. B., Marzi, A., Safronetz, D., Robertson, S. J., Feldmann, H., & Best, S. M. (2017). Immunobiology of Ebola and Lassa virus infections. *Nature Reviews Immunology*, *17*(3), 195–207. https://doi.org/10.1038/nri.2016.138

Pythoud, C., Rodrigo, W. W. S. I., Pasqual, G., Rothenberger, S., Martínez-Sobrido, L., de la Torre, J. C., & Kunz, S. (2012). Arenavirus nucleoprotein targets interferon regulatory factor-activating kinase IKKε. *Journal of Virology*, *86*(15), 7728–7738. https://doi.org/10.1128/JVI.00187-12

Qualai, J., Cantero, J., Li, L.-X., Carrascosa, J. M., Cabré, E., Dern, O., … Genescà, M. (2016). Adhesion Molecules Associated with Female Genital Tract Infection. *PLOS ONE*, *11*(6), e0156605. https://doi.org/10.1371/journal.pone.0156605

Raftery, M. J., Abdelaziz, M. O., Hofmann, J., & Schönrich, G. (2018). Hantavirus-Driven PD-L1/PD-L2 Upregulation: An Imperfect Viral Immune Evasion Mechanism. *Frontiers in Immunology*, *9*, 2560. https://doi.org/10.3389/fimmu.2018.02560

Rai, S. K., Micales, B. K., Wu, M. S., Cheung, D. S., Pugh, T. D., Lyons, G. E., & Salvato, M. S. (1997). Timed appearance of lymphocytic choriomeningitis virus after gastric inoculation of mice. *The American Journal of Pathology*, *151*(2), 633–639. Retrieved from http://www.ncbi.nlm.nih.gov/pubmed/9250174

Randall, R. E., & Goodbourn, S. (2008). Interferons and viruses: an interplay between induction, signalling, antiviral responses and virus countermeasures. *Journal of General Virology*, *89*(1), 1–47. https://doi.org/10.1099/vir.0.83391-0

Reddy, M., Eirikis, E., Davis, C., Davis, H. M., & Prabhakar, U. (2004). Comparative analysis of lymphocyte activation marker expression and cytokine secretion profile in stimulated human peripheral blood

mononuclear cell cultures: an in vitro model to monitor cellular immune function. *Journal of Immunological Methods*, *293*(1–2), 127–142. https://doi.org/10.1016/J.JIM.2004.07.006

Reese, T. A., Bi, K., Kambal, A., Filali-Mouhim, A., Beura, L. K., Bürger, M. C., … Virgin, H. W. (2016). Sequential Infection with Common Pathogens Promotes Human-like Immune Gene Expression and Altered Vaccine Response. *Cell Host & Microbe*, *19*(5), 713–719. https://doi.org/10.1016/j.chom.2016.04.003

Reiss, Y., Proudfoot, A. E., Power, C. A., Campbell, J. J., & Butcher, E. C. (2001). CC chemokine receptor (CCR)4 and the CCR10 ligand cutaneous T cell-attracting chemokine (CTACK) in lymphocyte trafficking to inflamed skin. *The Journal of Experimental Medicine*, *194*(10), 1541–1547. https://doi.org/10.1084/jem.194.10.1541

Richmond, J. K., & Baglole, D. J. (2003). Lassa fever: epidemiology, clinical features, and social consequences. *BMJ (Clinical Research Ed.)*, *327*(7426), 1271–1275. https://doi.org/10.1136/bmj.327.7426.1271

Rivera-Nieves, J., Burcin, T. L., Olson, T. S., Morris, M. A., McDuffie, M., Cominelli, F., & Ley, K. (2006). Critical role of endothelial P-selectin glycoprotein ligand 1 in chronic murine ileitis. *The Journal of Experimental Medicine*, *203*(4), 907–917. https://doi.org/10.1084/jem.20052530

Rivino, L. (2018). Understanding the Human T Cell Response to Dengue Virus. In *Advances in experimental medicine and biology* (Vol. 1062, pp. 241–250). Springer, Singapore. https://doi.org/10.1007/978-981-10-8727-1_17

Rivino, L., Kumaran, E. A., Thein, T.-L., Too, C. T., Hao Gan, V. C., Hanson, B. J., … MacAry, P. A. (2015). Virus-specific T lymphocytes home to the skin during natural dengue infection. *Science Translational Medicine*, *7*(278), 278ra35-278ra35. https://doi.org/10.1126/scitranslmed.aaa0526

Roberts, L. (2018). Nigeria hit by unprecedented Lassa fever outbreak. *Science*. https://doi.org/10.1126/science.359.6381.1201

Robins, H. S., Campregher, P. V, Srivastava, S. K., Wacher, A., Turtle, C. J., Kahsai, O., … Carlson, C. S. (2009). Comprehensive assessment of T-cell receptor beta-chain diversity in alphabeta T cells. *Blood*, *114*(19), 4099–4107. https://doi.org/10.1182/blood-2009-04-217604

Rosendahl Huber, S., van Beek, J., de Jonge, J., Luytjes, W., & van Baarle, D. (2014). T cell responses to viral infections - opportunities for Peptide vaccination. *Frontiers in Immunology*, *5*, 171. https://doi.org/10.3389/fimmu.2014.00171

Rot, A., & von Andrian, U. H. (2004). Chemokines in Innate and Adaptive Host Defense : Basic Chemokinese Grammar for Immune Cells. *Annual Review of Immunology*, *22*(1), 891–928. https://doi.org/10.1146/annurev.immunol.22.012703.104543

Rott, L. S., Rosé, J. R., Bass, D., Williams, M. B., Greenberg, H. B., & Butcher, E. C. (1997). Expression of mucosal homing receptor alpha4beta7 by circulating CD4+ cells with memory for intestinal rotavirus. *Journal of Clinical Investigation*, *100*(5), 1204–1208. https://doi.org/10.1172/JCI119633

Ruibal, P., Oestereich, L., Lüdtke, A., Becker-Ziaja, B., Wozniak, D. M., Kerber, R., … Muñoz-Fontela, C. (2016). Unique human immune signature of Ebola virus disease in Guinea. *Nature*, *533*(7601), 100–104. https://doi.org/10.1038/nature17949

Ruo, S. L., Mitchell, S. W., Kiley, M. P., Roumillat, L. F., Fisher-Hoch, S. P., & McCormick, J. B. (1991). Antigenic relatedness between arenaviruses defined at the epitope level by monoclonal antibodies. *Journal of General Virology*, *72*(3), 549–555. https://doi.org/10.1099/0022-1317-72-3-549

Russier, M., Pannetier, D., & Baize, S. (2012). Immune responses and Lassa virus infection. *Viruses*, *4*(11), 2766–2785. https://doi.org/10.3390/v4112766

Sackstein, R., Schatton, T., & Barthel, S. R. (2017). T-lymphocyte homing: an underappreciated yet critical hurdle for successful cancer immunotherapy. *Laboratory Investigation*, *97*(6), 669–697. https://doi.org/10.1038/labinvest.2017.25

Safronetz, D., Lopez, J. E., Sogoba, N., Traore', S. F., Raffel, S. J., Fischer, E. R., … Feldmann, H. (2010). Detection of Lassa virus, Mali. *Emerging Infectious Diseases*, *16*(7), 1123–1126. https://doi.org/10.3201/eid1607.100146

Sallusto, F., Kremmer, E., Palermo, B., Hoy, A., Ponath, P., Qin, S., … Lanzavecchia, A. (1999). Switch in chemokine receptor expression upon TCR stimulation reveals novel homing potential for recently activated T cells. *European Journal of Immunology*, *29*(6), 2037–2045. https://doi.org/10.1002/(SICI)1521-4141(199906)29:06<2037::AID-IMMU2037>3.0.CO;2-V

Sallusto, F., Lenig, D., Förster, R., Lipp, M., & Lanzavecchia, A. (1999). Two subsets of memory T lymphocytes with distinct homing potentials and effector functions. *Nature*, *401*(6754), 708–712. https://doi.org/10.1038/44385

Samaha, H., Pignata, A., Fousek, K., Ren, J., Lam, F. W., Stossi, F., … Taylor, M. D. (2018). A homing system targets therapeutic T cells to brain cancer. *Nature*, *14*, 17. https://doi.org/10.1038/s41586-018-0499-y

Sandoval, F., Terme, M., Nizard, M., Badoual, C., Bureau, M.-F., Freyburger, L., … Tartour, E. (2013). Mucosal Imprinting of Vaccine-Induced CD8+ T Cells Is Crucial to Inhibit the Growth of Mucosal Tumors. *Science Translational Medicine*, *5*(172), 172ra20-172ra20. https://doi.org/10.1126/scitranslmed.3004888

Santamaria Babi, L. F., Moser, R., Perez Soler, M. T., Picker, L. J., Blaser, K., & Hauser, C. (1995). Migration of skin-homing T cells across cytokine-activated human endothelial cell layers involves interaction of the cutaneous lymphocyte-associated antigen (CLA), the very late antigen-4 (VLA-4), and the lymphocyte function-associated antigen-1 (LFA-1). *Journal of Immunology (Baltimore, Md. : 1950)*, *154*(4), 1543–1550. Retrieved from http://www.ncbi.nlm.nih.gov/pubmed/7836740

Schaeffer, J., Carnec, X., Reynard, S., Mateo, M., Picard, C., Pietrosemoli, N., … Baize, S. (2018). Lassa virus activates myeloid dendritic cells but suppresses their ability to stimulate T cells. *PLoS Pathogens*, *14*(11), e1007430. https://doi.org/10.1371/journal.ppat.1007430

Schenkel, J. M., Fraser, K. A., Beura, L. K., Pauken, K. E., Vezys, V., & Masopust, D. (2014). Resident memory CD8 T cells trigger protective innate and adaptive immune responses. *Science*, *346*(6205), 98–101. https://doi.org/10.1126/science.1254536

Schenkel, J. M., & Masopust, D. (2014). Tissue-resident memory T cells. *Immunity*, *41*(6), 886–897. https://doi.org/10.1016/j.immuni.2014.12.007

Schmidt, M. E., & Varga, S. M. (2018). The CD8 T Cell Response to Respiratory Virus Infections. *Frontiers in Immunology*, *9*, 678. https://doi.org/10.3389/fimmu.2018.00678

Sckisel, G. D., Tietze, J. K., Zamora, A. E., Hsiao, H.-H., Priest, S. O., Wilkins, D. E. C., … Murphy, W. J. (2014). Influenza infection results in local expansion of memory CD8 $^{+}$ T cells with antigen non-specific phenotype and function. *Clinical & Experimental Immunology*, *175*(1), 79–91. https://doi.org/10.1111/cei.12186

Sgambelluri, F., Diani, M., Altomare, A., Frigerio, E., Drago, L., Granucci, F., … Reali, E. (2016). A role for CCR5+CD4 T cells in cutaneous psoriasis and for CD103+ CCR4+ CD8 Teff cells in the associated systemic inflammation. *Journal of Autoimmunity*, *70*, 80–90. https://doi.org/10.1016/j.jaut.2016.03.019

Shaffer, J. G., Grant, D. S., Schieffelin, J. S., Boisen, M. L., Goba, A., Hartnett, J. N., … Garry, R. F. (2014). Lassa Fever in Post-Conflict Sierra Leone. *PLoS Neglected Tropical Diseases*, *8*(3), e2748. https://doi.org/10.1371/journal.pntd.0002748

Sheridan, B. S., Pham, Q. M., Lee, Y. T., Cauley, L. S., Puddington, L., & Lefrançois, L. (2014). Oral infection drives a distinct population of intestinal resident memory cd8+ t cells with enhanced protective function. *Immunity*, *40*(5), 747–757. https://doi.org/10.1016/j.immuni.2014.03.007

Shimojima, M., Stroher, U., Ebihara, H., Feldmann, H., & Kawaoka, Y. (2012). Identification of Cell Surface Molecules Involved in Dystroglycan-Independent Lassa Virus Cell Entry. *Journal of Virology*, *86*(4), 2067–2078. https://doi.org/10.1128/JVI.06451-11

Shono, Y., Suga, H., Kamijo, H., Fujii, H., Oka, T., Miyagaki, T., … Sato, S. (2019). Expression of CCR3 and CCR4 Suggests a Poor Prognosis in Mycosis Fungoides and Sézary Syndrome. *Acta Dermato Venereologica*, *99*(9), 809–812. https://doi.org/10.2340/00015555-3207

Siddle, K. J., Eromon, P., Barnes, K. G., Mehta, S., Oguzie, J. U., Odia, I., … Happi, C. T. (2018). Genomic Analysis of Lassa Virus during an Increase in Cases in Nigeria in 2018. *The New England Journal of Medicine*, *379*(18), 1745–1753. https://doi.org/10.1056/NEJMoa1804498

Six, A., Mariotti-Ferrandiz, M. E., Chaara, W., Magadan, S., Pham, H.-P., Lefranc, M.-P., … Boudinot, P. (2013). The Past, Present, and Future of Immune Repertoire Biology – The Rise of Next-Generation Repertoire Analysis. *Frontiers in Immunology*, *4*, 413. https://doi.org/10.3389/fimmu.2013.00413

Snow, A. L., Pandiyan, P., Zheng, L., Krummey, S. M., & Lenardo, M. J. (2010). The power and the promise of restimulation-induced cell death in human immune diseases. *Immunological Reviews*, *236*(1), 68–82. https://doi.org/10.1111/j.1600-065X.2010.00917.x

Soler, D., Humphreys, T. L., Spinola, S. M., & Campbell, J. J. (2003). CCR4 versus CCR10 in human cutaneous TH lymphocyte trafficking. *Blood*, *101*(5), 1677–1682. https://doi.org/10.1182/blood-2002-07-2348

Speranza, E., Ruibal, P., Port, J. R., Feng, F., Burkhardt, L., Grundhoff, A., … Muñoz-Fontela, C. (2018). T-Cell Receptor Diversity and the Control of T-Cell Homeostasis Mark Ebola Virus Disease Survival in Humans. *The Journal of Infectious Diseases*, *218*(suppl_5), S508–S518. https://doi.org/10.1093/infdis/jiy352

Stanley Cheuk, A., Schlums, H., ne Gallais Sé ré zal, I., Stå hle, M., Bryceson, Y. T., Eidsmo Correspondence, L., … Eidsmo, L. (2017). CD49a Expression Defines Tissue-Resident CD8 + T Cells Poised for Cytotoxic Function in Human Skin Article CD49a Expression Defines Tissue-Resident CD8 + T Cells Poised for Cytotoxic Function in Human Skin. *Immunity*, *46*, 287–300. https://doi.org/10.1016/j.immuni.2017.01.009

Steinman, L. (2005). Blocking adhesion molecules as therapy for multiple sclerosis: natalizumab. *Nature Reviews Drug Discovery*, *4*(6), 510–518. https://doi.org/10.1038/nrd1752

Stephenson, E. H., Larson, E. W., & Dominik, J. W. (1984). Effect of environmental factors on aerosol-induced lassa virus infection. *Journal of Medical Virology*, *14*(4), 295–303. https://doi.org/10.1002/jmv.1890140402

Suwannasaen, D., Romphruk, A., Leelayuwat, C., & Lertmemongkolchai, G. (2010). Bystander T cells in human immune responses to dengue antigens. *BMC Immunology*, *11*(1), 47. https://doi.org/10.1186/1471-2172-11-47

Swain, S. L., & Bradley, L. M. (1992). Helper T cell memory: more questions than answers. *Seminars in Immunology*, *4*(1), 59–68. Retrieved from http://www.ncbi.nlm.nih.gov/pubmed/1350469

Swartz, M. A., Hubbell, J. A., & Reddy, S. T. (2008). Lymphatic drainage function and its immunological implications: From dendritic cell homing to vaccine design. *Seminars in Immunology*, *20*(2), 147–156. https://doi.org/10.1016/j.smim.2007.11.007

Tang, V. A., & Rosenthal, K. L. (2010). Intravaginal infection with herpes simplex virus type-2 (HSV-2) generates a functional effector memory T cell population that persists in the murine genital tract. *Journal of Reproductive Immunology*, *87*(1–2), 39–44. https://doi.org/10.1016/j.jri.2010.06.155

Tao, L., & Reese, T. A. (2017). Making Mouse Models That Reflect Human Immune Responses. *Trends in Immunology*, *38*(3), 181–193. https://doi.org/10.1016/j.it.2016.12.007

ter Meulen, J., Badusche, M., Kuhnt, K., Doetze, A., Satoguina, J., Marti, T., … Hoerauf, A. (2000). Characterization of human CD4(+) T-cell clones recognizing conserved and variable epitopes of the Lassa virus nucleoprotein. *Journal of Virology*, *74*(5), 2186–2192. https://doi.org/10.1128/jvi.74.5.2186-2192.2000

Ter Meulen, J., Koulemou, K., Wittekindt, T., Windisch, K., Strigl, S., Conde, S., & Schmitz, H. (1998). Detection of Lassa virus antinucleoprotein immunoglobulin G (IgG) and IgM antibodies by a simple recombinant immunoblot assay for field use. *Journal of Clinical Microbiology*, *36*(11), 3143–3148. Retrieved from http://www.ncbi.nlm.nih.gov/pubmed/9774554

Thome, J. J. C., Yudanin, N., Ohmura, Y., Kubota, M., Grinshpun, B., Sathaliyawala, T., … Farber, D. L. (2014). Spatial Map of Human T Cell Compartmentalization and Maintenance over Decades of Life. *Cell*, *159*(4), 814–828. https://doi.org/10.1016/j.cell.2014.10.026

Thompson, J. M., & Iwasaki, A. (2008). Toll-like receptors regulation of viral infection and disease. *Advanced Drug Delivery Reviews*, *60*(7), 786–794. https://doi.org/10.1016/j.addr.2007.11.003

Tomori, O., Fabiyi, A., Sorungbe, A., Smith, A., & McCormick, J. B. (1988). Viral hemorrhagic fever antibodies in Nigerian populations. *The American Journal of Tropical Medicine and Hygiene*, *38*(2), 407–410. https://doi.org/ 10.1136/bmj.311.7009.857

Torriani, G., Galan-Navarro, C., & Kunz, S. (2017). Lassa Virus Cell Entry Reveals New Aspects of Virus-Host Cell Interaction. *Journal of Virology*, *91*(4), e01902-16. https://doi.org/10.1128/JVI.01902-16

Troy, A. E., & Shen, H. (2003). Cutting Edge: Homeostatic Proliferation of Peripheral T Lymphocytes Is Regulated by Clonal Competition. *The Journal of Immunology*, *170*(2), 672–676. https://doi.org/10.4049/jimmunol.170.2.672

Van Breedam, W., Pöhlmann, S., Favoreel, H. W., de Groot, R. J., & Nauwynck, H. J. (2014). Bitter-sweet symphony: glycan–lectin interactions in virus biology. *FEMS Microbiology Reviews*, *38*(4), 598–632. https://doi.org/10.1111/1574-6976.12052

Walker, D. H., McCormick, J. B., Johnson, K. M., Webb, P. A., Komba-Kono, G., Elliott, L. H., & Gardner, J. J. (1982). Pathologic and virologic study of fatal Lassa fever in man. *The American Journal of Pathology*, *107*(3), 349–356. Retrieved from http://www.ncbi.nlm.nih.gov/pubmed/7081389

Walker, D. H., Wulff, H., Lange, J. V, & Murphy, F. A. (1975). Comparative pathology of Lassa virus infection in monkeys, guinea-pigs, and Mastomys natalensis. *Bulletin of the World Health Organization*, *52*(4–6), 523–534. Retrieved from http://www.ncbi.nlm.nih.gov/pubmed/821625

Warner, B. M., Safronetz, D., & Stein, D. R. (2018). Current research for a vaccine against Lassa hemorrhagic fever virus. *Drug Design, Development and Therapy*, *Volume 12*, 2519–2527. https://doi.org/10.2147/DDDT.S147276

Watanabe, R., Gehad, A., Yang, C., Scott, L. L., Teague, J. E., Schlapbach, C., … Clark, R. A. (2015). Human skin is protected by four functionally and phenotypically discrete populations of resident and recirculating memory T cells. *Science Translational Medicine*, *7*(279). https://doi.org/10.1126/scitranslmed.3010302

Wherry, E. J., & Kurachi, M. (2015). Molecular and cellular insights into T cell exhaustion. *Nature Reviews. Immunology*, *15*(8), 486–499. https://doi.org/10.1038/nri3862

WHO. (2016). *AN R&D BLUEPRINT FOR ACTION TO PREVENT EPIDEMICS*. Retrieved from www.who.int

WHO | Lassa Fever – Nigeria. (2018). *WHO*. Retrieved from https://www.who.int/csr/don/23-march-2018-lassa-fever-nigeria/en/

Winn, W. C., Monath, T. P., Murphy, F. A., & Whitfield, S. G. (1975). Lassa virus hepatitis. Observations on a fatal case from the 1972 Sierra Leone epidemic. *Archives of Pathology*, *99*(11), 599–604. Retrieved from http://www.ncbi.nlm.nih.gov/pubmed/1227472

World Health Organization. (2016). Weekly epidemiological record Relevé épidémiologique hebdomadaire. Retrieved from http://www.who.int/immunization/sage/en/index.html;

World Health Organization. (2018). *Introduction to Lassa fever: Managing infectious hazards*. Retrieved from http://www.who.int/emergencies/diseases/lassa-fever/geographic-distribution.png?ua=1

Wu, T., Hu, Y., Lee, Y.-T., Bouchard, K. R., Benechet, A., Khanna, K., & Cauley, L. S. (2014). Lung-resident memory CD8 T cells (TRM) are indispensable for optimal cross-protection against pulmonary virus infection. *Journal of Leukocyte Biology*, *95*(2), 215–224. https://doi.org/10.1189/jlb.0313180

Wulff, H., Lange, J. V., & Webb, P. A. (1978). Interrelationships Among Arenaviruses Measured by Indirect Immunofluorescence. *Intervirology*, *9*(6), 344–350. https://doi.org/10.1159/000148956

Xu, B., Wagner, N., Pham, L. N., Magno, V., Shan, Z., Butcher, E. C., & Michie, S. A. (2003). Lymphocyte homing to bronchus-associated lymphoid tissue (BALT) is mediated by L-selectin/PNAd, alpha4beta1 integrin/VCAM-1, and LFA-1 adhesion pathways. *The Journal of Experimental Medicine*, *197*(10), 1255–1267. https://doi.org/10.1084/jem.20010685

Yednock, T. A., Cannon, C., Fritz, L. C., Sanchez-Madrid, F., Steinman, L., & Karin, N. (1992). Prevention of experimental autoimmune encephalomyelitis by antibodies against α4βl integrin. *Nature*, *356*(6364), 63–66. https://doi.org/10.1038/356063a0

Yoneyama, M., Onomoto, K., Jogi, M., Akaboshi, T., & Fujita, T. (2015). Viral RNA detection by RIG-I-like receptors. *Current Opinion in Immunology*, *32*, 48–53. https://doi.org/10.1016/j.coi.2014.12.012

Yun, N. E., Poussard, A. L., Seregin, A. V., Walker, A. G., Smith, J. K., Aronson, J. F., … Paessler, S. (2012). Functional Interferon System Is Required for Clearance of Lassa Virus. *Journal of Virology*, *86*(6), 3389–3392. https://doi.org/10.1128/JVI.06284-11

Yun, N. E., & Walker, D. H. (2012). Pathogenesis of Lassa Fever. *Viruses*, *4*(10), 2031–2048. https://doi.org/10.3390/v4102031

Yun, N. E, Ronca, S., Tamura, A., Koma, T., Seregin, A. V, Dineley, K. T., … Paessler, S. (2015). Animal Model of Sensorineural Hearing Loss Associated with Lassa Virus Infection. *Journal of Virology*, *90*(6), 2920–2927. https://doi.org/10.1128/JVI.02948-15

Zajac, A. J., Blattman, J. N., Murali-Krishna, K., Sourdive, D. J. D., Suresh, M., Altman, J. D., & Ahmed, R. (1998). Viral Immune Evasion Due to Persistence of Activated T Cells Without Effector Function. *The Journal of Experimental Medicine*, *188*(12), 2205–2213. https://doi.org/10.1084/jem.188.12.2205

Zeng, R., Oderup, C., Yuan, R., Lee, M., Habtezion, A., Hadeiba, H., & Butcher, E. C. (2013). Retinoic acid regulates the development of a gut-homing precursor for intestinal dendritic cells. *Mucosal Immunology*, *6*(4), 847–856. https://doi.org/10.1038/mi.2012.123

Zhang, X., Sun, S., Hwang, I., Tough, D. F., & Sprent, J. (1998). Potent and Selective Stimulation of Memory-Phenotype CD8+ T Cells In Vivo by IL-15. *Immunity*, *8*(5), 591–599. https://doi.org/10.1016/S1074-7613(00)80564-6

Zhao, M., Chen, J., Tan, S., Dong, T., Jiang, H., Zheng, J., … Yu, H. (2018). Prolonged Evolution of Virus-Specific Memory T Cell Immunity after Severe Avian Influenza A (H7N9) Virus Infection. *Journal of Virology*, *92*(17). https://doi.org/10.1128/JVI.01024-18

10 APPENDIX

10.1 ACKNOWLEDGMENT

Three years is a long time to commit to one goal and walk the road towards it, and they would have been even longer if not for all the people who have shared those same three years with me and were by my side. May it be for the whole way or even just small stops along the way; I will always be grateful for your help I received along the way and I am grateful also for the time I was able to spend with you.

Cesar, I thank you for the opportunity to work in your lab, the endless time you committed to keeping me on course, forming me into a better scientist and giving me “just on minute” whenever I was (annoying) in need of help and knocked on your door. Your tireless commitment to getting funding, building international connections and coming up with crazy research ideas is the wheel that keep your lab rolling. I did not give you the easiest time, so I am grateful to have your support until the end and beyond. I know I have learned a lot under your supervision and I am sad to leave.
Lars, thank you for being my supervisor in Lübeck, for coming to Hamburg and listen to all the concerns and giving your full support. I am grateful that you were willing to walk this road with me. I know it must have been difficult from afar, but I was always sure you had our back and supported us fully. Thank you for helping make this thesis possible.
Thank you, Lisa, for adopting me into the Lassa family, being always ready to discuss ideas and help out with project planning and my training, not to mention showing me how to survive Nigeria politics (and saving from snakes along the way). Thanks for all the little moments where you were excited about my results and immediately bombarded me with 1000 ideas/questions to go further. I wish we had written down all those ideas we had when Nigeria was too hot to sleep, I think they would have made for a second PhD. I am still sad amazon refused to ship the strawberry gin to Irrua.

Thank you to my name-confuzzled team: Mufos, Virusimmunologists, Cesaren….in all honesty you will always be AwesomeGroup 62 to me! Thank you to Paula, Maite, Beatriu and Emilia, for your support. You thought me what matters, how to improve and to be better at staying on my toes (also literally). Beatriu, thank you for your support in figuring my s*** out and getting a move on with my non-zombified friends (NZFs). Emilia, thank you for

suffering through my attempt at your language and making it beautiful. Thank you for pushing me to step over my shadow. Maite, I will always remember your commitment and strive to mimic it. Thank you, Sergio, for keeping the lab alive and running. For showing me the ropes in the beginning and being there when needed. Also, Jürgen, all my thank to you, for bringing excitement and positive emotion wherever you go. The care packages you send were the best!

All my love to me fellow sufferers Moni and Cathy. Thank you for bouncing ideas, for talking science and for all the idle chitchat you let me indulge in. An n-lab society can have its benefits, also, I believe. The grass is always greener…but you made our lab the greenest. Cathy, thank you for giving me the emotional support I didn't know how to ask for. You made me smile, laugh and gave me the motivation to keep going when I felt like all motivation was gone. Thank you for not taking any bulls*** and letting be the excited fangirl with you. Moni, thank you for all the time spend at my side through the last three years. I do not know how I would have survived without you. Your help made the last year possible and I will always be grateful to you for supporting me with my NZFs. I know I must have driven you insane at times. I never told you how much I admire your persistence and the way you keep going even though it's hard. You will pull through at the end, I fully believe in you! There are too many diving vacations in your future to give up now.

My thanks also to the wonderful people from virology. Elly and Sabrina: Thank you for all your patience and help. I know that you guys get the worst with all the newbies, but you pull through and make us into better versions of ourselves. Be proud! I would have never survived the last year without your help and will forever remember everything I learned from you. Sabrina, you truly are the soul of the BSL-4 and always there to help. I hope you know how much that means to people, me included. Elly, thank you also for all your time and pulling me away to also have a life outside the institute. I am grateful for every Wednesday you stopped by our lab, and afraid you do not know how much that means to me.

Thank you, David! In honor of your own acknowledgments, I can say I agree with your analogy wholeheartedly. You were the best older (and taller) brother anyone could have asked for. Thank you for teaching me to make my first baby steps in the BSL-4, for bringing calm when I felt adrift in the storm and for not pushing me always when I was sure I left the line of polite annoyance long behind. You made me look forward, always! To Jonas, I hope you know that you were the annoying little brother I didn't know I needed in my life at that time. Even though I am afraid we caused Lisa some grey hairs. Your endless energy and ambition to "just get that assay right and perfect" are remarkable. Do not lose this part of yourself, please! Every time I clean my bench, I light a candle for you in my head.

Thank you Anke, for always bringing energy and helping me out, when I am sure you were drowning in your own work. Thank you Silke, for bringing sunshine wherever you go and bringing life to poor little Lassa rescues, that I thought would not see the light again. Thank you, Steffi, Nadia and Carola, for always having our back and taking the walkie.
Thank you, Constantin, for your patience, your help and your smile. Without you and your fellow animal caretakers we would all be lost. My gratitude also goes to all the other people, too numerous to name, in administration at BNI, and the sequencing team at HPI, that made everything possible. Thank you especially Jeanette, for being there for us. My love and thanks also to all the staff at ISTH, Nigeria. I am glad to have been able to meet all of you, learn from you and work with you. Thank you, Rita, Jennifer and Yemisi for going to the ward when I would not have been able to. Thank you Andras, for being the embodiment of summer, chasing the clouds away and bringing the sun into our lab! Thank you, Katha, Henry, Sandra and Santiago for sharing the road with me, even just for a short time.

And finally: Danke Mama, Danke Papa. Auf eure jeweils eigene, und viel unterschiedlicher hätten sie nicht sein können, Weisen, habt ihr das hier mit möglich gemacht. Ich war mir eurer Liebe und eurer Unterstützung und eurem Glauben an mich immer sicher. Ein größeres Geschenk hättet ihr mir nicht geben können.

10.2 VERSICHERUNG AN EIDES STATT

I hereby certify that this thesis has been composed by me and is based on my own work, unless stated otherwise. No other person's work has been used without due acknowledgement in this thesis. All references and verbatim extracts have been quoted, and all sources of information, including graphs and data sets, have been specifically acknowledged.

Lübeck, September 2019 Julia R. Po